TUM School of Life Sciences

Professur für Biotechnologie der Reproduktion, Prof. Dr. Benjamin Schusser

Generation and functional characterization of CRISPR/Cas9-expressing chickens to protect them from Marek´s disease virus

Natalie Denise Duda

Vollständiger Abdruck der von der TUM School of Life Sciences der Technischen Universität München zur Erlangung des akademischen Grades einer

Doktorin der Naturwissenschaften

genehmigten Dissertation.

Vorsitzende(r): Prof. Dr. Harald Luksch

Prüfende(r) der Dissertation:

1. Prof. Dr. Benjamin Schusser
2. Prof. Benedikt B. Kaufer, Ph.D.

Die Dissertation wurde am 12.04.2021 bei der Technischen Universität München eingereicht und durch die TUM School of Life Sciences am 20.07.2021 angenommen.

To my Family

Table of Contents

ABSTRACT

The adaptive immunity of procaryotes is based on the CRISPR/Cas9 system that relies on the endonuclease Cas9 and guide RNAs targeting nucleic acids in a sequence-specific manner. Further development of the CRISPR/Cas9 system has led to a precise and standardized genome editing technology with significant contributions to basic research, molecular biotechnology, and genetic engineering. Nevertheless, the simultaneous delivery of CRISPR/Cas9 components for efficient *in vivo* genome editing applications has been challenging as the size of the *Cas9* gene exceeds the packaging capacity of many delivery systems. This can be overcome by generating transgenic animals with ubiquitous Cas9 expression.

This work describes the generation of the first Cas9 transgenic chicken line. The ubiquitous expression of Cas9 was validated in all tested tissues. The functionality of the Cas9 endonuclease was confirmed *in vitro* as well as *in vivo* by using different delivery systems including retroviral vectors and *in ovo*-electroporation. This provides a powerful tool for efficient Cas9-mediated *ex vivo* and *in vivo* genome editing in the chicken by simply delivering guide RNAs and allows for precise gene editing with no need to generate germline modifications.

In the second part of this work, a transgenic chicken line was generated and tested in an infection experiment where it was challenged with the Marek´s disease virus (MDV). This chicken line ubiquitously expresses Cas9 and guide RNAs targeting essential genes of MDV. This ongoing work is fundamental to establish a CRISPR/Cas9-mediated *in vivo* protection against MDV in chickens.

ZUSAMMENFASSUNG

CRISPR/Cas9 ist eine effiziente Methode zur Genom-Editierung. Sie basiert auf dem Protein Cas9 und sogenannten Guide-RNAs und wurde erstmals als adaptiver Abwehrmechanismus in Prokaryoten beschrieben. Für die Anwendung der CRISPR/Cas9-Methode als Genomeditierungstechnologie wird sich der fehlerhafte DNA-Reparaturmechanismus von eukaryotischen Zellen zunutze gemacht. So können zum einen Gen-Knockouts durch das Herbeiführen von Insertionen und Deletionen erzeugt werden und zum anderen DNA-Stücke mittels homologer Rekombination effizient und präzise in das Zielgenom eingefügt werden. Eine effiziente Editierung von Genomsequenzen *in vivo* ist jedoch schwierig, weil dafür beide CRISPR/Cas9-Komponenten gleichzeitig in der Zelle vorhanden sein müssen und die Größe des *Cas9* Gens die Kapazität vieler Transportsysteme überschreitet. Eine Lösung für dieses Problem ist die Erzeugung transgener Tiere mit ubiquitärer Cas9-Expression.

Diese Arbeit beschreibt die erstmalige Erzeugung und Charakterisierung einer Cas9-exprimierenden Hühnerlinie. Die ubiquitäre Expression von Cas9 wurde in allen getesteten Geweben nachgewiesen und die Funktionalität der Cas9-Endonuklease in Cas9-exprimierenden Hühnern sowohl *in vitro* als auch *in vivo* bestätigt. Durch die Zugabe von Guide-RNAs per retroviralem Gentransfer als auch durch *in ovo*-Elektroporation, konnte das Hühnergenom ohne vorangehende Keimbahnmodifikation präzise und effizient verändert werden.

Im zweiten Teil dieser Arbeit wurde eine transgene Hühnerlinie mit ubiquitärer Expression von Cas9 und Guide-RNAs, die auf virale Gene des Marek Virus (MDV) abzielen und essentiell für dessen Replikation sind, generiert. Diese Tiere wurden in einem Infektionsexperiment mit MDV infiziert, um zu testen ob ein CRISPR/Cas9-vermittelter Schutz vor der Marekschen-Krankheit bei Hühnern etabliert werden kann.

1. INTRODUCTION

The chicken has become an indispensable animal model for many research areas with key findings in embryology, developmental biology and immunology. As it is a phylogenic distant species to humans with an easy access to the embryonated egg, it contributed to the discovery of gene functions [1], antibody-producing B-cells [2] and to the development of vaccines [3]. Moreover, poultry, and especially the chicken, is one of the most important livestock animals that already counts for almost 45 % of all meat that is consumed worldwide, therefore representing a significant nutritional source of animal-derived protein in our diet [4,5]. Until 2050, the global food production must increase by 70 % to meet our needs and feed the growing world population [5,6], while arable land for the production of food is constantly decreasing [7]. In contrast to beef and pork, poultry essentially contributes to this goal by providing an animal protein source which can be consumed independently of religion. Consequently, to meet these demands, a rapid change towards intensive agriculture use within the poultry industry, supported by technological transformation, is needed [8]. However, the downside of intensive agriculture use is accompanied by poor living conditions for the animals and the constant increase of infectious diseases, such as infectious bronchitis virus, infectious bursal disease virus, influenza A virus and Marek´s disease virus (MDV) which is one of the most deadly diseases in poultry [9]. MDV is a DNA-integrating herpesvirus that causes immunosuppression and the development of lymphomas. It causes an annual economic loss of up to $2 billion US dollars worldwide [10,11]. Although vaccines are applied, they do not provide a sterile immunity which is why the virus is able to overcome the protection and evolves towards higher virulence [12]. New genome editing technologies provide the possibility to establish disease resistance in chickens when conventional vaccination methods fail. Clustered Regularly Interspaced Short Palindromic Repeats (CRISPR) and its CRISPR-associated (Cas) nucleases were originally discovered as the “immune system of procaryotes” [13,14]. With further development of the CRISPR/Cas system towards a gene editing tool that is able to (in-)activate genes by site-specific targeting [15], it is now one of the most used techniques for genome editing [16] and a promising tool to fight MDV in chickens.

1.1. Marek´s disease virus

Herpesviruses have a long co-evolutionary history with their hosts and can be found in many species including humans, mammals, birds, reptiles, fish and frogs [17]. With their ability to integrate into the genome and thereby escaping the immune system of the host, latent infections can be established, enabling the virus to persist and occasionally reactivate which results in the outbreak of the disease [18].

The most prevalent avian herpesvirus is MDV, named after the Hungarian pathologist Jozef Marek [19]. It is an oncogenic herpesvirus which infects mainly domestic chickens (*gallus gallus domesticus*) and less commonly turkey, quail and geese [20,21] and causes typical symptoms such as severe immunosuppression, neurological disorders and neoplastic transformation, leading to peripheral and visceral lymphomas [12].

1.1.1. Classification and genomic structure

All herpesviruses are assigned to the order of Herpesvirales which can be divided into three families: *Herpes-*, *alloherpes-* and *malacoherpesviridae*. The family of *herpesviridae* infects mammals, birds, and reptiles whereas *alloherpesviridae* are found in fish and amphibians. The family of *malacoherpesviridae* infects invertebrates [22,23].

MDV-1, also known as Gallid herpesvirus 2 (GaHV-2), belongs to the family of *herpesviridae* which is further divided into three subfamilies: *alpha-, beta-* and *gammaherpesviridae*. Originally, MDV was classified into the group of *gammaherpesviridae* such as the human herpesvirus Epstein-Barr virus (EBV). However, sequencing of the complete MDV genome [24] revealed that the genomic organization is more similar to members of the *alphaherpesviridae* e.g. the Herpes simplex virus (HSV).

In 1975, Bulow and Biggs classified MDV into three serotype groups which can be distinguished by using serotype-specific monoclonal antibodies [25]: Serotype-1 MDV (GaHV-2), serotype-2 MDV (GaHV-3) and serotype-3 herpesvirus of turkey (HVT, meleagrid herpesvirus type 1). Among serotypes, only serotype-1 MDV is oncogenic and shows a wide variation in pathogenic potential ranging from avirulent to very virulent strains (Table 1) [26].

Table 1: MDV-1 isolates

MDV-1 isolates	**Pathogenic potential**
mMDV	Mild
vMDV	virulent
vvMDV	very virulent
vv+MDV	very virulent +

RB-1B and Md5 are well-known oncogenic strains, displaying a vvMDV pathogenic potential [27]. In contrast, CVI988 strains exhibit mMDV pathotypes which resemble the classical form of Marek´s disease (MD) [9]. Examples of non-oncogenic strains are vaccination strains such as HVT, SB-1 or CVI988/Rispens [28,29].

MDV is a double-stranded (ds) DNA virus with a size of 150-200 nm. Figure 1 shows the characteristic structure of herpesviruses consisting of glycosylated proteins on the cell surface, a tegument, an envelope and a nucleocapsid protecting the viral core containing the viral DNA [30,31].

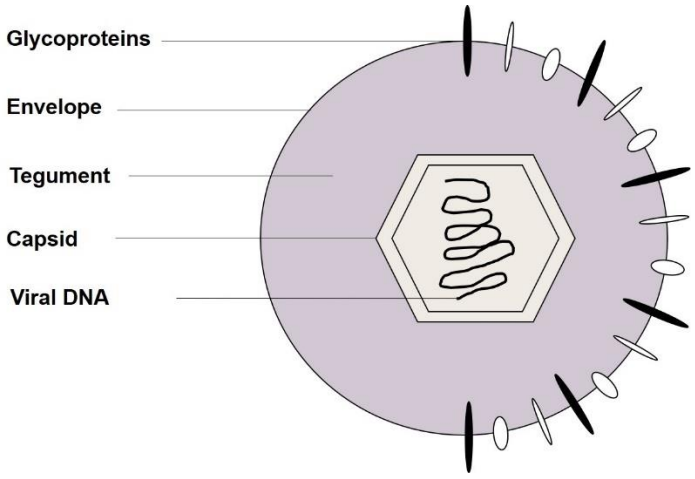

Figure 1: Characteristic structure of herpesviruses. MDV belongs to the family of *herpesviridae* and shares the same structure as several human herpesviruses including human herpes virus 6 (HHV-6). The MDV structure consists of surface glycoproteins, a tegument and envelope and a capsid with linear ds viral DNA. Figure modified from ViralZone [32].

Figure 2 shows a schematic mapping of the genomic structure of MDV. The DNA molecule is approximately 180 kilo base pairs (bp) long. It contains two unique regions (U_L, U_S) which are flanked by two internal repeats (IR_L, IR_S) and two terminal repeats (TR_L, TR_S) [24,33]. They contain α-like sequences that harbor telomeric repeats (TMR) with TTAGGG that are identical

to the host telomeres [30]. The shortening of these telomeres is prevented by the telomerase complex which contains two main components; the catalytic subunit telomerase reverse transcriptase (TERT), and the telomerase RNA (TR or TERC) which serves as a template for the addition of telomeric repeats to the 3' strands of chromosomes [34]. Telomerase activity is absent in most somatic cells, but is active in stem cells and cancer cells [35]. MDV encodes for viral TR (vTR) that shares 88 % sequence identity with the cellular TR of chickens (chTR) [36]. The MDV genome harbors two copies of the vTR gene in the TR_L and IR_L regions, interacting with the chicken TERT and resulting in higher telomerase activity which is thought to play a role in MDV-induced transformation [35].

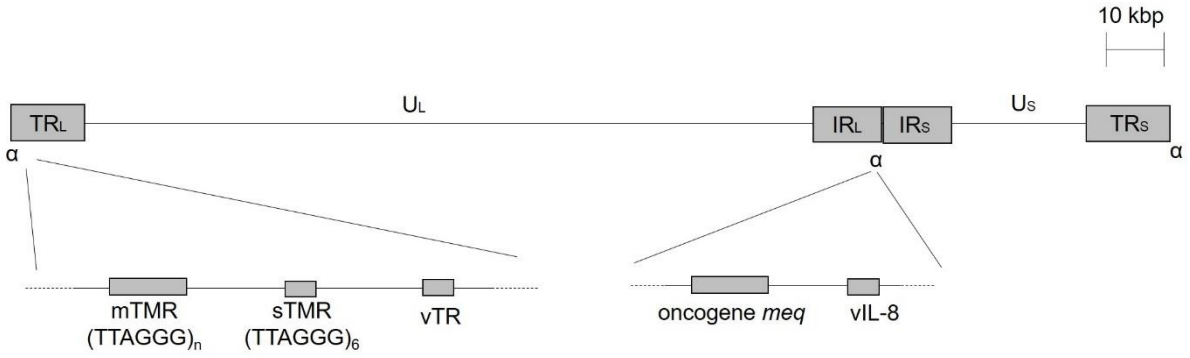

Figure 2: Genomic structure of MDV. The ds DNA molecule is linear and approximately 180 kilo bp long. It contains two unique regions, the unique long (U_L) and the unique short (U_S). These regions are flanked by two internal repeats [long (IR_L); short (IR_S)] and two terminal repeats [long (TR_L); short (TR_S)]. The $TR_{(L,S)}$ or $IR_{(L,S)}$ regions contain α-like sequences that harbour multiple telomeric repeats (mTMRs) and short telomeric repeats (sTMRs). Whereas mTMRs have a variable number of repeats [$(TTAGGG)_n$], sTMRs have a fixed number of 6 repeats [$(TTAGGG)_6$]. vTR encodes for the viral telomerase RNA, *meq* encodes for the basic leucine zipper transcription factor, and vIL-8 encodes for the viral chemokine IL-8. Figure modified from Kheimar et al. [35].

The MDV genome harbors two distinct TMR arrays: multiple telomeric repeats (mTMRs) and short telomeric repeats (sTMRs) [37], playing an important role in virus replication, integration and tumor formation [38,39]. The MDV genome encodes oncogenes leading to the transformation into tumor cells. The major MDV-oncogene is *meq* which encodes for a basic leucine zipper transcription factor [40]. As a potent transcription activator, it forms together with the proto-oncoprotein c-Jun a complex and represses lytic viral genes and modulates cell cycle regulators such as p53 and RB [30,41,42]. In addition to *meq*, several other factors are involved in MDV-induced tumorgenesis, including chemokines such as the viral IL-8 (vIL8). Based on its biological properties, the initially termed vIL-8 chemokine was

recently changed to vCXCL13 [43]. However, VIL8/vCXCL13 is known to be involved in recruiting immune cells to the site of viral replication [12,44]. More specifically, it attracts B-cells, the primary targets for lytic replication, and a subset of $CD4^+$ T-cells in which latency is established [43,44].

A cellular factor that is highly expressed by MDV tumor cells is CD30, a member of the tumor necrosis factor receptor (TNFR) II family [45]. CD30 was also identified as the Marek's-associated tumor surface antigen (MATSA) and is recognized by the monoclonal antibody AV37 [46]. Interestingly, specific antibodies against CD30 can be detected in more resistant chicken lines, suggesting immunity against CD30 could play a role in fighting tumors. CD30 signalling in normal lymphocytes promotes the survival and hyperproliferation of cells but can also lead to cell death [46]. However, its exact role of CD30 in lymphoma development is not fully understood.

1.1.2. Viral spread and host susceptibility

MDV infection is a global problem, distributed by backyard and migratory birds who represent a natural reservoir for the virus. To effectively control MD, it requires global surveillance and accurate reporting of cases [12]. Although the disease does not have to be reported according to the "World Organization of Animal Health" (IOE), more than half of the countries worldwide do report cases to keep track of its distribution and outbreaks. Endemic areas for MDV are countries such as China or Egypt reporting outbreaks on a yearly basis [12].

To prevent MDV outbreaks in commercial flocks, the spread from backyard and migratory birds to the industrial poultry must be prevented e.g. by biosecurity measurements. Nevertheless, it is typical that a large proportion of birds in commercial houses is infected [47], often by more than one MDV strain as serotypes 1 and 2 are the most prevalent ones. The outcome of infection and rate of virus spread within one flock is highly variable and depends on several factors:

- Virus serotype and its pathological potential [48,49]
- Time and level of initial exposure to the virus [50]
- Host susceptibility and genotype [51,52]

- Age of chickens [53]
- Presence of maternal antibodies that protect chicks the first weeks of life [19]
- Application of vaccines applied within the first day of life [19]
- Sex [54]

1.1.3. Pathogenesis and symptoms

MDV is highly oncogenic in its natural host and causes mortality rates of up to 100 % in unvaccinated flocks [55,56]. This is due to the complex pathogenesis of this highly cell-associated virus involving several cell types summarized in Figure 3.

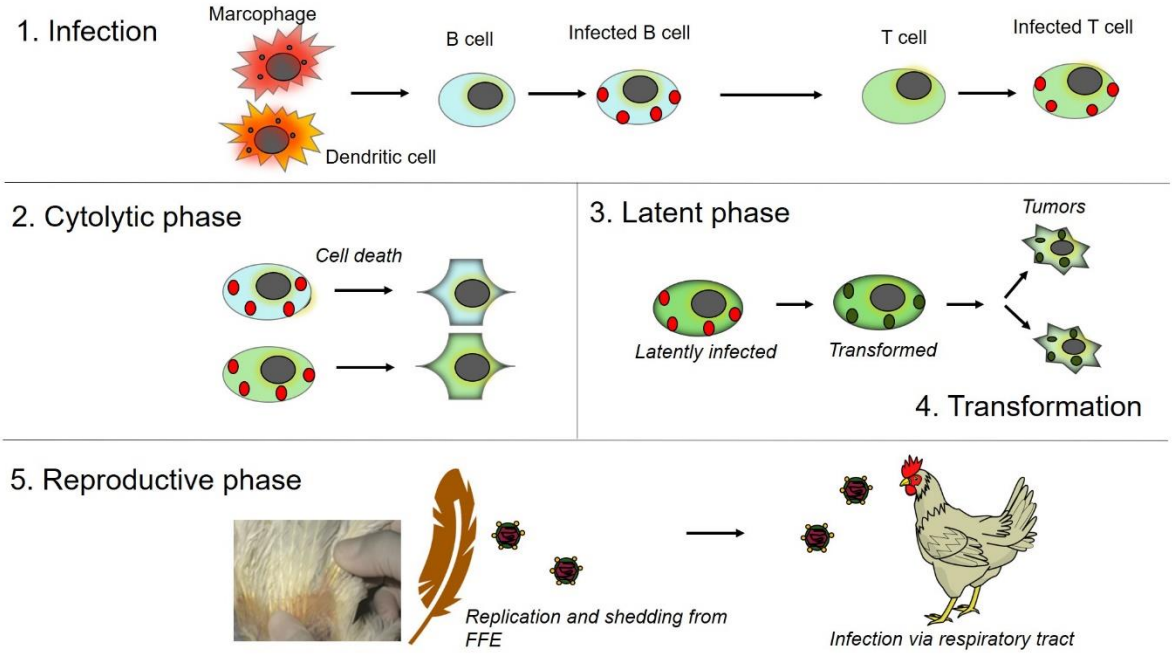

Figure 3: MDV pathogenesis. Macrophages and dendritic cells carry the virus to the primary lymphoid organs (bursa of Fabricius, spleen, thymus) where mainly B- and T-cells are infected (1). Infected cells undergo cytolytic phase resulting in cell death (2) or go into the latent phase (3) where latently infected T-cells undergo neoplastic transformation (4). The reproductive phase (5) takes place in the feather follicle epithelial (FFE) where the virus replicates in a second cytolytic phase and sheds infectious virions into the environment. Figure modified from Bertzbach et al. [27] and Boodhoo et al. [12].

Virus transmission occurs either direct or indirect with dust via the airborne route [57]. The infection begins in the respiratory tract with the inhalation of infectious particles from contaminated dust [58]. Within the early cytolytic phase, typically 3-5 days post infection (dpi) [12], immune cells such as macrophages and dendritic cells carry the virus to the primary lymphoid organs (bursa of Fabricius, spleen, thymus) where lytic replication of the virus occurs, mainly in B-cells as they appear to be the most susceptible cells for lytic replication [59]. It was long believed that infected B-cells amplify and transfer the virus, a process thought to be indispensable for MDV pathogenesis and tumor formation. Recently, Schusser et al. generated immunoglobulin (Ig) heavy chain J gene segment knockout (JH-KO) chickens that lack mature and peripheral B-cells [60]. These transgenic chickens were used in a study conducted by Bertzbach et al. who unraveled the role of B-cells in MDV infection and showed that the viral load in the blood of MDV infected animals was not altered in the absence of B-cells suggesting that mature and peripheral B-cells are dispensable for MDV pathogenesis [61]. Moreover, it has been shown that in the absence of B-cells, the virus replicates in $CD4^+$ and $CD8^+$ T-cells [61,62]. Bertzbach et al. also showed that MDV is replicating in natural killer (NK) cells [63].

Once the bird is infected, it can suffer from severe immunosuppression leading to an increased susceptibility to secondary infections e.g. with bacteria [64,65]. The neoplastic transformation of infected $CD4^+$ T-cells and their infiltration into the peripheral nervous system leads to neurological disorders such as ataxia, in extreme cases to the complete paralysis of legs and wings (Figure 4c). Although the virus can infect both $CD8^+$ and $CD4^+$ cells, mostly infected $CD4^+$ T-cells have the potential to transform into lymphomas [66]. Approximately 6-7 dpi, MDV integrates into the telomers of the host chromosomes by a homologous recombination pathway, establishing a latency in infected cells [30,38,39]. During latency, the virus stays dormant and expresses only a few viral genes [39]. Latently infected cells migrate to the skin where they reactivate and start the second cytolytic phase of virus replication in the feather follicle epithelial (FFE). Studies showed that viral DNA can already be detected after 5-7 dpi [67,68]. However, horizontal transmission occurs only between 12-14 dpi when infectious virions are shed into the environment [69]. Around 21-28 dpi, the transformed T-cells migrate to peripheral and visceral organs causing tumors in liver, spleen, ovaries, kidney, heart, proventriculus, skin, feather follicles and other tissues (Figure

4a,b) [66,70]. Further symptoms of the disease are depression, weight loss, anorexia and diarrhea [71]. An infection with vvMDV strains induces atrophy of lymphoid organs, resulting in a rapid disease progression and high mortality rates within the first two weeks of age[71,72].

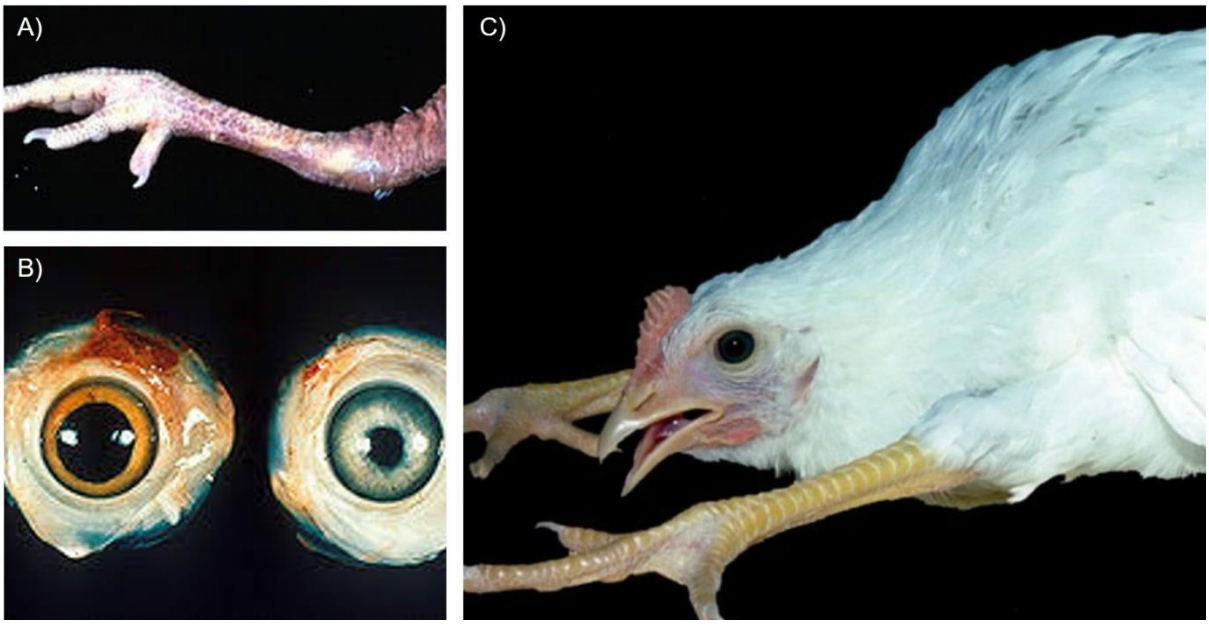

Figure 4: Marek´s disease. The development of symptoms can range from weeks to several months depending on the virulence of the MDV strain. Common symptoms are: Severe immunosuppression, neoplastic transformation of $CD4^+$ T-cells, leading to peripheral and visceral lymphomas (A: tumor skin; B: tumor in eye), neurological disorders (C: paralysis of legs). Figures adapted from [73–75].

1.1.4. MDV replication

MDV replication is a complex mechanism and can be divided into productive (lytic) and non-productive (persistent) replication forms which can be switched depending on the virus-cell interactions at different stages of the disease. Figure 5 shows the major replication steps with special focus on the proteins which are relevant for this thesis.

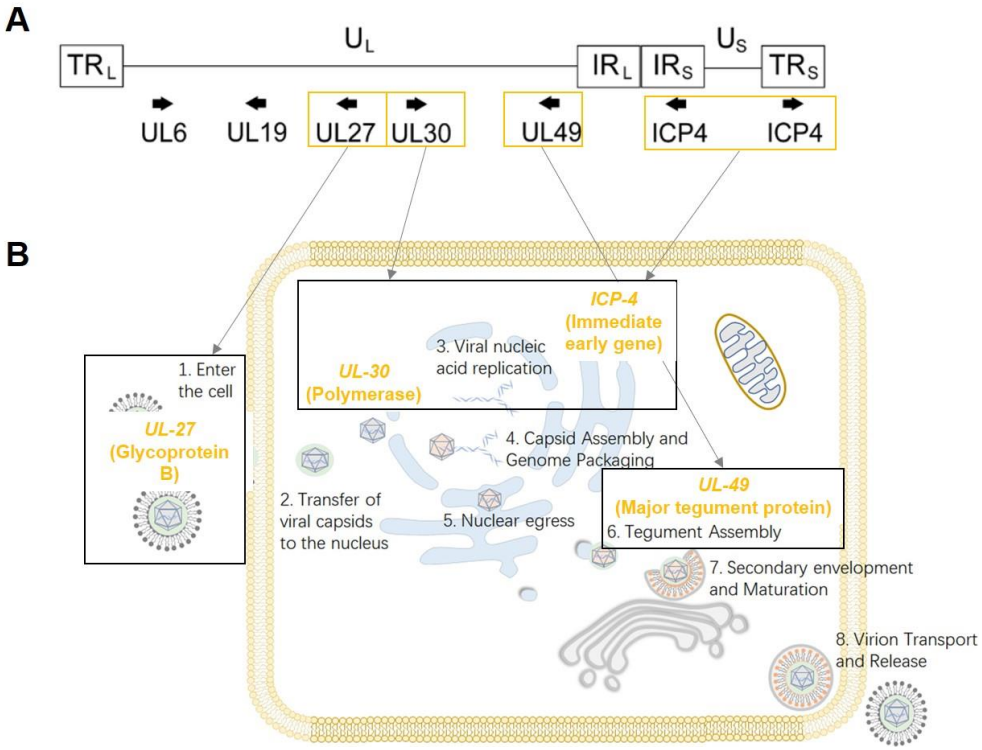

Figure 5: MDV replication. A) Genomic structure of MDV showing relevant genes for replication. *UL6* encodes the capsid portal protein, *UL19* encodes the major capsid protein, *UL27* encodes the glycoprotein B, *UL30* encodes the viral polymerase, *UL49* encodes the major tegument protein, *ICP4* encodes immediate early genes. B) MDV replication cycle. 1. Glycoproteins such as gB (UL27) facilitate membrane fusion. The virus enters the host cell. 2. Transport of the viral nucleocapsid to the nuclear pore. 3. Viral genome transcription and beginning of replication facilitated by the viral DNA polymerase UL30 in the nucleus. Immediate gene expression of major viral proteins such as ICP4 inhibits the host innate cellular defense. 4. Capsid assembly and subsequent packaging of newly synthesized viral genome. 5. Nuclear egress. Primary envelopment and de-envelopment occurs. 6. UL49 encodes for the viral tegument. The assembly on capsids occurs predominantly in the cytoplasm. 7. Virion maturation and secondary envelopment. 8. Virion transport and release of mature viruses from the cell. Figures modified from Wu et al. [76] and Hagag et al. [77].

The complete replication cycle takes about 18-20 hours [19]. The virus attaches to the host cell receptors via glycoproteins such as gB, gC and gD that mediate the fusion and, thus, releasing the viral genome into the cell. The uncoating of the virion is facilitated by cellular

enzymes. As the nucleocapsid enters the nucleus, the viral DNA polymerase UL30 synthesizes viral genomic DNA as long head to tail concatemers by rolling circle replication [78,79]. Subsequently, immediate gene expression of major viral proteins such as the infected cell protein 4 (ICP4) is initiated, leading to inhibition of the host innate cellular defence and serves as a strong transcriptional regulator for early and late viral genes [80–82]. Upon encapsulation of the viral genome, tegument proteins, including UL49, are necessary for nuclear egress and virion maturation of assembled viral nucleocapsids which acquire their final envelope via budding from trans-Golgi vesicles [55,83,84].

1.1.5. Strategies to control MDV

Vaccination represents until today the main strategy for MDV control. Shortly after the isolation of the virus in the 1960s, vaccines have been developed in England, Unites States and Netherlands [85]. It was the first example of a neoplastic disease that can be controlled by the use of a vaccine, long before this approach was applied to human medicine [86–88]. The first commercially available cell-culture-isolated MDV vaccine was developed at the Houghton Poultry Research Station (HPRS) in England (HPRS-16/att). However, HPRS-16/att vaccine never became widely used as it was soon replaced by the FC126 strain of herpesvirus of turkeys (HVT) [89,90]. With MDV evolving towards greater virulence, HTV was no longer protective against new emerging strains. The development of SB-1 or MD-11/75c strains improved, but none of these vaccines protected well against MD [91]. In the 1970s, Rispens el al. developed a live-attenuated vaccine (CVI988/Rispens), isolated from a very low pathogenic strain of hen number 988 of an MD antibody-positive flock which was free of avian leukosis virus and clinical signs of the disease [92,93].

Until today, CVI988/Rispens is the “gold standard vaccine” which efficiently protects chickens from vvMDV strains and prevents the onset of tumorigenesis [85,88,92]. Even though CVI988/Rispens vaccines are highly effective by preventing the outbreak of symptoms, the exact principles underlying successful vaccination are still not fully understood [94]. It is well accepted that live-attenuated MDV vaccines infect potential target cells so that these are not susceptible to the infection of wild-type (WT) MDVs. Although it stimulates the innate immune system, this response alone does not seem to last [94] by providing a long-term

sterile immunity. Thus, it allows the virus to spread and evolve in the field leading to increased virulence that eventually overcomes the vaccine hurdle [95]. Recent studies connected the increase of virulence in MDV strains to genomic changes that occurred during the evolutionary race between virus and host. Mutations in several open reading frames of genes such as *meq*, *UL6*, *UL15*, *UL36*, *UL37* and *ICP4* directly correlated to the change in virulence [96,97].

Since it is a matter of time how long the current vaccines can still control MD, there is a need for more potent vaccines or alternative interventions. One possible alternative to conventional vaccines was presented by Tischer et al. who developed a DNA-based vaccine containing the infectious BAC20 clone of serotype-1 MDV [98]. This method combines the advantages of vaccination with DNA and live-attenuated virus [94].

Previous studies presented a potential of vTR-based vaccines as “suicide switches” that are based on the mutation of the vTR template sequence from AATCCCAATC to ATATATATAT (AU5), resulting in telomere instability and thus leading to a reduced cancer cell proliferation [35,99]. That the effect of AU5 mutation was dependent on its incorporation into the telomere complex was confirmed as abrogation of the vTR-TERT interaction restored tumor formation [99]. Furthermore, resistant and susceptible chicken lines were vaccinated with vTR-AU5 mutants and challenged with a vvMDV strain, resulting in an efficient protection against the disease which appeared to be at least as good as the MDV vaccine CVI988/Rispens [99]. However, large scale vaccination trials have not been address to investigate if the vTR-AU5 mutant virus provides enhanced protection compared to the current vaccines [35,99].

Moreover, new genome editing technologies can contribute to the establishment of disease resistance in chickens. The CRISPR/Cas9 system, an adaptive immune mechanism originally found in bacteria and archaea that targets foreign nucleic acids [100,101] has been widely used as a genome editing tool to alter the genome of many species including bacteria, plant and several animals [102–106]. By the use of CRISPR/Cas9, Challagulla et al. developed an antiviral strategy to control MDV infection *in vivo* by sequence-specific virus interference. They used the Tol2 transposon system consisting of a miniTol2 plasmid that contained three guide RNAs (gRNAs) specific to immediate early ICP4 of MDV (gICP4) and a *Discosoma sp.* red fluorescent protein (DsRed) and one plasmid containing the transposase [107]. Each gRNA was expressed under the human U6 promoter. To generate transgenic chickens, direct *in vivo*

transfection of primordial germ cells as described by Tyack et al. [108] was applied. By breeding the Tol2-gICP4-DsRed line with chickens that constitutively express high-fidelity Cas9 (Cas9-HF1), green fluorescent protein (GFP) and two gRNAs targeting an endogenous gene as previously described by Challagulla et al. [109], the authors obtained transgenic chickens that constitutively express both gICP4-DsRed and Cas9-HF1-GFP transgenes. Upon challenging transgenic chickens via intraabdominal infection of MDV-1 Woodland strain passage-19 (p19), MDV replication was significantly reduced in transgenic chickens that expressed both, Cas9-HF1 and ICP4-gRNAs, compared to the control group consisting of Cas9-only and WT [107].

A similar approach was recently presented by Hagag et al. who identified (besides a gRNA against *ICP4*) other promising gRNAs that are conserved among different MDVs, leading in combination to the complete abrogation of viral replication *in vitro* [77]. Two independent gRNAs for each target gene were designed: 1+2 (5´and 3´) targeting the capsid portal protein (*UL6*), 4+5 (5´and 3´) targeting the glycoprotein B (*UL27*), 6+7 (5´and 3´) targeting the viral DNA polymerase (*UL30*), 8+9 (5´and 3´) targeting the tegument protein UL49 and 10+11 (5´and 3´) targeting the infected cell protein 4 (*ICP4*) (Figure 6a,b). One gRNA (gRNA 3) was designed targeting the 5´ of the major capsid protein (*UL19*). After infecting cells expressing Cas9 and gRNA with a vvRB-1B strain that expressed a GFP reporter gene, Hagag et al. performed plaque size assays and revealed that individual gRNAs (except for gRNA 2) significantly impaired virus replication and spread in cell culture (Figure 6b). Especially gRNAs 5, 6, 8 and 11 targeting *UL27*, *UL30*, *UL49* and *ICP4* significantly decreased plaque sizes by more than 50 % (Figure 6b). Moreover, the authors showed that the combination of two (5+6 and 8+11) or all four gRNAs (4x) completely stopped MDV replication (Figure 6c) and also prevented the emergence of escape mutants (Figure 7a) which were only observed for cultures containing single gRNAs 5 and 11 (Figure 7b,c) but not for gRNAs 6 and 8 [77].

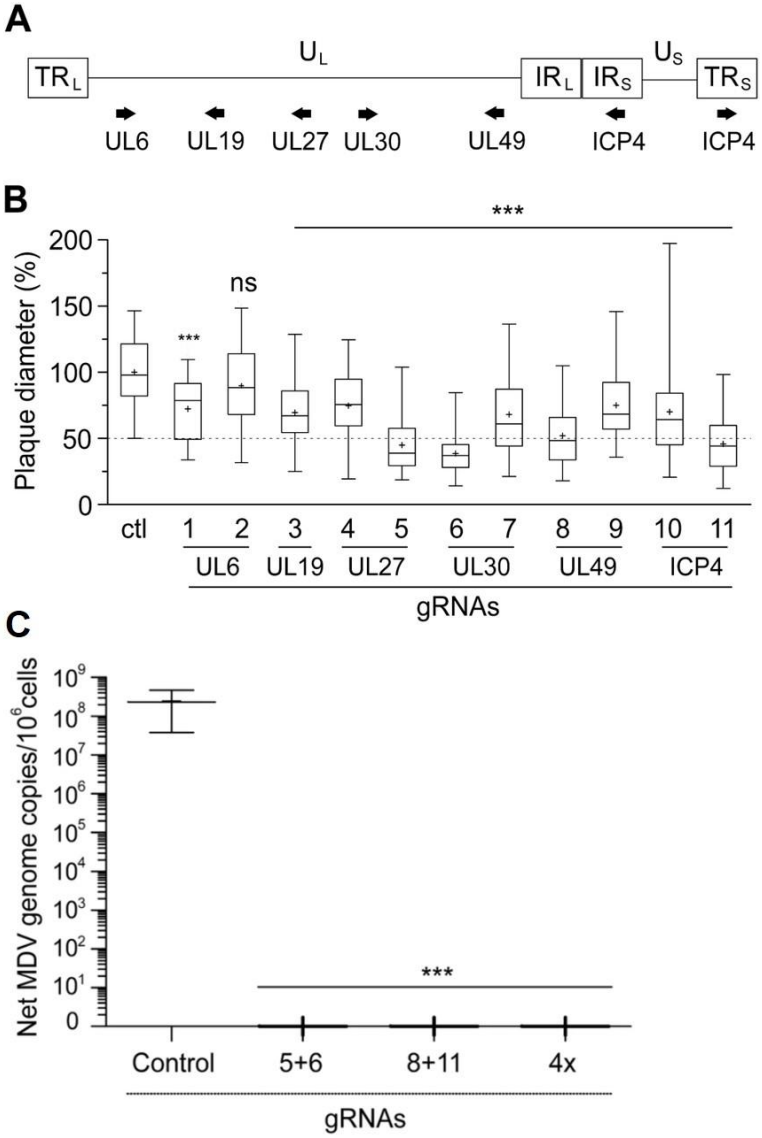

Figure 6: Targeting essential MDV genes by the use of the CRISPR/Cas9 system. Single gRNAs were chosen that partially impair genes important to virus replication (UL6, UL19, UL27, UL30, UL49, ICP4). A) Overview of the MDV genome showing the genes that were targeted. B) Plaque size assays of 11 different gRNAs targeting 6 different MDV essential genes; gRNAs 1 and 2 target the capsid portal protein (UL6, 5' and 3'); gRNA 3 targets the major capsid protein (UL19, 5'); gRNAs 4 and 5 target the glycoprotein B (UL27, 5' and 3'); gRNA 6 and 7 target the polymerase protein UL30 (5' and 3'); gRNAs 8 and 9 target the tegument protein (UL49, 5' and 3'); and gRNAs 10 and 11 target the infected cell protein (ICP4, 5' and 3'). Data were analyzed by ANOVA one-way analysis with Bonferroni correction. The error bars represent the standard deviations (***$p \leq 0.001$). C) Relative MDV genome copies detected by quantitative PCR at 5 days post-infection with 10,000 pfu. MDV genome copies were significantly (***$p \leq 0.001$, $n \geq 3$) reduced in multiplexed gRNAs (5+6, 8+11, 4x). Data set was analyzed by ANOVA one-way analysis with Bonferroni correction. The error bars represent the standard deviations. Figure adapted from Hagag et al. [77].

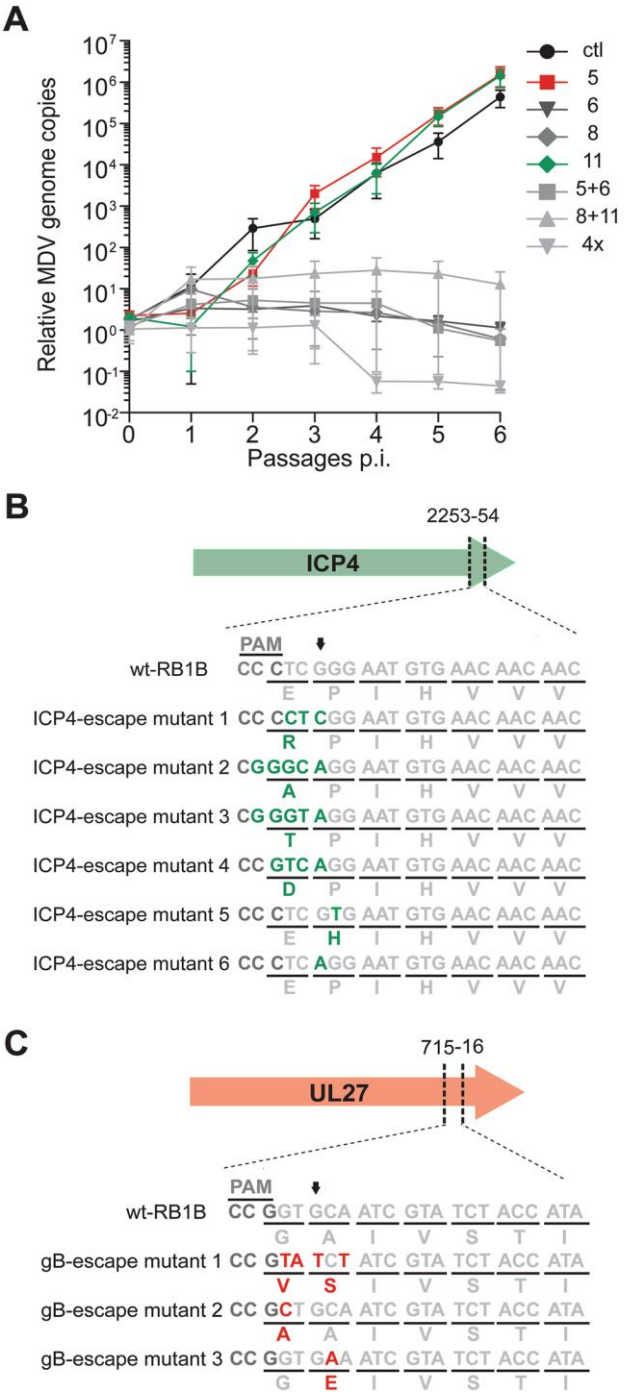

Figure 7: Evaluation of MDV escape mutants that evade inefficient single gRNAs. MDV growth kinetics in different CRISPR/Cas9-expressing cells. Relative MDV copies were determined by quantitative PCR. Cells were passaged up to six times (33 days). The data shows the average of three independent experiments (n = 3). The error bars represent the standard deviations ($p \leq 0.001$, ctl vs. 6, 8, 5 + 6, 8 + 11 and 4×; Kruskal–Wallis test). B) Sequence analysis of six MDV variants of 3´ ICP4 (single gRNA 11). The sequences on the top correspond to wild-type (wt) of RB-1B strain, the sequences at the bottom display the different CRISPR/Cas9 escape mutants detected. C) Sequence analysis of three MDV variants of 3´ UL27 (single gRNA 5). The sequences on the top correspond to wild-type (wt) of RB-1B strain, the sequences at the bottom display the different CRISPR/Cas9 escape mutants detected. Figure adapted from Hagag et al. [77].

1.2. Genome editing

Since the discovery of the molecular structure of DNA by Watson and Crick in 1953 [110], advances in genome editing technologies and the sequencing of genomes have allowed scientists to manipulate and alter the genetic material of many organisms [111–113]. Initially, genetically modified organisms have been widely used for the purpose of basic research to address amongst others the study of gene functions as well as genetic mechanisms and disorders. But genome editing has quickly been applied also within the agricultural and economic sector as the inefficiency of the natural selection process favors a targeted approach in the form of genome engineering [7].

The process of genome editing relies on the mechanism of DNA double-strand break (DSB) repair, a mechanism to maintain genomic integrity and viability in all organisms [114]. In eukaryotic cells, DSB repair is facilitated by two major mechanisms: Homology directed recombination (HDR) or non-homologous end joining (NHEJ) [115]. The mechanism of HDR relies on the presence of homologous sequences and results in an accurate repair of DSB [116]. In contrast, NHEJ re-ligates DSB without the presence of a repair template, generating insertions or deletions (INDELs). Meganucleases have the ability to induce sequence-specific DSB within the genome thus triggering one of the DNA repair mechanisms. While NHEJ is often used to generate a loss-of-function mutation in a particular gene, HDR enables the homologous recombination between the target site and donor template which can introduce precise modifications (Figure 8) [117].

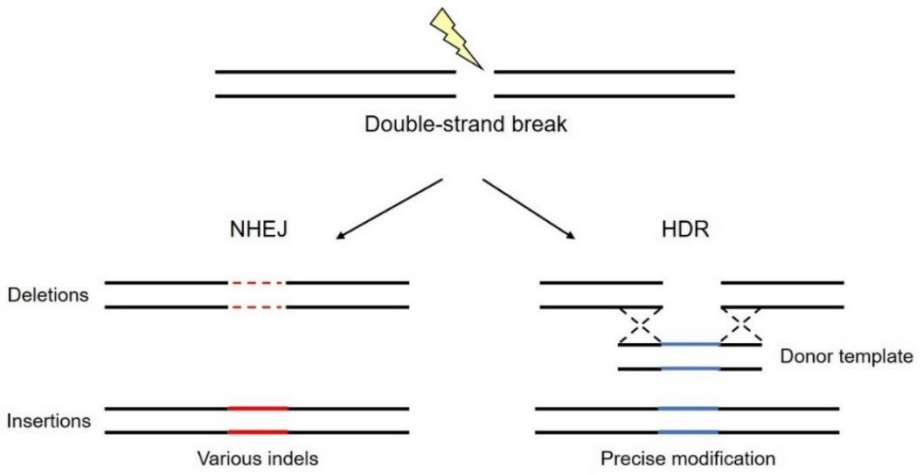

Figure 8: Mechanisms of double-strand break repair in eukaryotic cells. Upon nuclease-induce double strand break, two major repair mechanisms occur. Non-homologous end joining (NHEJ) introduces various INDELs, whereas homology directed repair (HDR) uses a donor template to repair the double-strand break. Figure adapted from Sander et al. [118].

1.2.1. Zinc finger and transcription activator-like effector nucleases

Prominent site-specific artificial nucleases are Zinc Finger Nuclease (ZFN) and Transcription Activator-Like Effector Nuclease (TALEN). TALENs and ZFNs are protein-based systems where a DNA-binding domain is coupled to the non-specific cleavage domain from type IIS restriction endonuclease FokI to initiate DNA breaks [119,120]. The DNA-binding domain of ZFNs typically binds DNA triplets (Figure 9B). As the dimerization of two FokI domains is required, a pair of ZFNs is needed for a site-specific cleavage [121]. The cleavage domains are fused to the C-terminus of each ZFN domain, thus binding of the individual ZFNs occurs at opposite strands with linker sequences between their C-termini [122].

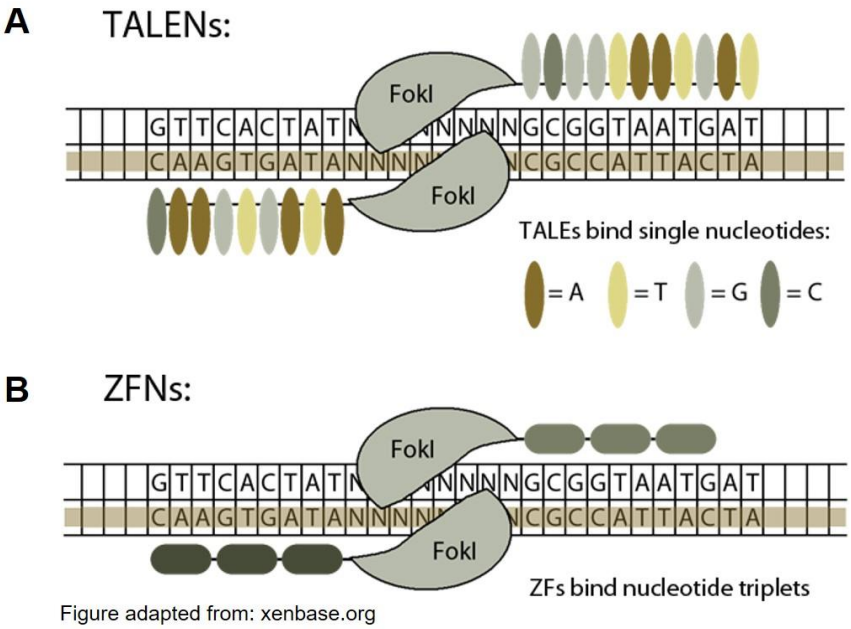

Figure 9: Transcription activator-like effector (TALEN) and zinc finger (ZFN) nucleases. Dimerization of the two cleavage domains of FokI restriction enzyme at desired DNA target site. Letters represent the four different DNA base pairs (A = adenine, T = thymine, G = guanine, C = cytosine). Whereas TALENs bind individual nucleotides (A.), ZFNs bind nucleotide triplets (B.). Figure adapted from xenbase.org [123].

The mechanism of TALENs is very similar but in contrast to ZFNs, the DNA-binding domain of TALEN consists of monomers, each binding to individual nucleotides (Figure 9A) which makes the engineering easier compared to ZFN. However, the generation of highly specific TALENs/ZFNs requires the individual design of new nucleases for each approach which is time consuming, cost intensive and limits the feasibility for large-scale gene editing [119].

1.2.2. The CRISPR/Cas system

The CRISPR/Cas9 system was originally identified as the "adaptive immune system of procaryotes". The immunity relies on CRISPRs (Clustered Regulatory Interspaced Short Palindromic Repeats) which are integrated sequences derived from invaded foreign nucleic acids that represent a unique fingerprint of infections. The immune response requires a second component, CRISPR-associated (Cas) genes, that encode proteins with site-specific nuclease activity to cut nucleic acids [124].

The CRISPR/Cas system has been further developed towards a precise and standardized genome editing technology with significant contributions to basic research, molecular biotechnology, genetic engineering and future therapeutics [125]. In contrast to ZFN and TALEN, CRISPR relies on a RNA-guided endonuclease [126] which is more feasible and preferred for most gene editing applications as it is more efficient and multiplexing by targeting multiple genes at the same time is possible [127].

While CRISPR/Cas is used in laboratories worldwide, this technology has also fascinated the general public to such an extent that interested people conduct research even outside of established laboratories [128]. In 2020, Emmanuelle Charpentier and Jennifer Doudna received the Nobel Prize in Chemistry for the development of the CRISPR/Cas tool, a technology that "had a revolutionary impact on the life sciences, is contributing to new cancer therapies and may make the dream of curing […] diseases come true" [129,130].

1.2.2.1. CRISPR/Cas – An adaptive immune system of procaryotes

Viruses are a common threat to cellular life, thus a variety of mechanisms to resist viral infections have evolved. It was long believed that adaptive immunity is limited to vertebrates [131,132]. However, the recent discovery of CRISPR/Cas showed that procaryotes do have an adaptive system to protect themselves against viruses and other mobile genetic elements by targeting DNA or RNA [133].

Immunity is achieved by integrating short sequences of viruses into the CRISPR locus (see step I. in Figure 10), a region present in the genome of bacteria and archaea [13,129,134]. This allows the cell to "remember, recognize and clear" viral infections by sequence-specific targeting [131]. The bacterial genome exhibits components necessary for this immunity

mechanism such as trans-activating CRISPR-RNA (tracrRNA), the Cas operon encoding CRISPR-associated (Cas) genes and the CRISPR repeat spacer array (CRISPRs). CRISPRs are arrays consisting of multiple, short and direct repeats that are separated by intervening spacers of unique nucleotides of a constant length [13]. These protospacers derive from nucleic acids of viruses that have infected the cell [135–137] and are used as recognition patterns that match to these viral genomes, thus destroy them and enable a sequence-specific resistance to a recurrent infection [100,133]. CRISPRs do not encode proteins, but appear to be transcribed into long pre-RNA molecules which are subsequently cleaved within the repeat sequence and further processed into mature small CRISPR-RNAs (crRNAs) (see step II. in Figure 10) [138].

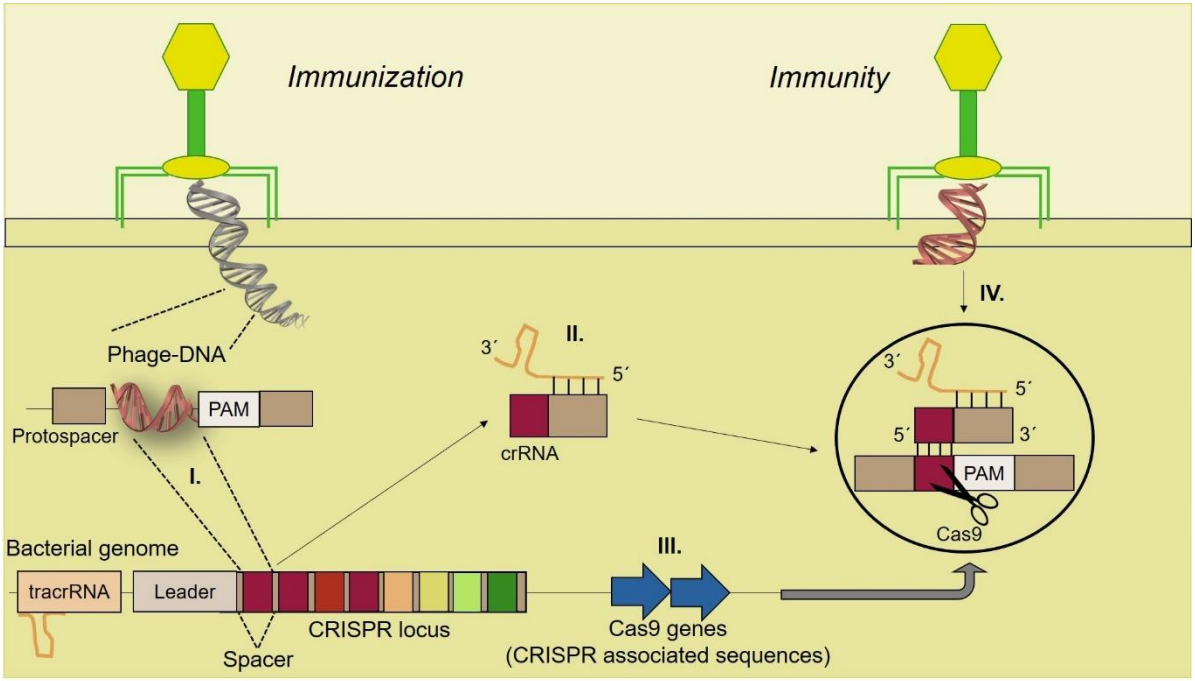

Figure 10: The CRISPR/Cas adaptive immune system of procaryotes. The process can be divided immunization and immunity and consist of four parts (I-IV). I. Adaption: Phage-DNA is inserted into the bacterial cell. Short fragments of the phage-DNA are integrated into the CRISPR locus of the bacterial genome. The CRISPR locus contains copies of a short direct repeat sequence, spacer (in brown), that separate the invader-derived sequences (multiple colors). Protospacer adjacent motifs (PAM) are found immediately adjacent to viral sequences selected for CRISPR integration (protospacers). II. crRNA biosynthesis: The CRISPR locus transcripts are processed first to long pre-crRNAs which are further processed to smaller mature crRNA. III. Expression: Expression of Cas genes, typically located adjacent to CRISPR loci. IV. Interference: The crRNA recognizes the target sequence, binds to it and initiates a site-specific cleavage facilitated by the Cas9 (marked with scissors). Figure modified from Ishino et al. [139] and trillium.de [140].

The incorporation of small fragments of foreign nucleic acids into the CRISPR locus is called spacer acquisition which heritably alters the genome of the host [141]. Interestingly, the addition of spacers occurs usually only on one side of the CRISPR locus so that infections can be chronologically retraced [131]. CRISPR activity requires the presence of Cas proteins that are found adjacent to the CRISPR locus (see step III. in Figure 10) [142]. Cas genes encode proteins with helicase and nuclease motifs [143] that are essential for the immune response. Several Cas proteins have been discovered [142] and their sequences are highly diverged probably due to the fast evolutionary processes [143]. Cas proteins can be classified into type I and type II proteins. Cas proteins that assemble into a large CRISPR-associated complex for antiviral defense belong to the class I system. Prominent examples of the type I classification are Cas1 and Cas3 [144]. The class II system is more simple and contains a multidomain that combines all the functions and activities necessary for interference [129]. The signature gene for the type II class is Cas9 which is found in *Streptococcus*-like species that target DNA [143] and Cas13 that has been shown to target RNA [145]. To discriminate between “self” and “non-self” sequences, short motifs next to the target sequences called the protospacer adjacent motif (PAM) sequences are necessary [146]. This prevents the systems from attacking its own CRISPR locus [131]. Upon a recurrent infection, the CRISPR/Cas complex is formed consisting of crRNA, tracrRNA and the nuclease. The crRNA recognizes the target sequence, binds to it and initiates a site-specific cleavage facilitated by Cas9, destroying the invading viral nucleic acids, thus establishing an immunization (see step IV. in Figure 10). Viruses that escape the CRISPR/Cas system carry point mutations in the protospacer, more precisely in the seed region, a region of only seven nucleotides [147]. Mutations outside of this region do not lead to a reduced immunity which limits the escape possibilities and allows single crRNA to efficiently target numerous related viruses [147].

Although the predominate role of CRISPR/Cas systems is the protection against foreign genetic material, they have been suggested to be involved in other cellular processes such as genome evolution [148], regulation of genes [149] and virulence [150], and in the elimination of defective proteins [151]. However, the processes behind these alternative functions are not well understood [131].

1.2.2.2. CRISPR/Cas9 – A tool for genome editing

The CRISPR/Cas type II system has been further developed for a various number of genome editing applications by making use of the DNA repair mechanism in eukaryotic cells. In contrast to the procaryotic defense mechanism, a dual crRNA:tracrRNA is fused into a single guide RNA (sgRNA) that guides Cas proteins to the DNA target site via base-pairing [124] (Figure 11). This was pathbreaking as these designed sgRNA molecules match to the desired target gene and are modifiable so that any DNA sequence of interest can be targeted as long as it is adjacent to the PAM sequence [146].

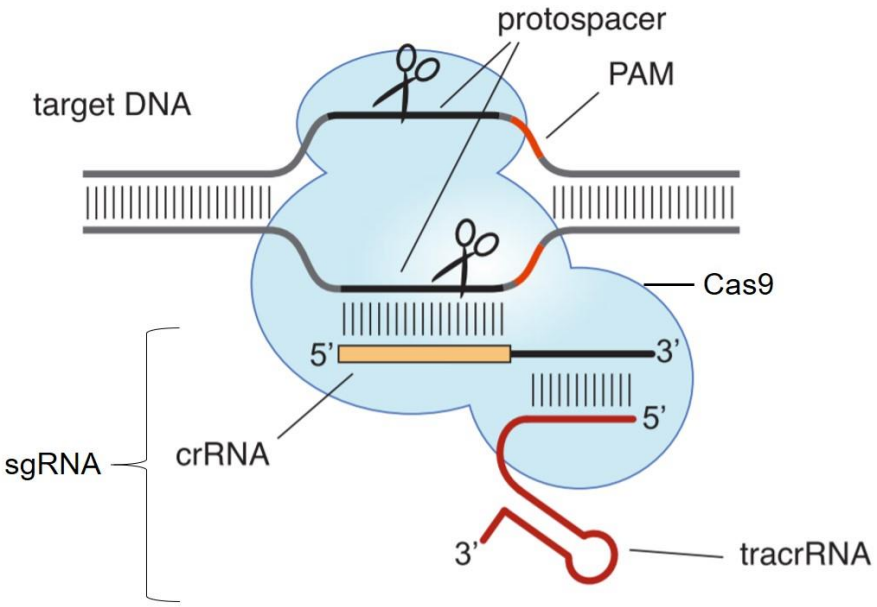

Figure 11: The CRISPR/Cas9 system, a tool for genome editing. Cas9 nuclease (in blue) from *Streptococcus pyogenes* is targeted to the genomic target sequence by a 20-nucleotide crRNA (yellow) and a scaffold tracrRNA (red). The crRNA guide sequence pairs with DNA target directly upstream of the 5´ NGG (with "N" representing a random nucleotide and "GG" two guanine nucleotides) PAM sequence (bright red). Cas9 cleaves each DNA strand and induces a double-strand break 3 bp upstream of the PAM (marked with scissors). Figure modified from Jinek et al. [124].

For most applications, the endonuclease Cas9 (CRISPR-associated protein 9) from *Streptococcus pyogenes* is used to facilitate the subsequent and sequence-specific cleavage [129]. Unlike Cas3, which degrades the target [131], Cas9 causes interference by producing blunt-end double-strand breaks, allowing the site-specific genome modifications by either

NHEJ or HDR [152]. NHEJ is the major repair pathway when using the CRISPR/Cas9 system [153] as it is error-prone and highly efficient for generating INDELs.

The Cas9 protein has a bilobed architecture consisting of target recognition and nuclease lobes [154]. The Cas9 activity relies on the 5´-NGG-3´ recognition pattern of the PAM sequence [155] which is located one base pair downstream of the crRNA binding sequence [124,135,146]. Moreover, Cas9 uses different nuclease domains (RuvC and HNH) to cut each DNA strand which can be independently inactivated (by mutation) to generate active site Cas9 mutants that cleave only a single strand [156].

1.2.3. Generation of genetically modified chickens

In contrast to mammals, the generation of genetically modified chickens has been hampered for decades, mainly because of the fact that avians lay eggs and have therefore an adapted unique reproductive system consisting of ovary and oviduct. Whereas the ovary comprises of a large number of preovulatory follicles and five prehierachical follicles (F1-F5), the oviduct is divided into the infundibulum, the magnum, the isthmus uterus and vagina (Figure 12) [157].

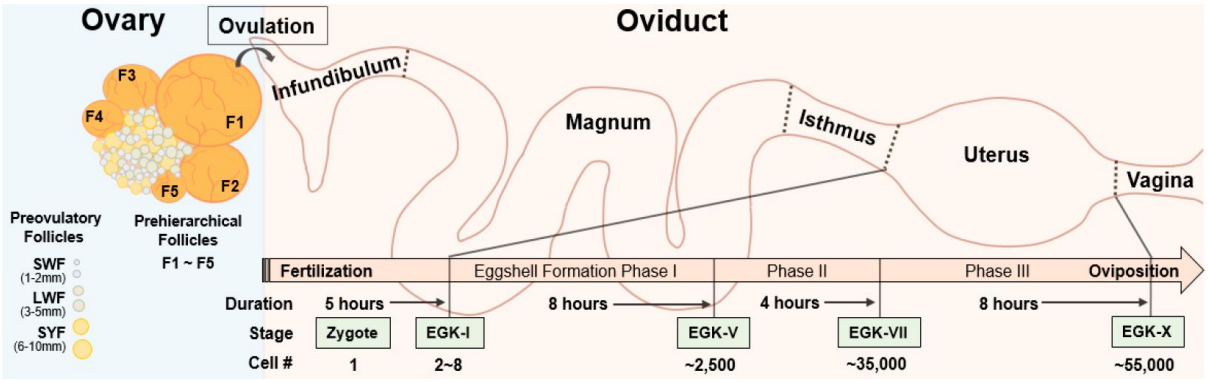

Figure 12: Overview of the avian reproductive system. The reproduction system consists of an ovary and an oviduct which can be further divided into infundibulum, magnum, isthmus, uterus and vagina. A large number of preovulatory follicles and five prehierachical follicles (F1-F5) are present in the ovary. After ovulation, the biggest F1 follicle enters the infundibulum where it gets fertilized. Whereas the accumulation of egg white takes place mainly in the magnum, the formation of outer and inner eggshell layers occurs in the isthmus. After passing the magnum and isthmus, the one-cell zygote starts to cleave in the uterus, transforming into an Eyal-Giladi and Kochav stage (EGK)-X-blastoderm by the time the egg is laid. Figure adapted from Bakst et al. [157] and Lee et al. [158].

The avian reproductive system allows for the embryonic development outside of the body, representing a practical feature to access and manipulate the living embryo. However, well-established methods used for the generation of transgenic mammals such as oocyte microinjection [159] or embryonic stem (ES) cell culture systems [160] are not suitable for avian species as the embryonic development begins in the oviduct of the hen and by the time the egg is laid, the embryo already consist of 40.000 – 60.000 cells [161,162]. In addition, chickens ES cells can only contribute to somatic tissues but not to the germline, making the generation of fully transgenic chickens by using ES cells impossible [163].

In 1987, the first transgenic chicken was generated by Salter et al. through direct injection of a recombinant avian leukosis virus (ALV), a member of the *retroviridae* family, into the yolk of a fertilized egg prior to incubation [164]. Retroviral vectors are widely used because they deliver foreign DNA into their hosts chromosomes as a natural process of their life cycle [38]. Since then, various retroviral vectors have been generated and used for the purpose of gene editing in chickens [165–169]. Even though the generation of transgenic chickens by the use of retroviral vectors is possible, the frequency of germline modification is low and the transmission into the offspring to generate fully transgenic animals appears to be even lower, probably because of host silencing of the viral sequences [170].

By the use of a lentivirus that as well belongs to the *retroviridae* family and has the ability to infect non-dividing cells [171], McGrew et al. demonstrated germline transmission rates between 4-45 % which was an 100-fold improvement compared to methods used before [170,172]. They showed that the transgene was stably inherited with no detectable epigenetic silencing between generations. The expression of different reporter genes including lacZ and enhanced green fluorescent protein (EGFP) simplified the analysis of transgenic animals [170]. Apart from the limited capacity size [172], a major concern of using retroviral vectors is the random genomic integration as well as the risk of recombination with WT viruses [173].

Only one report described the successful use of microinjection in birds to generate transgenic chickens [174] because it requires a fertilized oocyte at the one-cell stage, followed by modification of this oocyte and transfer back into a pseudopregnant animal [175]. In 1994, Love et al. generated transgenic chickens expressing neomycin resistance and a reporter gene lacZ by plasmid-DNA microinjection into the chicken zygote, followed by *ex vivo* embryo cell culture. Therefore, plasmid-DNA was injected into the pronucleus of the germinal disc [174].

The authors showed that approximately half of the embryos contained plasmid-DNA, 6 % at a level equivalent to one copy per cell. After they bred one chimeric rooster with WT hens, they obtained transmission rates of 3.4 %. However, this method is inefficient, labor-intensive and technically not practical and has never became widely used for the generation of transgenic birds.

The most recently established method to generate transgenic chickens is facilitated by the use of primordial germ cells (PGC) [176] which have typical characteristics of germline competent cells such as stem potency (= the ability to self-renew) and germline competency (= the ability to contribute to the germ cell lineage) [177]. PGCs are precursor cells of sperm and egg and undergo a unique migration process during embryogenesis in birds [178]. While in most animals, the development of germ cells occurs very early during the embryogenesis [179], avian germline cells can be found earliest 18 hours after onset of incubation [163]. At Hamburger Hamilton (H&H) stage 4, PGCs are located in the germinal crescent, which is the anterior marginal region between the area opaca and area pellucida [177,180]. PGCs circulate in the extraembryonic blood vessels until they settle in the developing gonad at H&H stage 17 [181], maturing into functional sperm and oocytes [180,182]. As the sex differentiation occurs approximately between embryonic day (ED) 5.5-6.5 (stage 28–30) [183], PGCs can be isolated from different regions of the embryo such as from the germinal crescent at H&H stage 4, extraembryonic blood vessels at ED 2.2 or gonads at ED 5-6 [177].

Significant progress in generating genetically modified chickens has been made in 2006 by van de Lavoir et al. who isolated PGCs from the blood of H&H stage 14-17 chicken embryos and cultured them *in vitro* for more than 150 days without influencing their germline competency [163,184]. By determining specific electroporation conditions, van de Lavoir et al. transfected PGCs with a linearized EGFP- and puromycin-expressing plasmid which improved the selection process for successfully transfected cells [163]. To avoid potential silencing of the transgenes, two copies of HS4 insulator sequences from the chicken β-globulin locus were inserted 5´and 3´of the transgenes [185]. The germline transmission of chimeras produced with PGCs cultured for up to 110 days ranged from <1 % to 86 % and resembled the transmission rates when freshly isolated PGCs are used [163].

Important insights regarding long-term culture conditions were gained by Whyte et al. who defined medium conditions without feeder cells and showed that the basic fibroblast growth

factor (bFGF) via MEK/ERK (also known as the Ras-Raf-MEK-ERK signaling pathway) plays an essential role in survival and proliferation of chicken PGCs [186,187].

The PGC culturing system offers the possibility of targeted mutations into the chicken genome. Figure 13 shows schematically the generation of transgenic chickens using genetically modified PGCs. The cells can be isolated from the embryonic blood during the migration into the gonads, expanded and modified *in vitro*. This provides the possibility to study transgene insertion in these cells *in vitro* before re-introducing them back into the embryonic vasculature of surrogate host embryos to form functional gametes and offspring [163,182].

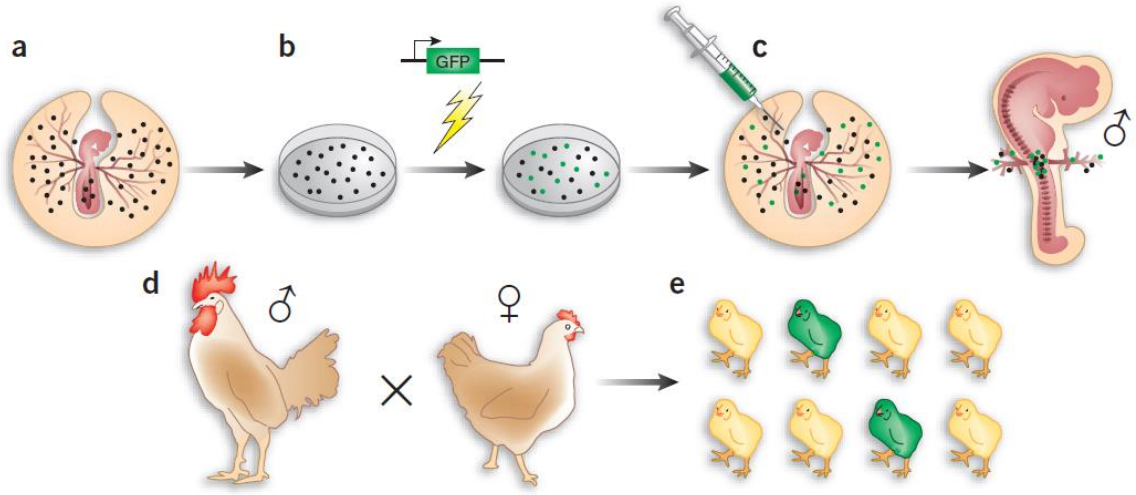

Figure 13: Production of transgenic chickens using genetically modified PGCs. a) PGCs (black) are isolated from the blood of chick embryos at H&H stage 10-12 (approximately two days of incubation). b) The embryonic blood is cultured under conditions that promote proliferation of PGCs. Electroporation of cultured cells with a transgene construct, here encoding green fluorescent protein (GFP). c) Transgenic PGCs (green) are injected into the circulatory system of embryos at H&H stage 13-15 (approximately 65 hours after incubation), the time point when endogenous PGCs migrate to the developing gonads. The recipient embryos are incubated until they hatch. d) After reaching sexual maturity, males are crossed with wild-type hens. e) The resulting offspring is screened to identify those derived from the GFP-expressing transgenic PGCs. Figure adapted from Sang [188].

Efforts have been made to stably transfect PGCs and efficiently increase the integration of transgenes. In 2008, Leighton et al. achieved stable transfection of PGCs at frequencies of 1-2 clones in 10^6 cells by electroporation of plasmid-DNA. The expression from integrated reporter constructs in this study was depended on the presence of flanking HS4 insulator

sequences [189]. In chickens, it has been shown that the frequencies of stable integration into PGCs were increased by ~20-fold using phiC31 integrase [189]. The site-specific recombinase phiC31 is a serin integrase originally found in the genome of a bacteriophage [190,191]. PhiC31 facilitates random integration by inserting transgenes into regions of the chicken genome containing repetitive DNA sequences that are presumably recognized as suitable non-coding sites [189]. The integrase catalyzes site-specific recombination between two attachment or att sites, called attP and attB, that originate from the phage or bacterial host, respectively. So called pseudo attP sites are present in regions of the target genome and resemble the native phage attP site [192]. The unidirectional integration of the attB/transgene-containing donor vector into the target genome requires the co-transfection with a phiC31 integrase expression vector [191]. Leighton et al. used phiC31 integrase to stably transfect EGFP-expressing PGCs with β-actin Cre-recombinase to generate transgenic chickens [190].

In addition, transposon-mediated transgenesis has been shown to be suitable for transgene insertion into the genome of PGCs [193,194]. Transposons are mobile genetic elements that are able to relocate within the genome. In eukaryotic genomes, transposable elements act in two different mechanisms according to whether their transposition intermediate is RNA (retro transposons class I, “copy and paste” principle) or DNA (DNA transposons class II, “cut and paste” principle) [195,196]. For the generation of transgenic animals, class II transposons have been adapted [197]. Two common systems are PiggyBac, isolated from cabbage looper moth *Trichoplusia ni* [198] and Tol2, identified in the genome of the medaka fish [199]. In 2012, MacDonald et al. published a study on the efficient use of PiggyBac and Tol2 transposons for the genetic modification of chicken PGCs by transfecting the cells with a vector containing an EGFP and puromycin resistance gene, resulting in 10.5 % EGFP-positive PGCs using PiggyBac and 45.2 % modified cells using Tol2 transposon [200]. In the same year, Park and Han injected recipient embryos with PGCs that were modified by a PiggyBac plasmid containing a GFP gene, resulting in germline transmission rates of up to 98.9 % [194]. Another study presented by Tyack et al. showed the successful generation of EGFP-expressing chickens by direct *in vivo* modification of PGCs using a miniTol2 plasmid containing EGFP and a plasmid containing the transposase [108]. By the injection of these plasmids together with lipofectamine 2000 transfection reagent into the vascular system of H&H stage 14 embryos,

the authors generated male germline chimeras, followed by breeding with WT hens to generate fully transgenic chickens. Two of the roosters showed a germline transmission of 1.5 % [108]. The direct modification of PGCs *in vivo* bypasses the necessity for *in vitro* culturing of these cells and displays an alternative for avian species where *in vitro* culture systems have not been established yet, e.g. Japanese quails [109].

The first study reporting on the successful use of homologous recombination with a targeted gene knock-out was demonstrated by Schusser et al. [60]. To delete the J gene segment of the immunoglobulin heavy chain (JH-KO), isogenic homology regions were assembled into a DNA targeting vector with a puromycin resistance cassette and EGFP flanked by LoxP-sites. To facilitate future integrase-mediated insertion of foreign genes into the chicken heavy chain locus, an attP site joined to a promotor less neomycin resistance gene was included. The authors showed that in 28 % of the antibiotic-selected clones, the marker cassette had been integrated at the desired locus. The resulting germline transmission rates were lower compared to previous reports [60]. Three years later, another study conducted by Schusser et al. demonstrated homologous recombination-induced knock-out of the immunoglobulin light chain (IgL) resulting in germline transmission rates of up to 48 % [201].

The CRISPR/Cas9 system has become an indispensable tool for genome editing in the chicken model. The first study of using CRISPR/Cas9-mediated genome engineering in chickens was published in 2015 where embryos were electroporated with plasmid-DNA coding for Cas9 and sgRNA against the transcription factor Pax7 [202]. Since then, numerous articles were published that used CRISPR/Cas9-mediated gene targeting in birds [203–205]. However, the *in vivo* application of this system in somatic tissue remains challenging due to the simultaneous delivery of CRISPR/Cas9 components which often exceeds, owing to the large size of Cas9, the packaging capacity of many delivery systems [206]. High-capacity viral vectors do exist but are often associated with higher immunogenicity, limited cell type specificity and tissue tropism [113,207]. To partially overcome these issues, alternative Cas9 variants such as split Cas [208] or small Cas9 orthologues such as *Staphylococcus aureus* Cas9 (SaCas9) (3.3 kb) [209] have been developed. A versatile system to enable efficient Cas9-mediated *in vivo* genome editing was demonstrated by Cas9 knock-in animals that constitutively express the Cas9 endonuclease [109,113,210]. Platt et al. demonstrated *in vivo* and *ex vivo* genome editing in Cas9 knock-in mice by using different delivery systems including

adeno-associated viruses (AAV), lentiviruses and particle-mediated delivery systems [113]. They generated a Cre-dependent Cas9 mouse by inserting a Cas9 expression cassette into the ROSA26 locus, a locus known to be a “safe harbor” for transgene expression without interrupting the function of essential endogenous genes [211,212]. Cas9 expression was driven by the ubiquitous CMV early enhancer-chicken-β-actin (CAG) promoter which was disrupted by a Lox-stop-Lox cassette to induce Cas9 expression by the use of Cre recombinase. The authors showed that constitutive Cas9-expressing mice are healthy with no morphological abnormalities. Moreover, the animals are fertile and can be bred to homozygosity [113].

1.3. Goals of the project

The aim of this project was to transfer the CRISPR/Cas9 system into chickens for the purpose of CRISPR/Cas9-mediated *in vivo* genome editing.

In the first step, chickens with ubiquitous expression of the Cas9 endonuclease from *Streptococcus pyogenes* (Cas9) were generated, the expression of Cas9 in these transgenic chickens was characterized and its functionality was tested *in vitro* and *in vivo*.

A further objective was to generate CRISPR/Cas9 chickens that ubiquitously express Cas9 and validated guide RNAs against MDV genes (MDV-gRNAs) to establish an *in vivo* disease resistance.

2. MATERIALS AND METHODS

2.1. Materials

2.1.1. Chemicals

Table 2: Chemicals and reagents

Chemical	**Supplier**
1 kb Plus DNA Ladder	Invitrogen, Carlsbad, USA
Acetate (CH_3COO)	AppliChem GmbH, Darmstadt, Germany
Acetic acid ($C_2H_4O_2$)	AppliChem GmbH, Darmstadt, Germany
Agarose low EEO	AppliChem GmbH, Darmstadt, Germany
Biocoll solution	Biochrom GmbH, Berlin, Germany
Boric acid (H_3BO_3)	AppliChem GmbH, Darmstadt, Germany
Bovine serum albumin (fraction V)	AppliChem GmbH, Darmstadt, Germany
DMSO $[(CH_3)_2SO]_2$	AppliChem GmbH, Darmstadt, Germany
dNTPs	New England Biolabs, Ipswich, USA
Disodium phosphate (Na_2HPO_4)	AppliChem GmbH, Darmstadt, Germany
Droplet generation oil for ddPCR	Bio-Rad Laboratories, Hercules, USA
DTT solution (1 M)	AppliChem GmbH, Darmstadt, Germany
EDTA Solution (0.5 M) pH 8.0	AppliChem GmbH, Darmstadt, Germany
Ethanol (EtOH), denatured	CLN GmbH, Niederhummel, Germany
Ethanol (EtOH), absolute	AppliChem GmbH, Darmstadt, Germany
Glycerol anhydrous ($C_3H_8O_3$)	AppliChem GmbH, Darmstadt, Germany
Glycerin ($C_2H_5NO_2$)	AppliChem GmbH, Darmstadt, Germany
IC Fixation Buffer	BD eBioscience™ Inc, Heidelberg, Germany
Isopropanol	AppliChem GmbH, Darmstadt, Germany
LB agar	AppliChem GmbH, Darmstadt, Germany
Luminol	AppliChem GmbH, Darmstadt, Germany
MagicMark™ XP Western Protein Standard	Invitrogen, Carlsbad, USA
Magnesium chloride ($MgCl_2$)	AppliChem GmbH, Darmstadt, Germany
Methanol (CH_3OH) for molecular biology	AppliChem GmbH, Darmstadt, Germany
Milk powder	AppliChem GmbH, Darmstadt, Germany
Orange G	AppliChem GmbH, Darmstadt, Germany
PageRuler, pre-stained	Thermo Fisher Scientific, Waltham, USA
Paraffin oil	AppliChem GmbH, Darmstadt, Germany
PCR water	AppliChem GmbH, Darmstadt, Germany
P coumaric acid	Sigma Aldrich, Saint-Louis, USA
Polyethylene glycol (PEG)	Sigma Aldrich, Saint-Louis, USA
PeqGreen	Peqlab GmbH, Erlangen, Germany
Permeabilization Buffer	BD eBioscience™ Inc, Heidelberg, Germany
Potassium chloride (KCl)	AppliChem GmbH, Darmstadt, Germany
Potassium phosphate (KH_2PO_4)	AppliChem GmbH, Darmstadt, Germany
RNAlater	Qiagen, Hilden, Germany
SDS grained pure	AppliChem GmbH, Darmstadt, Germany

Sodium acetate ($C_2H_3NaO_2$)	AppliChem GmbH, Darmstadt, Germany
Sodium azide (NaN_3)	AppliChem GmbH, Darmstadt, Germany
Sodium chloride (NaCl)	AppliChem GmbH, Darmstadt, Germany
Sodium desoxylate ($C_{24}H_{39}NaO_4$)	AppliChem GmbH, Darmstadt, Germany
Sucrose ($C_{12}H_{22}O_{11}$)	AppliChem GmbH, Darmstadt, Germany
Tetramethylethylendiamin (TEMED) ($C_6H_{16}N_2$)	AppliChem GmbH, Darmstadt, Germany
Thiogylerol	Promega, Madison, USA
Tris-HCl ($C_4H_{11}NO_3$xHCl)	AppliChem GmbH, Darmstadt, Germany
Triton-X100	AppliChem GmbH, Darmstadt, Germany
Trypanblue solution	Sigma Aldrich, Saint-Louis, USA
Trypsin	Biochrom GmbH, Berlin, Germany
Tween 20	Carl Roth GmbH, Karlsruhe, Germany
X-Gal	AppliChem GmbH, Darmstadt, Germany

2.1.2. Enzymes and enzyme buffers

Table 3: Enzyme and enzyme buffers

Enzyme or enzyme buffer	**Supplier**
5x FIREPol® Master Mix	Solis BioDyne, Tartu, Estland
5x HOT FIREPol® MultiPlex Mix	Solis BioDyne, Tartu, Estland
5x HOT FIREPol® Probe qPCR Mix Plus (no ROX)	Solis BioDyne, Tartu, Estland
Adenosine Triphosphate (ATP), 10 mM	New England Biolabs, Ipswich, USA
BshTI/AgeI	Thermo Fisher Scientific, Waltham, USA
Calf Intestinal Alkaline Phosphatase (CIAP) CIPA Buffer	Promega, Madison, USA
ddPCR Supermix for Probes (no dUTP) 2x	Bio-Rad Laboratories, Hercules, USA
DNAse I	Promega, Madison, USA
DNA Polymerase I, large (Klenow) fragment	New England Biolabs, Ipswich, USA
FastDigest Bbsl (Bpil)	Thermo Fisher Scientific, Waltham, USA
GoScript™ Enzyme Mix	Promega, Madison, USA
GoScript™ Reaction Buffer, Random Primer	Promega, Madison, USA
LongAmp® Taq DNA Polymerase, 5x LongAmp® Reaction Buffer	New England Biolabs, Ipswich, USA
NEBuilder® Hifi DNA Assembly Master	New England Biolabs, Ipswich, USA
Plasmid-Safe™ Exonuclease (DNAse) Plasmid-Safe™ Buffer (10x)	Lucigen Corporation, Middleton, USA
Pronase E (20 mg/ml)	AppliChem GmbH, Darmstadt, Germany
Proteinase K (20 mg/ml)	AppliChem GmbH, Darmstadt, Germany
Q5® High-Fidelity DNA Polymerase, 5x Q5® Reaction Buffer, 5x Q5® High GC Enhancer	New England Biolabs, Ipswich, USA
Restriction Endonucleases, Restriction Buffers 1.1, 2.1, 3.1, CutSmart®	New England Biolabs, Ipswich, USA
T4 DNA Ligase/PNK T4 DNA Ligation Buffer (10x)/PNK Buffer	New England Biolabs, Ipswich, USA

T7 DNA Ligase	New England Biolabs, Ipswich, USA
Tango Buffer (10x)	Thermo Fisher Scientific, Waltham, USA

2.1.3. Kits

Table 4: Kits

Kit	**Supplier**
AMAXA™ Cell Line Nucleofector™ Kit V	Lonza Cologne GmbH, Cologne, Germany
AMAXA™ Human T Cell Nucleofector™ Kit	Lonza Cologne GmbH, Cologne, Germany
eBioscience™ Fixation/Permeabilization	BD eBioscience™ Inc, Heidelberg, Germany
Eluator™ Vacuum Elution Device	Promega, Madison, USA
E.Z.N.A® Gel Extraction Kit	Omega Bio-tek, Inc., Norcross, USA
GoScript™ Reverse Transcription	Promega, Madison, USA
GoTaq® DNA Polymerase	Promega, Madison, USA
GoTaq® qPCR Master Mix	Promega, Madison, USA
HiPerFect Transfection Reagent	Qiagen, Hilden, Germany
NEBuilder® HiFi DNA Assembly Reaction Kit	New England Biolabs, Ipswich, USA
Neon™ Transfection Systems	Thermo Fisher Scientific, Waltham, USA
Overnight Mix2Seq Kit	Eurofins Genomics Germany GmbH, Ebersberg, Germany
pGEM® - T Easy Vector Systems	Promega, Madison, USA
PureYield™ Plasmid Miniprep System	Promega, Madison, USA
PureYield™ Plasmid Midiprep System	Promega, Madison, USA
ReliaPrep™ gDNA Blood and Tissue	Promega, Madison, USA
ReliaPrep™ RNA Cell Miniprep System	Promega, Madison, USA
ReliaPrep™ RNA Tissue Miniprep System	Promega, Madison, USA
SYBR® Green Master Mix	Promega, Madison, USA
Ultra-Sep® Gel Extraction Kit	Omega Bio-tek, Inc., Norcross, USA
Viafect™ Transfection Reagent	Promega, Madison, USA
Wizard® SV Gel and PCR Clean-Up System	Promega, Madison, USA
Xfect™ Transfection Reagent	Takara Bio Group, Shiga, Japan

2.1.4. Animals, cells and bacteria

Table 5: Chicken lines used or generated

Animal line	**Source**	**Breeding/use**
Lohmann´s selected Leghorn Classic (LSL Classic)	LSL Rhein-Main GmbH & Co. KG, Dieburg, Germany	Chicken line used for all breedings and PGC isolation
GFP 165-2	Ligand Pharmaceuticals, San Diego, USA	Chicken line used for PGC isolation
Cas9	Reproductive Biotechnology, TUM, Freising, Germany	Chicken line generated for ubiquitous expression of Cas9

MDV-gRNA	Reproductive Biotechnology, TUM, Freising, Germany	Chicken line generated for ubiquitous expression of MDV-gRNA
Cas9-MDV-gRNA	Reproductive Biotechnology, TUM, Freising, Germany	Chicken line generated for ubiquitous expression of Cas9-MDV-gRNA

Table 6: Cells used in cell culture

Cell type	**Genotypes**	**Source**
Chicken embryonic fibroblasts (CEF)	Wild-type, Cas9	Reproductive Biotechnology, TUM, Freising, Germany
Douglas Forster cells 1 (DF-1)	Wild-type, Cas9	Friedrich-Loeffler-Institute, Riems, Germany
Peripheral blood mononuclear cells (PBMC)	Wild-type, Cas9	Reproductive Biotechnology, TUM, Freising, Germany
Primordial germ cells (PGC)	Wild-type, Cas9, MDV-gRNA	Reproductive Biotechnology, TUM, Freising, Germany

Table 7: Bacteria

Bacteria	**Strain**	**Subtype**	**Supplier**
NEB 5-α competent *E. coli*	K12 strain	DH5α	New England Biolabs, Ipswich, USA
DH5α competent *E. coli*	K12 strain	DH5α	Self-produced

Table 8: Media for bacteria

Antibiotics	**Supplier**
Lysogeny Broth (LB) medium	AppliChem GmbH, Darmstadt, Germany
Super optimal broth with catabolite repression medium (SOC)	New England Biolabs, Ipswich, USA

Table 9: Antibiotics

Antibiotics	**Supplier**
Ampicillin	AppliChem GmbH, Darmstadt, Germany
Hygromycin	AppliChem GmbH, Darmstadt, Germany
Puromycin	Gibco, Waltham, USA

2.1.5. Cell culture media and supplements

Table 10: Media and supplements used in cell culture

Material	**Supplier**
Activin A	PeproTech Germany, Hamburg, Germany

Avian Knock-Out Dulbecco's Modified Eagle's Medium [163,213]	Thermo Fisher Scientific, Waltham, USA
B27 supplement (50x)	Thermo Fisher Scientific, Waltham, USA
β-mercaptoethanol	Thermo Fisher Scientific, Waltham, USA
Calcium chloride	Carl Roth GmbH, Karlsruhe, Germany
Chicken serum	Thermo Fisher Scientific, Waltham, USA
CO2-Independent Medium	Thermo Fisher Scientific, Waltham, USA
Dulbecco's Modified Eagle's Medium (DMEM) high glucose	Biochrom GmbH, Berlin, Germany/ Sigma Aldrich, Saint-Louis, USA
DMSO	AppliChem GmbH, Darmstadt, Germany
Fetal Bovine Serum (FBS) Superior	Biochrom GmbH, Berlin, Germany
Fibroblast-growth-factor (FGF)	R&D systems Minneapolis, USA
Glutamax	Thermo Fisher Scientific, Waltham, USA
Heparin sulfate	Sigma Aldrich, Saint-Louis, USA
Iscove´s Modified Dulbecco´s Medium	Sigma Aldrich, Saint-Louis, USA
MEM non-essential amino acids (100x)	Thermo Fisher Scientific, Waltham, USA
NEAA (100x)	Thermo Fisher Scientific, Waltham, USA
Nucleotides	Sigma Aldrich, Saint-Louis, USA
OptiMEM (1x)	Gibco, Waltham, USA
Ovalbumin	Sigma Aldrich, Saint-Louis, USA
Pen-Strep	Sigma Aldrich, Saint-Louis, USA
Pyruvate (100x)	Thermo Fisher Scientific, Waltham, USA
Roswell Park Memorial Institute (RPMI) 1640	Biochrom GmbH, Berlin, Germany
Sodium pyruvate solution	Thermo Fisher Scientific, Waltham, USA
Trypsin (10x)	Biochrom GmbH, Berlin, Germany

Table 11: Composition PGC medium

Material	**Volume (ml)**
Avian Knock-Out Dulbecco's Modified Eagle's Medium	46.225
B27 supplement (50x)	1
Glutamax (100x)	0.5
NEAA (100x)	0.5
Nucleotides (100 mM)	0.5
Pyruvate (100x)	0.2
β-mercaptoethanol (50 mM)	0.1
Pen/Strep (100x) *optional	0.1
$CaCl_2$ (20 mM)	0.375
Ovalbumin (20 %)	0.5
Heparin sulfate (50 mg/ml)	0.1

Table 12: Composition of Heparin sulfate solution (50 mg/ml)

Material	**Amount**
Heparin sulfate	0.25 g
Avian KO DMEM	5 ml

Table 13: Composition manipulation medium

Material	**Volume (ml)**
CO_2 independent medium	500
FBS Superior	56.8
Glutamax (100x)	5.7
Pen/Strep (100x)	5.7

Table 14: Composition freezing medium

Material	**Volume (%)**
Manipulation medium	90
DMSO	10

Table 15: Composition DF-1 medium

Material	**Volume (ml)**
DMEM high glucose	500
FBS Superior	50
Glutamax (100x)	5

Table 16: Composition CEF medium

Material	**Volume (ml)**
Basal ISCOVE	460
FBS Superior	25
Chicken serum	10
Pen/Strep (100x)	5

Table 17: Composition medium splenic PBMC

Material	**Volume (ml)**
RPMI 1640	440
FBS Superior	50
Glutamax (100x)	5
Pen/Strep (100x) *optional	5

Table 18: Composition for 0.25x Trypsin/EDTA

Material	**Volume (ml)**
PBS/EDTA	37.5
Trypsin (1x)	12.5

2.1.6. Buffers and solutions

Table 19: Composition of TBE buffer (10x)

Component	**Amount**
Tris(hydroxymethyl)aminomethane	108 g
Boric acid	55 g
EDTA (pH 8.0)	40 ml
dH_2O	Add to 1 l

Table 20: Composition of TAE buffer (50x)

Component	**Amount**
Tris(hydroxymethyl)aminomethane	242 g
Acetic acid	57.1 ml
EDTA (0.5 M)	100 ml
dH_2O	Add to 1 l

Table 21: Composition of 1 % agarose gel (calculated for 50 ml)

Component	**Amount**
1x TBE or TAE	50 ml
Agarose	0.5 g
PeqGREEN	2 µl

Table 22: Composition of 6x Orange G Loading dye

Component	**Amount**
DNA glycerol	60 ml
0.5 M EDTA	12 ml
6x Orange G Loading Dye	100 mg
dH_2O	Add to 100 ml

Table 23: Composition of 1 kb DNA ladder

Component	**Volume (µl)**
DNA Ladder	4.5
6X Orange G Loading Dye	25
dH_2O	120.5

Table 24: Composition of APS (10 %)

Component	**Amount**
Ammonium persulfate	1 g
dH_2O	Add to 10 ml

Table 25: Composition of SDS (10 %)

Component	**Amount**
Sodium dodecyl sulfate (SDS)	10 g
dH_2O	Add to 100 ml

Table 26: Composition of PBS and PBS-T (pH 7.2)

Component	**Amount**
Sodium chloride	40 g
Di-sodiumhydrogenphosphate-dihydrate	7.25 g
Potassiumhydrogenphosphate	1.0 g
Potassium chloride	1.0 g
dH_2O (pH 7.2)	Add to 5000 ml
For PBS-T add additionally:	
Tween20	0.05 %

Table 27: Composition RIPA buffer for Western blot

Component	**Final concentration**
Sodium chloride	150 mM
Triton X-100	1.0 %
Sodium deoxycholate	0.5 %
Sodium dodecyl sulfate (SDS)	0.1 %
Tris (pH 8.0)	50 mM

Table 28: Composition of 4x Tris Cl/SDS buffer (pH 6.8)

Component	**Amount**
Tris 0.5 M	6.05 g
Sodium dodecyl sulfate (SDS)	0.4 g
dH_2O	Add to 100 ml

Table 29: Composition of 4x Tris Cl/SDS buffer (pH 8.8)

Component	**Amount**
Tris 1.5 M	91 g
Sodium dodecyl sulfate (SDS)	2 g
dH_2O	Add to 500 ml

Table 30: Composition of 6x Laemmli buffer

Component	**Amount**
4x Tris-Cl/SDS buffer (pH 6.8)	7 ml
Glycerol anhydrous	3 ml
Sodium dodecyl sulfate (SDS)	1 g
Bromphenol blue	1 mg

Table 31: Composition of 5x electrophoresis running buffer (pH 8.3) for Western blot

Component	**Amount**
Tris	15 g
Glycine	72 g
Sodium dodecyl sulfate (SDS)	5 g
Aqua dest.	Add to 1000 ml

Table 32: Composition of Towbin buffer

Component	**Amount**
Tris	3.03 g
Glycine	14.4 g
Methanol	100 ml
Aqua dest.	Add to 1000 ml

Table 33: Composition of homemade enhanced chemiluminescence (ECL) solution A

Component	**Amount**
Tris-HCl 0.1 M (pH 8.6)	200 ml
Luminol	50 mg

Table 34: Composition of homemade enhanced chemiluminescence (ECL) solution B

Component	**Amount**
Para-Hydroxycoumarin acid	11 mg
DMSO	10 ml

Table 35: Composition Fluo-buffer for fluorescence-activated cell sorting (FACS)

Component	**Amount**
Bovine Serum Albumin - Fraction V9	5 g
Sodium azide	50 mg
PBS (pH 7.2)	Add to 500 ml

Table 36: Composition of TEN buffer for genomic DNA isolation (Protocol Quick & Dirty)

Component	**Final concentration**
Tris-Cl (pH 8.0)	10 mM
EDTA	1 mM
NaCl	10 mM

Table 37: Composition of STM buffer (Protocol Quick & Dirty)

Component	**Final concentration**

Sucrose	64 mM
Tris-Cl (pH 7.5)	20 mM
$MgCl_2$	10 mM
Triton X-100	0.5 %

Table 38: Composition of Pronase E

Component	**Amount**
Protease E from Streptomyces griseus	20 mg
H_2O	1 ml

Table 39: Composition Lysis Buffer tissue digest

Component	**Final concentration**
Sodium dodecyl sulfate (SDS)	0.2 %
EDTA (0.5M)	5 mM
Tris-HCl (pH 8.5)	100 mM
NaCl	200 mM

2.1.7. Antibodies

Table 40: Primary and secondary antibodies

Primary antibodies				
Antibody, clone	**Isotype**	**Supplier**	**Conjugate**	**Concentration**
Mouse anti-chicken beta actin (loading control)	IgG2b	Thermo Fisher Scientific, Waltham, USA	UNLB	1 µg/ml (WB)
Mouse anti-Cas9, clone 7A9 3A3	IgG	Thermo Fisher Scientific, Waltham, USA	UNLB	1.25 µg/ml (WB)
Fixable Viability Dye eFluor 780		eBioscience™ Inc., San Diego, USA	eFluor 780	1 µl/ml = 1:1000 dilution (FACS)
7AAD viability dye		Biozol Diagnostica Vertrieb GmbH, Eching, Germany	7AAD	1:100 dilution (FACS)
Mouse anti-chicken MHC (B2M), FL21-21 (cell culture supernatant)	IgG1	Kindly provided by Jim Kaufman, Department of Pathology, University of Cambridge, UK	UNLB	1:5 dilution (FACS)
Mouse anti-chicken Bu1-FITC	IgG1	Biozol Diagnostica Vertrieb GmbH, Eching, Germany	FITC	2.5 µg/ml (FACS)

Mouse anti-chicken CXCR4, clone 9D9	IgG2a	Bio-Rad Laboratories, Hercules, USA	UNLB	2 µg/ml (FACS)
Mouse anti-chicken CD45-FITC, clone LT40	IgG1	Biozol Diagnostica Vertrieb GmbH, Eching, Germany	FITC	5 µg/ml (FACS)
Mouse anti-chicken CD4-FITC, clone CT-4	IgG1	Biozol Diagnostica Vertrieb GmbH, Eching, Germany	FITC	0.625 µg/ml (FACS)
Mouse anti-chicken CD8a-Pacific Blue, clone CT-8	IgG1	Biozol Diagnostica Vertrieb GmbH, Eching, Germany	Pacific Blue	0.625 µg/ml (FACS)
Mouse anti-chicken Kul01, clone KUL01	IgG1	Biozol Diagnostica Vertrieb GmbH, Eching, Germany	UNLB	2.5 µg/ml (FACS)
Mouse anti-chicken TCRγδ (TCR1)	IgG1	Biozol Diagnostica Vertrieb GmbH, Eching, Germany	UNLB	0.625 µg/ml (FACS)
Mouse anti-chicken TCRγδ - BIOTIN	IgG1	Biozol Diagnostica Vertrieb GmbH, Eching, Germany	Biotin	0.625 µg/ml (FACS)
Mouse anti-chicken TCR αβ-1 (TCR2)	IgG1	Biozol Diagnostica Vertrieb GmbH, Eching, Germany	UNLB	2.5 µg/ml (FACS)
Mouse anti-chicken TCR αβ-1-BIOTIN	IgG1	Biozol Diagnostica Vertrieb GmbH, Eching, Germany	Biotin	2.5 µg/ml (FACS)
Mouse anti-chicken TCR αβ-2 (TCR3)	IgG1	Biozol Diagnostica Vertrieb GmbH, Eching, Germany	UNLB	2.5 µg/ml (FACS)
Mouse anti-chicken TCR αβ-2-BIOTIN	IgG1	Biozol Diagnostica Vertrieb GmbH, Eching, Germany	Biotin	2.5 µg/ml (FACS)
Mouse anti-FLAG, clone M2	IgG1	Sigma Aldrich, Saint-Louis, USA	UNLB	1.375 µg/ml (FACS)
Secondary antibodies				
Antibody, clone	**Isotype**	**Supplier**	**Conjugate**	**Concentration**
Goat anti-mouse APC	IgG (H+L)	Biozol Diagnostica Vertrieb GmbH, Eching, Germany	APC	0.625 µg/ml (FACS)
Streptavidin-APC		VWR International GmbH, Darmstadt, Germany	APC	0.2 µg/ml (FACS)
Goat anti-mouse, human ads PE-Cy7	IgG2a	Southern Biotech, Birmingham, USA	PE-Cy7	1.25 µg/ml (FACS)
Donkey anti-mouse	IgG (H+L)	Jackson ImmunoResearch Laboratories Inc., West Grove, USA	HRP	0.04 µg/ml (WB)

2.1.8. Oligonucleotides

2.1.8.1. Primer and probes

Table 41: Primer and probes. Oligonucleotides were obtained from Eurofins, Ebersberg, Germany and Integrated DNA Technologies (IDT), USA

Internal No.	Sequence (5´→3´)	Target name	Tm (°C)	Purpose
Gene detection				
14015	AAGGACGACGGCAACTACAAGACC	EGFP	64	Detection of EGFP
14016	CTTGATGCCGTTCTTCTGCTTGTC	EGFP	61	Detection of EGFP
593	GAGAGAATGAAGCGGATCGAAGAG	Cas9_RT_fw	59	Detection of Cas9
594	CAGTTCCTGGTCCACGTACATATC	Cas9_RT-rv	59	Detection of Cas9
440	TTGCTGTAGAAGAAGTACTTGGCG	Cas9	59	Detection of Cas9
1	AAGCATAGAAACAATGTGGGAC	Z-chromosome 12027	55	Sexing primer
2	AACTCTGTCTGGAAGGACTT	Z-chromosome (CPE15R) 12028	55	Sexing primer
3	CTATGCCTACCACMTTCCTATTTGC	W-chromosome (USP1) 12029	58-60	Sexing primer
4	AGCTGGAYTTCAGWSCATCTTCT	W-chromosome (USP3) 12030	58-60	Sexing primer
672	ATGGTGAGCAAGGGCGAGGAGCT	672_GFP_fw	68	GFP INDEL detection
14149	CGTCCTCGATGTTGTGGCGGATC	GFP 14149	65	GFP INDEL detection
677	ACTTGTAGACCTGCGGCTC	677_B2M_INDEL_RP	60	B2M INDEL detection
676	CAAGGTGCAGGTGTACTCC	676_B2M_INDEL_FP	58	B2M INDEL detection
815	CAATGTCGAGGAAGGGGTTCC	815_rv	61	Detection of gRNA array
653	GGCAAGTTTGTGGAATTGGTTTAAC	IT32-SalI-overhang-4X FP	57	Detection of gRNA array
277	TACCACAATGTACCCTGGC	Beta actin fw	57	Detection of beta actin
278	CTCGTCTTGTTTTATGCGC	Beta actin rv	54	Detection of beta actin
Sequencing primer				
651	TCGACGTTTCAGACCCACCTCCCAAC	IT31-SalI-overhang-2X FP	75	Sequencing primer
652	CGGGTGGTAGACGAAACGTC	crRNA_IT9_rv	61	Sequencing primer
654	GTTGGGAGGTGGGTCTGAAACGTCGA	IT31-SalI-overhang-2X RV	75	Sequencing primer
656	GACGTTTCGTCTACCACCCG	crRNA-IT9_fw	61	Sequencing primer
662	GTTGTTGTTCACATTCCCGA	662_crRNA-IT12_fw	55	Sequencing primer
663	TCGGGAATGTGAACAACAAC	663_crRNA-IT12_rv	55	Sequencing primer
683	CGAAGCAGTTGAGGACGTTC	gRNA 1445 rev	59	Sequencing primer
684	AATGGCTTATCATTTTCCAC	684_IT7_fw	49	Sequencing primer
685	GTGCAATCGTATCTACCATA	685_IT6_rv	51	Sequencing primer
686	TATGGTAGATACGATTGCAC	686_IT6 fw	51	Sequencing primer

678	CCGGCAAGCTGCCCGTGCCC	EGFP_sgRNA_rv	74	Sequencing primer
675	CATATTTGCATATACGATACAAGGC	hu6_prom_fw	53	Sequencing primer
684	AATGGCTTATCATTTTCCAC	684_IT7_fw	49	Sequencing primer
685	GTGCAATCGTATCTACCATA	685_IT6_rv	51	Sequencing primer
686	TATGGTAGATACGATTGCAC	686_IT6 fw	51	Sequencing primer
28(14017)	TAATACGACTCACTATAGGG	T7 14017	49	Sequencing primer
Cloning and Gibson primer				
417	GTGGCCTCGCGTACCACTGTGGCATCGATTTTCCCATGATTCCTTCATATTTG	RCAS(BP) A_gRNA_FW	60	Gibson primer PX330 into RCAS(BP) A
418	CGTATATCTGGCCCGTACATCGCATCGATCTAGAGCCATTTGTCTGC	RCAS(BP) A_gRNA_RV	60	Gibson primer PX330 into RCAS(BP) A
646	TTAGGCTGAACTAGCTAGTCTCGAGATTATCGTTTCAGACCCACCTCCC	IT7+IT6+IT12+IT9__GA_fw	71	Gibson Primer for cloning
647	TAAGCTGCAATAAACAAGTTAACGCACCGGAGCCACTCGAG	IT7+IT6+IT12+IT9_GA_rv	70	Gibson Primer for cloning
856	CCGGGCTGCAGGAATTCGATATCCGATTTTCCCATGATTCC	856_Gibson_pBlueScript_gRNA1445_fw	71	Gibson primer used for cloning
857	ACGGTATCGATAAGCTTGATATCATCTAGAGCCATTTGTCTG	857_Gibson_pBlueScript_gRNA1445_rv	65	Gibson primer used for cloning
664	CACCGGTCTTGGTGCCCGCAGAGGCG	664_sgRNA 1444	76	Primer used for cloning
665	AAACCGCCTCTGCGGGCACCAAGACC	665_sgRNA 1444	73	Primer used for cloning
1003	AGCTTATCGATACCGTCGACTGACCGACAATTGCATGAAGA	1003_Gibson_CMV-EGFP-BGHpA_Fw	69	Gibson primer for cloning
1004	AAGCTGGTACCGGGCCCCCCCATAGAGCCCACCGCATC	1004_Gibson_CMV-EGFP-BGHpA_Rv_new	81	Gibson primer for cloning
ddPCR primer and probes				
491	CAGGATGCAGAAGGAGATCA	ddPCR beta actin fw	59	ddPCR primer b-actin
492	TCCACCACTAAGACAAAGCA	ddPCR beta actin rv	59	ddPCR primer b-actin
500	GTGGGTGGAGGAGGCTGAGC	ddPCR beta actin probe (5´HEX 3´BHQ1)	66	ddPCR probe b-actin
648	CATATGCGCGATTGCTGATC	ddPCR hygro fw	57	ddPCR primer hygromycin
649	GTCAATGACCGCTGTTATGC	ddPCR hygro rv	56	ddPCR primer hygromycin
650	TCGTGCACGCGGATTTCGGCTCCAA	ddPCR hygro probe (5´FAM 3´BHQ1)	70	ddPCR probe hygromycin
q-RT PCR primer and probes				
322	CATGTCTAAGTACACACGGGCGGTA	18S fw	63	SYBR® Green 18S primer
323	GGCGCTGCTGGCATGTATTA	18S rv	61	SYBR® Green 18S primer
656	GACGTTTCGTCTACCACCCG	IT9 fw	61	SYBR® Green IT9 primer
1087	CACCGAATGGCTTATCATTTTCCACG	1087_IT7_fw	61	SYBR® Green IT7 primer
1088	CACCGTATGGTAGATACGATTGCACGT	1088_IT6_fw	62	SYBR® Green IT6 primer
1089	CACCGGTTGTTGTTCACATTCCCGA	1089_IT12_fw	64	SYBR® Green T12 primer
1090	AGCACCGACTCGGTGCCACTTTTT	1090_scaffold_RNA_rv	66	SYBR® Green rv primer
817	CTTGGCTTTATATATCTTGTGGAAAGG	817_Taqman™_Primer_fw	55	Taqman™ qPCR primer
818	CAAGTTGATAACGGACTAGCCT	818_Taqman™_Primer_rv	56	Taqman™ qPCR primer

819	ACTCGGGAATGTGAACAACAACC	819_Taqman™_Probe_IT12 (5´FAM 3´BHQ1)	60	Taqman™ qPCR probe – detection IT12
820	CCGTATGGTAGATACGATTGCACG	820_Taqman™_Probe_IT6 (5´FAM 3´BHQ1)	60	Taqman™ qPCR probe – detection IT6
821	CCGAATGGCTTATCATTTTCCACG	821_Taqman™_Probe_IT7 (5´FAM 3´BHQ1)	59	Taqman™ qPCR probe – detection IT7
822	AAACCGGGTGGTAGACGAAAC	822_Taqman™_Probe_IT9 (5´FAM 3´BHQ1)	60	Taqman™ qPCR probe – detection IT9

2.1.8.2. gRNA oligonucleotides

Table 42: sgRNA oligonucleotide sequences. Oligonucleotides were obtained from Eurofins, Ebersberg, Germany

Name	**Target site**	**Target sequence (5´→ 3´) PAM**	**Oligo sequences**	**Origin**
sgRNA 1408	EGFP	GGGCACGGGCAGCTTGCCGG	5´ – CACCGGGGCACGGGCAGCTTGCCGG – 3´ 5´ – AAACCCGGCAAGCTGCCCGTGCCCC – 3´	Addgene pFYF1320 EGFP Site#1
sgRNA 1430	IFNAR1	GTGTGCCTCTGGGCGGCTAGCGG	5´ – CACCGGTGTGCCTCTGGGCGGCTAG – 3´ 3´ – AAACCTAGCCGCCCAGAGGCACACC – 3´	Reproductive Biotechnology, TUM, Freising, Germany
sgRNA 1434	CXCR4	AAATTCAATGAGTATGCCAGAGG	5´ – CACCGGAAATTCAATGAGTATGCCAG – 3´ 5´ – AAACCTGGCATACTCATTGAATTTCC – 3´	Reproductive Biotechnology, TUM, Freising, Germany
sgRNA 1435	CXCR4	ATTTGCTGACAATGGCTCGGAGG	5´ – CACCGGATTTGCTGACAATGGCTCGG – 3´ 5´ – AAACCCGAGCCATTGTCAGCAAATCC – 3´	Reproductive Biotechnology, TUM, Freising, Germany [214]
sgRNA 1444	B2M	TCTTGGTGCCCGCAGAGGCGAGG	5´ – CACCGGTCTTGGTGCCCGCAGAGGCG – 3´ 5´ – AAACCGCCTCTGCGGGCACCAAGACC – 3´	Department of Pathology, University of Cambridge, UK
sgRNA 1445	B2M	GAACGTCCTCAACTGCTTCGTGG	5´ – CACCGGAACGTCCTCAACTGCTTCG – 3´ 5´ – AAACCGAAGCAGTTGAGGACGTTCC – 3´	Department of Pathology, University of Cambridge, UK

Table 43: Synthetic sgRNA sequences. Oligonucleotides were purchased from SYNTHEGO, Redwood City, USA

Name	**Target site**	**Oligo sequences**	**Origin**
sgRNA 1408	EGFP	5´ – GGGCACGGGCAGCUUGCCGG – 3´	SYNTHEGO, Redwood City, USA
sgRNA 1434	CXCR4	5´ – A*A*A*UUCAAUGAGUAUGCCAG – 3´	SYNTHEGO, Redwood City, USA
sgRNA 1435	CXCR4	5´ – A*U*U*UGCUGACAAUGGCUCGG – 3´	SYNTHEGO, Redwood City, USA
sgRNA 1444	B2M	5´ – U*C*U*UGGUGCCCGCAGAGGCG – 3´	SYNTHEGO, Redwood City, USA
sgRNA 1444	B2M	5´ – UCUUGGUGCCCGCAGAGGCG – 3´	SYNTHEGO, Redwood City, USA
sgRNA 1445	B2M	5´ – G*A*A*CGUCCUCAACUGCUUCG – 3´	SYNTHEGO, Redwood City, USA
sgRNA 1445	B2M	5´ – GAACGUCCUCAACUGCUUCG – 3´	SYNTHEGO, Redwood City, USA

* chemically 2'-O-methyl phosphorothioate linkage modified

Table 44: gRNA sequences in the MDV genome. Sequences were obtained from the group of Prof. Benedikt Kaufer (see also Hagag et al. [77])

Name	**Name according to Hagag et al. [77]**	**Target gene in MDV**	**Target sequence (5´→ 3´)**	**Origin**
IT6	gRNA 5	UL27 (glycoprotein B)	TATGGTAGATACGATTGCAC	Institute of Virology, FU Berlin, Germany
IT7	gRNA 6	UL30 (viral DNA polymerase)	AATGGCTTATCATTTCCAC	Institute of Virology, FU Berlin, Germany
IT9	gRNA 8	UL49 (tegument protein)	GACGTTTCGTCTACCACCCG	Institute of Virology, FU Berlin, Germany
IT12	gRNA 11	ICP4 (infected cell protein 4)	GTTGTTGTTCACATTCCCGA	Institute of Virology, FU Berlin, Germany

2.1.9. DNA vectors and constructs

Table 45: Constructs used in this work

Construct name (Internal No.)	Resistance genes	Source
2B-E attB70 EGFP (K27/177)	Ampicillin, Hygromycin	University of California, Davis, USA
pKL05-hU6-MDV-gRNA (K182)	Ampicillin	Institute of Virology, FU Berlin, Germany
pKL05-IT6	Ampicillin	Institute of Virology, FU Berlin, Germany
pKL05-IT7	Ampicillin	Institute of Virology, FU Berlin, Germany
pKL05-IT12	Ampicillin	Institute of Virology, FU Berlin, Germany
pKL05-IT9	Ampicillin	Institute of Virology, FU Berlin, Germany
pBS II K26 (K103) - Addgene Plasmid #212205	Ampicillin	Addgene, Massachusetts, USA kindly provided by Stratagene
pBS attB 70 Hygro Cas9 (K146) (Figure 14)	Ampicillin, Hygromycin	Reproductive Biotechnology, TUM, Freising, Germany
pGEM-T-Easy (K147) - Addgene Plasmid #A1360	Ampicillin	Addgene, Massachusetts, USA kindly provided by Promega
PhiC31 integrase (K158) - Addgene Plasmid #18935	Ampicillin	Addgene, Massachusetts, USA kindly provided by Michele Calos [215]
pX330-U6-Chimeric_BB-CBh-hSpCas9 - Addgene Plasmid #42230	Ampicillin	Addgene, Massachusetts, USA kindly provided by Feng Zhang [216]
pX333-2x-U6-Chimeric_BB-CBh-hSpCas9 - Addgene Plasmid #64073	Ampicillin	Addgene, Massachusetts, USA kindly provided by Andrea Ventura [217]
RCAS(BP)A (K023)	Ampicillin	Addgene, Massachusetts, USA [218]
RCAS(BP)A-sgRNA-EGFP (1408) (K130)	Ampicillin	Reproductive Biotechnology, TUM, Freising, Germany
RCAS(BP)A-sgRNA-INFAR (1430) (K140)	Ampicillin	Reproductive Biotechnology, TUM, Freising, Germany
pBlueScript-sgRNA-EGFP (1408) (K168)	Ampicillin	Reproductive Biotechnology, TUM, Freising, Germany
pBlueScript-sgRNA-porcine-B2M + CMV-EGFP-BGHpA	Ampicillin	Chair of Livestock Biotechnology, TUM, Freising, Germany

Table 46: Constructs generated within this work

Construct No.	Insert	Restriction/ Gibson insert	Original vector	Restriction site vector	Assembly	Seq primer
2B-E attB70 MDV-gRNA (183) Clone 53 (Figure 15)	MDV-gRNA from K182	HindIII-HF, XhoI	2B-E attB70 EGFP (K27/177)	XhoI, HpaI	Blunt end T4 DNA ligase	651, 652, 653, 654
RCAS(BP)A B2M-sgRNA 1445 (K187) Clone 4 (Figure 16)	sgRNA 1445 (B2M) from px330	Gibson primers 417, 418	RCAS (BP) A sgRNA EGFP(K180)	Cla1	Gibson assembly	335
pBS-B2M-sgRNA 1445 (K245) Clone 2 (Figure 17)	sgRNA 1445 (B2M) from K187	Gibson primers 865, 866	pBS II K26 (K103)	EcoRV	Gibson assembly	28 (T7 14017)
pBS-B2M-sgRNA 1445 + CMV-EGFP-BGHpA	sgRNA 1445 (B2M) + CMV-EGFP-BGHpA	Gibson primers 1003, 1004	pBS sgRNA 1445 (B2M) (K245)	XhoI	Gibson assembly	26 (for EGFP seq) 17 (for sgRNA 1445)

(K301) Clone 4 (Figure 18)						

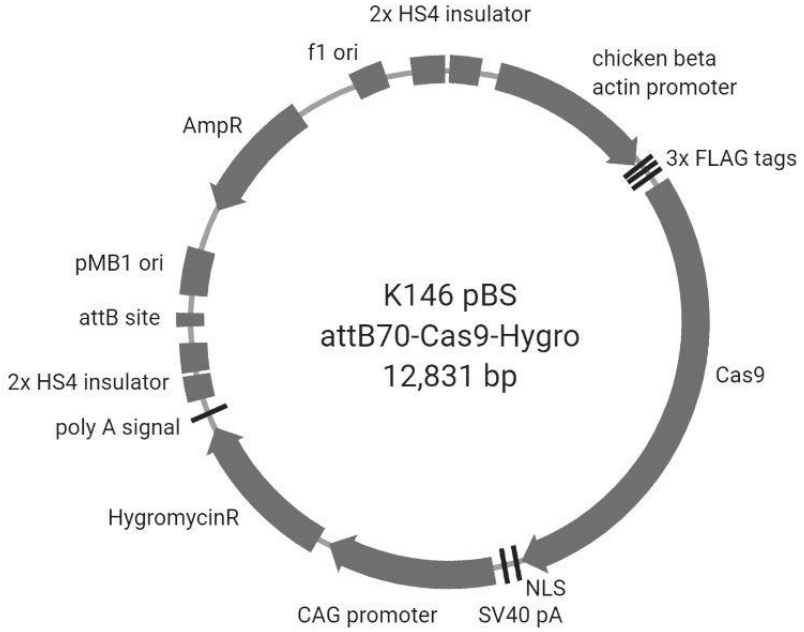

Figure 14: Cas9 expression construct (K146). This construct was used for the generation of Cas9-expressing PGCs. Stable integration of the Cas9 gene was ensured by attB70 using phiC31 integrase. The plasmid map was created with BioRender.com.

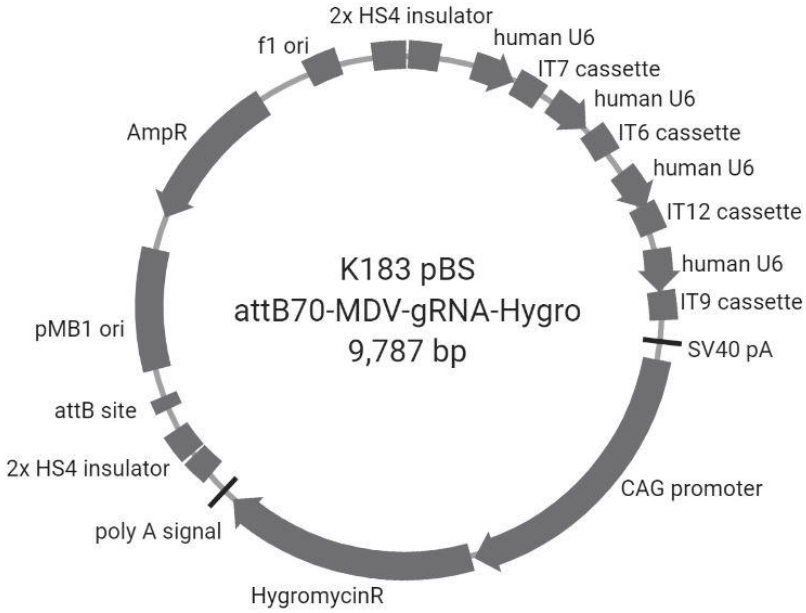

Figure 15: MDV-gRNA expression construct (K183). This construct was used for the generation of MDV-gRNA-expressing PGCs. For stable integration into PGCs, the Cas9 expression plasmid contained an attB70 site to ensure the insertion of the transgene using phiC31 integrase. The plasmid map was created with BioRender.com.

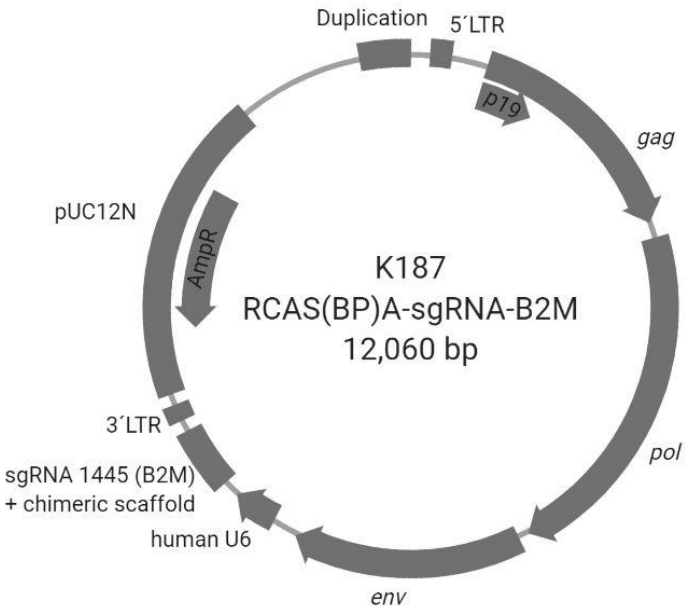

Figure 16: RCAS(BP)A-sgRNA-1445(B2M) (K187). The construct contains a 5´LTR, 3´LTR, *gag*, *pol*, *env* and an ampicillin resistance gene (AmpR). SgRNA 1445 (B2M) expression is driven by the human U6 promoter and followed by a chimeric scaffold sequence. The plasmid map was created with BioRender.com.

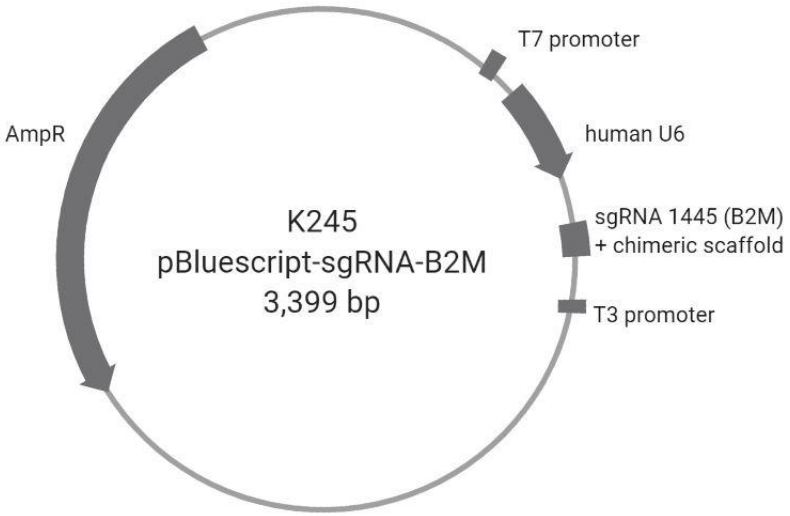

Figure 17: pBlueScript-sgRNA-1445(B2M) (K245). SgRNA 1445 (B2M) expression was driven by the human U6 promoter and followed by a chimeric scaffold sequence. The construct contained an ampicillin resistance gene (AmpR). The plasmid map was created with BioRender.com.

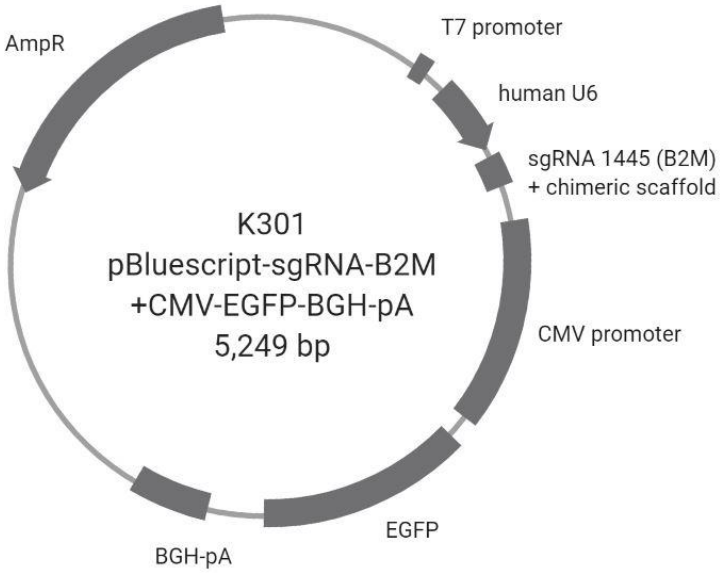

Figure 18: pBlueScript-sgRNA-1445(B2M)+CMV-EGFP-BGH-pA (K301). EGFP expression was driven by the CMV promoter and followed by a BGH-pA signal. SgRNA 1445 (B2M) expression was driven by the human U6 promoter and followed by a chimeric scaffold sequence. The construct contained an ampicillin resistance gene (AmpR). The plasmid map was created with BioRender.com.

2.1.10. Laboratory equipment

Table 47: Instruments

Instrument	**Supplier**
Attune Nxt Flow Cytometer	Thermo Fisher Scientific, Waltham, USA
AMAXA™ Nucleofector® II Device	Lonza Cologne GmbH, Cologne, Germany
Bio-Rad CFX	Bio-Rad Laboratories, Hercules, USA
Blue Light Table	SERVA Electrophoresis GmbH, Heidelberg, Germany
BTX Electroporator	BTX, Holliston, USA
Candling light with fixation system	Self-made construction
Centrifuge, SIGMA 3-16K	SciQuip Ltd, Newtown, UK
Centrifuge, 5424R	Eppendorf, Wesseling, Germany
Centrifuge, 5810R	Eppendorf, Wesseling, Germany
Cell Counting Chamber (Neubauer)	Laboroptik Ltd, Lancing, United Kingdom
Cryo-container, Cool Cell -1 °C/min	BioCision, San Rafael, USA
CO2-Incubator	Thermo Fisher Scientific, Waltham, USA
Digital Black & White Medical Printer P95E	Mitsubishi Electric, Germany
Digital Heat Block	VWR International GmbH, Darmstadt, Germany
DREMEL® 3000-15	Conrad GmbH, Munich, Germany
Erlenmeyer 10-1000 ml	VWR International GmbH, Darmstadt, Germany

Freezer (-20 °C), GNP3056 Pr	Liebherr, Biberach, Germany
Freezer (-80 °C), SN30407588	Thermo Fisher Scientific, Waltham, USA
Fridge (+4 °C), TP410 Comfort	Liebherr, Biberach, Germany
Fusion Fx	Vilber Lourmat, Eberhardzell, Germany
Gel comb 6-12 pockets	Peqlab GmbH, Erlangen, Germany
Gel Documentation, Quantum ST5	Vilber Lourmat, Eberhardzell, Germany
Gel slide Thermo EC Classic CSSU911	Thermo Fisher Scientific, Waltham, USA
HEKA incubator	HEKA Brutgeräte GmbH, Rietberg, Germany
Ice Maker	Eurfrigor, Lainate, Italy
Innuspeed Homogenizer	Analytik Jena GmbH, Jena, Germany
Incubator for eggs (Flächenbrüter Modell 400)	Bruja Brutmaschinen-Janeschitz GmbH, Hammelburg, Germany
Microcentrifuge, MiniStar	VWR International GmbH, Darmstadt, Germany
Microscope, Axiovert 25	Zeiss AG, Oberkochen, Germany
Microwave	MDA, Rüsselsheim, Germany
Multi-channel pipette EX3	Eppendorf, Wesseling, Germany
PCR-Cycler, peqSTAR 2x	Peqlab GmbH, Erlangen, Germany
PCR-Cycler T100 Thermal Cycler	Bio-Rad Laboratories, Hercules, USA
PCR workstation Pro HEPA	VWR International GmbH, Darmstadt, Germany
Pipette, pipetteman P2, P10, P20, P100, P200 and P1000	Gilson Inc, Middleton, USA
Precision scale 440-33N	KERN & SOHN GmbH, Balingen, Germany
Procon incubator	Grumbach Brutgeräte GmbH, Aßlar, Germany
QuantStudio Real-Time PCR system	Thermo Fisher Scientific, Waltham, USA
QX200™ Digital Droplet PCR (ddPCR) reader	Bio-Rad Laboratories, Munich, Germany
Rocking shaker	VWR International GmbH, Darmstadt, Germany
Spectrophotometer, Nanodrop™ Lite	Thermo Fisher Scientific, Waltham, USA
Speed Mill Plus	Analytik Jena GmbH, Jena, Germany
Standard Analog Shaker, Orbital	VWR International GmbH, Darmstadt, Germany
Steri-Cycle ™ CO_2-Incubator	Thermo Fisher Scientific, Waltham, USA
Sterile Surgical Instruments (tweezer, scissors)	Henry Schein VET GmbH, Hamburg, Germany
Sterile Workbench, Herasafe	Heraeus Holding GmbH, Hanau, Germany
Thermo Cycler, peqSTAR	Peqlab GmbH, Erlangen, Germany
Thermal Cycler, T100	Bio-Rad Laboratories, Munich, Germany
Vortex Mixer, ZX3	VELP Scientifica, Usmate, Italy
Water Bath	Memmert GmbH + Co. KG, Schwabach, Germany
Weight scale	VWR International GmbH, Darmstadt, Germany
Wet Tank Blotting System	Bio-Rad Laboratories, Munich, Germany

2.1.11. Consumables

Table 48: Consumables

Material	**Supplier**
Acetate foil for Microtest	Sarstedt, Nümbrecht, Germany
Biosphere® Filter Tips, 1250 µl	Sarstedt, Nümbrecht, Germany
Biosphere® Filter Tips, 0,1-10 µl	Sarstedt, Nümbrecht, Germany
Biosphere® Filter Tips, 2-20 µl	Sarstedt, Nümbrecht, Germany
Biosphere® Filter Tips, 2-100 µl	Sarstedt, Nümbrecht, Germany
Biosphere® Filter Tips, 2-200 µl	Sarstedt, Nümbrecht, Germany
Centrifuge Tube	VWR International GmbH, Darmstadt, Germany
Cellstar Tubes	Greiner Bio-one International GmbH, Kremsmünster, Austria
Chromatographie Paper	Sigma Aldrich, Saint-Louis, USA
Corning cell strainer (100 µM)	Sigma Aldrich, Saint-Louis, USA
Cover slips	Thermo Fisher Scientific, Waltham, USA
Cryo vials	Thermo Fisher Scientific, Waltham, USA
DG8™ cartridge for QX200™	Bio-Rad Laboratories, Hercules, USA
DG8™ gasket for QX200™	Bio-Rad Laboratories, Hercules, USA
EDTA microvette tubes	Sarstedt, Nümbrecht, Germany
Electroporation cuvettes	Lonza Cologne GmbH, Cologne, Germany
FrameStar® FastPlate 96	4titude, Wotton, UK
Glas beads, 5 ± 0,3 mm	Carl Roth GmbH, Karlsruhe, Germany
Injekt®-F Solo, 1 ml	B. Braun Melsungen AG, Hessen, Germany
InnuSpeed Lysis Tube A	Analytik Jena GmbH, Jena, Germany
Insulin syringe, one-way (0.3x1.2 mm)	Henry Schein VET GmbH, Hamburg, Germany
Megablock® (96-well)	Sarstedt, Nümbrecht, Germany
Microcapillary pipet (40 µm)	Hilgenberg GmbH, Malsfeld, Germany
Needles (27G – 20G)	B. Braun Melsungen AG, Hessen, Germany
NitrilBestGen (powder-free, latex-free gloves)	Meditrade, Kiefersfelden, Germany
Nitrocellulose membrane	GE Healthcare Life Science, Amersham, UK/ Sigma Aldrich Saint-Louis, USA
Nunc™ CryoTube Vials	Thermo Fisher Scientific, Waltham, USA
Nunc™ EasYFlask 25 cm^2	Thermo Fisher Scientific, Waltham, USA
Nunc™ EasYFlask 75 cm^2	Thermo Fisher Scientific, Waltham, USA
Nunclon Delta Surface, 6 well	Thermo Fisher Scientific, Waltham, USA
Nunclon Delta Surface, 12 well	Thermo Fisher Scientific, Waltham, USA
Nunclon Delta Surface, 24 well	Thermo Fisher Scientific, Waltham, USA
Nunclon Delta Surface, 48 well	Thermo Fisher Scientific, Waltham, USA
Nunclon Delta Surface, 96 well	Thermo Fisher Scientific, Waltham, USA
Omnifix syringes (3 ml, 5 ml, 10 ml)	MarMed GmbH, Cölbe, Germany
Parafilm	Sigma Aldrich, Saint-Louis, USA
PCR Mulitply µstripe pro 8-strip	Sarstedt, Nümbrecht, Germany
Petri dish, unsterile	Sarstedt, Nümbrecht, Germany

Petri dish, sterile	Thermo Fisher Scientific, Waltham, USA
Plastic foil Saran Cling Plus	SC Johnson, Racine, USA
Reagent Reservoir	VWR International GmbH, Darmstadt, Germany
SafeSeal 1.5 ml tube	Sarstedt, Nümbrecht, Germany
Seal foil for PCR plates	Sarstedt, Nümbrecht, Germany
Serologic Pipette 2 ml	Sarstedt, Nümbrecht, Germany
Serologic Pipette 5 ml	Sarstedt, Nümbrecht, Germany
Serologic Pipette 10 ml	Sarstedt, Nümbrecht, Germany
Serologic Pipette 25 ml	Sarstedt, Nümbrecht, Germany
Serologic Pipette 50 ml	Sarstedt, Nümbrecht, Germany
Sterile filter 0.22 µm	VWR International GmbH, Darmstadt, Germany
Sterile Scarpel	neoLab Migge GmbH, Heidelberg, Germany
Tube 50 ml, 114x28 mm, PP	Sarstedt, Nümbrecht, Germany
Tube 15 ml, 129x17 mm, PP	Sarstedt, Nümbrecht, Germany
Vacuum Filtration	VWR International GmbH, Darmstadt, Germany
Waste disposal bags	VWR International GmbH, Darmstadt, Germany
Weight boat	neoLab Migge GmbH, Heidelberg, Germany

2.1.12. Software and online tools

Table 49: Software and online tools

Software	**Supplier**	**Usage**
Benchling	Benchling, San Francisco, USA	Sequence maps and alignments
BioRender	BioRender, Toronto, Canada	Plasmid maps
CRISPR design tool (http://crispr.mit.edu [219])	Zhang Lab, MIT, Cambridge, USA	Design CRISPR guide RNA
Digital droplet “QuantaSoft”	Bio-Rad Laboratories, Hercules, USA	Copy number analysis
DNASTAR Lasergene (v17)	DNASTAR, Madison, USA	Sequence maps and alignments
FileMaker Pro (v19.2.1.14)	FileMaker, Inc, Santa Clara, USA	Management of data and documentation
FlowJo (v10.4.1)	FlowJo LLC., Ashland, USA	Processing FACS data & analysis
Genome databases (www.ncbi.nlm.nih.gov; www.ensembl.org [220,221])	EMBL, Hinxton, Great Britain NCBI, USA	BLAST function and genome database
GraphPad Prism (v8.0.1)	San Diego, USA	Generation of graphs and images
ICE: Interference of CRISPR edits	SYNTHEGO, Redwood City, USA	Analysis of INDEL formation
Leica Application Suite X (v.3.7.4.23463)	Leica Camera, Wetzlar, Germany	Microscopy imaging
Microsoft Office 2010	Microsoft, Redmond, USA	Excel, Word, PowerPoint
Primer design tool “Primer3“	Whitehead Institute for Biomedical Research, Cambridge, USA	Primer design
QuantStudio 3	Thermo Fisher Scientific, Waltham, USA	Real-time quantitative PCR analysis
SPSS24 statistics (v24.0.0.0)	IBM, USA	Statistical analysis
TIDE: Tracking of INDELs by Decomposition (http://shinyapps.datacurators.nl/tide/ [222])	Deskop Genetics, London, Great Britain	Analysis of INDEL formation (Brinkman et al. [223])
VisionCapt „Quantum ST5“ (v16.15)	Vilbert Lourmat, Eberhardzell, Germany	Agarose gel documentation

2.2. Methods

2.2.1. Cell culture

2.2.1.1. Isolation and cultivation of primordial germ cells

PGC isolation from blood was done at H&H stage 14-16 [224,225]. Therefore, eggs were incubated for 65 h at 37.8 °C and 55 % humidity. The embryonated eggs were scored around the middle line so that the egg could be divided by carefully opening it with a scalpel. The embryo (with egg white and yolk) was transferred to a weight boat and 1-2 µl blood was taken with a microcapillary pipet. Subsequently, the blood was resuspended in 100 µl of prewarmed PGC medium at 37 °C (Table 11). The needle was washed with manipulation medium between the embryos. The cells were collected from the bottom of the 0.5 ml Eppendorf tube and the supernatant was discarded. The cells were resuspended in 300 µl of 5 % CO_2-equilibrated PGC medium and plated onto 48 well plates. On a daily basis, the cells were observed, the medium replaced and cells passaged if necessary. After approximately 14 days in culture, other cells such as erythrocytes died out.

PGCs were passaged every 2-3 days and cultured at 37.0 °C and 5 % CO_2. For counting, cells were transferred to a 50 ml falcon. After centrifugation (225 x g, 10 min) at room temperature (RT), the cells were resuspended in PGC medium ($^2/_3$ new PGC medium, $^1/_3$ supernatant of old PGC medium after centrifugation) and plated at concentration of 125.000 cells per ml. Over the weekend, the cells were plated at the concentration of 100.000 cells per ml.

2.2.1.2. Isolation and cultivation of chicken embryonic fibroblasts

The genotype of ED10 embryos was determined one day before CEF isolation if desired. Therefore, blood was collected as described in section 2.2.2.3. One day later (ED11), CEF isolation was performed. Before the beginning of the isolation, the egg was cleaned with 80 % ethanol. The embryo was removed from the egg and quickly decapitated. Legs and arms were removed and the torso was placed onto a sterile petri dish and washed with sterile PBS. The torso was cut with a sterile scalpel into small pieces and pushed through a cell strainer to obtain single cells. The cell suspension was placed in a 50 ml falcon and filled with PBS to wash the cells. The suspension was placed on ice and sedimented for 10 min. The supernatant was placed into a new 50 ml falcon and cells were centrifuged for 10 min at 300 x g at RT. The

pellet was resuspended in CEF medium (Table 16) and cells were cultured at a temperature of 40.0 °C with a 5 % CO_2. The cells were split every 2-3 days in ratio of 1:10 or 1:20 at a confluence of 90 %. The cells were washed with 3-4 ml PBS, trypsinized with 1.5 ml of 25 % trypsin (PBS/EDTA) and incubated for 10 min at 37 °C. 3.5 ml CEF medium was added and the cells were centrifuged for 10 min at 300 x g. The supernatant was discarded, and the cell pellet was resuspended in 5 ml CEF culture medium and plated at desired dilution into a T25 flask.

2.2.1.3. Isolation and cultivation of splenic lymphocytes

For splenic lymphocyte culture, spleens from 20-50 week old animals were used. The spleen was removed aseptically and placed into a 50 ml falcon filled with sterile PBS on ice for the transport. The spleen capsule was removed and the organ was homogenized by passing it through a cell strainer. The cell suspension was centrifuged (10 min, 225 x g, 4 °C), the pellet was resuspended in 10 ml PBS and cells were isolated by Ficoll density gradient separation (12 min, 650 x g without break, RT). The resulting PBMCs were taken from the interphase, washed with PBS and centrifuged for 10 min at 475 x g (4°C). The cells were counted and directly used for electroporation before plating onto a 24 well plate ($5x10^6$cells/well). Due to the short culture time (48 h), the cells were not passaged.

2.2.1.4. Cultivation of DF-1 cells

DF-1 cells were cultured at 40.0 °C and 5 % CO_2. The cells were split every 2-3 days in ratio of 1:10 at a confluence of 90 %. The cells were washed with 3-4 ml PBS, trypsinized with 1.5 ml of 0.25x trypsin (PBS/EDTA) and incubated for 10 min at 37 °C. 3.5 ml DF-1 medium was added and the cells were centrifuged for 10 min at 300 x g. The supernatant was discarded, and the cell pellet was resuspended in 5 ml DF-1 culture medium and plated 1:10 into a T25 flask.

2.2.1.5. Electroporation and transfection of cells

PGCs were electroporated using AMAXA™ Cell Line Nucleofector™ Kit V. Briefly, cells were centrifuged (225 x g, 10 min, RT) and the supernatant was removed. The cells were washed in PBS, centrifuged (300 x g, 4 min, RT) and $3\text{-}5x10^6$ cells were resuspended in 100 µl

Nucleofector solution added with 10-20 µg plasmid DNA. For stable integration, 10 µg of plasmid and 10 µg of phiC31 integrase was used as described in [226]. The cells were transferred into an electroporation cuvette and placed into BTX electroporator. The following settings were used: 8 pulses, 350 V for 100 µsec/pulse. 500 µl of PGC medium was added to the electroporated cells and the cuvette was placed into the incubator for 5 min. The cells were cultured by adding $^2/_3$ fresh and $^1/_3$ old PGC medium and cells were plated on a 48 well plate.

Splenic lymphocytes were electroporated using AMAXA™ Human T Cell Nucleofector™ Kit. Before starting with the electroporation, a 12 well plate was prepared with 1.5 ml culture medium per well and pre-equilibrated in a humidified at 40.0 °C with 5 % CO_2 incubator for at least 30 minutes as it is recommended by the manufacturer´s protocol. $5x10^6$ cells were resuspended in 100 µl Human T Cell Nucleofector® Solution, supplemented with entire supplements. The cells were combined with either 2 µg pmaxGFP® Vector (electroporation control) or 25 pmol/µl of guide RNA oligonucleotides. The suspension was transferred into the electroporation cuvette and program V-001 of the AMAXA™ Nucleofector® II Device was used for electroporation. 500 µl of the pre-equilibrated culture media was added to the cells before gently transferring the sample to the 12 well plate (final volume 2 ml media per well). 6 h after electroporation, the medium was changed, and cells were analyzed 48 h post electroporation.

Adherent cells (DF-1 and CEF) were transfected with plasmid DNA using ViaFect™ Transfection Reagent. One day before the transfection, the cells were seeded onto the desired culture plate format so that the cells were at confluence of ~70 % when transfected. The next day, the cells were transfected using Viafect™ Transfection Reagent at ratio 6:1 (transfection reagent : DNA) according to manufacturer´s instructions. Briefly, 3 µl Viafect™ Transfection Reagent was used for 500 ng DNA and filled up to 50 µl with OptiMEM. If stable DNA integration was desired, 250 ng of the phiC31 integrase and 250 ng of the construct containing an attB site to facilitate genomic integration was used. The transfection mix was incubated for 15 min at RT. The medium was changed and transfection complexes were added dropwise to the cells. If desired, cells were selected by antibiotics. Therefore 24 h after transfection, the medium was supplemented with hygromycin (at concentration of 1 µg/ml)

or puromycin (at concentration 2.5 µg/ml). The clones were frozen down as described in 2.2.1.6.

For the transfection with synthetic gRNAs, Xfect™ Transfection Reagent kit was used. Briefly, one day prior to the transfection, the cells were seeded onto a 6 well plate so that the cells were at confluence ~70 % on the day of transfection. For the transfection, two tubes were prepared: Tube 1 contained 100 µl of 25 pmol of gRNA and Xfext™ Reaction Buffer and Tube 2 contained 1.5 µl of Xfect™ Polymer and 98.5 µl Xfect™ Reaction Buffer. The tubes were mixed and incubated for 10 min at RT to allow nanoparticles to form. The entire 200 µl of nanoparticle complexes were added to the cells and incubated under normal culture conditions. After 4 h, the medium was removed and replaced with fresh culture medium until further analysis.

2.2.1.6. Cryopreservation

Adherent cells were washed with PBS to remove FBS residuals. The cells were trypsinized with 1.5 ml of 0.25x trypsin (diluted in PBS/EDTA) and incubated for 10 min at 37 °C. 3.5 ml medium supplemented with FBS was added and the cells were counted. After centrifugation (10 min, 300 x g, RT), the supernatant was removed and 1-3x10^6cells were first resuspended in 900 µ of manipulation medium before another 900 µl of manipulation medium supplemented with 20 % DMSO (final concentration in 1800 µl is 10 %) was added. The cells were transferred into cryovials which were placed into a cryo-container and stored as soon as possible at -80 °C. After 24 h, the cells were transferred to the liquid nitrogen storage.

Frozen cells were thawed at 37 °C (water bath) and transferred to a 50 ml falcon. Two times 10 ml of manipulation medium was added, first dropwise, then at once, to dilute DMSO. After centrifugation for 10 min at 300 x g (RT), the supernatant was discarded, the cell pellet was resuspended in 5 ml culture medium and the cells were seeded into a T25 flask.

2.2.2. Animals

Within this work the following chicken lines were generated:

- Chickens that ubiquitously express the endonuclease Cas9 from *Streptococcus pyogenes* (Cas9)
- Chickens that ubiquitously express four gRNAs against essential genes of MDV (MDV-gRNA)
- Chickens that ubiquitously express both Cas9 and the four gRNAs against MDV (Cas9-MDV-gRNA)

Animals used or generated originated from LSL-classic (Lohmanns selected Leghorn classic). The EGFP 165-2 chicken line originated from Crystal Bioscience and was used for the derivation of PGCs. Chickens hatched exclusively at the animal facility Versuchstation Thalhausen, TUM School of Life Sciences. Eggs were incubated at 37.8 °C and 50-60 % humidity until ED17 before they were transferred to the hatcher and incubated at 37.2 °C. On ED20, the humidity was raised to 80 %. Animals were kept at the animal facility in a conventional housing system and received standard diet and water *ad libitum*. Permission for animal experiments in this work was issued by the government of upper Bavaria, Germany (experimental license: ROB-55.2-2532.Vet_02-17-101).

2.2.2.1. Generation of germline chimeras

PGCs were isolated from blood as described in Chapter 2.2.1.1 and genetically modified as described in 2.2.1.5. On the day of injections, the modified cells were counted, adjusted to the concentration of 3000 cells per µl and resuspended in manipulation medium.

For the injection of modified PGCs into the embryo, LSL-classic eggs were incubated for 65 h (H&H stage 14-16) under normal conditions. The embryonated eggs were scored and carefully opened with a scalpel. The embryo (including egg white and yolk) was transferred to a weight boat. Only embryos with intact membranes and yolk were further used as damaged embryos die during the incubation until hatch. To inject the embryo´s vascular blood system with 1 µl of cell solution, a glass microcapillary pipet was used. A sterile filter between mouth and pipe was used to avoid contamination. The needle was washed with manipulation medium between the embryos. Turkey eggs were used as a surrogate eggshell. The weight of the egg

was determined to ensure that turkey egg was 30-40 g heavier than the chicken egg. On the day of injections, turkey eggs were scored at their point side, opened and the egg content was discarded. 1 ml of 20 % Penicillin-Streptomycin-solution was placed into the empty turkey surrogate eggshell. After transferring the injected embryo into the surrogate egg shell, it was sealed with Saran wrap and albumin around the egg opening. The embryos were controlled daily and dead embryos were removed from the incubator. Hatching of the chicks was accompanied and monitored. On ED19/ED20, air holes were applied to the sealing foil dependent on the hatching progress of the chick. When the chorioallantoic membranes (CAM) were successfully removed, the chicks were placed into carton boxes for hatching.

2.2.2.2. Sperm collection

To test germline chimeras for germline transmission, the sperm of sexual mature roosters was collected. Therefore, the roosters had to be trained for sperm collection procedure. The feathers around the cloaca were cut and animals were placed onto a soft cover on the table. One person applied an abdominal massage to stimulate the gonads. The second person massaged the abdominal region of the cloaca and squeezed it. The sperm sample was collected in a 1.5 ml Eppendorf tube. Samples displaying high quality (white and viscous without faeces or blood contaminations) were further analyzed, otherwise the sample was discarded.

2.2.2.3. Blood collection

Blood from chicken embryos was taken on ED10-ED12. Therefore, the eggs were candled and a triangle window (approximately 1 cm x 1 cm x 0.5 cm) was drawn onto the eggshell where the underlaying blood vessel was clearly visible. The egg was carefully scored, the eggshell removed and a drop of paraffin oil was applied to the membrane to visualize the blood vessel. Blood draw was performed with a PBS/EDTA coated 30G insulin syringe and blood was placed onto a 96 well plate for further analysis. The eggshell was put back and sealed with tape.

Blood from hatched chicks and adult animals was taken from the *vena jugularis dextra*. In brief, the neck was sprayed with 70 % ethanol and blood volumes not more than the volumes

according to the governmental regulation guidelines of GV-Solas were taken. The blood was immediately placed into an EDTA coated microvette tube and mixed to avoid coagulation.

2.2.2.4. Injection of RCAS infected cells into the egg and bursa preparation

Chicken eggs were incubated 3 days before the injection. DF-1 cells were transfected with the desired "Replication Competent ALV LTR with a Splice acceptor" (RCAS) vector and expanded over several passages. Per injection $1x10^6$ cells/ embryo were needed. Shortly before the injection, the cells were detached by using 0.25x Trypsin-EDTA, washed with PBS, adjusted to $1x10^7$ cells/ml and transferred into a 1-ml syringe. The egg was disinfected with 70 % ethanol and scored at the flat pole without destroying the egg membrane. The cells were mixed by moving the syringe up and down. Per embryo, 100 µl of the cell suspension (correlates to $1x10^6$ cells) were injected into the egg. Note that the cannula is vertically inserted (ca. 2/3 of its length into the egg). The hole in the egg shell was sealed with tape. After the injection, the egg was quickly placed back into the incubator. At ED18, the bursa of Fabricius was isolated for B-cell preparation. B-cells were particularly chosen because the isolation of this cell type is a well-established method. The bursa was dissected, placed into an Eppendorf tube prepared with 1 ml sterile PBS and placed on ice. The bursa was homogenized by passing through a cell strainer. Another 1 ml sterile PBS was added to the cell suspension before Ficoll density gradient separation (12 min, 650 x g without break, RT) was performed. The resulting cells were taken from the interphase, washed with 5 ml PBS and centrifuged for 10 min at 475 x g (4 °C) before cells were counted and stained as described in 2.2.6.

2.2.2.5. *In vivo* infection with MDV strain RB-1B

The infection with a vvMDV strain RB-1B was performed in a specialized animal facility for viral infection experiments in Berlin and was conducted in collaboration with Prof. Benedikt Kaufer (Institute of Virology, FU Berlin, Germany).

Eggs from a heterozygous (+/-) Cas9 x MDV-gRNA breeding (LSL-classic) were collected and sent to the cooperation partner in Berlin. Blood was collected as described in 2.2.2.3 and genotyping to distinguish between WT, Cas9 and/or MDV-gRNA positive animals as described in 2.2.3.6 (see Figure 20 and Figure 21). Vaccine-Lohmann Specific-Pathogen-Free (Valo-SPF)

chickens were used as contact birds (i.e. not infected). After completing the genotyping, the flock was divided into a control group consisting of WT, Cas9-only- and MDV-gRNA-only-expressing animals (n=24) and a test group containing Cas9-MDV-gRNA animals (n=16). A scheme of the experimental workflow is shown in Figure 19. Valo-SPF contact birds hatched on the same day and were housed next to the groups (n=11) (Figure 19a,b). One day after the hatch, chicks from control and test group were infected with 1000 plaque forming units (pfu) of strain RB-1B as it was done in previous studies [61]. In order to determine and quantify the presence or absence of MDV genome copies during the experiment, blood and feather samples were collected (Figure 19c) and analyzed by MDV-*ICP4*-qPCR as described in [61]. The birds were monitored on a daily basis for MD-induced symptoms and tumorous lesions that included severe ataxia, paralysis, torticollis and somnolence. If symptoms appeared, chickens were euthanized and organs (spleen, bursa, thymus) collected (Figure 19d) for further analysis. In a final necropsy at the end of the experiment, all animals were examined. The RNA was isolated from spleen samples (see 2.2.3.3), followed by cDNA synthesis (see 2.2.3.5) and SYBR® Green q-RT-PCR analysis for Cas9 and MDV-gRNA (see 2.2.3.12).

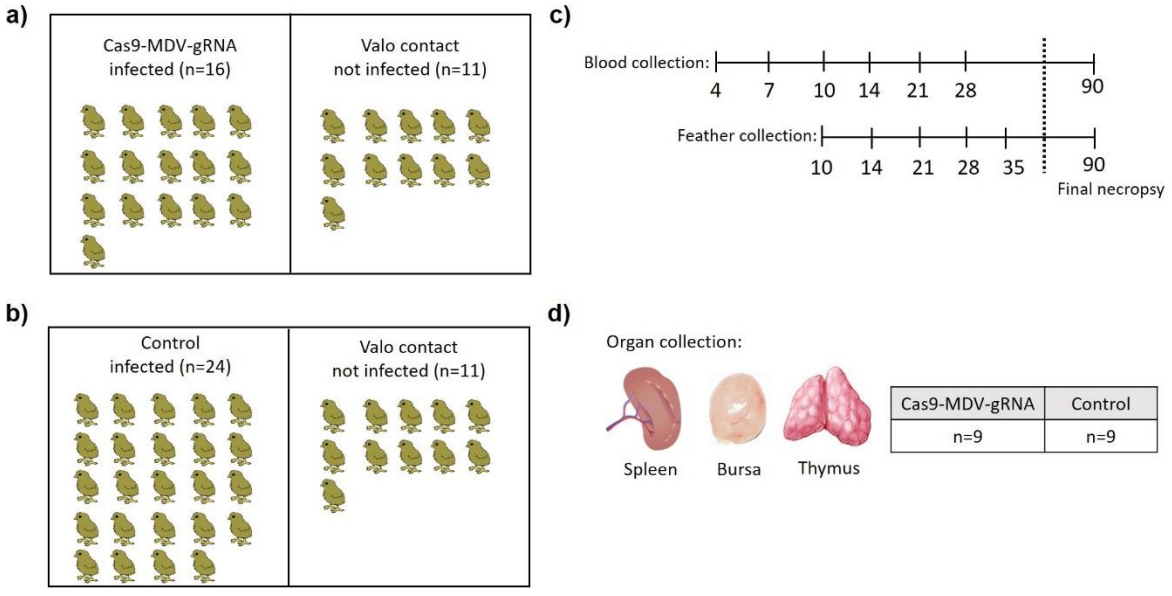

Figure 19: Experimental setup of the RB-1B infection challenge. a) Cas9-MDV-gRNA-expressing chicks (n=16) were infected with 1000 plaque forming units (pfu) on day one post hatch. Valo-SPF contact birds (n=11) were housed next to the test group and were not infected. b) Control animals (WT, Cas9-only and MDV-gRNA-only) (n=24) were infected with 1000 plaque forming units (pfu) on day one post hatch. Valo-SPF contact birds (n=11) were housed next to the control group and were not infected. c) Blood and feather samples were collected to determine MDV genome copies by MDV-*ICP4*-qPCR. Blood samples were collected on day 4, 7, 10, 14, 21, 28

post hatch. Feather samples were collected on day 10, 14, 21, 28, 35. Final necropsy was done at day 90 post hatch. d) Organs (spleen, bursa, thymus) were collected for both groups (n=9) and used for further analysis.

2.2.3. Molecular biology

2.2.3.1. Isolation of genomic DNA

Genomic DNA (gDNA) from cell pellets was isolated using ReliaPrep™ Blood gDNA Miniprep System. Approximately $1x10^6$ cells were pelleted and instructions according to manufacturer were followed. Briefly, the cell pellet was resuspended in 200 µl of Cell Lysis Buffer (CLD) and 20 µl of Proteinkinase K. The cells were vortexed and incubated for 10 min at 56 °C. 250 µl of Binding Buffer (BBA) was added and vortexed for 10 sec. The content was transferred to Reliaprep™ Binding Columns and centrifuged for 1 min at 16.000 x g. The flow through was discarded and 500 µl of Colum Wash Solution (CWD) was added to the column, followed by centrifugation for 3 min at maximum speed. The washing step was repeated for a total of three washes. The Column was transferred to a clean 1.5 ml Eppendorf tube and gDNA was eluted in 100 µl nuclease-free water. The gDNA was stored at -20 °C.

Genomic DNA from tissue samples was isolated by the "Quick & Dirty Protocol". Briefly, per sample 250 µl of the Lysis Buffer (Table 39) and 10 µl of Proteinkinase K (20 mg/ml) was added. The samples were vortexed and incubated overnight (12-20 h) at 56 °C (350 rpm). The day after, the samples was vortexed and centrifuged for 20 min at 3600 rpm (RT). After centrifugation, 50 µl of the supernatant was mixed with 50 µl of 100 % isopropanol. The samples were centrifuged for 15 min at 3600 rpm (RT). The supernatant was discarded and the pellet was dried for at least 10 min. The pellet was resuspended in 100 µl nuclease-free H_2O and incubated for 30 min at 56 °C (350 rpm). The gDNA was stored at -20 °C. Genomic DNA from 4 % paraformaldehyde (PFA) fixed tissue was isolated as described above with minor changes. The fixed tissue was washed with PBS to remove the residual PFA solution. The tissue was digested with 250 µl Lysis Buffer tissue and 10 µl Proteinkinase K (20 mg/ml), vortexed and incubate overnight at 56 °C, 500 rpm. The next day, the digested tissue was vortexed and gDNA isolation according to "Quick & Dirty Protocol" as described above was followed. The pellet was resuspended in 50 µl nuclease-free H_2O.

Genomic DNA from blood was isolated by either "Quick and Dirty Protocol" or ReliaPrep™ Blood gDNA Miniprep System. For large sample sizes, gDNA isolation by "Quick & Dirty"

method was used. Briefly, per sample 200 µl of STM buffer (Table 37) were mixed with 1µl of the EDTA-blood. After centrifugation at 1000 x g for 5 minutes (RT), the supernatant was discarded by flipping of the deep well 96 well plate. The last remains of fluid were thoroughly discarded by tapping the deep well 96 plate multiple times on a paper towel. Each pellet was resuspended in 400 µl TEN buffer (Table 36) supplemented with 100 µg/ml Pronase E. The deep well 96 plate was sealed and incubated for 1 h at 37 °C and 300 rpm. The reaction was stopped by heat inactivation at 65 °C for 20 minutes. If higher gDNA quality was required, ReliaPrep™ Blood gDNA Miniprep System was used. Briefly, 5 µl blood was mixed with 195 µl PBS and manufacturer´s instructions were followed. The gDNA was stored at -20 °C.

Genomic DNA from sperm samples was isolated by the "Quick & Dirty Protocol". Briefly, 5 µl sperm were mixed with 200 µl TEN buffer (Table 36) supplemented with 100 µg/ml Pronase E (Table 38) and incubated at 37 °C overnight. The next day, the reaction was heat inactivated at 65 °C for 10 minutes. The gDNA was stored at -20 °C.

2.2.3.2. Isolation of plasmid DNA

Transformed *E.coli* form colonies on Ampicillin containing lysogeny broth (LB) plates when incubated over night at 37 °C. The next day, plates were removed from the bacteria incubator, sealed with parafilm and placed in the fridge. In the afternoon, LB media was supplemented with ampicillin (100 µg/µl). The colonies were picked with a pipette tip and the tip was placed in the prepared tubes for shaking overnight at 37 °C and 250 rpm. On the next day, a glycerol stock was prepared (150 µl glycerol and 850 µl of the bacteria) before plasmid purification was done.

PureYield™ Plasmid Miniprep was used when lower DNA yields were desired. The protocol was followed according to manufacturer´s instructions. In brief, two times 1.5 ml of the DH5α bacterial culture was centrifuged for 1 min at 18.000 x g (RT) and the supernatant was removed. The cell pellet was resuspended in 600 µl nuclease-free H_2O, then 100 µl Cell Lysis Buffer was added and inverted at least 6 times for mixing. 350 µl Neutralization Buffer (stored at 4 °C in the fridge) was added and mixed by inverting at least 6 times. After centrifugation (3 min at 18.000 x g), the supernatant was transferred to a PureYield™ Mini Column and placed into a collection tube. The suspension was centrifuged (30 sec, 18.000 x g) and the

flowthrough was discarded. Subsequently, 200 µl of Endotoxin Removal Wash Solution was added and centrifuged for 30 sec at 18.000 x g. To wash the column, 400 µl of Column Wash Solution was added before centrifuging for another 30 sec 18.000 x g. speed. Plasmid DNA was eluted by adding 50-100 µl nuclease-free H_2O to the column, incubating for 1 min at RT, and followed by centrifugation for 30 sec at 18.000 x g.

PureYield ™ Plasmid Midiprep was used when large DNA yields were desired. Therefore, a bacterial day culture (4 ml LB + 4 µl Ampicillin) was transferred to a bigger volume of 250 ml LB medium + 250 µl Ampicillin and placed at 37 °C, 250 rpm overnight. On the next day, the cells were centrifuged (4000 x g, 12 min, RT) and the bacterial pellet was resuspended in 6 ml of Cell Resuspension Solution. 6 ml of Cell Lysis Solution was added and the solution was mixed by inverting several times. After incubating for 3 min at RT, 10 ml Neutralization Solution was added and again mixed by inverting the tube. The lysate was centrifuged (12.000 x g, 20 min, RT) and the supernatant was transferred to a PureYield™ Clearing Column placed into a PureYield™ Binding Column stacked onto a vacuum system. The vacuum was applied to suck the solution through. The PureYield™ Clearing Column was removed and 5 ml of Endotoxin Removal Wash Solution was added to the Column. By applying the vacuum, the suspension went through, followed by addition of 20 ml of Column Wash Solution. After letting the membrane dry out for 5 min, the Column was assembled in the Eluator™ Vacuum Elution Device. 400 – 500 µl nuclease-free H_2O was added and incubated for 1 min at RT before applying the vacuum.

2.2.3.3. Isolation of RNA

RNA isolation from cells was done by using ReliaPrep™ RNA Cell Miniprep System according to manufacturer´s instructions. Briefly, 1-5x10^6 cells were harvested and washed with PBS. After centrifugation at 300 x g for 5 min at RT, the cell pellet was carefully resuspended in BL and TG Buffer according to manufacturer´s instructions. The recommended amount of 100 % isopropanol was added and mixed by vortexing for 5 sec. The lysate was transferred to a Mini Column and centrifuged for 30 sec at 13.000 x g (RT). The flowthrough was discarded and 500 µl of RNA Wash Solution was added. After centrifugation for 30 sec at 13.000 x g (RT), DNAse I incubation mix was prepared by combining per sample 24 µl of Yellow Core Buffer, 3 µl of $MgCl_2$ (0.09 M) and 3 µl of DNAse I on ice. 30 µl of mix was added directly to the Mini Column

and incubated for 15 min at RT. 200 µl Column Wash Solution was added and the Column was centrifuged for 30 sec at 13.000 x g (RT). The flowthrough was discarded and first 500 µl, then after centrifugation (30 sec, 13.000 x g, RT), 300 µl of RNA Wash Solution was applied. The Mini Column was transferred to a clean 1.5 ml Eppendorf tube and RNA was eluted in 30 µl nuclease-free water. The RNA was stored at -80 °C.

RNA isolation from tissue was done by ReliaPrep™ RNA Tissue Miniprep System. Briefly, tissue samples were collected and stored in RNAlater until further use or processed directly. Each sample (max. 20 mg) was mixed with LBA+TG Buffer in an InnuSpeed lysis tube and homogenized in the continuous mode for 30 seconds. The liquid phase was used to isolate RNA according to manufacturer´s instructions. For fibrous tissues, an equal volume of RNA Dilution Buffer (RDB) was added and mixed by vortexing for 10 seconds. After incubating for 1 min at RT, a visible precipitate appeared. The homogenates were cleared by centrifugation for 3 min at 10.000 x g (RT) to pellet insoluble debris. The cleared lysates were transferred to Mini Columns and RNA isolation protocol was followed as described above.

2.2.3.4. Determination of DNA and RNA concentration

DNA and RNA concentrations were determined using a Nanodrop light spectrophotometer according to the manufacturers' protocol.

2.2.3.5. cDNA synthesis

For cDNA synthesis, GoScript™ Reverse Transcription Mix, Random Primers was conducted. Per sample, 10 µl of GoScript™ Transcription Mix containing 4 µl nuclease-free water, 4 µl GoScript™ Reaction Buffer Random Primers and 2 µl GoScript™ Enzyme Mix were mixed on ice. 400 ng RNA were diluted in nuclease-free water to a total volume of 10 µl. 10 µl of the GoScript™ Transcription Mix was mixed with 10 µl of RNA and placed into a thermocycler (25 °C, 5 min; 42 °C, 60 min; 70 °C, 15 min). After completion of the thermocycler run, the reaction was directly placed on ice for 5 min and diluted with another 20 µl nuclease-free water to a total volume of 40 µl. cDNA was stored at -20 °C.

2.2.3.6. Polymerase chain reaction

The polymerase chain reaction (PCR) is a molecular biological tool to amplify DNA fragments by using sequence specific primers. In this work, different polymerases were used which will be further depicted below. Table 41 summarizes the primers used in this work. The annealing temperatures were calculated by using the online tool "Tm Calculator" from NEB [227].

FIREPol® DNA polymerase is a thermostable *Taq* DNA polymerase with 5´ to 3´ enzyme activity and the ability to attach polyA tails. Its error rate can range between $2x10^{-4}$ - $2x10^{-5}$ [228,229]. FIREPol® DNA polymerase was used in order to amplify target fragments from genomic and plasmid DNA. Set up of the PCR mix was done under the laminar hood until DNA was added. PCR was performed with 5x FIREPol® DNA polymerase as described in Table 50. Thermocycler settings were used as recommended and are listed in Table 51.

Table 50: Composition of a FIREPol® reaction mix with a total volume of 20 µl

Component	**Amount**	**Final concentration**
5x FIREPol® Mastermix (5 U/µl)	4 µl	1 U/µl
Forward Primer [5 pmol/µl]	1 µl	0.25 µM
Reverse Primer [5 pmol/µl]	1 µl	0.25 µM
DNA	x µl	5-50 ng/µl
Nuclease-free water	Add to 20 µl	

Table 51: Thermocycler settings for PCR with FIREPol® DNA polymerase

Step	**Temperature**	**Time**	**Cycles**
Initial Denaturation	95 °C	3 minutes	1
Denaturation	95 °C	30 seconds	25-35
Annealing	50-68 °C	30 seconds	
Elongation	72 °C	~ 1 min/ 1 kb	
Final Elongation	72 °C	5 minutes	1
Hold	12 °C	Infinite	

For Cas9 genotyping, FIREPol® Cas9 PCR as described in Figure 20 was performed.

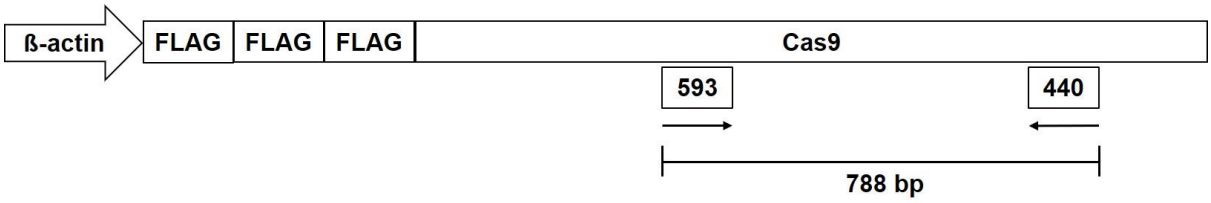

Figure 20: FIREPol® Cas9 PCR used for genotyping. The forward primer 593 and the reverse primer 440 were used. Annealing temperature was 58 °C and elongation time 1 minute. The expected amplicon was 788 bp. Figure not to scale: The chicken β-actin promoter is 1340 bp long, each FLAG tag is 24 bp long and the Cas9 sequence is 4272 bp long.

FIREPol® MultiPlex Mix was used for sex determination with W- and Z-chromosome specific primers (Table 41). PCR was performed as described in Table 52. Thermocycler settings were used as recommended and are summarized in Table 53.

Table 52: Composition of a FIREPol® MultiPlex Mix with a total volume of 20 µl

Component	**Amount**	**Final concentration**
5x FIREPol® MultiPlex Mix	4 µl	1x
Forward Primer 1 + 3 [5 pmol/µl]	1 µl each	0.25 µM
Reverse Primer 2 + 4 [5 pmol/µl]	1 µl each	0.25 µM
DNA	x µl	5-50 ng/µl
Nuclease-free water	Add to 20 µl	

Table 53: Thermocycler settings for PCR with FIREPol® MultiPlex Mix for sexing

Step	**Temperature**	**Time**	**Cycles**
Initial Denaturation	95 °C	12 minutes	1
Denaturation	95 °C	30 seconds	25-35
Annealing	56 °C	30 seconds	
Elongation	72 °C	~ 1 min/ 1 kb	
Final Elongation	72 °C	5 minutes	1
Hold	12 °C	Infinite	

Q5® High-Fidelity DNA polymerase is a thermostable DNA polymerase with 3´ to 5´exonuclease activity. With its error rate being $5.3x10^{-7}$ [230], it is approx. 280-fold lower

than the error rate of the *Taq* DNA polymerase [231]. The proof-reading function of the Q5® High-Fidelity DNA polymerase was used for cloning and amplifying PCR fragments for INDEL analysis. The reaction mix was pipetted according to Table 54. The assembly of the reaction components was performed on ice and quickly transferred to the thermocycler. Thermocycler settings were used as recommended and listed in Table 55.

Table 54: Composition of Q5® reaction mix for one reaction

Component	**25 µl Reaction**	**50 µl Reaction**	**Final concentration**
5x Q5® Reaction Buffer	5 µl	10 µl	1x
dNTPs (10 mM)	0.5 µl	1 µl	200 µM
Forward Primer [10 pmol/µl]	1.25 µl	2.5 µl	0.5 µM
Reverse Primer [10 pmol/µl]	1.25 µl	2.5 µl	0.5 µM
Template DNA	variable	Variable	< 1 µg
Q5® DNA Polymerase (2 U/µl)	0.25 µl	0.5 µl	0.02 U/ µl
5x Q5® Enhancer *optional	5 µl	10 µl	1x
Nuclease-free H_2O	Add to 25 µl	Add to 50 µl	

Table 55: Thermocycler settings for PCR with Q5® DNA polymerase

Step	**Temperature**	**Time**	**Cycles**
Initial Denaturation	98 °C	30 seconds	1
Denaturation	98°C	10 seconds	25-35
Annealing	50-72 °C	30 seconds	
Elongation	72 °C	~20-30 seconds/ 1 kb	
Final Elongation	72 °C	2 minutes	1
Hold	12 °C	Infinite	

LongAmp® *Taq* DNA polymerase was used for long range PCRs, especially for genotyping of MDV-gRNA animals. The composition of one reaction is shown in Table 56. The assembly of these reaction components was performed on ice and quickly transferred to the thermocycler. The program of the thermocycler is summarized in Table 57.

Table 56: Composition of a LongAmp® reaction mix for one reaction

Component	**25 µl Reaction**	**50 µl Reaction**	**Final Concentration**
5x LongAmp® Taq Reaction Buffer	5 µl	10 µl	1x
dNTPs (10 mM)	0.75 µl	1.5 µl	300 µM
Forward Primer [10 pmol/µl]	1 µl	2 µl	0.4 µM
Reverse Primer [10 pmol/µl]	1 µl	2 µl	0.4 µM
Template DNA	variable	variable	<1,000 ng
LongAmp® Taq DNA Polymerase (2.5 U/µl)	1 µl	2 µl	0.1 U/µl
Nuclease-free H_2O	Add to 25 µl	Add to 50 µl	

Table 57: Thermocycler settings for PCR with LongAmp® *Taq* DNA polymerase

Step	**Temperature**	**Time**	**Cycles**
Initial Denaturation	94 °C	30 seconds	1
Denaturation	94 °C	30 seconds	30
Annealing	45-65 °C	15-60 seconds	
Elongation	65 °C	~50 seconds/ 1 kb	
Final Extension	65 °C	10 minutes	1
Hold	12 °C	Infinite	

Genotyping of MDV-gRNA-expressing animals was done by LongAmp® PCR as described in Figure 21.

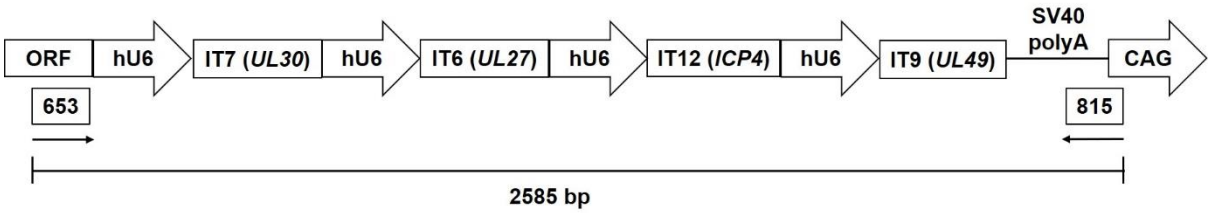

Figure 21: LongAmp® MDV-gRNA genotyping PCR covering the four MDV-gRNA cassettes. The forward primer 653 is binding to the open reading frame (ORF) region. The reverse primer 815 is binding after the SV40 polyA sequence. The resulting amplicon is 2585 bp long. Figure is not to scale. The human U6 promoter is 236 bp long, the gRNA sequences are 20 bp long, and the gRNA scaffold sequences are 79 bp long.

2.2.3.7. Agarose gel electrophoresis

Agarose gel electrophoresis is a method to separate DNA by mass and thus by size [232]. The negatively charged DNA is running towards a cathode. If the DNA fragment is relatively small, it will pass quickly through the gel. Bigger fragments need more time to cover the same distance.

Tris-Borate-EDTA-Buffer (TBE) gel electrophoresis was used for detection of amplicons after PCR reaction or DNA detection after control restriction digests. Tris-Acetate-EDTA-Buffer (TAE) was used when DNA fragment was cut out from gel for purification.

If not otherwise mentioned, 1 % TBE agarose gels were used. For a 50 ml gel, 0.5 g agarose was mixed with 50 ml buffer and heated in the microwave. The bottle was cooled down to ~50 °C before 2 µl peqGREEN /50 ml buffer was added. PeqGREEN is a DNA-binding dye and makes DNA molecules detectable by UV- or blue light. The fluid was poured into a gel chamber and a comb was placed into it. Upon gel polymerization, the gel with its chamber was placed into a buffer filled gel electrophoresis apparatus. A total volume of 10 µl sample were loaded in each pocket consisting of 2-5 µl DNA product, diluted with 5-8 µl of dH_2O and 2 µl of 6x Orange G Loading Dye. To determine the band size of the sample, 8 µl of 1 kb DNA ladder was loaded in a separate pocket. The voltages ranged dependent on the size of the gel between 90 and 140 V. After 30-90 minutes, the run was stopped and the DNA was detected by using Quantum ST5.

2.2.3.8. DNA purification from agarose gel

DNA was extracted from 1 % TAE agarose gels as recommended by Ultra-Sep® Gel Extraction Kit. Briefly, 700 µl of the Binding Buffer and 10 µl of the beads were placed in an Eppendorf tube and vortexed before it was incubated for 10 min at 50 °C in the thermos mixer. The tube was vortexed every 2 min during the incubation. After centrifugation for 1 min at 10.000 x g (RT), the liquid was discarded and 300 µl of Binding Buffer was added. The tube was centrifuged for 1 min at 10.000 x g (RT) and the liquid was discarded. 750 µl of DNA Wash Buffer was added and centrifuged for 1 min at 10.000 x g (RT). The pellet was air-dried for 30 min before the DNA was eluted by adding 15-30 µl of Elution Buffer. The pellet was

resuspended and incubated for 5 min at 50 °C. The DNA concentration was measured by using a Nanodrop. The DNA was stored at -20 °C.

2.2.3.9. Purification of PCR product

To purify a PCR product the Wizard® SV Gel and PCR Clean-Up System was used. The DNA Purification Protocol by Centrifugation was followed. An equal volume of Membrane Binding Solution was added to the PCR product and pipetted onto a SV Mini Column placed into a Collection Tube. After incubating for 1 min at RT, the Eppendorf tube was centrifuged for 1 min at 16.000 x g (RT). The flow through was discarded and 700 µl Membrane Wash Solution was added. The tube was centrifuged for 1 min at 16.000 x g (RT) and the flow through was discarded. 500 µl Membrane Wash Solution was added and the solution was centrifuged for 5 min at 16.000 x g (RT). The flowthrough was discarded and the tube was centrifuged for 1 min at 16.000 x g (RT) with the lid open to let the ethanol residuals evaporate. DNA was eluted by adding 25 µl of nuclease-free H_2O, followed by 1 min incubation at RT. After a final centrifugation step for 1 min at 16.000 x g (RT), the DNA concentration was measured using a Nanodrop. The DNA was stored at -20 °C.

2.2.3.10. Digital droplet PCR

Droplet digital polymerase chain reaction (ddPCR) is a method to quantify nucleic acids within a single droplet and was used to calculate the copy number of a target gene (hygromycin). A reference gene is needed for this purpose.

The template DNA was digested for 1 h at 37 °C with XbaI, as this restriction enzyme has many restriction sites within most DNA sequences (Table 58). Note that the enzyme should not cut within the desired amplicon sequence. After heat inactivation at 65 °C for 20 min, the samples were used directly or stored at -20 °C.

Table 58: XbaI digestion mix for a reaction of 50 µl

Component	**Amount**	**Final concentration**
XbaI enzyme (20 U/µl)	1 µl	0.4 U/µl
CutSmart® Buffer (10x)	5 µl	1x

DNA template	500 ng	
Nuclease-free H_2O	Add to 50 µl	

The digested samples were diluted, 5 µl DNA + 5 µl H_2O, to a final concentration of 5 ng/µl. 2 µl (= 10 ng) from this dilution were used per one ddPCR supermix reaction. Components were mixed on ice. Volumes and concentrations for one ddPCR supermix reaction of 25 µl are listed in Table 59.

Table 59: ddPCR supermix for one reaction of 25 µl

Component	**Volume**	**Final concentration**
2x ddPCR supermix for probes	12.5 µl	1x
20x target primer/probe mix (FAM)	1.25 µl	250 nM probe; 900 nM primer
20x reference primer/probe mix (HEX)	1.25 µl	250 nM probe; 900 nM primer
Template DNA	2 µl	10 ng
Nuclease-free H_2O	Add to 25 µl	

Droplets were generated using a QX200™ Digital Droplet Generator. 20 µl of the mastermix + template (middle row) and 70 µl of droplet oil (lower row) was placed onto the cartridge, covered with the red gasket and placed into the droplet generator. 40 µl of the generated emulsion was placed onto a 96 well plate and sealed with aluminum foil. The plate was inserted into a PCR thermocycler and ddPCR program was applied (Table 60).

Table 60: Thermocycler program for ddPCR

Step	**Temperature**	**Time**	**Ramp rate**	**Cycles**
Initial denaturation	95 °C	10 minutes	2 °C/sec	1
Denaturation	94 °C	30 seconds		40
Annealing/extension	59 °C	1 minutes		
Signal stabilization	4 °C	5 minutes		1
	98 °C	5 minutes		1
Infinite hold	12 °C	Infinite		

After the cycler run, the plate was either placed directly into the QX200 digital droplet reader or stored overnight at 4 °C before readout was done the next day.

2.2.3.11. Taqman™ quantitative PCR

For MDV-gRNA genotyping, probes for each MDV-gRNA were designed (Figure 22) and Taqman™ quantitative real-time PCR (q-RT-PCR) was performed according to manufacturer´s instructions, briefly displayed in Table 61 and Table 62.

Table 61: 5x HOT FIREPol® Probe qPCR Mix Plus (no ROX) for one reaction of 20 µl

Component	**20 µl Reaction**	**Final Concentration**
5x HOT FIREPol® Probe qPCR Mix Plus (no ROX)	4 µl	1x
Forward Primer [10 pmol/µl]	0.4 µl	200 nM
Reverse Primer [10 pmol/µl]	0.4 µl	200 nM
Probe [10 pmol/µl]	0.2 µl	100 nM
Template DNA	2 ng	
Nuclease-free H_2O	Add to 20 µl	

Table 62: Thermocycler settings recommended for Taqman™ qPCR

Step	**Temperature**	**Time**	**Cycles**
Initial activation	95 °C	12 minutes	1
Denaturation	95 °C	15 seconds	40
Annealing/elongation	60 °C	60 seconds	

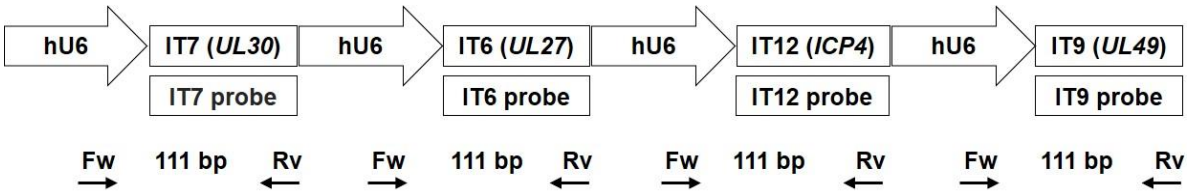

Figure 22: Taqman™ q-RT-PCR assay to detect MDV-gRNAs. Established primers (817, 818) and 5´FAM/3´BHQ1-labelled probes for the detection of individual MDV-gRNAs. Arrows represent forward and reverse primers. Plot is not to scale.

2.2.3.12. SYBR® GREEN qPCR

SYBR® Green q-RT-PCR was used to measure the expression levels of Cas9 (Figure 23) and individual four MDV-gRNAs (Figure 24) in different samples. The reaction mix in Table 63 and thermocycler settings summarized in Table 64 were used. The reaction mix was calculated for each primer pair individually. The housekeeping gene 18S was used for data normalization. Expression levels were calculated according to the following equations:

$$\Delta ct = ct\ (target\ gene) - ct\ (housekeeping\ gene)$$

$$\Delta\Delta ct = \Delta ct\ (sample) - \Delta ct\ (wt)$$

$$n\text{-}fold\ expression = 2^{-\Delta\Delta ct}$$

Table 63: Composition of SYBR® Green qPCR Master Mix

Component	**Amount**	**Final concentration**
2x Gotaq® qPCR Master Mix	12.5 µl	1x
Forward Primer [5 pmol/µl]	1.5 µl	300 nM
Reverse Primer [5 pmol/µl]	1.5 µl	300 nM
cDNA Template DNA	5 µl	10 ng
Nuclease-free H_2O	Add to 25 µl	

Table 64: Thermocycler settings for SYBR® Green qPCR reaction

Step	**Temperature**	**Time**	**Cycles**
Initial activation	95 °C	2 minutes	1
Denaturation	95 °C	15 seconds	40
Annealing	59 °C	30 seconds	
Extension	72 °C	10 seconds	
Dissociation stage	95 °C	15 seconds	1
	57 °C	30 seconds	
	95 °C	15 seconds	

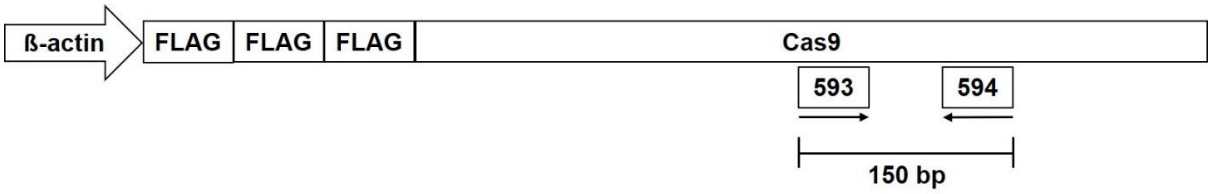

Figure 23: SYBR® Green q-RT-PCR established to detect Cas9. Short amplicon RT-PCR primers 593 and 594 were used. Arrows represent forward and reverse primers. The amplicon size is 150 bp. Figure not to scale: The chicken β-actin promoter is 1340 bp, each FLAG tag is 24 b and the Cas9 sequence is 4272 bp long.

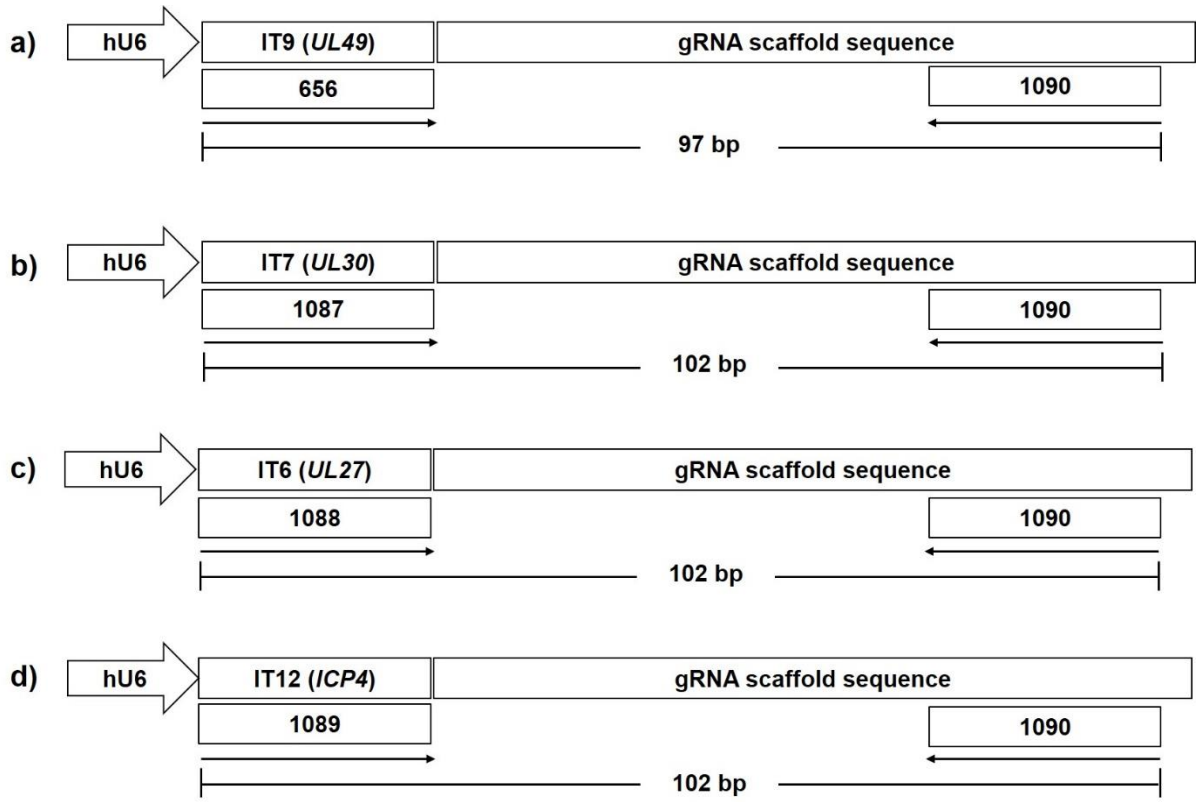

Figure 24: SYBR® Green q-RT-PCR established to detect individual MDV-gRNA sequences. The forward primers were design for each MDV-gRNA individually. The same reverse primer 1090 was used in each reaction as it binds to the gRNA scaffold sequence present in all gRNAs. Arrows represent forward and reverse primers. Assay adapted from Aparicio et al. [233] a) Detection of MDV-gRNA IT9 (*UL49*). b) Detection of MDV-gRNA IT7 (*UL30*). c) Detection of MDV-gRNA IT6 (*UL27*). d) Detection of MDV-gRNA IT12 (*ICP4*). Expected amplicon size was 102 bp, except for IT9 detection (97 bp). Figure not to scale: human U6 promoter = 236 bp; gRNA sequences = 20 bp; gRNA scaffold sequence: 79 bp.

2.2.4. Cloning

2.2.4.1. Gibson Assembly

Gibson assembly is a commonly used method to assemble DNA fragments to generate plasmid constructs. After generating DNA fragments with overlapping ends by either

restriction digest or PCR, the fragments can form a circular plasmid due to complementary base pairing of these overlapping ends.

All Gibson assembly reactions were performed by using 10 µl of NEBuilder® HiFi DNA Assembly Mastermix, 100 ng of the backbone DNA and 200 ng of the insert DNA. For two fragments, the ratio of vector to insert was 1:2. For three fragments, the DNA was mixed in the ratio vector to inserts 1:2:2. The assembly was performed in a thermocycler at 50 °C for 60 min.

2.2.4.2. Transformation of chemically competent *E. coli*

The *E. coli* strains DH5α or NEBalpha were used for transformation. The bacteria were thawed slowly on ice before 2 µl of the assembled product was added and incubated for 30 min on ice. After a heat shock (42 °C, 30 sec), the cells were transferred for 2 min back on ice. 950 µl of SOC medium was added. The tube was placed on a shaker for 60 min at 37 °C and 200 rpm. The transformed bacteria were plated in three different volumes on Ampicillin (Amp) selected plates (50 µl, 100 µl, remaining volume). After 20 min of incubation at RT, the plates were stored overnight upside-down in the bacteria incubator at 37 °C.

2.2.4.3. Blunting (Klenow)

Blunting was used to ligate DNA fragments with incompatible ends by using the DNA polymerase I, large (Klenow) fragment. Klenow is able to remove sticky ends from the 3`-end and fills up nucleotides at the 5`-overhangs so that blunt ends are created. Briefly, after performing a restriction digest as further described in section 2.2.4.9, 2 µl of 2 mM dNTPs and 1 U/µg of DNA polymerase I, large (Klenow) fragment was added to a 50 µl reaction mix and incubated at 25 °C for 15 min in the heat block. The reaction was inactivated by heating for 20 min at 75 °C.

2.2.4.4. Dephosphorylation with CIAP

To avoid religation of the backbone vector, 5`-phosphates were removed by using Calf Intestinal Alkaline Phosphatase (CIAP). After restriction digest and blunting as described in

2.2.4.9 and 2.2.4.3, 1 µl of CIAP Enzyme and 5 µl of CIAP Buffer was added to a 20 µl reaction. The reaction was incubated for 30 min at 37 °C, then again 1 µl of CIAP Enzyme was added for another 30 min at 37 °C. The product was purified by using Wizard® SV Gel and PCR Clean-Up System.

2.2.4.5. T4 Ligation

Digested and dephosphorylated DNA vector backbone and digested insert DNA fragments were ligated by using T4 DNA ligase. Reactions were set up according to Table 65 and incubated overnight at 4 °C. The ratio of vector and insert was calculated according to the following equation:

$$Vector\ amount\ (ng) \div Vector\ size\ (bp) = X \div Insert\ size\ (bp)$$

Table 65: Composition of T4 DNA ligation reaction

Component	**Amount**	**Final concentration**
DNA backbone vector	100 ng	
DNA insert	Dependent on ratio 1:2-1:8 (vector : insert)	
T4 DNA Ligase (400 U/µl)	0.5 µl	20 U/µl
T4 DNA Ligase Buffer (10x)	1 µl	1x
Nuclease-free H_2O	Add to 10 µl	

2.2.4.6. Colony PCR

Colony PCR was performed to determine positive clones after correct assembly. Briefly, single colonies were picked and placed into a deep well 96 plate filled with 600 µl LB medium + Ampicillin (100 µg/µl). The colonies were incubated for 3.5 h at 37 °C and 500 rpm. 2 µl of the bacteria suspension was used for FIREPol® PCR as described in section 2.2.3.6.

2.2.4.7. CRISPR cloning

CRISPR cloning describes the process of integrating sgRNAs into a CRISPR vector (e.g. px330). The procedure can be divided into three parts: 1. Phosphorylation and oligonucleotide annealing; 2. Digestion ligation reaction; 3. PlasmidSafe reaction [115,216].

In the first part, two oligonucleotides coding for the sgRNA were phosphorylated and annealed together according to the following instruction described in Table 66 and Table 67.

Table 66: Phosphorylation and oligonucleotide annealing (step 1)

Component	**Amount**	**Final concentration**
Oligo 1 [100 pmol/µl]	1 µl	10 µM
Oligo 2 [100 pmol/µl]	1 µl	10 µM
T4 Polynucleotide Kinase Buffer (10x)	1 µl	1x
T4 Polynucleotide Kinase (10 U/µl)	0.5 µl	0.5 U/µl
Nuclease-free H_2O	Add to 10 µl	

Table 67: Thermocycler settings - phosphorylation and oligonucleotide annealing (step 1)

Step	**Temperature**	**Time**	**Cycles**
Step 1	37 °C	30 minutes	Ramp down to 25 °C (5 °C/min)
Step 2	95 °C	5 minutes	

In the second part, a digestion & ligation step is need to assemble the CRISPR vector with the sgRNA oligonucleotides from step 1. Table 68 shows the components needed for the reaction. The annealed oligonucleotides from step 1 were diluted 1:250 before use. Table 69 shows the thermocycler settings used for the digestion & ligation step.

Table 68: Digestion & ligation of annealed oligonucleotides (step 2)

Component	**Amount**	**Final concentration**
DNA backbone vector	100 ng	
Diluted annealed oligos from step 1 (1:250)	2 µl	
Tango Buffer (10x)	2 µl	1x
DTT (10 mM)	1 µl	0.5 mM
ATP (10 mM)	1 µl	0.5 mM
FastDigest Bbsl (Bpil) (10 U/µl)	1 µl	0.5 U/µl
T7 Ligase (3.000 U/µl)	0.5 µl	75 U/µl
Nuclease-free H_2O	Add to 20 µl	

Table 69: Thermocycler settings – Digestion & ligation (step 2)

Step	**Temperature**	**Time**	**Cycles**
Digestion	37 °C	5 minutes	6
Ligation	23 °C	5 minutes	
Hold	12 °C	Infinite Hold	

To prevent unwanted recombination products, a PlasmidSafe reaction was performed according to the following instructions (Table 70). The reaction was incubated at 37 °C for 30 min in the thermocycler before 2 µl from the reaction were used for transformation into chemically competent *E. coli* as described in 2.2.4.2.

Table 70: PlasmidSafe reaction (step 3)

Component	**Amount**	**Final concentration**
Ligation Reaction (from step 2)	11 µl	
PlasmidSafe Exonuclease (DNAse) (10 U/µl)	1 µl	0.66 U/µl
PlasmidSafe Buffer (10x)	1.5 µl	1x
ATP (10 mM)	1.5 µl	1 mM

2.2.4.8. Cloning by pGEM®-T Easy Vector Systems

Cloning PCR products with pGEM®-T Easy Vector Systems was used to verify all four MDV-gRNA sequences in MDV-gRNA-expressing animals. First, FIREPol® PCR was performed to generate amplicons with A tails as this is essential for further pGEM®-T Easy cloning. The protocol according to manufacturer´s instruction was used. Briefly, the following ligation reaction was set up as described in Table 71. The vector : insert ration was calculated as followed:

$$\frac{Vector\ (ng)\ x\ Size\ of\ insert\ (kb)}{Size\ of\ vector\ (kb)}\ x\ Insert{:}Vector\ molar\ ratio = \ Insert\ (ng)$$

The reaction was incubated for 1 h at RT or alternatively overnight at 4 °C. 2 µl of the ligation reaction was used for transformation into chemically competent *E. coli* as described in Chapter 2.2.4.2, except that bacteria was incubated for 20 min on ice, followed by heat shock at 42 °C for 45 sec. The bacteria were plated onto ampicillin (100 µg/µl) and X-Gal (120 µl/plate) coated plates before they were incubated overnight at 37 °C. The next day, only white colonies were selected.

Table 71: Components for pGEM®-T Easy cloning

Component	**Amount**	**Final concentration**
2x Rapid Ligation Buffer, T4 DNA Ligase	5 µl	1x
pGEM®-T Easy Vector	X µl	50 ng
PCR product (depending on calculated ratio)	X µl	
T4 DNA Ligase (3 Weiss U/ µl)	1 µl	0.3 U/µl
Nuclease-free H_2O	Add to 10 µl	

2.2.4.9. Restriction enzyme digest

Plasmid digest after cloning was used to determine site specific insertion of DNA fragments into a vector. As restriction enzymes bind to specific target sequences, they cleave DNA into fragments and can therefore be used as a molecular cloning tool. The program SeqBuilder and the online tool Benchling [234] were used. Restriction digestion was performed according to manufacturer´s instructions and composition for one reaction of 20 µl can be found in Table 72.

Table 72: Restriction digest mix for one reaction of 20 µl

Component	**Amount**	**Final concentration**
Plasmid DNA	X µl	500 ng - 1 µg
Buffer	2 µl	
Enzyme 1 (20 U/µl)	0.5 µl	0.5 U/µl
Enzyme 2 (20 U/µl)	0.5 µl	0.5 U/µl
Nuclease-free H_2O	Add to 20 µl	

2.2.5. Western blot analysis

Protein was isolated from tissue samples of Cas9-expressing chickens by homogenization with cold radioimmunoprecipitation assay buffer (RIPA buffer) in InnuSPEED Lysis Tubes using a speedmill homogenizer. To ensure complete homogenization, tissue was homogenized three times á 30 sec in continuous mode. The homogenates were centrifuged at 4 °C at 1000 x g for 5 min and supernatants were used for further analysis. The samples were boiled with 6x Laemmli sample buffer for 5 min at 95 °C. Protein samples were separated by SDS-PAGE electrophoresis using a 9 % Tris-Cl/SDS-separation stacked onto a 4 % Tris-Cl/SDS collection gel (Table 73) for 15 min at 80 V followed by 45 min at 200 V.

Table 73: Composition of separation and collection gel for Western blot analysis

9 % Separation gel		**4 % Collection gel**	
Component	**Volume**	**Component**	**Volume**
30 % acrylamide	3.0 ml	30 % acrylamide	650 µl
4x Tris-Cl/SDS (pH 8.8)	2.5 ml	4x Tris-Cl/SDS (pH 6.8)	1.25 ml
APS	50.0 µl	APS	25.0 µl
TEMED	10.0 µl	TEMED	7.5 µl
dH_2O	4.5 ml	dH_2O	3.05 ml

PageRuler Pre-stained and MagicMark™ XP Western Protein Standard were mixed 1:1 and used as protein markers. Mixing both marker together has the advantage that protein marker and samples can easier be overlayed as the MagicMark™ XP Western Protein Standard can also be detected by a HRP conjugated secondary antibody. Using PageRuler Pre-stained has the advantage that the marker is visible so that the progress of the SDS-PAGE can be followed while it is running. Proteins were transferred from the gel onto nitrocellulose membranes and surrounded with filter paper and foam pads as displayed in Figure 25. The transfer was facilitated at 100 V for 60 min using the Bio-Rad wet tank blotting system. Membranes were blocked for 1 hour at room temperature or at 4 °C overnight with 4 % nonfat milk in PBS-T. The membranes were separated through cutting them into half so that membranes could be incubated in parallel. The upper part of the membrane where the Cas9 protein was expected (165 kDa) was incubated with a primary mouse IgG anti-Cas9 (1.25 µg/ml); the lower part of the membrane where the beta-actin protein was expected (42 kDa) was incubated with a primary mouse IgG anti-chicken beta-actin (1.0 µg/ml) as a loading control. The primary antibodies were diluted in 4 % milk/PBS-T and membranes incubated for 1 hour at room temperature or at 4°C overnight. After washing the membranes for three times with PBS-T for 10 min, the membranes were incubated with a peroxidase-conjugated donkey anti-mouse antibody (0.04 µg/ml) in 4 % milk/PBS-T for 1 hour at RT. The secondary antibody was removed be washing six times for 10 mins with PBS-T. The membranes were exposed to clarity enhanced chemiluminescence (ECL) reagents for 1 min. The proteins were visualized using Fusion FX by detecting the chemiluminescent signal produced by the reaction with horseradish peroxidase.

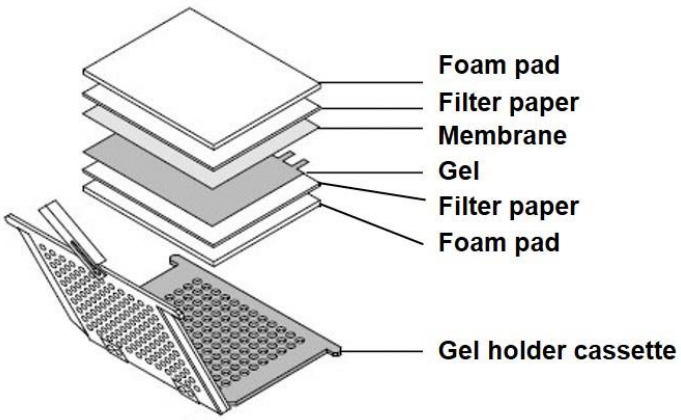

Figure 25: Instructions for Western blotting. The order of the stacking is essential for correct blotting. Figure modified from Trans-Blot® Cell (Bio-Rad) [235].

2.2.6. Flow cytometry analysis

Extracellular staining was performed with $1x10^6$ cells per well plated onto a 96 well plate. All incubation steps were done on ice and in the dark. The cells were pelleted at 700 x g for 1 min and the supernatant was discarded. The cell pellet was resuspended in 50 µl of the primary antibodies (Table 40) diluted in Fluo-buffer (Note: One or more primary antibodies can be mixed together depending on conjugation, isotypes and specificity). After 20 minutes, the cells were washed by adding 150 µl of Fluo-buffer to remove unbound primary antibodies. The cells were centrifuged at 700 x g for 1 min and the supernatant was discarded. The cells were washed again with 200 µl of Fluo-buffer and centrifuged. The cells were resuspended with the secondary antibody (Table 40) diluted in Fluo-buffer. After 15 minutes incubation, the cells were washed as described above, resuspended in 400 µl Fluo-buffer and transferred to FACS tubes.

Live/dead staining was performed to focus on living cells. The staining was done with 7 Amino actinomycin D (7AAD) viability dye (diluted 1:100 in Fluo-buffer) at the end or with Fixable Viability Dye eFluor 780 (diluted 1:1000 in Fluo-buffer) in the beginning before the first antibody was applied.

Intracellular staining was performed for the detection of antigens that are not located on the cell surface. Briefly, $1x10^6$ cells were plated on a 96 well plate and the cells were treated as described above, additionally the cells were fixed and permeabilized before staining procedure. Fixation and permeabilization was performed according to eBioscience™ Intracellular Fixation/Permeabilization protocol.

Analysis was performed by using Attune NxT Flow Cytometer. Data analysis was done with FlowJo v10.4.1. software (FlowJo, LLC 2006-2017, USA). All antibodies used in this work are listed in Table 40.

2.2.7. Statistical analysis and graphs

Statistical analysis was carried out in this thesis to find significant differences between datasets. Therefore, SPSS24 statistics v24.0.0.0 or Python v3.7 depending on the task and convenience of access was used. In a first step, the data was tested for normality with a Shapiro-Wilk test. If the *p*-value was larger than 0.05, the data was assumed to be normally distributed. In cases where the sample size was insufficiently large, or biased by double occurrences, data was assumed to be normally distributed if comparable datasets were normally distributed as well. To determine if the mean between two normally distributed datasets is significantly different, a Student's t-test was employed. Data that was not normally distributed was tested for significance by means of a Mann-Whitney U test unless stated otherwise. Table 74 shows definitions of significances.

Table 74: Definitions for statistical analysis

Meaning (Symbol)	***p*-value**
Not significant (NS)	$p>0.05$
Significant (*)	$p\leq0.05$
Significant (**)	$p\leq0.01$

Graphs were constructed using GraphPad Prism v8.0.1. Plasmid maps were generated using BioRender [236].

3. RESULTS

3.1. Generation of chickens with ubiquitous Cas9 expression

3.1.1. Highest Cas9 germline transmission in C4

The first step of generating genetically modified chickens requires successful genome editing in PGCs and the colonization of the gonads by these cells to create chimeric animals [163]. To generate Cas9 germline chimeras, EGFP-expressing PGCs (LSL-EGFP 165-2 Line 54) that already carried the EGFP transgene were stably transfected with the Cas9 expression construct (see Figure 14) (Cas9-EGFP) and single cell clones were selected with hygromycin. Three single cell clones (C2, C4, C5) were further expanded and injected into 65 h old (H&H stage 13-15) embryos as described in Chapter 2.2.2.1. Table 75 summarizes the number of injected embryos, the number of total chimeras hatched and chimeric roosters that resulted from the injections, respectively. Six chimeric roosters were obtained from PGC single cell clone 2, 19 from clone 4 and 22 from clone 5.

Table 75: Overview of Cas9 injections

Cell line (age at injection)	Injected embryos	Total chimeras	Males
LSL EGFP PGC (54) Cas9 C2 (93 days old)	103	7	6
LSL EGFP PGC (54) Cas9 C4 (97 days old)	60	39	19
LSL EGFP PGC (54) Cas9 C5 (100 days old)	59	41	22

Upon sexual maturity, sperm was collected from chimeras and analyzed for the presence of the transgene by PCR with primers specifically detecting the Cas9 gene. The highest transmissions were observed in chimeras originating from PGC single cell clone C4 (4.68 % for EGFP and 3.12 % for Cas9). The transmission of chimeras originating from PGC single cell clone C2 was 1.54 % for EGFP and 0.69 % for Cas9. The transmission of chimeras originating from PGC single cell clone C5 was 0.42 % for EGFP and 0 % for Cas9 (Table 76). Chimeric roosters #42545, #42563, #42567 and #42569 (C4) were bred with WT hens resulting in five non-chimeric heterozygous animals. Four Cas9-positive embryos were observed in the offspring from chimeras originated from clone 2. No Cas9-positive embryo or chick was derived from roosters originated from clone 5.

Table 76: Overview of Cas9 transmission. The transmission rate was calculated according to the number of fertilized eggs

Clone	Eggs set for hatch	Fertilized eggs	Hatched	EGFP	EGFP/ Cas9	Cas9 embryo	Cas9 chick	EGFP (%)	Cas9 (%)
C2	629	583	278	9	1	4	0	1.54	0.69
C4	668	577	427	27	5	13	5	4.68	3.12
C5	273	238	168	1	0	0	0	0.42	0

3.1.2. Cas9 copy number analysis

Cas9 copy numbers in PGC single cell clones (C2, C4, C5) and tissue from a dead embryo (derived from C2) were analyzed via ddPCR. This revealed Cas9 copy numbers of 1.94 (±0.28) for clone 2 and 1.60 (±0.24) copies for clone 5 (Figure 26). PGC single cell clone C4 had only a single integration of the Cas9 gene displaying 0.94 (±0.15) copies. It was observed that Cas9-positive embryos originating from PGC single cell clone C2 died between ED18-21. Investigation of Cas9 copy numbers from tissue of a dead embryo (derived from C2) revealed 1.96 (±0.16) Cas9 copies (Figure 26).

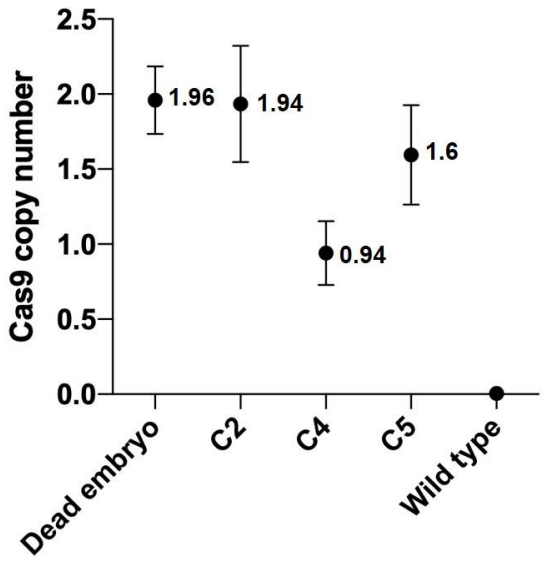

Figure 26: Cas9 copy number analysis in PGC single cell clones. The hygromycin resistance gene was used to determine Cas9 integration numbers by ddPCR. PGC clones (C2, C4 and C5) and tissue from a C2 dead embryo (ED18-21) were analyzed. PGC C2 and C5 had two integrations (C2 = 1.94 ±0.28, C5 = 1.60 ±0.24) while PGC C4 had a single Cas9 integration (0.94 ±0.15). 1.96 (±0.16) copies were observed in tissue from a C2 dead embryo. The figure shows the mean and standard deviation of the copy numbers. Figure adapted from Rieblinger et al. [237] and Bartsch et al. [238].

3.1.3. No phenotypic abnormalities in heterozygous Cas9-expressing chickens

Development and health of heterozygous Cas9-expressing chickens that originated from PGC single cell clone C4 were monitored to exclude negative effects due to transgene overexpression. Interestingly, EGFP (resulting from LSL-EGFP 165-2 Line 54) and the Cas9 gene segregated independently in the offspring. The following generations of this transgenic line were established without EGFP. Cas9-EGFP-expressing embryos, however, were used for functionality testing of the Cas9 endonuclease. To oversee the development of transgenic animals, their weight was measured weekly over 10 weeks and compared to WT animals from the same hatch. No significant differences in weight (n=3, p>0.05) were observed (Figure 27a). Upon sexual maturity, the birds showed no abnormalities, were fertile and gave rise to the next generation of heterozygous Cas9 chickens (Figure 27b).

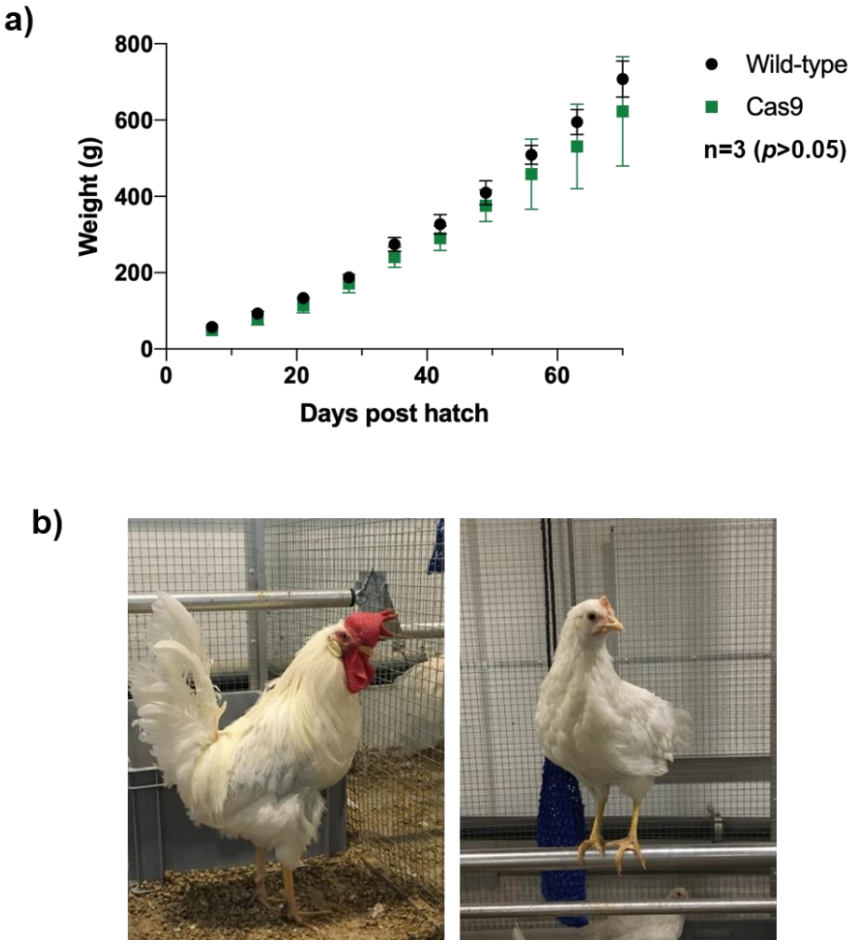

Figure 27: Monitoring of Cas9-expressing chickens. a) Comparison of the weight between Cas9-expressing and wild-type birds from the same hatch. The weight of males was measured over 70 days post hatch. No significant differences (n=3, p>0.05) were determined. The error bars represent the standard deviation. b) Exemplary images of the Cas9-expressing chickens. Figure adapted from Rieblinger et al. [237] and Bartsch et al. [238].

3.1.4. Ubiquitous expression of Cas9 in transgenic animals

Due to the expression driven by the chicken β-actin promoter (see Cas9 expression construct Figure 14), it was expected that the Cas9 gene is expressed in all tissues derived from a Cas9-expressing chicken. To test this, Cas9 expression was analyzed on mRNA level by reverse transcription (RT)-PCR (Figure 28) and on protein level by Western blot analysis (Figure 29). For RT-PCR, short amplicon generating primers were established (Table 41) and the following tissues were tested for Cas9 and β-actin expression: stomach glands, spleen, duodenum, cecal tonsil, liver, caecum, brain, thymus, kidney, gonad, lung, pectoral muscle, pancreas and heart. β-actin (300 bp) served as a control and was present in all tested samples. The expression of Cas9 (150 bp) was confirmed in all samples from the Cas9-expressing animal. No Cas9 expression was observed in the WT animal.

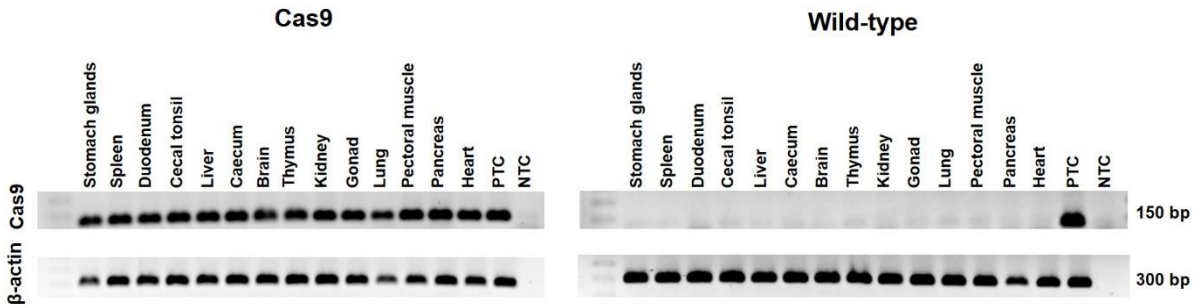

Figure 28: Cas9 expression analysis on mRNA level. RNA from stomach glands, spleen, duodenum, cecal tonsil, liver, caecum, brain, thymus, kidney, gonad, lung, pectoral muscle, pancreas and heart was isolated, followed by cDNA synthesis and RT-PCR. β-actin RT-PCR (lower row) served as a control (amplicon size: 300 bp). Cas9 RT-PCR (upper row) resulted in an amplicon of 150 bp in Cas9 samples but not in WT. Figure adapted from Rieblinger et al. [237] and Bartsch et al. [238].

In Western blot analysis, stomach glands, kidney, duodenum, cecal tonsil, liver, brain, thymus, spleen, gonad and lung of a Cas9-expressing chicken were analyzed to verify Cas9 expression on protein level. β-actin (42 kDa) served as a loading control and was present in all tested samples. β-actin bands in thymus, spleen and lung were stronger. The Cas9 protein was expected at 165 kDa and expressed in all tested samples confirming a ubiquitous Cas9 expression on a protein level. However, lower Cas9 expression compared to the rest of the samples was observed in the gonad (Figure 29).

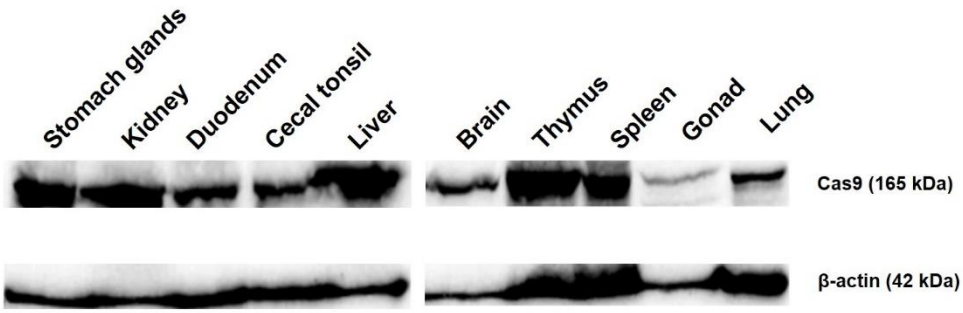

Figure 29: Cas9 expression analysis on protein level. Tissue samples (stomach glands, kidney, duodenum, cecal tonsil, liver, brain, thymus, spleen, gonad, lung) of a Cas9-expressing animal were lysed with RIPA buffer. 10 µl of the lysates were used for Western blot analysis. Proteins were separated in a 9 % SDS-PAGE gel and transferred to a nitrocellulose membrane. The Cas9 protein (165 kDa) (upper row) was detected by using a mouse anti-Cas9 primary antibody, followed by donkey anti-mouse-HRP antibody. β-actin (lower row) was detected by using a mouse anti-chicken-β-actin primary antibody, followed by donkey anti-mouse-HRP antibody and served as a loading control (42 kDa).

A SYBR® Green q-RT-PCR assay was established (see Chapter 2.2.3.12, Figure 23) to quantify Cas9 expression in different Cas9-expressing cells and tissues (Figure 30). The highest Cas9 expression was observed in cells that were stably transfected with Cas9 (CR = embryonic retinal cells from duck and DF-1).

The average expression level between the two cell lines was 18-fold, 49-fold, 3-fold higher compared to spleen, liver and heart tissues from a ubiquitously Cas9-expressing animal, respectively. Amongst tissues, the heart showed the highest expression levels being 7-fold higher compared to the spleen and 18-fold higher compared to the liver.

A comparison between CEF and tissues shows that the expression levels in primary derived CEF on average was 3 times higher than the average value between liver and spleen but three times lower than the heart. The expression levels in stably transfected cells was 9-fold higher than for CEF (Figure 30). As the measurement was performed once for each sample, no statistical analysis was performed.

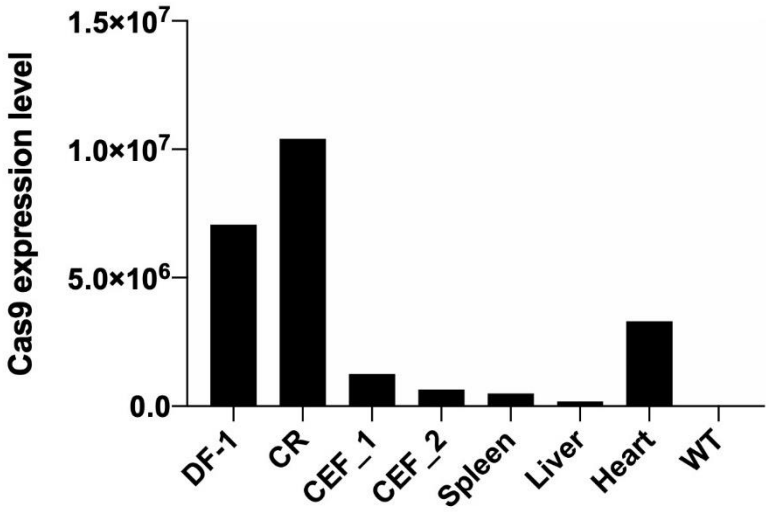

Figure 30: Cas9 expression levels in different Cas9-expressing cells and tissues. Cas9-expressing DF-1, CR and two different primary derived Cas9-CEF lines (CEF_1 derived from a Cas9-expressing embryo; CEF_2 derived from a Cas9-MDV-gRNA-expressing embryo) were analyzed. Tissue samples (spleen, liver, heart) were harvested from a Cas9-expressing animal. The RNA was isolated, followed by cDNA synthesis and q-RT-PCR using SYBR® Green. CEF WT was used as control. 18S served as an expression control.

3.1.5. Off-target analysis of single guide RNAs

Several sgRNA were used in this study to test Cas9 functionality (Table 42). Two sgRNAs (1444, 1445) were directed against β 2 microglobulin (B2M), a subunit of the major histocompatibility complex 1. Two sgRNAs (1434, 1435) were directed against CXCR4, a chemokine receptor type 4. A sgRNA against EGFP (1408) and a sgRNA against the interferon α/β receptor 1 (IFNAR1) (1430) were used.

On- and off-target analyses revealed scores for CXCR4 (1434) of 69.8/41.2 (on/off-target), for CXCR4 (1435) scores of 68.1/46.7 (on/off-target), for B2M (1444) scores of 41.3/82.5 (on/off-target), for B2M (1445) scores of 45.4/92.0 (on/off-target), for EGFP (1408) scores of 47.8/75.3 (on/off-target) and for IFNAR1 (1430) scores of 57.5/48.4 (on/off-target) (Table 77).

Table 77: On- and off-target analysis of gRNAs. SgRNAs against CXCR4, B2M, EGFP and IFNAR1 were compared to the genome of *gallus gallus* to predict on- and off-targets. Scores ranging from 0-100 and higher is better. The nuclease Cas9 from *Streptococcus pyogenes* was used. Scores were obtained from benchling.com.

sgRNA target (internal No.)	**On-target score[1]**	**Off-target score[2]**
CXCR4 (1434)	69.8	41.2
CXCR4 (1435)	68.1	46.7
B2M (1444)	41.3	82.5
B2M (1445)	45.4	92.0
EGFP (1408)	47.8	75.3

IFNAR1 (1430)	57.5	48.4

[1] On-target score: Based upon Doench et al. [239]

[2] Off-target score: Based on Hsu et al. [240]

3.1.6. Generation of target plasmids

The cloning of sgRNA 1445 into the RCAS(BP)A vector was done as described in Chapters 2.2.4.7 and 2.2.4.1. After CRISPR cloning of the sgRNA 1445 sequence into the px330 vector, four positive clones at expected size of 8500 bp were obtained (Figure 31a). The sequence was amplified with overhangs to the RCAS(BP)A vector, resulting in an amplicon of 437 bp (Figure 31b). Sanger sequencing confirmed the correct insertion of sgRNA 1445 into the RCAS(BP)A vector (Figure 31c).

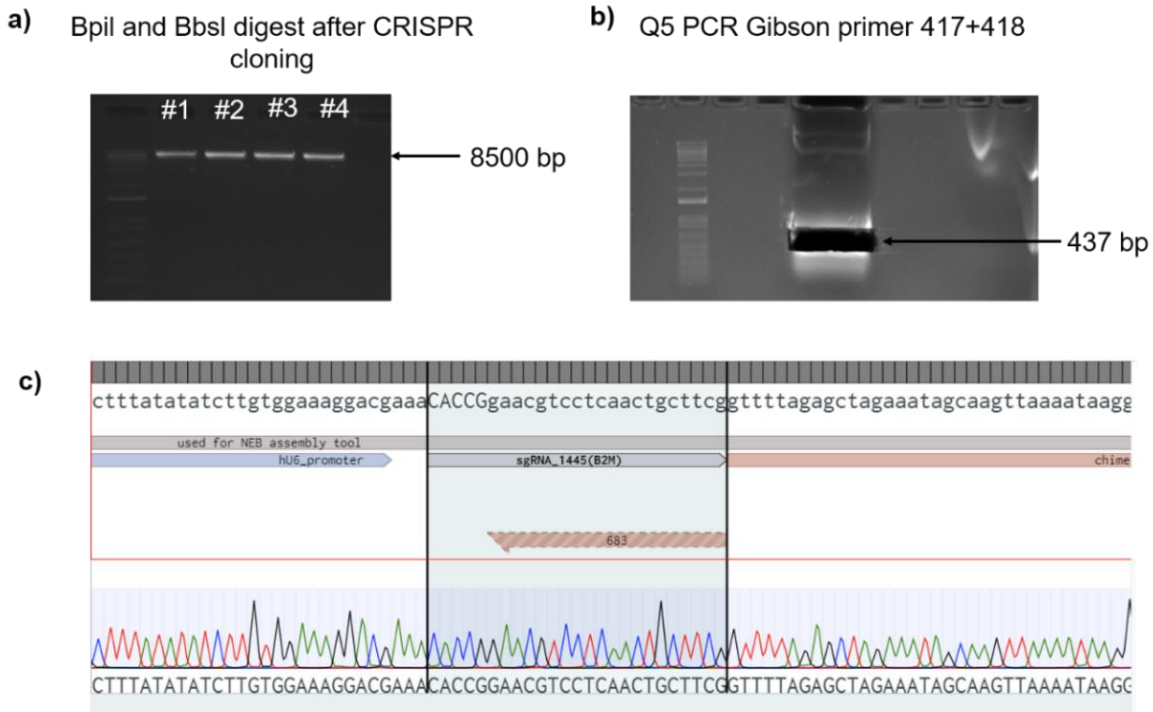

Figure 31: Cloning of RCAS(BP)A sgRNA 1445 (B2M) construct (K187). a) Successful cloning of sgRNA 1445 (B2M) into px330 vector. b) Q5® PCR with Gibson primers (417+418) containing overhangs to the RCAS(BP)A vector. The resulted amplicon was 437 bp long. c) Sequencing results showing correct insertion of sgRNA 1445 (B2M) into the RCAS(BP)A vector.

The sgRNA 1445 (B2M) was cloned into the pBlueScript II SK (+) vector. The backbone vector was digested (see Chapter 2.2.4.9), resulting in a linearized product with a band at the expected size of 2961 bp (Figure 32a). The sequence was amplified with overhangs to the

pBlueScript II SK (+) vector (see Chapter 2.2.4.1), resulting in an amplicon of 477 bp (Figure 32b). Sanger sequencing confirmed the correct insertion of the sgRNA 1445 sequence into the vector (Figure 32c).

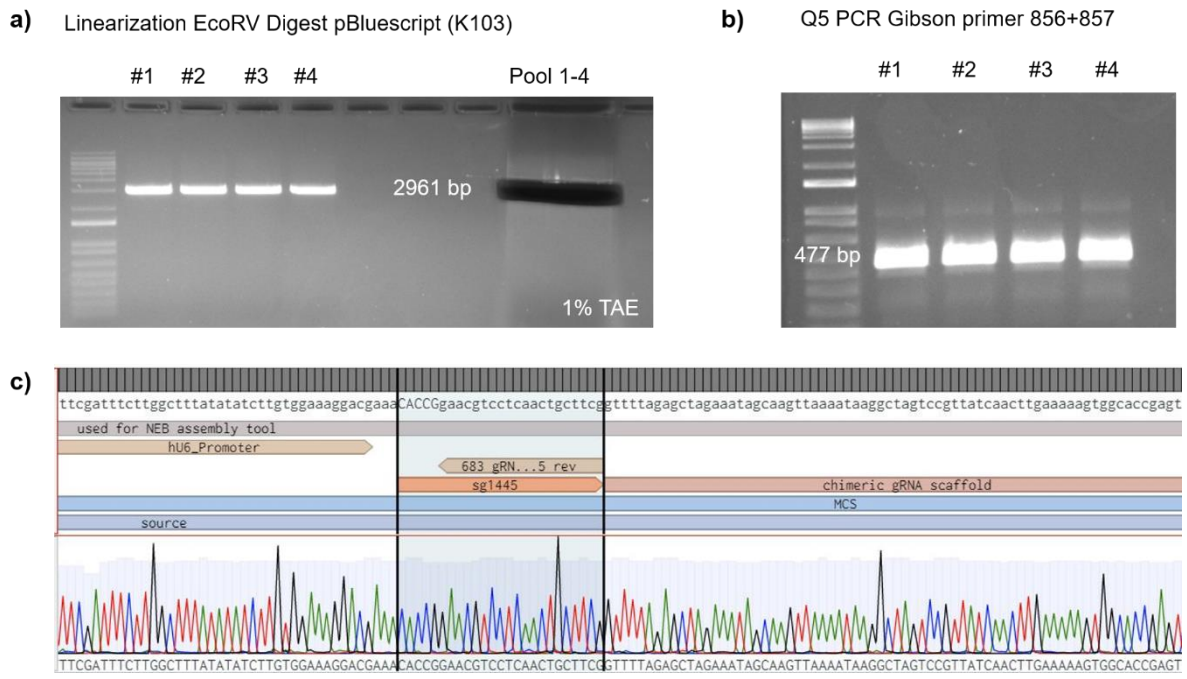

Figure 32: Cloning of pBlueScript sgRNA 1445 (B2M) construct (K245). a) Linearization of pBlueScript II SK (+) (K103) with EcoRV. All four restriction digest reactions showed band at expected size of 2961 bp. The reactions were pooled (pool #1-4) on a 1 % TAE agarose gel and linearized construct was purified. b) Q5® PCR with Gibson primers (856+857) containing overhangs to the pBlueScript II SK (+) vector. The resulted amplicon was 477 bp long. c) Sequencing results from clone 2 showing correct insertion of sgRNA 1445 (B2M) into the pBlueScript II SK (+) vector.

The sgRNA 1445 (B2M) sequence was cloned into the pBlueScript II SK (+) vector that also contained EGFP under the CMV promoter. The bovine growth hormone polyA (BHGpA) signal allowed for polyadenylation and thereby provided transcription termination. The construct K245 as generated above (Figure 32) was linearized and the CMV-EGFP-BGHpA sequence was amplified with overhangs to the pBlueScript II SK (+) vector, resulting in an amplicon of 1857 bp (Figure 33a). Colony PCR revealed 10 out of 16 positive clones (Figure 33b). Restriction digest of clone four showed bands at expected sizes of 3994 bp and 1255 bp (Figure 33c). Sanger sequencing confirmed the correct insertion of sgRNA 1445 (Figure 33d) and EGFP insert into the vector. The same construct was generated except that the sgRNA against the chicken B2M was replaced by a sgRNA against the porcine B2M (data not shown).

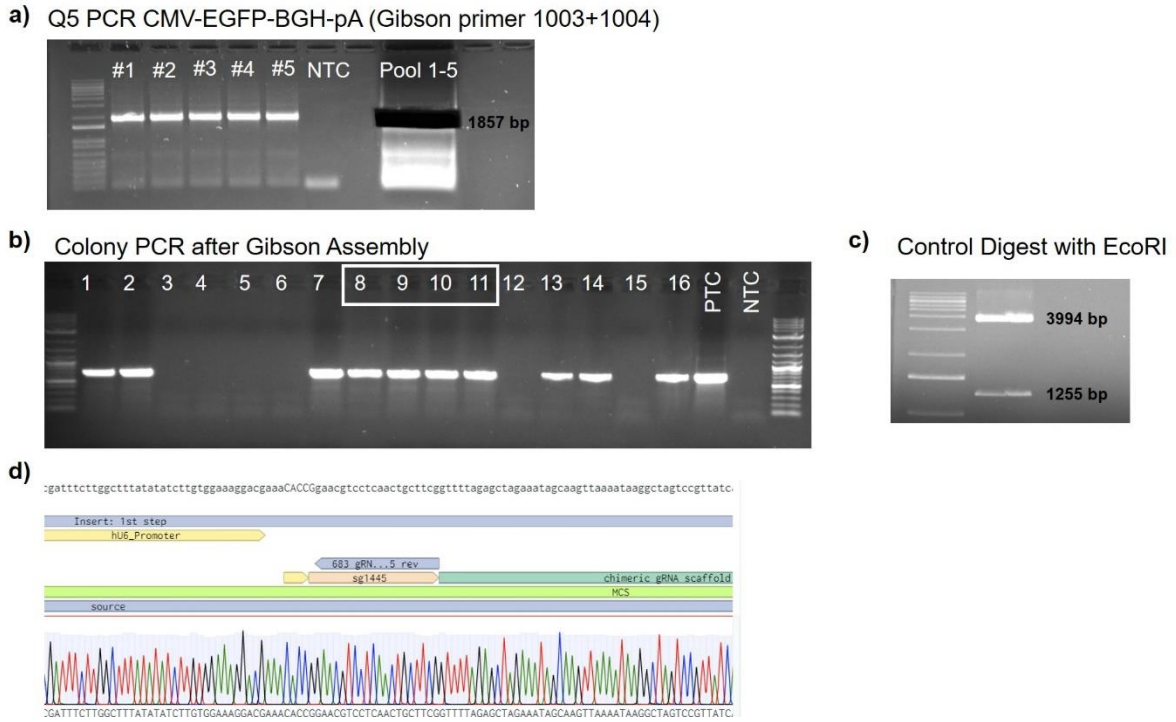

Figure 33: Cloning of pBlueScript-B2M-sgRNA-CMV-BGH-pA (K301). a) Q5® PCR to amplify CMV-BGH-pA sequence with Gibson primers (1003+1004) containing overhangs to the pBlueScript II SK (+) vector. The resulted amplicon was 1857 bp long. The reactions were pooled (pool #1-5) on a 1 % TAE agarose gel and purified from the gel. b) Colony PCR performed after Gibson assembly. 10 out of 16 clones were positive; four clones - marked with white box (8, 9, 10, 11) were used for the isolation of plasmid DNA (Miniprep). c) A control digest with EcoRI was performed on clone 4, resulting in bands at expected sizes of 3994 bp and 1255 bp. d) Sequencing results showing correct insertion of sgRNA 1445 (B2M) sequence.

3.1.7. *In vitro* Cas9-mediated genome editing

3.1.7.1. Reduced EGFP expression in Cas9-CEF after gRNA delivery

Cas9-EGFP-expressing CEF were isolated from a Cas9-EGFP-expressing embryo as described in Chapter 2.2.1.2. To show that the Cas9 nuclease is functional, the cells were transfected with the RCAS(BP)A vector containing a sgRNA against EGFP (see Table 45). The successful inactivation of the target gene was assessed by flow cytometry. FACS analysis after 20 days post transduction showed that 69.3 % of the cells lost EGFP fluorescence when treated with sgRNA against EGFP. In contrast, only 4.1 % lost EGFP signal in the MOCK-transfected control (Figure 34).

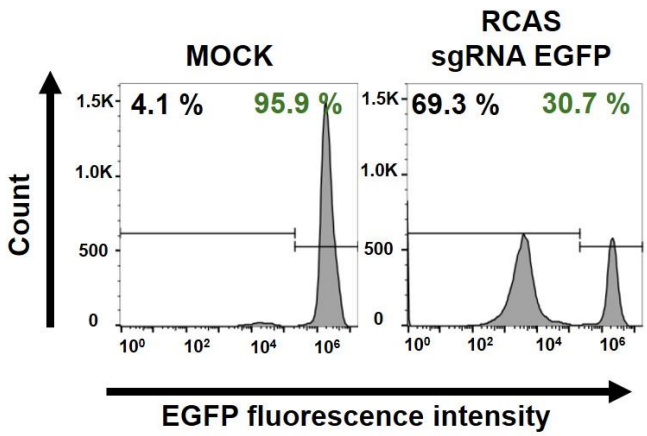

Figure 34: EGFP targeting in primary Cas9-EGFP-CEF with RCAS(BP)A. Cas9-EGFP-CEF were transfected with 500 ng of RCAS(BP)A containing a sgRNA against EGFP (1408) or a sgRNA against the interferon receptor (INFAR 1430) as control. FACS analysis for EGFP expression were performed 20 days post transduction and resulted in 69.3 % loss of EGFP in cells. In the MOCK-transfected control 4.1 % of the cells lost EGFP fluorescence. Figure adapted from Rieblinger et al. [237] and Bartsch et al. [238].

In addition, Cas9-EGFP-CEF were transfected with synthetic sgRNAs against EGFP (see Table 43) as described in Chapter 2.2.1.5. FACS analyses were performed 72 h, 96 h and 8 days after the transfection and revealed a reduction in EGFP signal by 15.8 % after 72 h, by 27 % after 96 h and by 27.2 % after 8 days when treated with sgRNA against EGFP but not in MOCK-transfected or untransfected controls (Figure 35a). The EGFP signal was not further reduced after 96 h post transfection.

The TIDE analysis tool was used to determine the cleavage efficiency in EGFP targeted CEF by synthetic sgRNA. An amplicon across the expected target site was amplified by PCR, followed by Sanger sequencing. The analysis of INDELs revealed a total on-target cleavage efficiency of 34.1 % (R^2=0.89) (Figure 35b) which resembles the reduction in EGFP expression observed by FACS analysis (up to 27.2 %, Figure 35a).

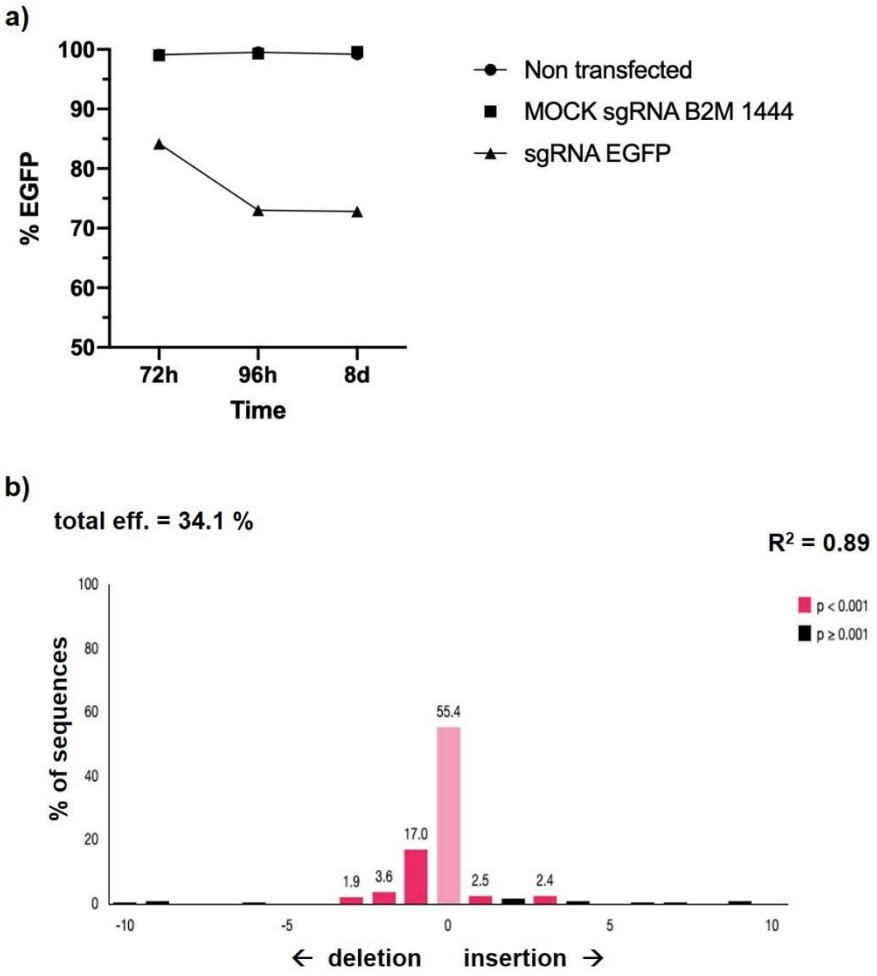

Figure 35: EGFP targeting in primary Cas9-EGFP-CEF with synthetic sgRNA. Cas9-EGFP-expressing CEF were transfected with 25 pmol of synthetic sgRNA against EGFP (1408) or B2M (1444) as a MOCK-transfected control. a) FACS analyses for EGFP expression were performed 72 h, 96 h and 8 days post transfection revealing a decline in EGFP when targeted with sgRNA against EGFP but not in untransfected or MOCK control. b) TIDE analysis of Cas9-EGFP-expressing CEF upon treatment with synthetic sgRNA against EGFP. gDNA was isolated from the cell pellet and an amplicon across the target site was amplified by PCR, followed by sequencing. The INDEL spectrum shows a total cleavage efficiency of 34.1 % (R^2=0.89). As a control an unedited samples was used.

3.1.7.2. Reduced B2M expression in Cas9-CEF after gRNA delivery

B2M was targeted in non-fluorescent Cas9-expressing CEF by using the pBlueScript-B2M-sgRNA-1445-CMV-EGFP-BGHpA construct (see Figure 33). The expression of CMV-EGFP-BGHpA enabled the analysis of only transfected (= EGFP positive) cells. 48 hours after transfection, the cells were analyzed by fluorescence microscopy imaging and FACS analysis (Figure 36). Fluorescence microscopy images showed EGFP expression in MOCK-transfected (sgRNA against porcine B2M) and targeted (sgRNA against chicken B2M) but not in untransfected cells, as expected (Figure 36a-c).

An anti-chB2M staining was performed to detect surface B2M expression in EGFP-positive and living single cells. The results showed that the expression of B2M in MOCK-transfected cells was reduced by 3.24 % (Figure 36d), while targeting with sgRNA against the chicken B2M resulted in a reduction of B2M expression by 19.86 % (Figure 36e).

The experiment was repeated four times and demonstrated that the reduction was significant (n=4, $p<0.05$). While 98.43 % (±0.15 %) of the cells in the MOCK-transfected control still expressed B2M on the cell surface, only 79.63 % (±9.17 %) showed B2M expression in targeted cells (Figure 36f).

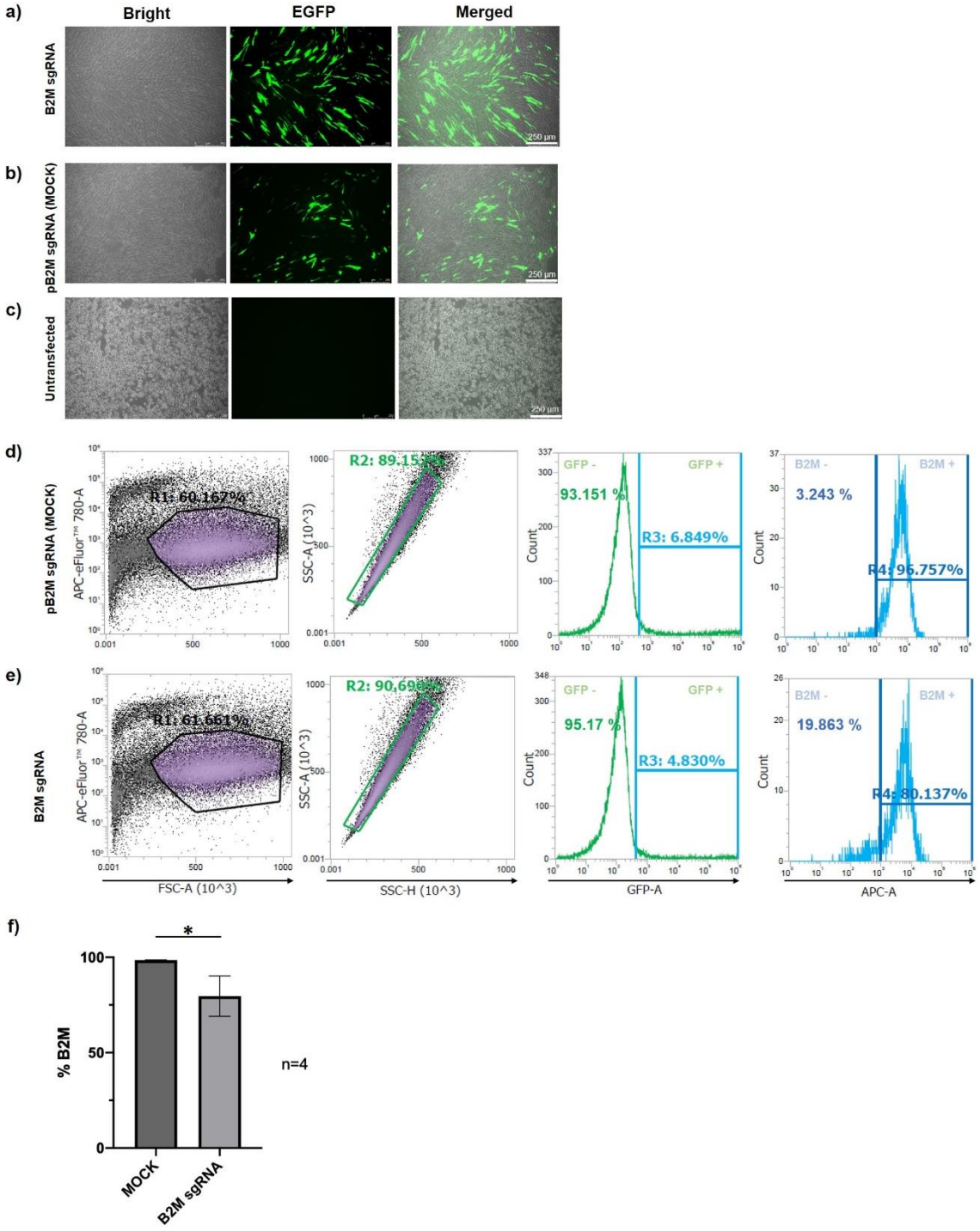

Figure 36: B2M targeting in EGFP-positive Cas9-expressing CEF. Fluorescence microscopy imaging and FACS analysis of Cas9-expressing CEF transfected with 750 ng of pBlueScript-CMV-EGFP-BGH-pA vector (K301) containing either a sgRNA against the chicken B2M (1445) or a sgRNA against the porcine B2M (pB2M) (MOCK). a-c) Fluorescence microscopy images were taken 48 h post transfection showing that EGFP was expressed in targeted and MOCK-transfected, but not in untransfected cells. Left: Bright field image, middle: EGFP fluorescence, right: merged images are shown. The size of the scale bar is 250 µm. d,e) Exemplary results of FACS analysis 48 h post transfection. The cells were gated on living cells (APC-eFluor-780-A:FSC-A), single cells (SSC-A:SSC-H) and EGFP-positive cells. B2M was stained with a mouse IgG1 anti-chB2M primary antibody, followed by a goat IgG (H+L) APC secondary antibody. f) Statistical analysis of four independent replicates. The B2M surface expression on Cas9-expressing CEF was significantly (n=4, p<0.05) reduced when cells treated with a sgRNA against B2M (79.63 % ± 9.17 %) compared to the MOCK control (98.43 % ± 0.15 %). Error bars denote the standard deviation.

3.1.8. *In vivo* Cas9-mediated genome editing

3.1.8.1. Reduced B2M expression in RCAS-transduced bursal B-cells

In vivo genome editing was done by delivering a sgRNA against B2M into chicken embryos as described in Chapter 2.2.2.4. DF-1 cells were transfected with a RCAS(BP)A vector containing a sgRNA against B2M (1445) (see Figure 31) and passaged over several passages to ensure transduction of the cells before they were injected into embryos at ED3. RCAS transduction and Cas9 expression was confirmed in heart tissues of transduced embryos that were harvested at ED18 (Figure 37a). Figure 37b shows FACS results for five Cas9-expressing embryos (#82, #90, #99, #114, #116) that were treated with a sgRNA against B2M and four Cas9-expressing embryos (#49, #78, #54, #56) that were treated with a sgRNA against EGFP (MOCK).

Bursal B-cells were stained to detect B2M expression on the cell surface. B2M was significantly ($n \geq 4$, $p < 0.05$, Figure 37c) reduced in B2M-sgRNA-treated embryos with a reduction of 56.0 % in embryo #82, 77.8 % in embryo #90, 69.6 % in embryo #99, 58.9 % in embryo #114 and 75.8 % in embryo #116 (Figure 37b, lower row). In contrast, a reduction of 5.4 % in embryo #49, 3.2 % in embryo #78, 16.9 % in embryo #54 and 4.75 % in embryo #56 was observed in MOCK-treated embryos (Figure 37b, upper row).

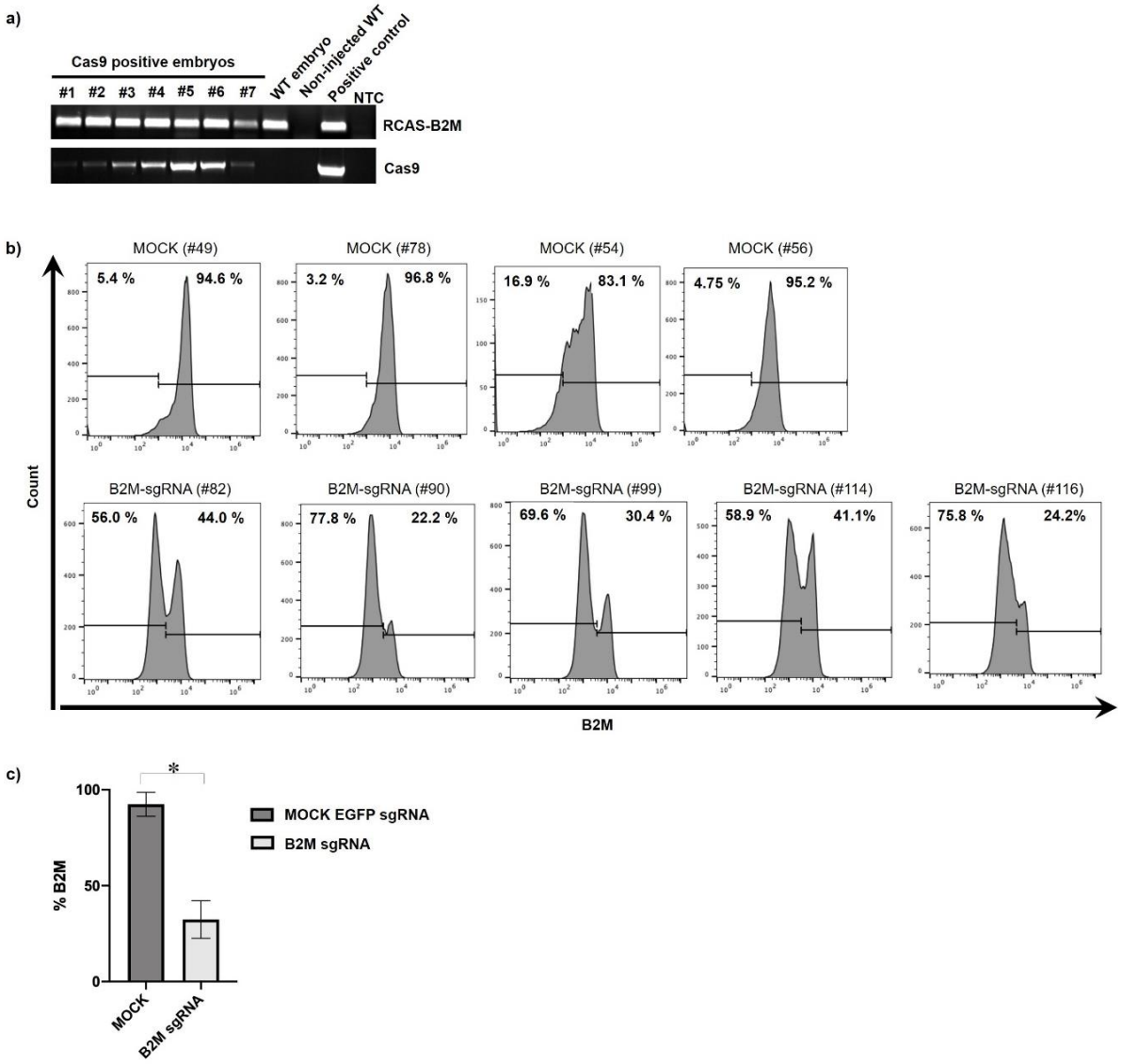

Figure 37: *In vivo* B2M targeting in bursal B-cells of Cas9-expressing embryos. a) Genotyping of embryos to detect Cas9 positive embryos (lower row) and B2M sgRNA expression (upper row) by PCR. b) FACS analysis of bursal B-cells from five Cas9-expressing embryos (#82, #90, #99, #114, #116) that were targeted *in vivo* by the delivery of RCAS(BP)A vector containing a sgRNA against B2M (1445); and four Cas9-expressing embryos (#49, #78, #54, #56) treated with RCAS(BP)A vector containing a sgRNA against EGFP (1408) (MOCK). Live/dead staining was performed with 7AAD viability dye, followed by B2M staining with a mouse IgG1 anti-chB2M primary antibody and a goat IgG (H+L) anti-mouse-APC secondary antibody. c) B2M surface expression on bursal B-cells was significantly reduced (n≥4; $p<0.05$) when treated with sgRNA against B2M (32.38 % ± 8.78 %) compared to MOCK control (sgRNA against EGFP, 92.43 % ± 5.44 %). Error bars denote the standard deviation. Figure adapted from Rieblinger et al. [237] and Bartsch et al. [238].

3.1.8.2. Reduced EGFP and B2M expression in embryonic chicken midbrains

To further confirm Cas9 functionality *in vivo*, *in ovo*-electroporation as previously described [241–244] was done in cooperation with the Chair of Zoology, TUM, Freising, Germany.

In the first experiment, the pBlueScript II SK (+) vector containing a sgRNA against EGFP (see Table 45) or B2M (MOCK) (see Figure 32) was delivered into the central nervous system of developing Cas9 x EGFP embryos in H&H stage 10-13. The embryos were incubated further until ED12 when embryonic midbrains were dissected for analysis. Embryo #5 and #7 showed high losses of EGFP signal in epifluorescence imaging (data not shown). The gDNA from fixed tissue was isolated as described in Chapter 2.2.3.1. The EGFP target site was amplified by PCR and sequenced. TIDE analysis of embryo #5 and embryo #7 showed INDEL formation with total efficiencies of 6.8 % (R^2=0.93) and 11.5 % (R^2=0.91), respectively (Figure 38a,b).

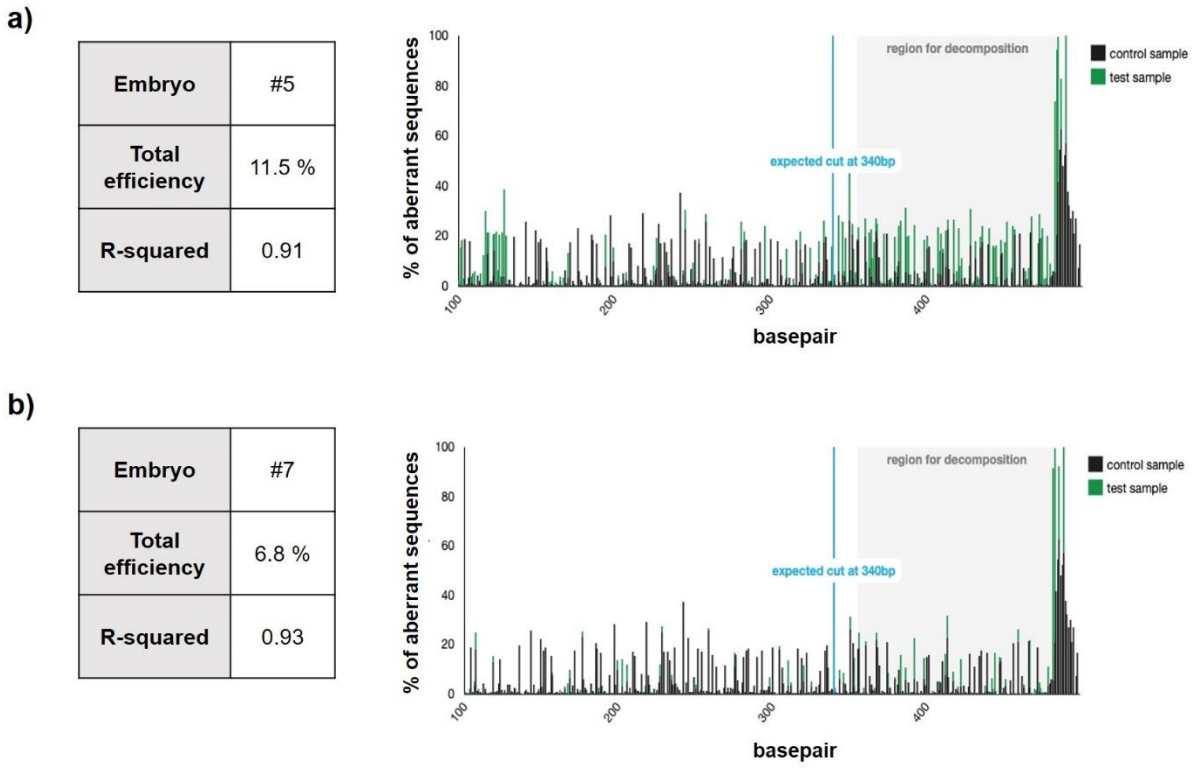

Figure 38: EGFP targeting by *in ovo*-electroporation of Cas9 x EGFP embryos. Cas9-expressing embryos (#5, #7) were electroporated with a pBlueScript II SK (+) vector containing sgRNA against EGFP (1408) or B2M (1445) (MOCK). TIDE analysis (right) shows aberrant sequence signal in control (black) and treated samples (green), the expected cut site (vertical blue line) and the region used for decomposition (grey shade). The INDEL spectrum analysis is summarized at the left (table). a) Analysis of Cas9-expressing embryo #5 revealing a total cleavage efficiency of 11.5 % (R^2 = 0.91). b) Analysis of Cas9-expressing embryo #7 revealing a total cleavage efficiency of 6.8 % (R^2 = 0.93). Figure adapted from Rieblinger et al. [237].

In the second experiment, the pBlueScript II SK (+) vector containing a sgRNA against B2M (see Figure 32) or EGFP (MOCK) (see Table 45) was delivered to the central nervous system of developing Cas9 x WT embryos in H&H stage 10-13. TIDE analysis on PCR-amplified amplicons revealed total efficiencies of 11.1 % (embryo #22, R^2 =1.0), 11.8 % (embryo #12, R^2 =0.97) and 13.8 % (embryo #6, R^2 =0.97) with INDELs around the expected cutting site (Figure 39a-c).

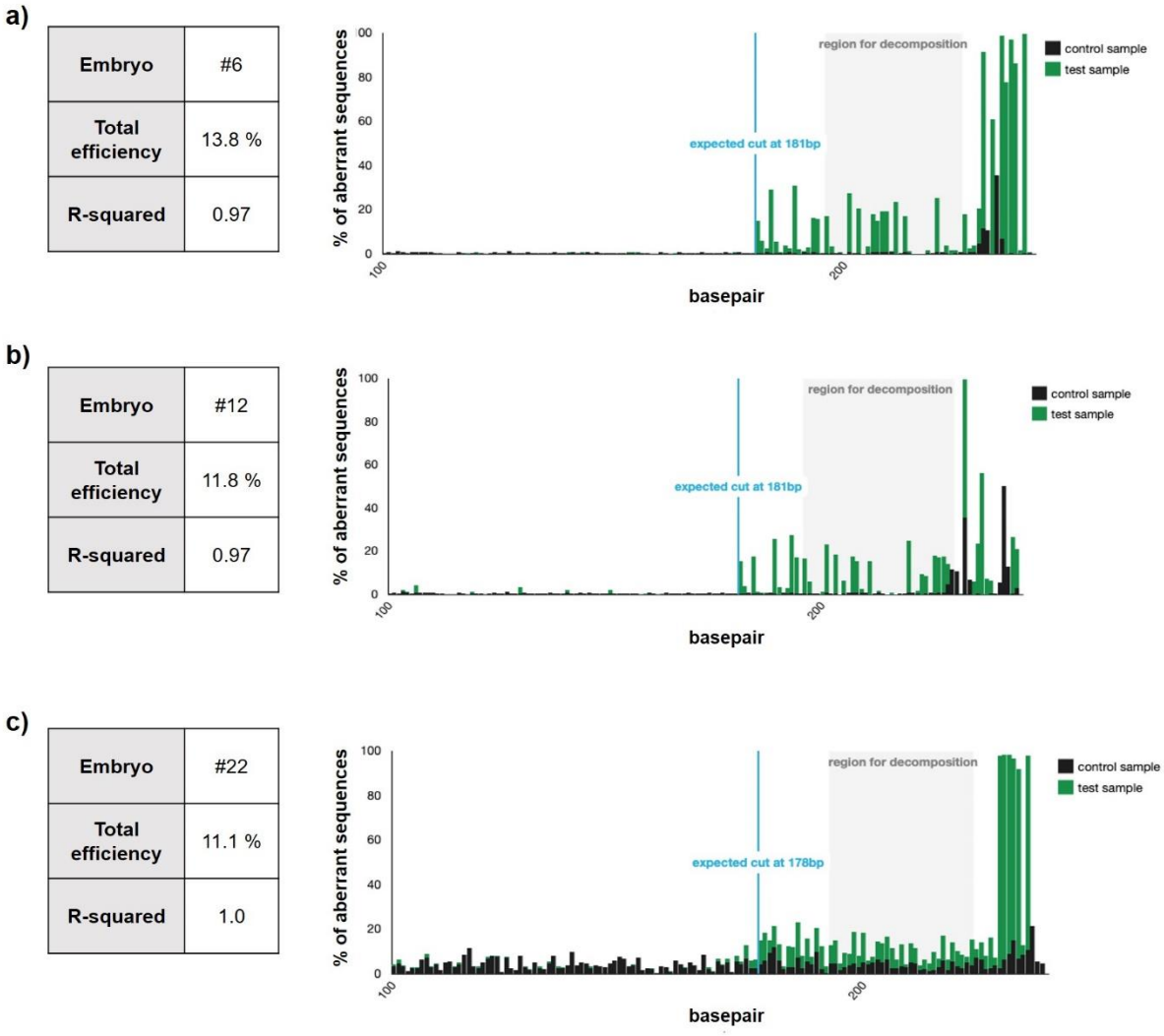

Figure 39: B2M targeting by *in ovo*-electroporation of midbrains in Cas9 x WT embryos. Cas9-expressing embryos (#6, #12, #22) were electroporated with a pBlueScript II SK (+) vector containing sgRNA against B2M (1445) or EGFP (1408) (MOCK). TIDE analysis images (right) show aberrant sequence signal in control (black) and treated samples (green), the expected cut site (vertical blue line) and the region used for decomposition (grey shade). The INDEL spectrum analysis is summarized at the left (table). a) Analysis of Cas9-expressing embryo #6 revealing a total cleavage efficiency of 13.8 % (R^2 =0.97). b) Analysis of Cas9-expressing embryo #12 revealing a total cleavage efficiency of 11.8 % (R^2 =0.97). c) Analysis of Cas9-expressing embryo #22 revealing a total cleavage efficiency of 11.1 % (R^2 =1.0). Figure adapted from Rieblinger et al. [237].

3.1.9. Reduced CXCR4 and B2M expression in primary Cas9-expressing lymphocytes

Deriving primary cells from a Cas9-expressing chicken has the advantage that also cells that are usually hard to transfect, such as lymphocytes, can be targeted with high efficiencies as only the sgRNA has to be delivered.

To test if Cas9 was able to efficiently induce INDEL formation in primary lymphocytes, PBMCs were isolated from the spleen of a Cas9-expressing chicken as described in Chapter 2.2.1.3. Multiple transfection and transduction protocols have been tried out within this work (RCAS system, HiPerFect Transfection Reagent, Neon™ Transfection Systems) but none of these protocols led to gene editing as most of the cells died after the treatment. Several modifications of these protocols did not increase the survival of the cells. The most efficient method was AMAXA™ Human T Cell Nucleofector™ Kit with cell deaths up to 50 %. Directly after isolation, the cells were electroporated with chemically modified sgRNAs against CXCR4 (1434, 1435) or B2M (1444, 1445) (Table 43). An anti-chCXCR4 or anti-chB2M staining was performed to analyze the expression of CXCR4 and B2M, respectively, on the cell surface. Co-staining with an anti-chCD45 was performed to focus on the expression in lymphocytes.

Figure 40a shows FACS results of $CD45^+$ PBMCs that were targeted with sgRNAs against CXCR4 (1434 and 1435). Two sgRNAs against B2M (1444 and 1445) were used as controls. The expression of CXCR4 was not impaired in controls as 98.3 % (±0.6 %) (untransfected), 94.7 % (±1.1 %) (sgRNA B2M 1444) and 92.1 % (±1.8 %) (sgRNA B2M 1445) of the cells still displayed CXCR4 at the cell surface. In contrast, only 64.7 % (±13.0 %) and 86.8 % (±5.6 %) of the cells showed CXCR4 expression upon targeting with sgRNA 1434 and 1435, respectively (Figure 40a). Statistical analysis revealed that the reductions of CXCR4 expression at the cell surface by 35.3 % (±13.0 %) for sgRNA 1434 and 13.2 (±5.5 %) for sgRNA 1435 were significant (n=3; $p<0.05$) compared to the untransfected control (Figure 40b).

Figure 40c shows the FACS results of $CD45^+$ PBMCs that were targeted with sgRNAs against B2M (1444 and 1445). SgRNAs against CXCR4 (1434 and 1435) were used as controls. The expression of B2M was not impaired in controls as 98.3 % (±0.8 %) (untransfected), 97.9 % (±0.6 %) (sgRNA CXCR4 1434) and 98.4 % (±0.8 %) (sgRNA CXCR4 1435) of the cells expressed B2M at the cell surface. In contrast, 82.5 % (±3.8 %) and 93.7 % (±2.8 %) of the cells displayed

B2M expression upon targeting with sgRNA 1444 and 1445, respectively (Figure 40c). Statistical analysis showed that the reduction of B2M on the cell surface by 17.3 % (±3.8 %) for sgRNA 1444 was significant (n=3; p<0.01) compared to the untransfected and MOCK controls (Figure 40d). The reduction in B2M expression by 6.3 (±2.8 %) for sgRNA 1455 targeted cells was not significant compared to the controls.

a)

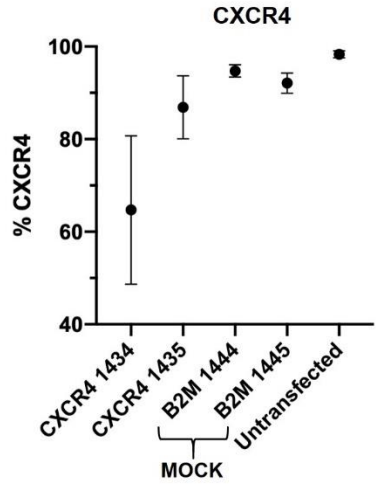

b)

CXCR4 target	B2M 1444	B2M 1445	Untransfected
CXCR4 1434	p<0.05	p<0.05	p<0.05
CXCR4 1435	NS	NS	p<0.05

c)

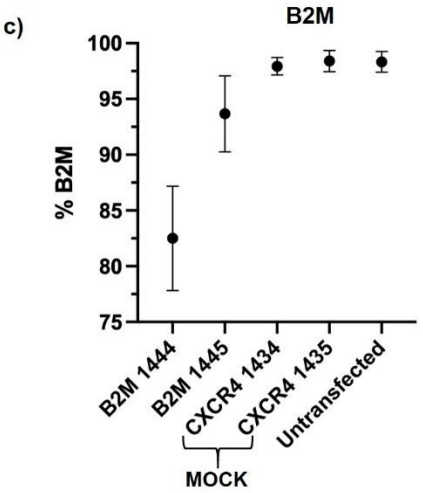

d)

B2M target	CXCR4 1434	CXCR4 1435	Untransfected
B2M 1444	p<0.01	p<0.01	p<0.01
B2M 1445	NS	NS	NS

Figure 40: FACS and statistical analysis of CXCR4 and B2M targeted CD45$^+$ PBMCs. Splenic CD45$^+$ PBMCs were treated with 25 pmol of chemically modified synthetic gRNA against CXCR4 (1434, 1435) or B2M (1444, 1445). 48 h post electroporation (AMAXA^{TM} Human T Cell Nucleofector^{TM} Kit), the cells were stained with Fixability Viability Dye eFluor780, followed by CXCR4 (mouse IgG2a anti-chCXCR4) or B2M (mouse IgG1 anti-chB2M) staining. The primary antibody was detected using a goat IgG (H+L) ani-mouse APC-labeled secondary antibody. The co-staining with mouse IgG1 anti-chCD45-FITC allowed the analysis of lymphocytes. a) CXCR4 targeting in CD45$^+$ PBMCs showing a 35.3 % (±13.0 %) and 13.2 % (±5.5 %) reduction in CXCR4 expression when cells were treated with a sgRNA against CXCR4 1434 or 1435, respectively. b) Statistical analysis for CXCR4 targeting. The data from three independent replicates are shown. CXCR4 expression was significantly reduced upon treatment with sgRNAs 1434 and 1435 (n=3; p<0.05). Error bars denote the standard deviation. c) B2M targeting in CD45$^+$ PBMCs showing a 17.3 % (±3.8 %) and 6.3 % (±2.8 %) reduction in B2M expression when cells were treated with a sgRNA against B2M 1444 or 1445, respectively. d) Statistical analysis for B2M targeting. The data from three independent replicates are shown. B2M expression was significantly reduced upon treatment with sgRNA 1444 (n=3; p<0.01). The difference in reduction by sgRNA 1445 was not significant (NS). Error bars denote the standard deviation. Figure adapted from Rieblinger et al. [237].

TIDE analysis was performed on splenic PBMCs which were obtained from the previous experiment (see Figure 40), targeted with chemically modified sgRNAs against CXCR4 and B2M. The analysis of spectrum and frequency of INDELs at the CXCR4 target site targeted with sgRNA 1434 resulted in gene editing efficiencies of 44.3 % (R^2=0.82), 45.1 % (R^2=0.89) and 20.5 % (R^2=0.95) displaying mainly deletions (Figure 41).

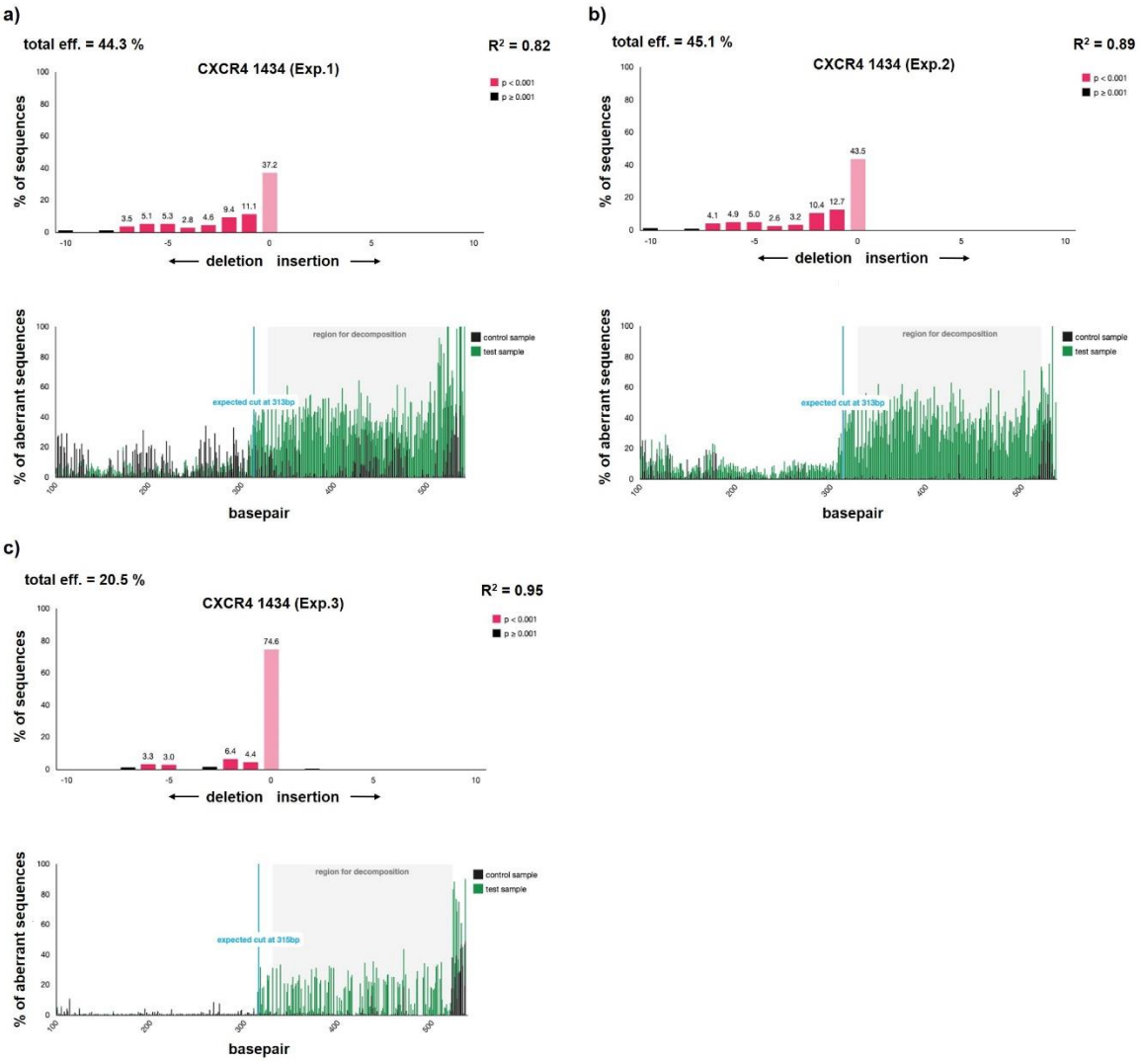

Figure 41: TIDE analysis of CXCR4 targeting with sgRNA 1434 in CD45$^+$ PBMCs. Results from three independent experiments (exp.) are shown. A sgRNA against B2M 1444 was used as a control. The gDNA from cells was isolated and an amplicon across the expected target site was amplified by PCR, followed by Sanger sequencing. The lower images show the aberrant sequence signal in control (black) and treated samples (green), the expected cut site (vertical blue line) and the region used for decomposition (grey shade). The upper images show the INDEL spectrum analysis for each experiment, respectively. a) Exp.1: The analysis of spectrum and frequency of INDELS at the CXCR4 1434 target site mediated by functional Cas9 revealed a total efficiency of 44.3 % (R^2=0.82). b) Exp.2: The analysis of spectrum and frequency of INDELS at the CXCR4 1434 target site mediated by functional Cas9 revealed a total efficiency of 45.1 % (R^2=0.89). c) Exp.3: The analysis of spectrum and frequency of INDELS at the CXCR4 1434 target site mediated by functional Cas9 revealed a total efficiency of 20.5 % (R^2=0.95).

Targeting with a sgRNA against CXCR4 (1435) resulted in gene editing efficiencies of 30.1 % (R^2=0.93), 18.6 % (R^2=0.95) and 6.2 % (R^2=0.98) (Figure 42).

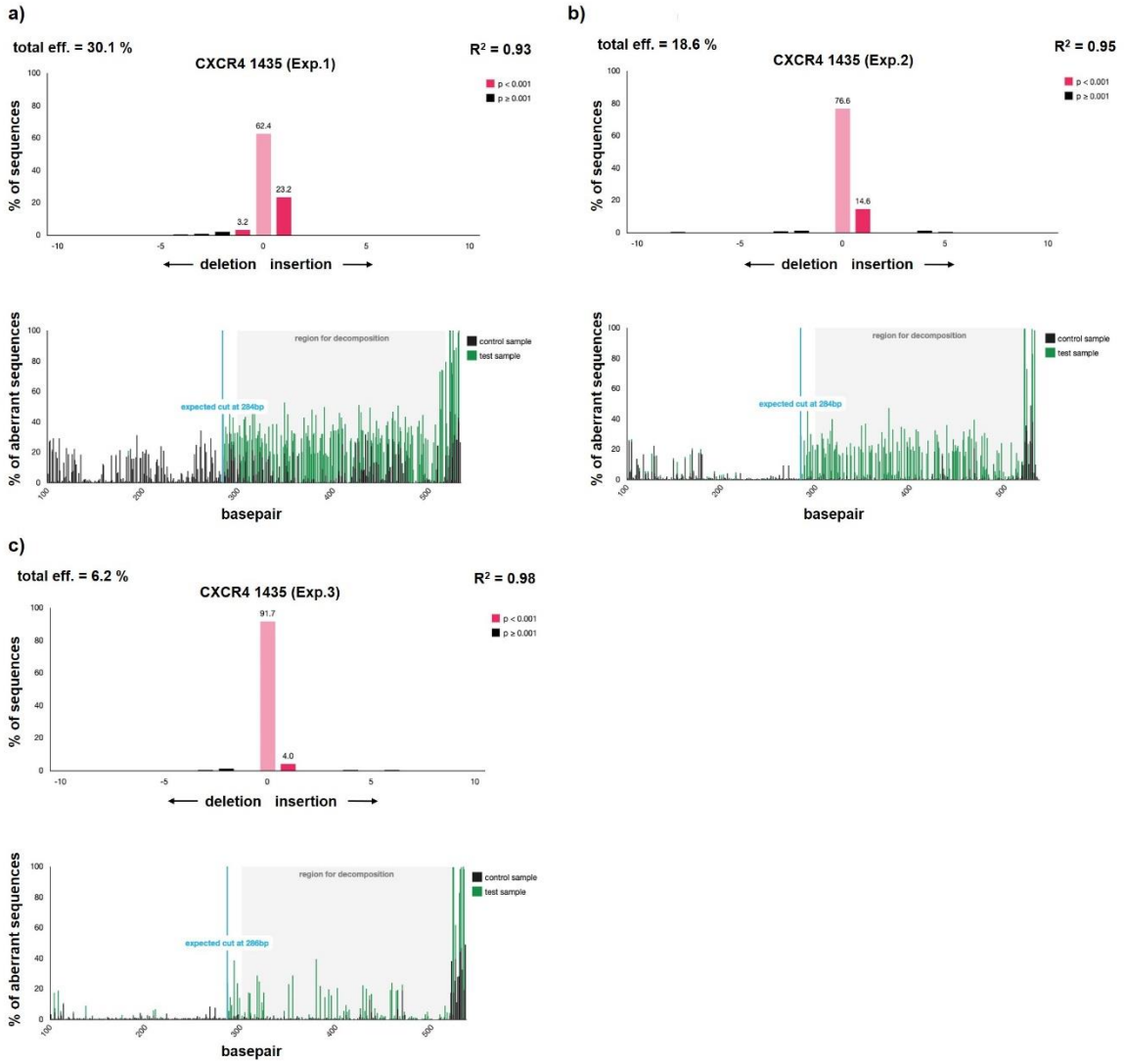

Figure 42: TIDE analysis of CXCR4 targeting with sgRNA 1435 in $CD45^+$ PBMCs. Results from three independent experiments are shown. A sgRNA against B2M (1444) was used as a control. The gDNA from cells was isolated and an amplicon across the expected target site was amplified by PCR, followed by Sanger sequencing. The lower images show the aberrant sequence signal in control (black) and treated samples (green), the expected cut site (vertical blue line) and the region used for decomposition (grey shade). The upper images show the INDEL spectrum analysis for each experiment, respectively. a) Exp.1: The analysis of spectrum and frequency of INDELs at the CXCR4 1435 target site mediated by functional Cas9 revealed a total efficiency of 30.1 % (R^2=0.93). b) Exp.2: The analysis of spectrum and frequency of INDELs at the CXCR4 1435 target site mediated by functional Cas9 revealed a total efficiency of 18.6 % (R^2=0.95). c) Exp.3: The analysis of spectrum and frequency of INDELs at the CXCR4 1435 target site mediated by functional Cas9 revealed a total efficiency of 6.2 % (R^2=0.98).

Targeting with a sgRNA against B2M (1444) resulted in gene editing efficiencies of 15.1 % (R^2=0.96) and 13.6 % (R^2=0.95) (Figure 43).

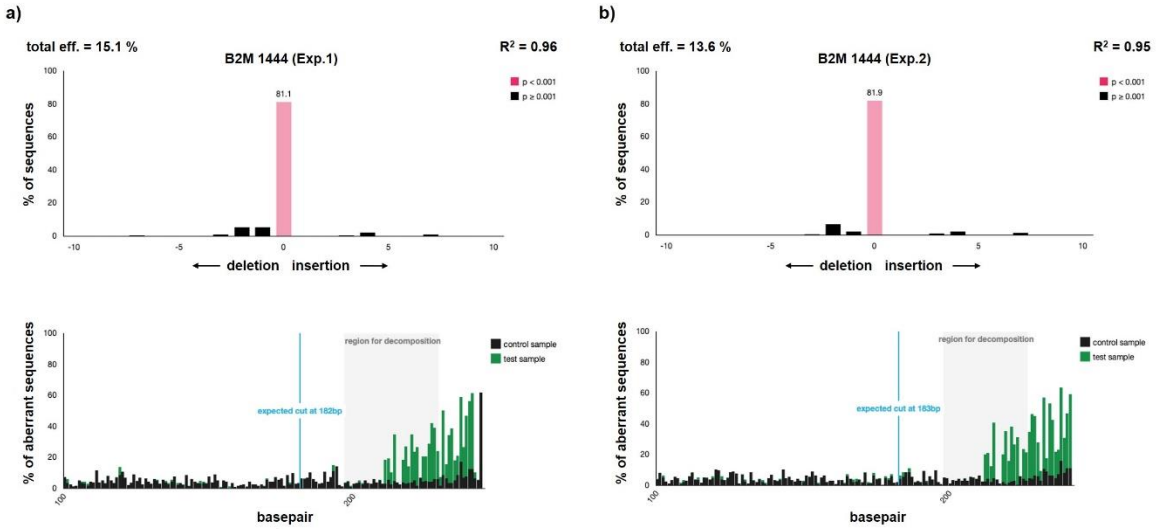

Figure 43: TIDE analysis of B2M targeting with sgRNA 1444 in CD45⁺ PBMCs. Results from two independent experiments are shown. As a reference control, unedited cells were used. The gDNA from cells was isolated and an amplicon across the expected target site was amplified by PCR, followed by Sanger sequencing. The lower images show the aberrant sequence signal in control (black) and treated samples (green), the expected cut site (vertical blue line) and the region used for decomposition (grey shade). The upper images show the INDEL spectrum analysis for each experiment, respectively. a) Exp.1: The analysis of spectrum and frequency of INDELs at the B2M 1444 target site mediated by functional Cas9 revealed a total efficiency of 15.1 % (R^2=0.96). b) Exp.2: The analysis of spectrum and frequency of INDELs at the B2M 1444 target site mediated by functional Cas9 revealed a total efficiency of 13.6 % (R^2=0.95).

Targeting with a sgRNA against B2M (1445) revealed targeting efficiencies of 16.1 (R^2=0.99) and 12.3 % (R^2=0.99) (Figure 44).

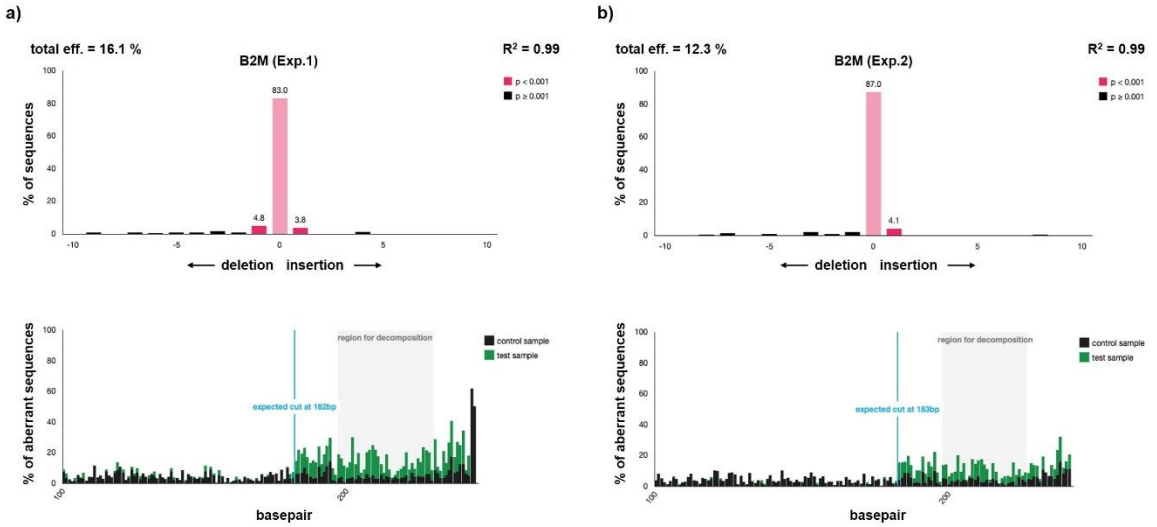

Figure 44: TIDE analysis of B2M targeting with sgRNA 1445 in CD45⁺ PBMCs. Results from two independent experiments are shown. As a reference control, unedited cells were used. The gDNA from cells was isolated and

an amplicon across the expected target site was amplified by PCR, followed by Sanger sequencing. The lower images show the aberrant sequence signal in control (black) and treated samples (green), the expected cut site (vertical blue line) and the region used for decomposition (grey shade). The upper images show the INDEL spectrum analysis for each experiment, respectively. a) Exp.1: The analysis of spectrum and frequency of INDELs at the B2M 1445 target site mediated by functional Cas9 revealed a total efficiency of 16.1 % (R^2=0.99). b) Exp.2: The analysis of spectrum and frequency of INDELs at the B2M 1445 target site mediated by functional Cas9 revealed a total efficiency of 12.3 % (R^2=0.99).

To further evaluate targeting efficiencies within the $CD45^+$ cell population, splenic PBMCs were isolated and electroporated with chemically modified sgRNA against CXCR4 (1434) as it was the most efficient sgRNA with gene editing efficiencies up to 45.1 % (R^2=0.89) (Figure 41b). The living cell population was co-stained with anti-chCXCR4 and antibodies to detect B-cells (anti-chBu1), macrophages (anti-chKul01), γδ-T-cells (anti-chTCR1) and αβ-T-cells (anti-chTCR2-3) (Table 40). T-cells were further divided into $CD4^+$ and $CD8^+$ cell populations. The CXCR4 expression was reduced by 17.1 % in B-cells (Figure 45a), by 25.2 % in macrophages (Figure 45b), by 16.2 % in TCR1 $CD8^+$ (Figure 45c), by 11.4 % TCR2-3 $CD4^+$ (Figure 45d) and by 16.7 % in TCR2-3 $CD8^+$ (Figure 45e). A sgRNA against B2M was used as a MOCK control. Due to the lack of independent repetitions of the experiment, no statistical analysis was done.

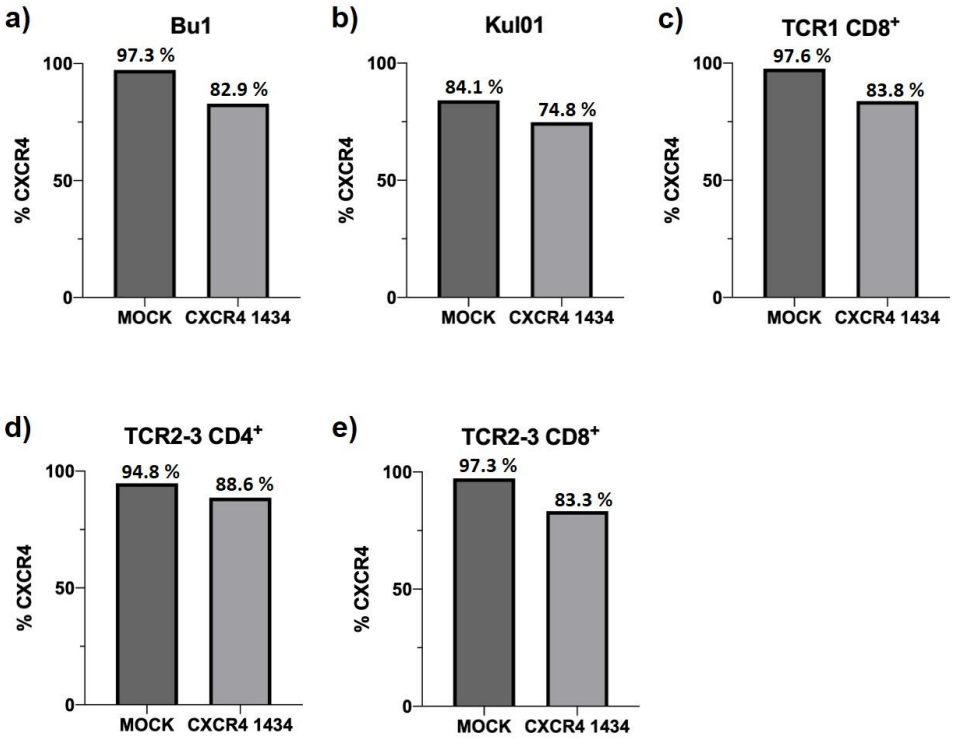

Figure 45: Targeting efficiencies within the CD45$^+$ cell population. Splenic CD45$^+$ PBMCs were electroporated with 25 pmol of chemically modified sgRNA against CXCR4 (1434) or B2M (1445) (MOCK). 48 h post electroporation, the cells were stained with Fixability Viability Dye eFluor780 and CXCR4 expression was analyzed in different cell populations. a) CXCR4 was detected using a mouse IgG2a anti-chCXCR4 primary antibody, followed by goat anti-mouse IgG (H+L) APC secondary antibody staining. B-cells were detected using a direct-labeled mouse IgG1 anti-chBu1-FITC antibody. The analysis revealed that 97.3 % of the cells expressed CXCR4 in MOCK control while only 82.9 % of the cells expressed CXCR4 in targeted sample. b) Macrophages were detected using a mouse IgG1 anti-chKul01 primary antibody, followed by a goat anti-mouse IgG (H+L) APC secondary antibody. CXCR4 was stained using a mouse IgG2a anti-chCXCR4 antibody, followed by a goat anti-mouse IgG2a PE-Cy7 secondary antibody. The analysis revealed that 84.1 % of the cells expressed CXCR4 in MOCK control while only 74.8 % of the cells expressed CXCR4 in targeted sample. c) γδ-T-cells were stained using a mouse anti-chTCR1-BIOTIN-labeled primary antibody, followed by an anti-mouse Streptavidin-APC secondary antibody. CD8$^+$ cells in the TCR1 cell population were detected using a direct-labeled mouse IgG1 anti-chCD8a-Pacific Blue antibody. The analysis revealed that 97.6 % of the cells expressed CXCR4 in MOCK control while only 83.8 % of the cells expressed CXCR4 in targeted sample. d) αβ-T-cells were stained using mouse anti-chTCR2-3-BIOTIN-labeled primary antibodies, followed by an anti-mouse Streptavidin-APC secondary antibody. CD4$^+$ cells in the TCR2-3 cell population were detected using a direct-labeled mouse IgG1 anti-chCD4-FITC antibody. The analysis revealed that 94.8 % of the cells expressed CXCR4 in MOCK control while only 88.6 % of the cells expressed CXCR4 in targeted sample. e) The same staining as described in d) was applied, except that here CD8$^+$ cells in the TCR2-3 cell population were detected using a direct-labeled mouse IgG1 anti-chCD8a-Pacific Blue antibody. The analysis revealed that 97.3 % of the cells expressed CXCR4 in MOCK control while only 83.3 % of the cells expressed CXCR4 in targeted sample.

3.2. Generation of chickens with ubiquitous MDV-gRNA expression

A relevant application of the generated ubiquitously Cas9-expressing chickens is the establishment of disease resistance against MDV by the use of appropriate gRNAs that were obtained from the group of Prof. Benedikt Kaufer (Institute of Virology, FU Berlin, Germany) (see Table 44). IT6 is directed against *UL27*, IT7 targets *UL30*, IT9 is directed against *UL49* and IT12 targets *ICP4* (for more detail see Chapter 1.1.4). The MDV-gRNAs were tested *in vitro* (see Hagag et al. [77] and Chapter 1.1.5) and showed the complete abrogation of viral replication when combined.

3.2.1. Cloning of an MDV-gRNA expression construct

An expression construct was generated to introduce the four MDV-gRNAs (IT7, IT6, IT12, IT9) into the chicken genome. The expression of each gRNA was driven by the human U6 promoter and followed by a poly-A signal. The four expression cassettes (each consisting of hU6 promoter, gRNA and scaffold RNA sequence) and the selectable marker were flanked with duplicated copies of the core 300 bp HS4 insulators from the chicken β-globin gene to ensure proper transgene expression (see Figure 15).

The generated construct contained an ampicillin resistance and a hygromycin selectable marker cassette under the CAG promoter. For stable integration into PGCs, the MDV-gRNA expression plasmid contained an attB70 site to ensure the insertion of the transgene using phiC31 integrase.

The cloning was done as described in Chapters 2.2.4.3, 2.2.4.4 and 2.2.4.5. Colony PCR as described in Chapter 2.2.4.6 was done to select for positive clones. Restriction digest of clone 53 showed bands at expected sizes of 6082 bp and 3705 bp (Figure 46a) confirming the insertion of the four MDV-gRNA cassettes into the expression construct. The correct sequence of each gRNA (IT7, IT6, IT12, IT9) was confirmed by Sanger sequencing (Figure 46b-e).

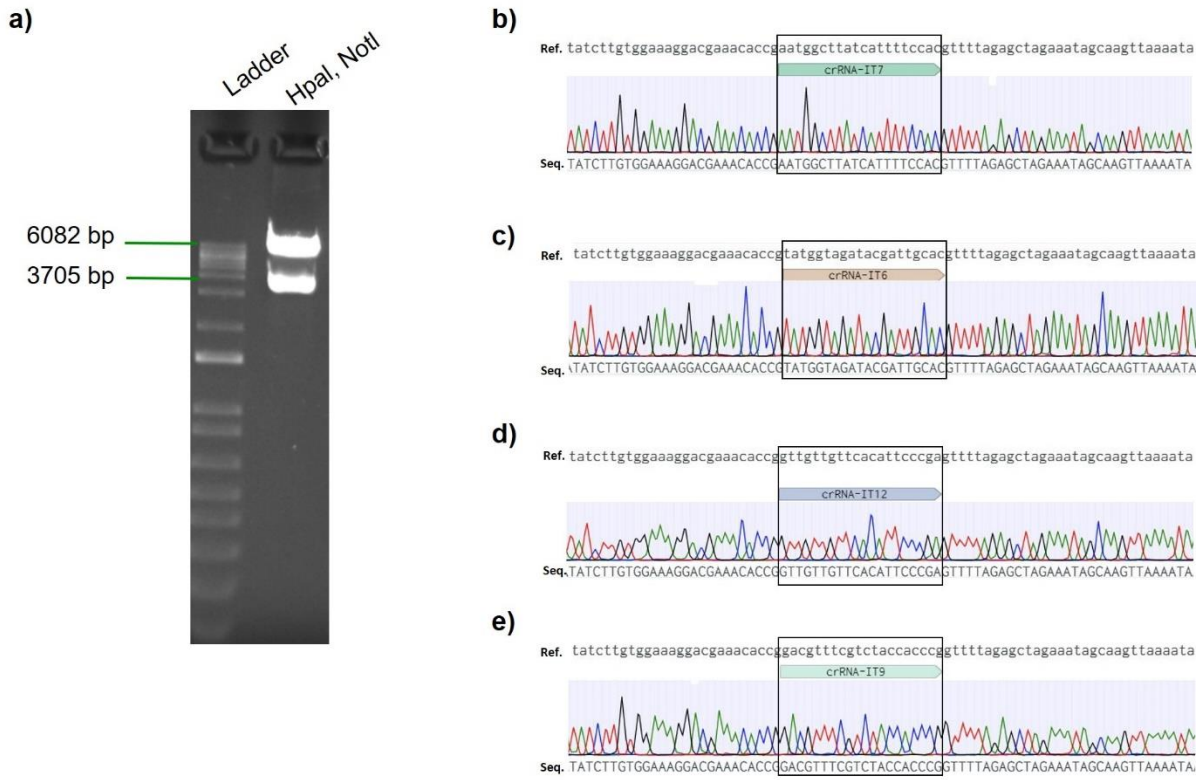

Figure 46: Cloning and sequencing of MDV-gRNA expression construct (K183). a) Control digest of positive clone 53 with restriction enzymes HpaI and NotI showing bands at expected sizes of 6082 bp and 3705 bp. b-e) Sequencing over the four MDV-gRNA sequences (black box) with the reference sequence (Ref.) on the top and sequencing results (Seq.) at the bottom.

3.2.2. Single integration of MDV-gRNAs in PGC clones (C2, C3, C6)

EGFP-expressing PGCs (LSL-EGFP 165-2 Line 54) derived from embryos at H&H stage 13-15 were stably transfected with the MDV-gRNA construct as described in Chapter 2.2.1.5. Three cell clones (C2, C3, C6) showed integration of the MDV-gRNA construct confirmed by PCR (Figure 47).

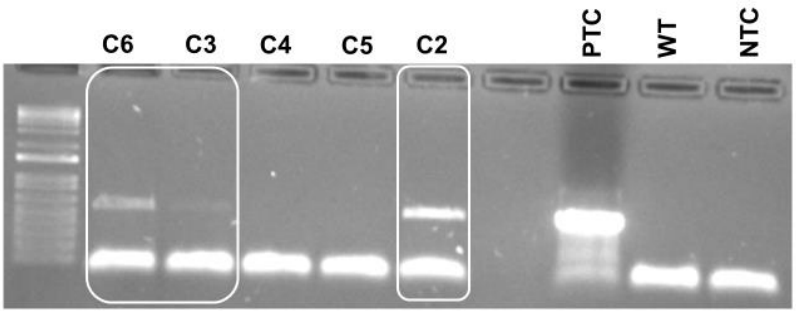

Figure 47: Detection of MDV-gRNAs in PGC clones by PCR. Three positive cell clones (C6, C3, C2) were observed (white boxes). Primers 653 and 651 were used to amplify an amplicon of 1317 bp. The annealing temperature

was 60 °C and the elongation time 1 minute and 30 seconds. As a positive control (PTC), the MDV-gRNA construct (K183) was used. A no template control (NTC) was used as a negative control.

MDV-gRNA copy numbers in PGC single cell clones (C2, C3 and C6) were examined. Figure 48 shows that all three clones had a single integration of MDV-gRNA with copy numbers of 0.84 (±0.14), 0.80 (±0.15) and 0.77 (±0.15) for C6, C3 and C2, respectively.

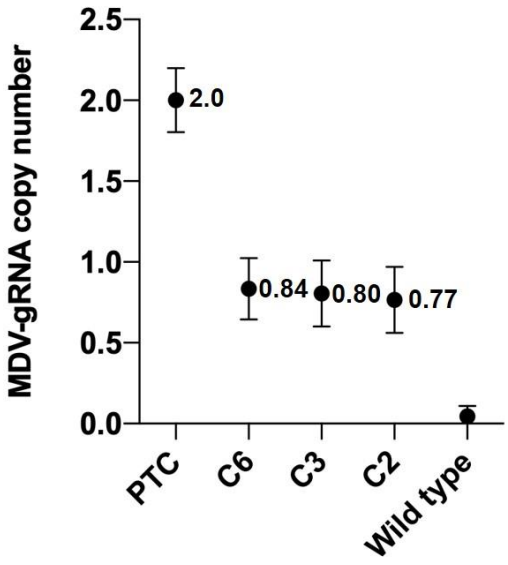

Figure 48: Analysis of MDV-gRNA copy numbers. The hygromycin resistance gene was used to determine MDV-gRNA copy numbers by ddPCR in PGC cell clones C2, C3, C6. As a positive control (PTC), Cas9-expressing tissue was used. Wild-type was used as a negative control. The error bars represent the standard deviation.

3.2.3. Colonization of the gonads by MDV-gRNA-expressing PGCs

The analyzed three PGC single cell clones (C2, C3, C6) were injected into 65 h old (H&H stage 13-15) embryos as described in Chapter 2.2.2.1. Modified PGCs successfully colonized the gonad (Figure 49).

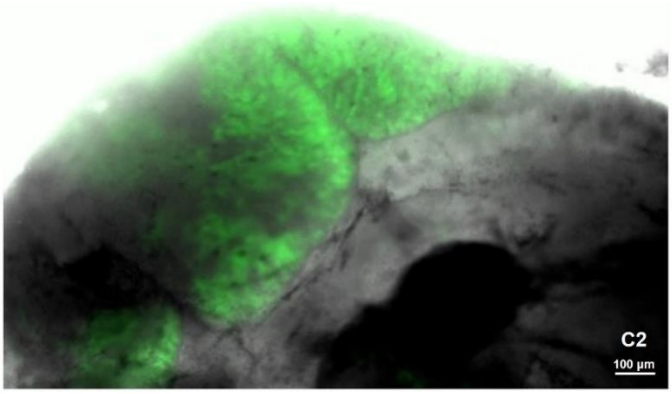

Figure 49: Colonization of a female gonad by MDV-gRNA-EGFP-expressing PGCs. Microscopy image shows the colonization of female gonad by PGCs stably expressing MDV-gRNAs and EGFP (C2). The size of the scale bar is 100 µm.

Table 78 summarizes the number of injected embryos, the number of total chimeras hatched and chimeric roosters that resulted from the injections, respectively. 36 embryos were injected with clone 2, resulting in 14 male chimeras. 29 embryos were injected with clone 3, resulting in two male chimeras. 40 embryos were injected with clone 6, resulting in 14 male chimeras.

Table 78: Overview of MDV-gRNA injections

Cell line (age at injection)	Injected embryos	Hatched chickens	Males
LSL EGFP PGC (54) MDV-gRNA C2 (108 days old)	36	24	14
LSL EGFP PGC (54) MDV-gRNA C3 (104 days old)	29	13	2
LSL EGFP PGC (54) MDV-gRNA C6 (103 days old)	40	23	14

3.2.4. Transmission of MDV-gRNAs to the offspring

Upon sexual maturity, sperm was collected from chimeric roosters and analyzed for transgene expression. Roosters with wing band numbers #47166, #47164, #47159, #47170 (C2) and #47190, #47192 (C6) were the most promising candidates for breeding as they showed gRNA specific bands at expected size in PCR (Figure 50).

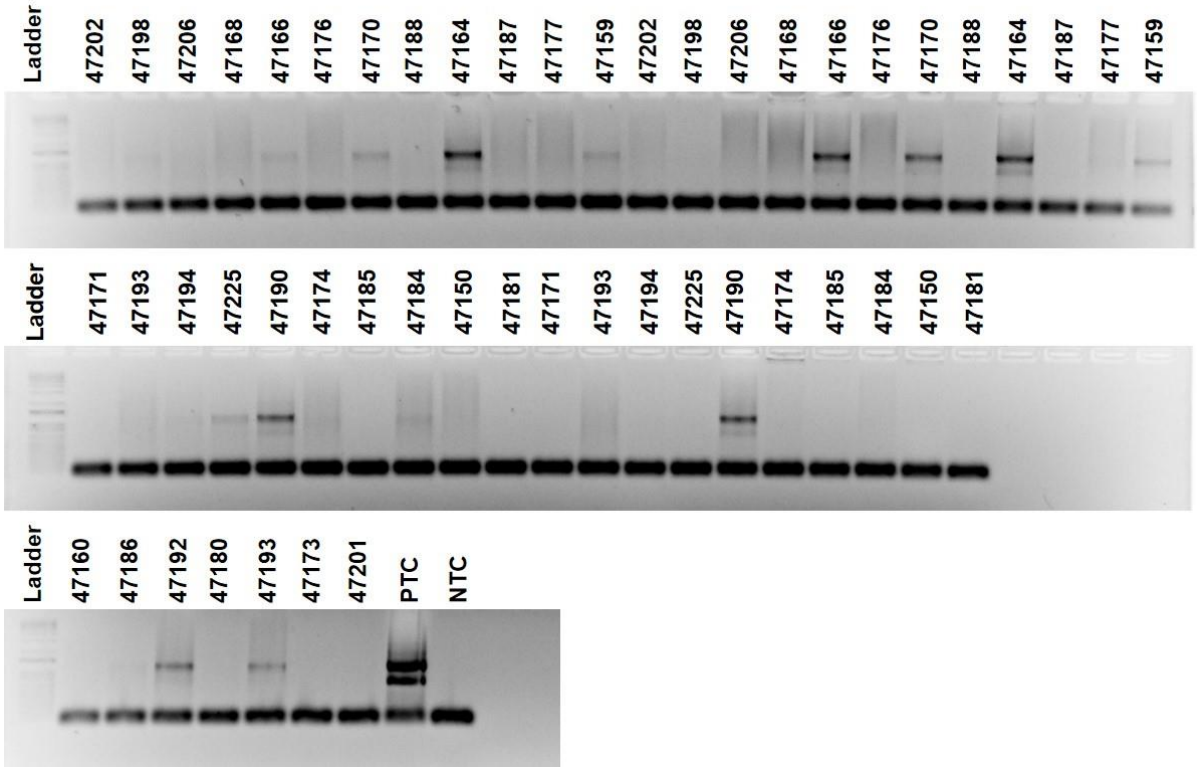

Figure 50: Analysis of sperm from MDV-gRNA germline chimeras. Sperm was collected over several days and analyzed for transgene expression by PCR. Roosters with germline modification displayed bands at size of expected amplicon of 1317 bp. Depending on how often the roosters were giving sperm, the number of the rooster appears several times on the gel picture. The most promising roosters were #47166, #47164, #47159, #47170 (C2) and #47190, #47192 (C6).

Chimera #47164 (C2) was chosen to be bred with WT hens to obtain heterozygous animals expressing ubiquitously MDV-gRNAs. The transmission rates were 16.32 % for EGFP and 12.24 % for MDV-gRNA (Table 79). Roosters from different PGC single cell clones were not tested due to the high transmission rates observed in #47164 (C2).

Table 79: Overview of MDV-gRNA transmission. The transmission rate was calculated according to the number of fertilized eggs

Clone	Fertilized	Hatched	EGFP	MDV-gRNA	EGFP/MDV-gRNA	EGFP (%)	MDV-gRNA (%)
C2	49	33	8	6	3	16.32	12.24

3.2.5. No phenotypic abnormalities in heterozygous MDV-gRNA-expressing chickens

Heterozygous MDV-gRNA-expressing chickens that originated from PGC single cell clone C2 were further analyzed. As observed for Cas9-expressing chickens (see Chapter 3.1.3), EGFP (resulting from LSL-EGFP 165-2 Line 54) and MDV-gRNAs segregated independently in the offspring. The following generations of this transgenic line were established without EGFP. Ubiquitously MDV-gRNA-expressing animals were observed on a daily basis and showed no physiological abnormalities. The weight of transgenic birds was measured over 10 weeks and compared to WT siblings. Figure 51a shows that there was no significant difference in weight between MDV-gRNA-expressing and WT animals (n≥3, p>0.05). After they reached sexual maturity, birds were fertile and gave rise to the next generation (Figure 51b).

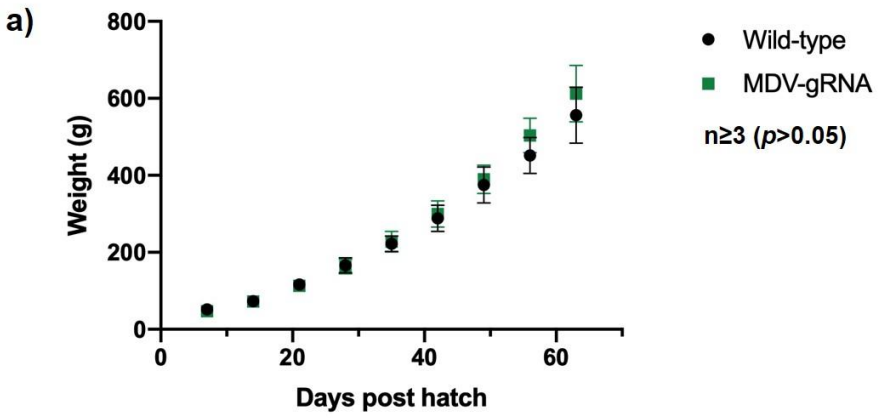

b)

Figure 51: Monitoring of MDV-gRNA-expressing chickens. a) Comparison of the weight between heterozygous MDV-gRNA-expressing and wild-type birds from the same hatch. The weight of male and female birds was measured over 70 days post hatch. No significant differences (n≥3, p>0.05) were determined. The error bars represent the standard deviation. b) Exemplary image of the MDV-gRNA-expressing chickens.

3.2.6. Expression of MDV-gRNAs in transgenic animals

To ensure that transgenic animals expressed all four MDV-gRNAs, a genotyping PCR covering the four MDV-gRNA cassettes was established (see Chapter 2.2.3.6, Figure 21). To test this PCR, gDNA was isolated from blood of MDV-gRNA-expressing animals. Figure 52 shows that all four MDV-gRNAs were present in transgenic animals.

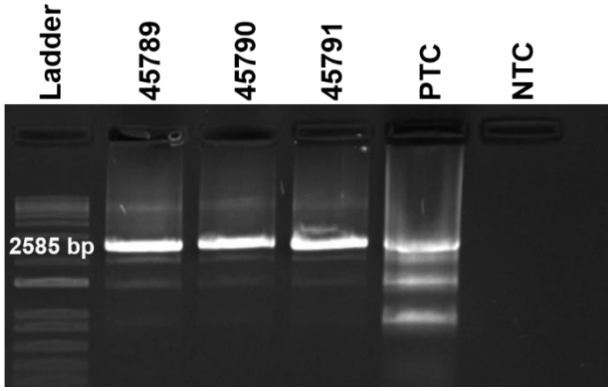

Figure 52: Genotyping of MDV-gRNA-expressing animals. LongAmp® PCR was performed on gDNA isolated from blood of animals #45789, #45790 and #45791. The expected amplicon was 2585 bp. As a positive control (PTC) the MDV-gRNA expression construct K183 was used. A no template control (NTC) was used as a negative control.

To examine MDV-gRNA expression in transgenic animals, a Taqman™ q-RT-PCR assay was established (see Chapter 2.2.3.11, Figure 22). Fluorescein amidite (FAM)-labeled oligonucleotide probes specific for each MDV-gRNA (IT7P, IT6P, IT12P, IT9P) were designed. The allelic discrimination plot was used as a basis to separate controls such as WT and negative samples from positive samples (Figure 53). The threshold was specified by the QuantStudio software. The MDV-gRNA expression construct (K183) (Table 46) and single pKL-IT plasmids containing only one of the gRNAs (Table 45) were used as positive controls. The analysis was performed on blood samples from animals with wing band numbers #47575, #47589 and #47590. Figure 53 shows that animal #47575 did not express MDV-gRNAs as no signal was observed above the threshold. In contrast, the expression of all four gRNAs was confirmed in animals #45789 and #45790 which is consistent with the results obtained from the genotyping (see Figure 52).

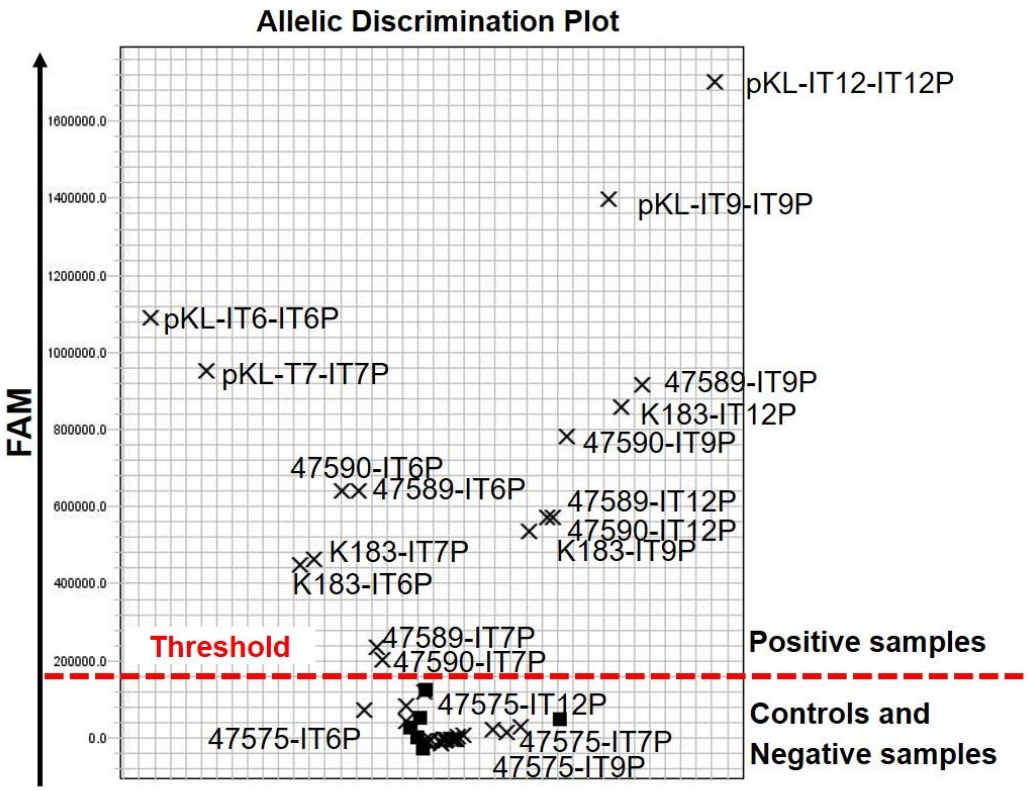

Figure 53: Allelic discrimination plot to detect MDV-gRNAs. RNA was isolated from PBMCs from the blood, followed by cDNA synthesis and Taqman™ q-RT-PCR assay. The plot shows FAM-labeled samples on the y-axis. The threshold separates controls such as wild-type and negative samples from positive samples. IT"x"-P represents the respective probe that labels the individual MDV-gRNAs (IT9, IT7, IT6, IT12). The preceding term (before the dash) represents the sample that was analyzed. pKL-IT9, pKL-IT7, pKL-IT6 and pKL-IT12 are the single plasmids for respective MDV-gRNA. As a positive control (PTC) that combines all four MDV-gRNAs, the MDV-gRNA construct K183 was used. The numbers 47575, 47589, 47590 represent animals.

Another q-RT-PCR assay based on SYBR® Green was established (see Chapter 2.2.3.12, Figure 24). The analysis shown in Figure 54 confirms that all four MDV-gRNAs were expressed in animals #47589, #47590 and #47591 but levels varied between animals. Averaged for animals #47589, #47590 and #47591, MDV-gRNA expressions were 1600 (±1200), 260 (±334), 370 (±289) and 10.5 (±6.6) for IT9, IT7, IT12 and IT6, respectively. All animals showed lower expressions of the respective gRNA compared to animal #45600 which was used as a positive control (Figure 54).

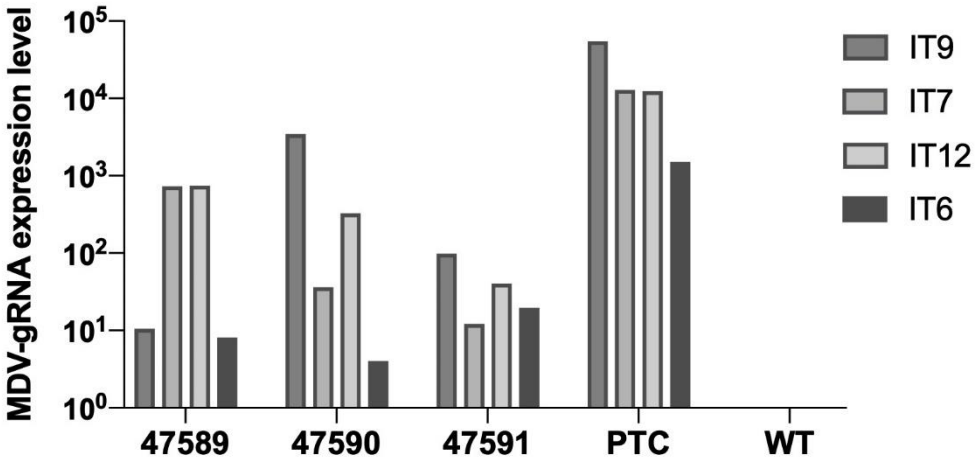

Figure 54: MDV-gRNA expression levels in transgenic animals. RNA was isolated from PBMCs from the blood, followed by cDNA synthesis and SYBR® Green q-RT-PCR assay. The figure shows expression of MDV-gRNAs (IT9, IT7, IT12, IT6) in animals with wing numbers #47598, #47590 and #47591. Animal #45600 was used as a positive control (PTC). A wild-type (WT) animal was used as a negative control. 18S served as an expression control.

To verify that the MDV-gRNA sequences were correctly expressed, the individual gRNA sequences were cloned into the pGEM® T Easy vector system as described in Chapter 2.2.4.8. Sequencing over each MDV-gRNA region showed that IT6, IT7 and IT12 were correctly expressed (Figure 55a,b,d). A deletion of one base pair that is located two base pairs upstream of the IT6 sequence (marked in red) was observed (Figure 55a). More importantly, IT9 (gRNA against *UL49*) was not correctly expressed according to this result. All nucleotides which did not match the correct IT9 sequence were marked in red (Figure 55c).

Since the *in vitro* experiments to initially test the MDV-gRNAs (see Chapter 1.1.5) showed that the combination of only two of the gRNAs, IT6 (*UL27*) combined with IT7 (*UL30*) or IT9 (*UL49*) combined with IT12 (*ICP4*), are necessary to completely abrogate MDV replication, the animals were further used for the purpose of this thesis.

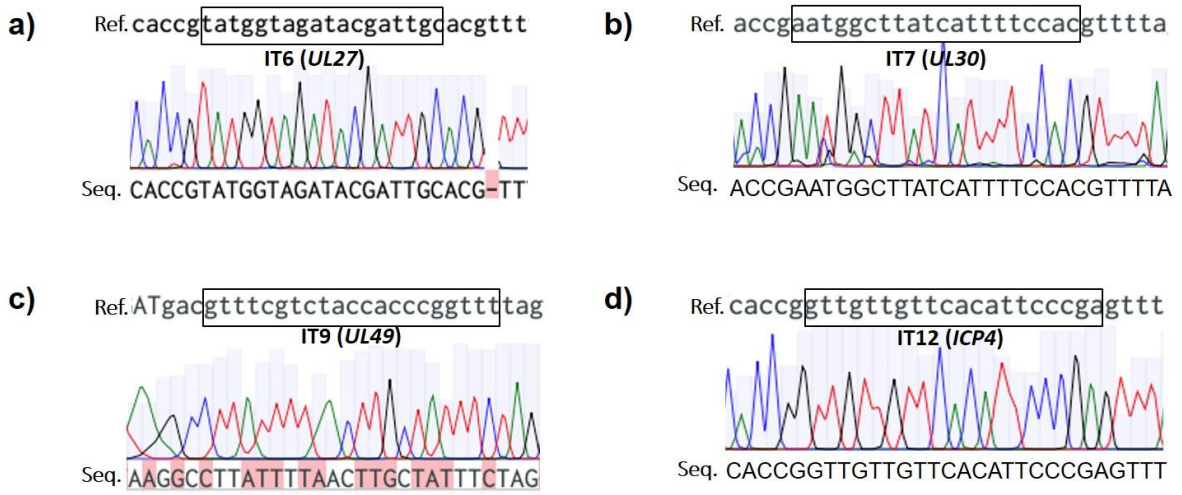

Figure 55: Sequencing results after cloning individual MDV-gRNAs into pGEM® T Easy. The amplified sequences were cloned into the pGEM® T Easy vector system. The figure shows the four MDV-gRNA sequences (black box) with the reference sequence (Ref.) on the top and sequencing results (Seq.) at the bottom. a) Sequencing result for IT6 (*UL27*) showing that sequence is correctly expressed. There was a -1bp deletion two base pairs upstream of the gRNA sequence which is marked in red. b) Sequencing result for IT7 (*UL30*) showing that the sequence is correctly expressed. c) Sequencing result for IT9 (*UL49*) showing that the sequence was not correctly expressed as indicated in red. d) Sequencing result for IT12 (*ICP4*) showing that the sequence is correctly expressed.

3.3. No phenotypic abnormalities in heterozygous Cas9-MDV-gRNA-expressing chickens

Upon reaching sexual maturity, animals from both transgenic lines were bred together to generate chickens that express Cas9 and MDV-gRNA together. Because both transgenic chicken lines contained hygromycin resistance cassettes, it was important to ensure that double transgenic animals exhibit no negative side effects due to the overexpression of the antibiotic resistance. The animals were monitored on a daily basis but no physiological abnormalities such as crop enlargement were observed. The weight of Cas9-MDV-gRNA animals was measured once a week over 10 weeks and compared to WT birds from the same hatch and revealed that there was no significant difference (n≥4, p>0.05) between both groups (Figure 56).

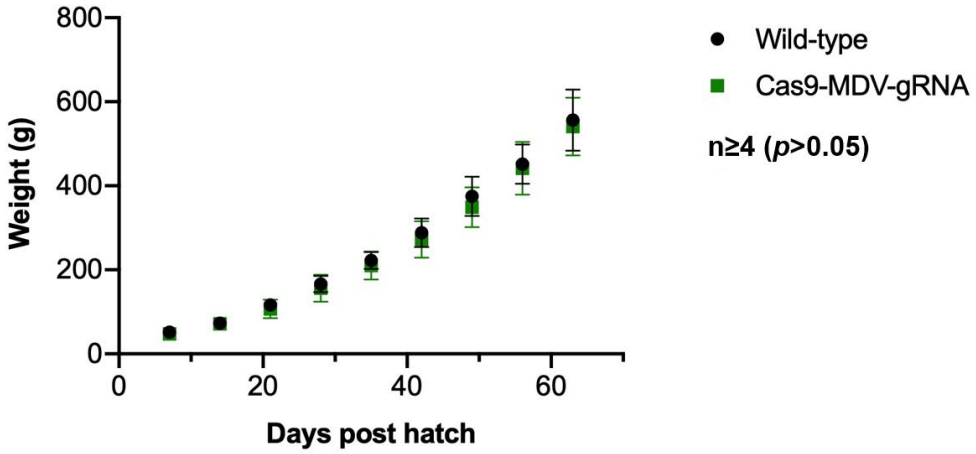

Figure 56: Comparison of the weight of Cas9-MDV-gRNA-expressing and wild-type chickens. The weight of male and female birds was measured over 70 days post hatch. No significant differences (n≥4, p>0.05) were determined. The error bars denote the standard deviation.

3.4. *In vivo* infection challenge – Cas9-MDV-gRNA-expressing chickens were not protected against MDV

To test the hypothesis that the CRISPR/Cas9 system can be used to protect chickens from MDV, the double transgenic Cas9-MDV-gRNA animals were used for an *in vivo* infection challenge. One day after hatch, the chickens were infected with a vvMDV strain RB-1B. It was expected that the ubiquitous expression of both CRISPR/Cas9 components in these animals allows for the inactivation of the virus replication upon infection. WT birds or birds that expressed only Cas9 or MDV-gRNA alone should therefore not be protected and were used as control animals. Additionally, it was examined whether the virus can be stopped from shedding through the natural airborne route and thus from transmitting to non-transgenic birds.

The infection experiment was performed in collaboration with Prof. Benedikt Kaufer (Institute of Virology, FU Berlin, Germany)* and conducted as described in Chapter 2.2.2.5. Results obtained by the group of Prof. Kaufer will be clearly marked.

Out of 159 eggs from a Cas9 (+/-) x MDV-gRNA (+/-) breeding, 63 birds hatched. In Figure 57 and Figure 58 the genotyping of MDV-gRNA and Cas9 is shown. According to Mendel´s laws of inheritance, a quarter of the animals were Cas9-only (25.4 %), MDV-gRNA-only (23.8 %), WT (25.4 %) and both Cas9-MDV-gRNA (25.4 %).

The animals were divided into a test (Cas9-MDV-gRNA) and a control (Cas9-only, MDV-gRNA-only, WT) group and infected with RB-1B as described in Chapter 2.2.2.5. Valo-SPF contact birds were housed next to the animals but were not infected.

*Unfortunately, travel restrictions due to the Covid-19 pandemic in 2020 prohibited me from traveling to Berlin to assist the infection experiment in person. Samples were shipped to TUM for further analysis.

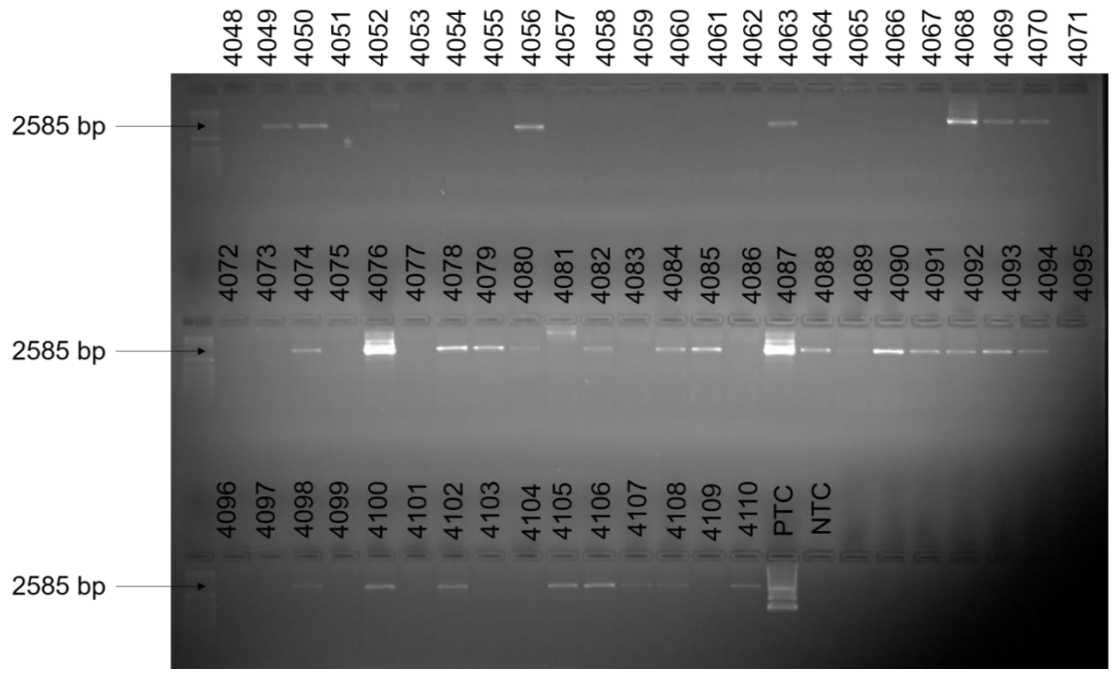

Figure 57: MDV-gRNA genotyping of 63 chicks that hatched for RB-1B infection challenge. LongAmp® PCR was used. MDV-gRNA-positive animals showed band at expected size of 2585 bp. As a positive control (PTC), the MDV-gRNA expression construct (K183) was used. A no template control (NTC) was used as a negative control.

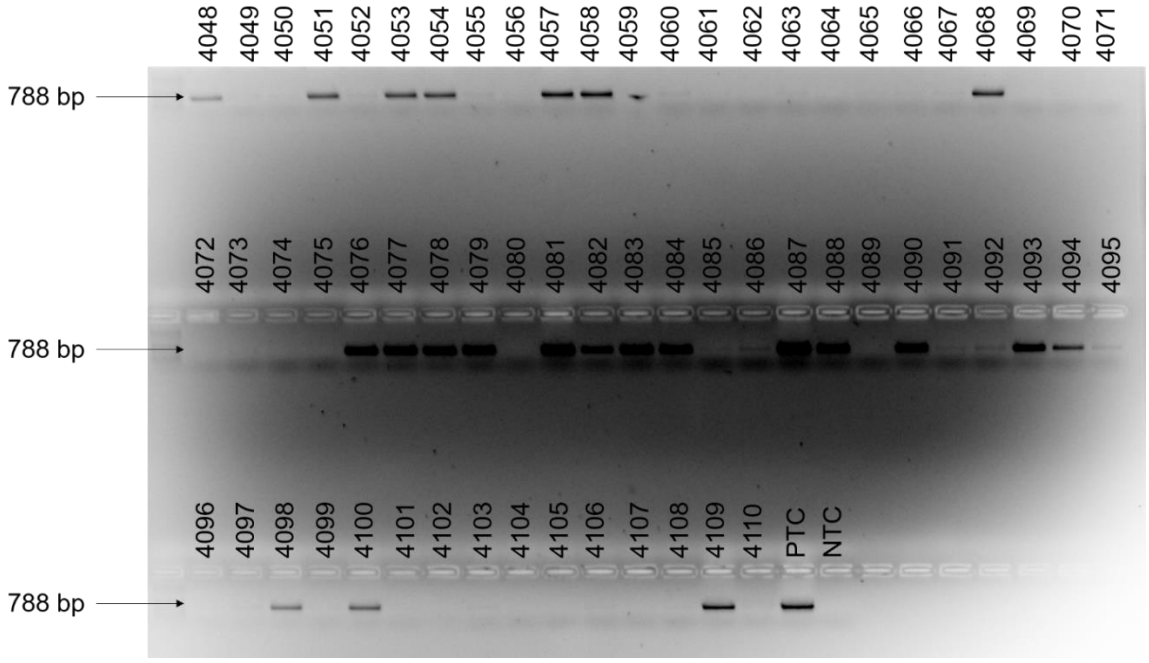

Figure 58: Cas9 genotyping of 63 chicks that hatched for RB-1B infection challenge. FIREPol® PCR was used. Cas9 positive animals showed band at expected size of 788 bp. As a positive control (PTC), the Cas9 expression construct (K146) was used. A no template control (NTC) was used as a negative control.

The results from the infection experiment show that infected birds from both groups exhibited tumorous lesions mostly in the spleen and kidney (Table 80). Organ samples from nine animals of test group and control group were collected (Table 80). In the control group, five out of nine animals (#4064, #4070, #4072, #4096 and #4097) showed MD-induced symptoms (ataxia, immunosuppression) and the formation of tumors. In the test group, five out of nine animals (#4082, #4085, #4087, #4088 and #4090) showed MD-induced symptoms (ataxia, immunosuppression) but not all of them had tumors. As pointed out in Table 80 animal #4063 was falsely placed into the Cas9-MDV-gRNA group as the genotyping showed the presence of MDV-gRNA in this animal but no expression of Cas9 (Figure 57, Figure 58). Also Valo-SPF contact birds showed MD-induced symptoms in two birds from the control contact (2 out of 11) and two from the Cas9-MDV-gRNA contact group (2 out of 11). The data is not shown.

Table 80: Summary of MDV infection experiment. The data was collected from Kaufer and colleagues. The table shows number of birds from control and test groups, day of death post infection (pi), MDV incidences, tumor incidences and samples that were taken during or at the end of the experiment (90 days final necropsy). Animal No. 4063 (marked in grey) was falsely placed into the Cas9-MDV-gRNA group as it only expressed MDV-gRNA but no Cas9

Bird Number	Group	Death (days pi)	MDV incidence	Tumor incidence	Samples taken
4051	Control	90	Final Necropsy	No	Spleen, Bursa, Thymus
4052	Control	90	Final Necropsy	No	Spleen, Bursa, Thymus
4053	Control	90	Final Necropsy	No	Spleen, Bursa, Thymus
4056	Control	90	Final Necropsy	No	Spleen, Bursa, Thymus
4064	Control	71	Atactic	Yes (Spleen, Liver)	Spleen, Liver
4070	Control	71	Atactic	Yes (Spleen, Gonad, Kidney)	Spleen, Gonads, Kidney
4072	Control	45	Weak	Yes (Spleen, Gonad)	Spleen, Gonads
4096	Control	85	Weak	Yes (Spleen, Breast muscle)	Spleen
4097	Control	59	Yes	Yes (Spleen, Kidney)	Spleen, Kidney
4063	Cas9-MDV-gRNA	90	Final necropsy	No	Spleen, Bursa, Thymus
4068	Cas9-MDV-gRNA	90	Final necropsy	No	Spleen, Bursa, Thymus
4078	Cas9-MDV-gRNA	90	Final necropsy	No	Spleen, Bursa, Thymus
4082	Cas9-MDV-gRNA	52	Weak	No	Spleen

4085	Cas9-MDV-gRNA	34	Yes	Yes (Liver, Kidney, Gonad, Spleen)	Spleen, Kidney
4087	Cas9-MDV-gRNA	62	Atactic	Yes (Spleen, Kidney)	Spleen, Kidney
4088	Cas9-MDV-gRNA	85	Atactic	No	Spleen, Bursa, Thymus
4090	Cas9-MDV-gRNA	35	Weak	Yes (Spleen)	Spleen
4100	Cas9-MDV-gRNA	90	Final necropsy	No	Spleen, Bursa, Thymus

Kaplan-Meier analysis of MD incidences in test and control group revealed that Cas9-MDV-gRNA-expressing animals developed MD-induced symptoms starting from day 34 post infection (pi) reaching incidences of 31.25 %; and control animals developed MD-induced symptoms starting from day 45 pi reaching incidences of 20 % (Figure 59a). In addition, the ratio of tumor incidences were calculated for both groups which was 5 % higher in Cas9-MDV-gRNA-expressing chickens (with a tumor incidence of 30 %) than in the control group (with a tumor incidence of 25 %) (Figure 59b).

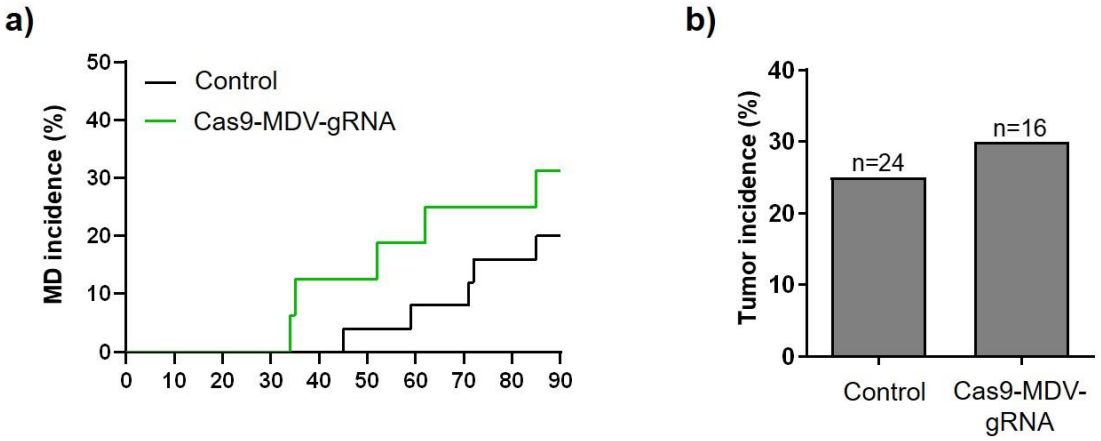

Figure 59: MD and tumor incidences. Figure shows data from infected birds of the control group (n = 24) and Cas9-MDV-gRNA (n = 16) group. a) MD incidences (%) over 90 days. Control group = black line; Cas9-MDV-gRNA group = green line. b) Tumor incidence (%) of animals that developed tumors during the experiment and at the final necropsy. The data was collected, analyzed and presented by Andelé Conradie (Institute of Virology, FU, Berlin, Germany).

Figure 60 shows the mean number of MDV genome copies in the blood (Figure 60a) and feather follicles (Figure 60b) in the control and Cas9-MDV-gRNA group and revealed no significant reduction (p>0.05, Kruskal-Wallis). In both groups viral genome copies increased in the blood starting from day 4 pi with titers of $1.5x10^1$ copies/10^6 cells in the control and

3.2x10[1] copies/10[6] cells in the Cas9-MDV-gRNA group, reaching up to 1.1x10[4] copies/10[6] cells at day 28 pi for both groups (Figure 60a). In the feather follicles, the number of viral genome copies was for both groups low (3.1x10[1] copies/10[6] cells) until day 10 pi and then increased rapidly, reaching up to 1.7x10[7] copies/10[6] cells in the control and 2.2x10[6] copies/10[6] cells in the Cas9-MDV-gRNA group at day 35 pi (Figure 60b).

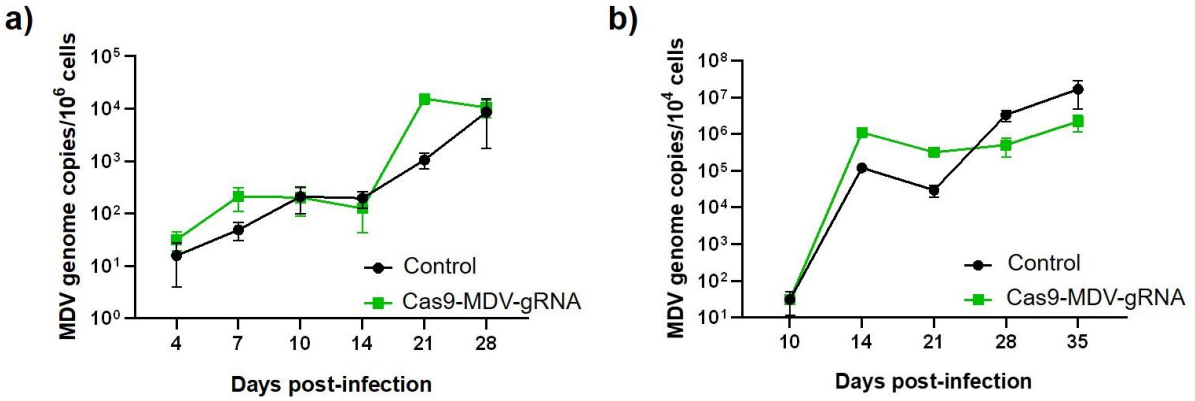

Figure 60: MDV genome copies detected by MDV-*ICP4*-qPCR in blood or feathers of infected chickens. Figure shows data from infected birds of the control group (n = 24) and Cas9-MDV-gRNA (n = 16) group. a) Mean MDV genome copies in blood per one million cells are shown for the indicated time points collected at 4, 7, 10, 14, 21 and 28 dpi. b) Feathers were collected at 10, 14, 21, 28 and 35 dpi. No significant differences were observed (p>0.05, Kruskal-Wallis test). The data was collected, analyzed and presented by Andelé Conradie (Institute of Virology, FU, Berlin, Germany).

The tissue samples collected over the period of the experiment or at the final necropsy were further analyzed for Cas9 and MDV-gRNA expression. Figure 61a shows that there was no difference for Cas9 expression within the Cas9-MDV-gRNA group between animals that survived (#4078 and #4100) and animals that died (#4082 and #4087). Animal #4100 (survivor) expressed ten times less of the Cas9 endonuclease compared to the other animals analyzed.

The expression analysis of individual MDV-gRNAs revealed that there was a 18-fold reduction of gRNA IT9 and a 10-fold reduction of gRNA IT7 in birds that died (#4085, #4087) compared to the ones that survived (#4078, #4100) until the end of the experiment (Figure 61b). Because of insufficient number of samples it was not possible to test for statistical significances.

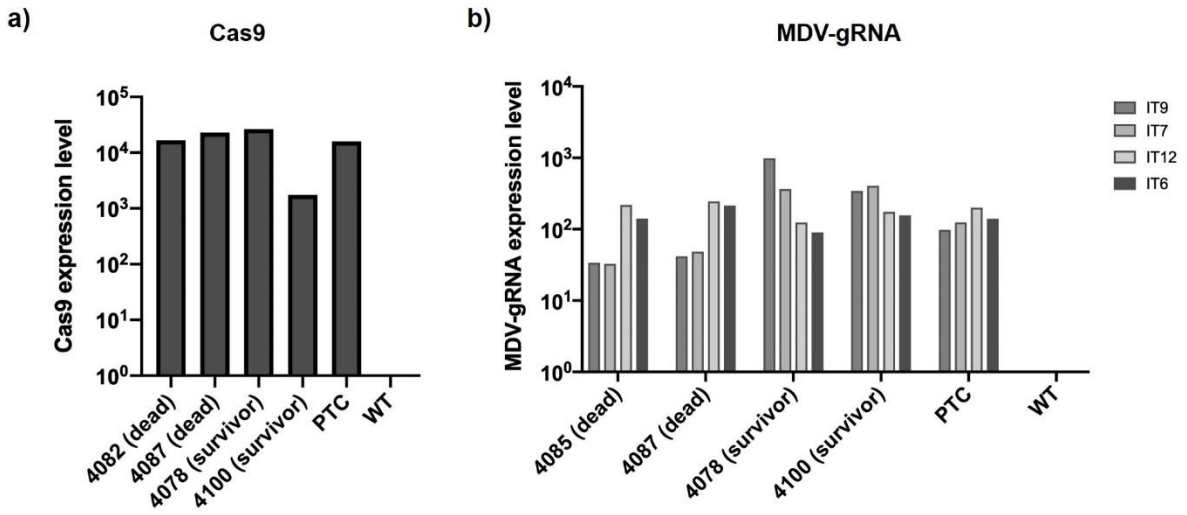

Figure 61: Cas9 and MDV-gRNA expression levels in survivor and dead birds. a) Cas9 SYBR® Green q-RT-PCR was done on spleen samples of infected Cas9-MDV-gRNA-expressing chickens (survived = #4078 and #4100; dead = #4082 and #4087). cDNA from the spleen of a Cas9-expressing animal was used as a positive control (PTC). cDNA from a wild-type (WT) animal was used as a negative control. 18S served as an expression control. b) MDV-gRNA SYBR® Green q-RT-PCR was done for each MDV-gRNA on spleen samples of infected Cas9-MDV-gRNA-expressing birds (survived = #4078 and #4100; dead = #4085 and #4087). MDV-gRNAs were detected individually. cDNA from the spleen of a MDV-gRNA-expressing animal was used as a positive control (PTC). cDNA from the spleen of a wild-type (WT) animal was used as a negative control. 18S served as an expression control.

3.5. Breeding of heterozygous MDV-gRNA-expressing chickens led to homozygosity

To investigate, if MDV-gRNA animals could possibly be bred to homozygosity, 17 eggs from a MDV-gRNA (+/-) x MDV-gRNA (+/-) breeding (Figure 62a) were incubated. Eleven animals hatched and were genotyped, showing that six animals #40333, #40334, #40335, #40336, #40337 and #40338 were MDV-gRNA-positive (Figure 62b).

These six animals were analyzed regarding MDV-gRNA copy numbers by ddPCR, revealing that one animal (#49336) was homozygous with 1.79 (±0.08) copies. All other animals had a single integration of MDV-gRNA (0.90±0.08 (#49333), 0.90±0.07 (#49334), 0.90±0.05 (#49335), 0.90±0.06 (#49337) and 0.91±0.07 (#49338)) (Figure 62c).

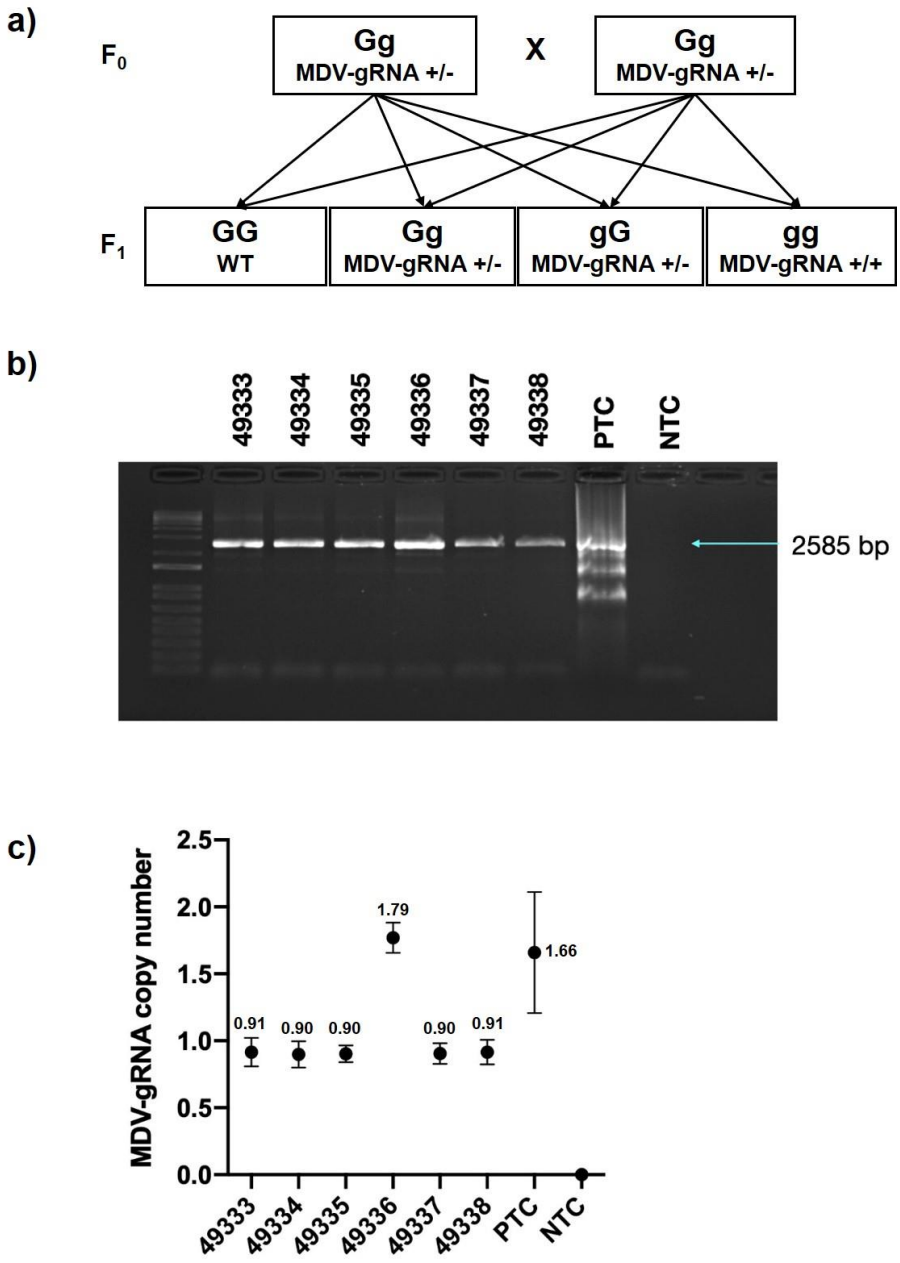

Figure 62: MDV-gRNA homozygous (+/+) chicken. a) Breeding scheme to obtain homozygous MDV-gRNA chickens. Breeding of two heterozygous (+/-) animals in the F_0 generation results in a quarter of WT, a quarter of homozygous and half of heterozygous animals in the F_1 generation. Note: Capital letters code for wild-type alleles; lowercase letters code for genetically modified alleles. b) MDV-gRNA genotyping by LongAmp® PCR resulting in an amplicon of 2585 bp. Animals (#49333, #49334, #49335, #49336, #49337 and #49338) were MDV-gRNA positive. As a positive control (PTC), the MDV-gRNA expression construct was used. No template control (NTC) was used as a negative control. c) Copy number analysis by ddPCR to determine homozygous MDV-gRNA animals. One animal (#49336) had two copies while the rest had one copy of MDV-gRNA. The error bars represent the standard deviation.

3.6. Attempt to breed homozygous Cas9-expressing chickens failed

To investigate if it is possible to breed C4 originated heterozygous Cas9-expressing chickens to homozygosity, 72 eggs from a Cas9 (+/-) x Cas9 (+/-) breeding (Figure 63a) were incubated. Interestingly, only 11 animals hatched from this breeding as 52 eggs dropped out at ED7 after candling. Four embryos were dead and 48 eggs were unfertilized or embryos did not develop.

Cas9 genotyping was done (Figure 63b) and six Cas9 positive animals were further investigated regarding their Cas9 copy numbers. None of these animals was homozygous for Cas9 displaying copy numbers of 0.97±0.08 (#49340), 0.97±0.07 (#49341), 0.95±0.07 (#40343), 0.95±0.08 (#40344), 0.91±0.07 (#40345) and 0.95±0.07 (#40347) (Figure 63c).

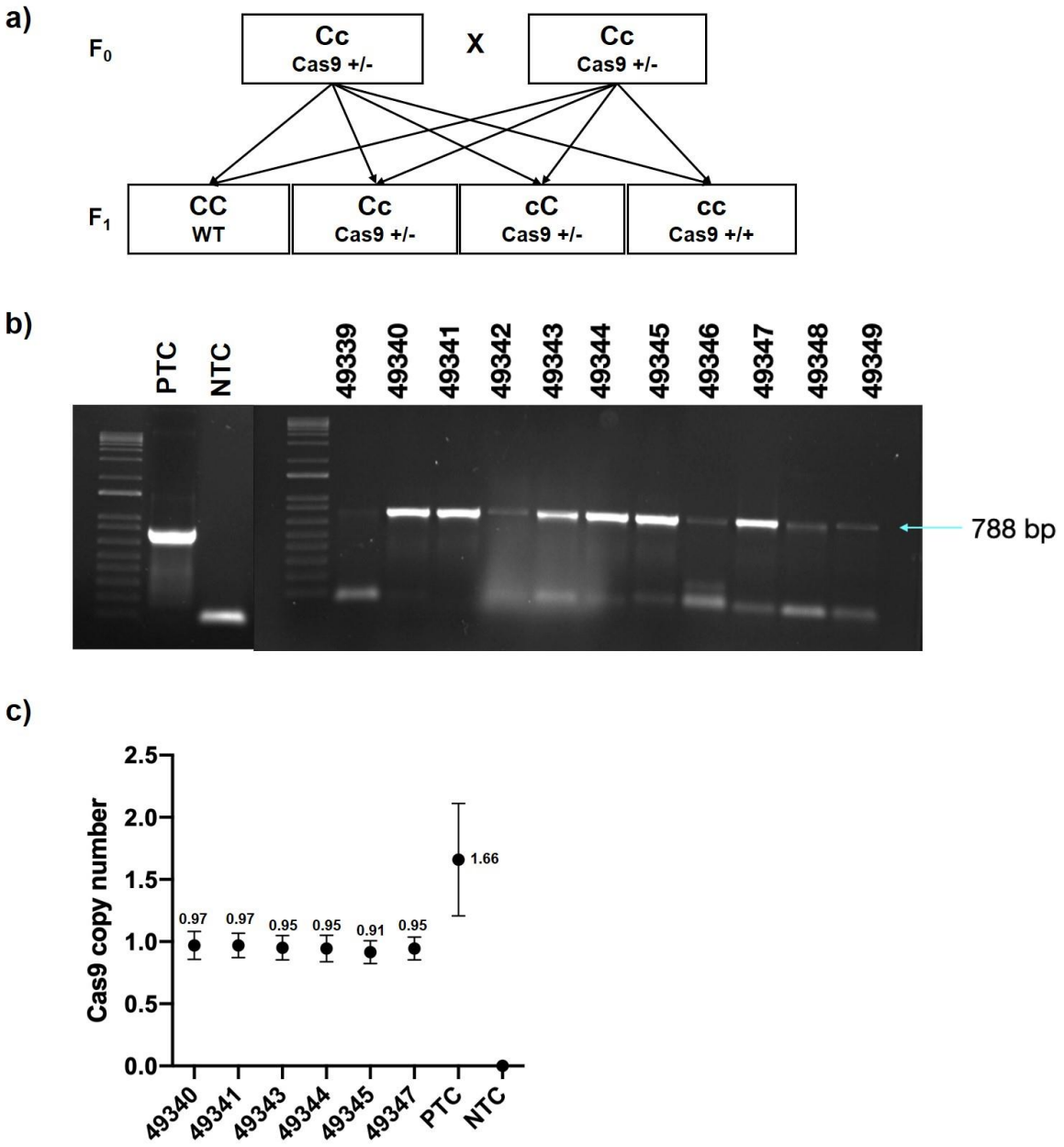

Figure 63: Attempt to breed Cas9 homozygous (+/+) chickens. a) Breeding scheme to obtain homozygous Cas9 chickens. Breeding of two heterozygous (+/-) animals in the F0 generation results in a quarter of WT, a quarter of homozygous and half of heterozygous animals in the F1 generation. Note: Capital letters code for wild-type alleles; lowercase letters code for genetically modified alleles. b) Cas9 genotyping by FIREPol® PCR resulting in an amplicon of 788 bp. As a positive control (PTC), the Cas9 expression construct was used. A no template control (NTC) was used as a negative control. c) Six Cas9 positive embryos (#49340, #49341, #49343, #49344, #49345 and #49347) were analyzed for Cas9 integration numbers to determine possible homozygous animals. None of the animals had more than one copy of Cas9. The error bars represent the standard deviation.

4. DISCUSSION

The goal of this work was the implementation of the CRISPR/Cas9 system into chickens to provide a platform for *in vivo* genome editing. The first objective was to establish a ubiquitously Cas9-expressing chicken line for the purpose of efficient *in vivo* and *ex vivo* genome editing which will be discussed in Chapter 4.1. The second goal of this project was to make use of the novel Cas9-expressing chicken model and establish an *in vivo* CRISPR/Cas9-mediated resistance against MDV in chickens (Chapter 4.2).

4.1. Cas9-expressing chickens – A tool for *in vivo* genome editing

Genome editing requires the simultaneous delivery of the sgRNA and Cas9 endonuclease. This can be difficult due to insufficient packaging capacities of many delivery vectors and the potential safety risks when human and animal target sequences are highly homologous [206]. To overcome these constraints, transgenic animals that ubiquitously express Cas9 were generated, providing an efficient and safe platform for Cas9-mediated *in vivo* genome editing. This has the advantage that only sgRNAs need to be delivered via viral vectors or non-viral delivery methods such as electroporation. This allows for efficient tissue-specific genome editing and multiplexing by combining multiple gRNAs into one vector.

So far, mainly Cas9-expressing mammals such as mice and pigs were generated [113,210]. Nevertheless, phylogenetically distant species such as chickens offer the opportunity to study gene functions for basic research questions as well as cross-species comparisons which are important to understand how genes are conserved over evolution. In this thesis, transgenic chickens that ubiquitously express the Cas9 endonuclease from *Streptococcus pyogenes* were generated and characterized. The results were published on *bioRxiv* as a preprint in April 2020 [238], followed by peer review and publication in the journal of *Proceedings of the National Academy of Sciences* (PNAS) in January 2021 [237].

Generation of ubiquitous Cas9-expressing chickens. In July 2020, three months after our preprint was published, a research group also reported on the generation of Cas9-expressing chickens [109]. Challagulla et al. generated fully transgenic chickens constitutively expressing Cas9-HF1, GFP and gRNAs targeting exon 1 of the endogenous interferon alpha and beta receptor subunit 1 gene (IFNAR1-gRNAs). To facilitate stable transgene integration into the chicken genome, the authors transfected PGCs *in vivo* with a miniTol2 plasmid containing

Cas9-HF1 under the CMV promoter, GFP expression driven by the CAGG promoter and two IFNAR1-gRNAs each under the human U6 promoter. After breeding chimeras with wild-type animals, 1/301 chickens was fully transgenic. The low transgenesis rate probably originated from the direct injection system which often results in low efficiencies as was shown by other studies that used direct *in vivo* transfection of PGCs [108]. In addition, the authors speculated that the low transgenesis rate resulted from the large cargo size, mainly due to the Cas9 endonuclease, that was inserted within the ITRs of the Tol2 transposon [109]. The major disadvantage of transposon-mediated transgenesis lies in the unpredictability of these mobile genetic elements to transpose to new locations which can interfere with endogenous genes, resulting in effects which are unwanted, especially for *in vivo* applications [245]. Although no difference in phenotype between wild-type and transgenic chickens was observed, the authors mentioned that they could not neglect the possibility of off-target events by the stable expression of both, Cas9-HF1 and IFNAR1-gRNAs [109].

In this thesis, a transgenic chicken line was generated that ubiquitously expresses Cas9 without the presence of additional gRNAs. Transgenic chickens were generated by phiC31 integrase-mediated integration of a Cas9 expression construct into a chicken endogenous pseudo attP site, which has previously been reported to increase the integration frequency in PGCs [190] and which, in contrast to transposons, does not allow for genetic mobility. Health-related risks in animals are more foreseeable by using phiC31 which is important with respect to animal welfare and the approval of new transgenic lines for science and agriculture. Furthermore, the use of *in vitro*-modified PGCs enables the screening of transgenes and their integration before the cells are re-introduced back into a surrogate embryo which is an advantage over direct injection.

The presence of a hygromycin resistance gene in the Cas9 expression construct enabled the selection of single cell clones in cell culture. The PGC clones were screened by immunofluorescence and flow cytometry (data not shown) and confirmed Cas9 expression and functionality in these cells [237,238]. Consequently, all embryos that were injected with PGCs from one clone carried the same modification, ensuring a uniform expression profile. To avoid potential silencing of the Cas9 transgene, HS4 insulator sequences were used, acting as enhancers together with endogenous transcriptional elements to activate promoters on the constructs [189].

The PGCs used to generate chimeric germline roosters already carried an EGFP transgene which simplified analysis of transgenic animals due to the fluorescence of the reporter gene [170]. It was observed that both transgenes, EGFP and Cas9, were two independent integration events, therefore they were segregated or inherited together in the offspring. Since the expression of EGFP in adult animals is thought to be accompanied with poor phenotypes such as crop enlargement, the following generations of the Cas9 transgenic line were established without EGFP and only Cas9-EGFP-expressing embryos were used for functionality testing of the Cas9 endonuclease. The Cas9 germline transmissions observed in this study are in line with other studies reporting frequencies ranging from < 1 % to 86 % [189].

Homozygote Cas9-expressing chickens are not viable. Interestingly, no Cas9-expressing chicks hatched from chimeric roosters originated from PGC single cell clones C2 and C5 (Table 76). Therefore, the assumption was made that these animals died during embryogenesis, possibly because of potential toxic effect of high Cas9 expression as observed for Cre-recombinase expressing mice [246] and/or insertional mutagenesis that can occur during random integration. Although transgene insertion aims for the insertion of a foreign gene into a genomic region that will not disrupt the function of the host genome, random integration does not provide a direct control over the site of integration which can lead to variable copy numbers per cell and unpredictable gene expressions [247–249]. As mentioned above, the phiC31 integrase preferably integrates into att-bearing regions of the chicken genome that contains repetitive DNA sequences of which it is presumed that these are suitable sites in non-coding regions [189]. It is possible that endogenous genes are affected by this random insertion, leading to deleterious effects that influence development, health and longevity of these animals [189]. This effect is even more dangerous when animals are homozygous and the transgene is integrated into both of the alleles. The analysis of transgene copy numbers revealed that PGC single cell clone C4 had only a single integration, in contrast to C2 and C5 that had two integrations of the Cas9 gene (Figure 26). It can be assumed that thus homozygous animals are not viable and that clone 4 originating animals are viable because they are heterozygous, expressing still one wild-type allele. The attempt of breeding C4 heterozygous animals to homozygosity failed (Figure 63), emphasizing the fact that Cas9 overexpression and/or insertional mutagenesis leads to lethality. Furthermore, it was observed that C4 and C2 originating homozygous embryos probably died at different stages during embryogenesis as more than half of the C4 homozygous embryos died already very

early (until ED7) and C2 homozygous embryos died at a later time between ED18-21. It should be tested if lethal effects of ED7 dead embryos correlate with homozygosity. DNA from the germinal crescent should be isolated from these embryos and analyzed regarding Cas9 copy numbers which was, however, not done within the scope of this work.

Ubiquitous expression of Cas9 in transgenic animals. Despite the fact that homozygosity in Cas9 transgenic animals seems to be lethal, heterozygous animals show no phenotypic abnormalities and are fertile. The expression of Cas9 was analyzed on mRNA and protein level (Figure 28, Figure 29), and quantitatively by q-RT-PCR (Figure 30). As expected, Cas9 was ubiquitously expressed due to the use of the chicken β-actin promoter. However, differences in Cas9 expression between Cas9-expressing cells and tissues were observed. Cell lines that were stably transfected with Cas9 showed higher Cas9 expression compared to primary cells such as isolated Cas9-CEF or tissues from a Cas9-expressing animal (Figure 30). Studies showed that the gene expression can strongly differ from cells to tissue due to transcription and epigenetic factors [250] and due to inter-individual difference between tissues [251]. This was also observed in this study as e.g. Cas9 expression in the heart tissue was 18-fold higher than in the liver. In addition differences between cells and tissues might be explained by the fact that cDNA is required for q-RT-PCR analysis and the isolation of RNA followed by cDNA synthesis is more difficult to realize for tissue samples because of the time needed to isolate and prepare tissue samples (e.g. homogenization) compared to cells. Nonetheless, these were results from one animal and no statistical analysis was performed due to the lack of tissue samples available from different animals. Analysis on more Cas9-expressing animals would be interesting to further investigate Cas9 expression levels in tissues.

The Cas9 endonuclease is functional. In proof-of-principle experiments, the functionality of Cas9 was confirmed *in vitro* and *in vivo* by delivering only sgRNAs to Cas9-expressing cells or embryos from a heterozygous animal, resulting in the formation of INDELs by the mechanism of NHEJ after DSB. The biggest downside of Cas9 and other site-specific nucleases are possible off-target effects, resulting from off-target cleavage and accidental inactivation of non-target genes. These unintended cleavages can occur at sites that differ by up to 5 bases from the target sequence and can result in phenotypic consequences unrelated to the on-target gene editing effect [250]. The prediction of off-target events is crucial but their identification is not trivial. Most of the online off-target algorithms assume that off-target sequences are closely

related to the on-target site which potentially misses off-target cleavage sites with less sequence similarity. In this work, suitable gRNAs were used that have been tested in previous studies [214,251] and showed high predicted on-target and low off-target binding (Table 77).

***In vitro* studies**: Primary CEF from a Cas9-expressing embryo were transfected with sgRNAs directed against EGFP (in case of Cas9-EGFP-expressing CEF) or B2M by employing different methods for gRNA delivery, such as transfection with plasmid-DNA, synthetic gRNAs or viral-based delivery methods (RCAS). All approaches resulted in editing of the target locus. Nevertheless, the efficiencies were strongly dependent on the gRNA delivery method ranging from 27.2 % for synthetic gRNAs (Figure 35) to 69.3 % homozygous gene inactivation in RCAS-transduced Cas9-EGFP-expressing CEF (Figure 34). As expected, targeting efficiencies in RCAS-transduced cells were higher and increased over time compared to cells targeted with synthetic gRNAs. This is due to the fact that synthetic gRNAs are small oligonucleotides that are not translated into proteins, leading to an immediate double-strand break in the presence of Cas9 endonuclease with no increased potential for gene inactivation (see Figure 35a). In contrast, RCAS is a derivative of the retroviral Rous sarcoma virus [218,252] that has been shown to efficiently deliver foreign DNA into chicken cells and embryos [253,254]. The infection of cells is dependent on specific interactions between the envelope glycoprotein on the surface of the virus and the cognate receptor on the surface of the cell. As mammalian cells do not display these functional receptors necessary for infection, the use of RCAS is relative biosafe compared to other viral-based delivery methods. Some amphotropic (= wide host range) RCAS variants may infect mammalian cells, but are not able to replicate in these cells [255]. Avian cells such as DF-1 and CEF can be efficiently infected by subgroup A viruses [255,256] which was used in this study (RCAS(BP)A vector). Although it was recently shown that RCAS vectors can infect non-dividing cells in culture, a reduced efficiency relative to infection of dividing cells is expected as the productive infection and/or transduction requires host cell division [257,258].

The Cas9 endonuclease was tested in CEF that were transfected with plasmid-DNA containing a sgRNA directed against B2M (Figure 36). As a MOCK-transfected control, the chicken sgRNA B2M sequence was replaced by a sgRNA against porcine B2M as it was expected that the chicken and porcine target sequences will not cross-react in the B2M locus [259]. This displayed the most exact MOCK-transfection control because except for the 20 nucleotide

sgRNA sequence, the construct was identical. The co-expression with EGFP enabled the analysis of only transfected cells, resulting in targeting efficiencies that were slightly lower than for the delivery with synthetic sgRNA. This might be due to the fact that synthetic gRNAs were delivered by a polymer-based transfection which is highly efficient compared to lipofectamine-based transfection usually done for large plasmid constructs in fibroblasts [260]. In addition, CEF were transfected with DNA isolated by PureYield^{TM} Plasmid Miniprep which exhibits lower DNA yields compared to PureYield^{TM} Plasmid Midiprep DNA.

***In vivo* studies**: The chicken embryo has been widely used to address research questions in cell and developmental biology [261,262] due to its accessibility and ease to manipulate a living embryo in the egg. The functionality of Cas9 was demonstrated *in vivo* by delivering sgRNA into Cas9-expressing embryos. Previous studies reported successful *in vivo* genome editing in avian species by direct injection of adenoviral delivered CRISPR/Cas9 components into the blastoderm of a newly laid egg [205]. However, the need to deliver the Cas9 endonuclease has generally been the limiting factor due to its large size. The ubiquitous availability of Cas9 in the transgenic chicken line allows for efficient *in vivo* genome editing by simply delivering sgRNAs. The RCAS-mediated delivery of a sgRNA efficiently inactivated B2M in avian B-cells, revealing a significant reduction of B2M surface expression in targeted Cas9-expressing embryos (Figure 37c). The differences in B2M reduction between individual embryos (ranging from 56.0 % to 77.8 %) probably resulted from different transduction efficiencies. Although any cell type could have been analyzed, this study focused on B-cells as bursa preparation, followed by B-cell isolation is a well-established method in our lab. As studies showed that RCAS-delivered proteins and inserted transgenes are expressed in a mosaic pattern but mainly detectable in the skin, blood vessels and heart [263,264], a piece of heart tissue was examined to confirm RCAS transduction and Cas9 expression (Figure 37a).

Furthermore, tissue-specific *in vivo* genome editing without the need for viral vectors was demonstrated. *In ovo*-electroporation of chicken embryos is a widely used technique to manipulate cells or brain regions with plasmid-DNA [242]. Here, plasmids containing a sgRNA against EGFP or B2M were introduced by electric pulses that caused pores in the cell membrane, allowing the uptake of DNA into the cell where together with the cellular availably of Cas9, gene targeting occurred. The electroporation by short-term high-voltage pulses is a standard method commonly used for bacteria or eukaryotic cells [265]. However, in this

process, about 50-75 % of cells die which is acceptable for bacteria but not for living embryos [241]. By modifying the electroporation protocol towards low fixed voltages, the cell viability was enhanced [266], making *in ovo*-electroporation applicable for tissue-specific genome editing in vertebrate embryos [267,268]. The advantage of *in ovo*-electroporation with plasmid-DNA is that it is quick, inexpensive and more biosafe than the delivery via viral vectors [269]. Targeting efficiencies between individual embryos were similar for both target genes ranging from 6.8 % to 11.5 % for sgRNA against EGFP and 11.1 % to 13.8 % for sgRNA against B2M. These efficiencies are rather low compared to other studies that used *in ovo*-electroporation for CRISPR/Cas9-mediated genome engineering in the chicken embryo [202]. This might have several reasons including that *in ovo*-electroporation results in a mosaic population of transfected cells [202]. The electroporation process itself is very unprecise which makes it difficult to determine the exact application area. The supplementation of dyes to the plasmid-DNA or the use of reporter genes can be used to trace the electroporation site and monitor the expression efficiency [241]. Véron et al. designed an experimental system that allowed the identification of CRISPR-targeted cells within the electroporated tissue [202] resulting in the analysis of only targeted cells and probably therefore higher efficiencies. Furthermore, tissues from EGFP-expressing embryos in this study were fixed with PFA in order to analyze them by microscopy imaging confirming EGFP deletion upon targeting (data not shown, see Rieblinger et al. [237]). The isolation of DNA from fixed tissue is possible but the cross-linking of peptides complicates this process and interferes with the polymerase during PCR [270]. Nevertheless, the R^2-values obtained from TIDE analyses showed a high goodness-of-fit and the microscopic analysis clearly showed the loss of EGFP fluorescence in Cas9-expressing sgRNA-treated but not in MOCK-treated embryos (data not shown, see Rieblinger et al. [237]).

Based on the results obtained by the delivery of sgRNAs via the RCAS system or by electroporation into the brain of chicken embryos, *in vivo* genome editing in ubiquitously Cas9-expressing chickens was clearly demonstrated. However, one should note that *in vivo* genome editing events were performed in chickens before hatching. While *in ovo* genome editing events did not lead to embryonic lethality, *in vivo* genome editing should be performed using live animals in order to analyze phenotypic changes in animals post hatch.

Ubiquitous expression of Cas9 - a tool for hard to transfect cells. T-cells remain one of the most challenging cells to be transfected and are most commonly transduced by using lentiviral vectors [271]. In this work, gene editing in chicken lymphocytes was demonstrated by isolating cells from the spleen of adult Cas9-expressing chickens. Different transfection and transduction protocols were tested but most of these approaches were not successful because most of the cells died after the treatment. A protocol from "AMAXA™ Human T Cell Nucleofector™ Kit", which is usually used to modify human T-cells, was adjusted to chicken cells and resulted in the successful modification of chicken lymphocytes by using chemically 2'-O-methyl phosphorothioate linkage-modified synthetic gRNAs which have been shown to enhance genome editing efficiencies in human primary T-cells by increasing their stability in primary cell culture [272].

A sgRNA against CXCR4 or B2M was applied to the cells directly after isolation resulting in significant reductions of surface expression for both target genes (Figure 40). As expected, the analysis of spectrum and frequencies of INDELs showed that results resemble the results obtained from flow cytometry. The differences between individual experiments can probably be explained by different transfection efficiencies. Although all sgRNAs were able to induce homozygous INDELs at respective target sites, CXCR4 targeting was more efficient compared to B2M. This is not surprising as it is well known that not all gRNAs work equally well [273]. Particularly the sgRNA 1434 against CXCR4 was the most efficient gRNA with targeting efficiencies up to 45.1 % (Figure 41b).

The cells were directly electroporated after splenic isolation and analyzed shortly after (2 days later), thus it was not necessary to treat the cells with cytokines such as interleukin 12 (IL12) and IL2 which is commonly done to stimulate the proliferation of γδ T-cells [274,275], implicating that these cells are a mixture consisting of B-cell, T-cells and other $CD45^+$ immune cells present in the spleen. To analyze targeting efficiencies within the $CD45^+$ cell population, co-stainings with antibodies detecting B-cells, T-cells and macrophages were established (Figure 45). The T-cell populations were further discriminated between $CD4^+$ and $CD8^+$, except for TCR1 as these cells do not display $CD4^+$ cells [276,277]. This proof-of-principle experiment demonstrates the ease to perform gene editing in primary isolated chicken lymphocytes, with a great potential to contribute to a better understanding of immune cell function in the chicken model.

4.2. *In vivo* CRISPR/Cas9-mediated resistance against MDV

The avian herpesvirus MDV infects chickens and causes one of the most frequent cancers in the animal kingdom [27]. The ability to integrate into the genome helps the virus to escape the host´s immune system and by means of establishing persistent infections, it can occasionally reactivate resulting in unpredictable outbreaks of the disease [11]. Although vaccines prevent the formation of cancer, they do not provide sterile immunity, allowing the virus to infect and evolve towards higher virulence. To protect chickens from this deadly virus, genetic resistance by transgenesis was suggested [278].

The CRISPR/Cas9 system can directly act on viral DNA, representing a strategy to fight MDV *in vivo*. The induction of targeted DSBs can impair the packaging of the viral genome, disrupt the expression of essential proteins or affect viral replication indirectly by NHEJ which often produces deleterious mutations [77]. Recently, the MDV genome has been sequenced revealing more than 100 gene products [94] of which approximately 30 proteins are needed for infectious particles [279]. Previous studies used RNA interference (RNAi) to control MDV by knocking down ICP4 and gB genes [280–282] leading to the selective disruption, and thus to the abrogation of MDV replication in host cells. However, viruses can produce viral suppressors of RNAi through long-term coevolution, limiting the efficiency of RNAi technology [283]. Moreover, using small interfering RNAs (siRNAs) targets mRNA transcripts by Dicer-targeting which is thought to be less efficient than CRISPR/Cas9-mediated interference which directly targets viral genes in the host cell [107].

A study from Challagulla et al. reported on *in vivo* inhibition of MDV replication in transgenic chickens by CRISPR/Cas9 [107]. Using a miniTol2 vector containing three gRNAs against ICP4, each under the human U6 promoter and co-expressed with DsRed (gICP4-DsRed), transgenic chickens were generated by direct *in vivo* transfection of PGCs as described by Tyack et al. [108]. As previously mentioned, the authors recently presented a fully transgenic chicken line with constitutive expression of Cas9-HF1, GFP and IFNAR1-gRNAs [109]. To ensure that the additional presence of IFNAR1-gRNAs in Cas9-transgenic chickens does not interfere, the authors performed *in vitro* infection of Cas9-CEF and WT-CEF with the MDV-1 Woodland strain and found no significant differences in MDV replication [107]. By mating, transgenic chickens were generated that expressed Cas9-HF1-GFP-IFNAR1-gRNAs and gICP4-DsRed. Upon infection with the MDV-1 Woodland strain, viral replication was significantly reduced in

transgenic chickens compared to the control group (Cas9-only and WT) [107]. However, this approach only reduced but did not completely abrogated viral replication which raises concerns regarding viral reactivation under the influence of stress, infection with immunosuppressive viruses or other MD-inducing factors. Furthermore, it has not been tested if transgenic chickens are resistant to tumor development [107]. Though unlikely, because it requires the mutation of three locations at the same time, the authors speculated that targeting of only the *ICP4* gene with three gRNAs is not sufficient, leading to the development of escape mutants, and that the combination of two or more gRNAs against different MDV genes might increase the efficiencies against viral replication *in vivo* [107].

Generation of MDV-gRNA-expressing chickens. In this work, the combination of four gRNAs targeting four essential genes (UL27, UL30, UL49, ICP4) of MDV were used to generate transgenic chickens for the purpose of *in vivo* resistance. Each gRNA was expressed under the human U6 promoter which is commonly used for high, ubiquitous expression of gRNAs [284]. As presented by Hagag et al., MDV-gRNAs impaired the viral replication *in vitro* by targeting viral sequences in the genome of infected Cas9-expressing CR cells without compromising cellular genes. Certain combinations of at least two gRNAs, or all four gRNAs, completely stopped MDV replication and prevented the emergence of escape mutants *in vitro* [77]. The authors speculated that this is due to the additive effect of combining multiple gRNAs that led to the loss of large parts of the viral genome and subsequently to the loss of genomic integrity and fragments essential for replication [77]. In addition, abrogation of the expression of multiple essential genes blocked the formation of infectious viral particles [77].

To generate transgenic chickens, the four gRNAs were cloned into an expression construct which was, however, challenging because of the repetitive pattern of promoter and gRNA scaffold sequences present in each expression cassette. Blunt-end cloning was conducted to merge all four gRNAs into one expression construct. Although the stacking of multiple gRNAs under individual promoters is widely used [285–287], recent studies suggested the use of expression of multiple gRNAs driven by a single promoter [288,289]. This avoids the issue of repetitive sequences that can interfere with sequence-dependent analyses such as PCRs. Nevertheless, Sanger sequencing across the four expression cassettes confirmed that all four gRNAs were correctly expressed (Figure 46b-e). Stable integration onto the chicken genome was ensured by phiC31 integrase-mediated random integration into EGFP-expressing PGCs.

Three PGC single cell clones with a single integration of the transgene were obtained and injected into surrogate embryos to generate germline chimeras and germline transmission frequencies observed are in line with other studies [189]. No differences in phenotype or weight between transgenic and wild-type chicks were observed (Figure 51) indicating that transgenic animals are healthy.

The analysis of MDV-gRNA-expressing chickens was challenging due to the repetitive sequences as mentioned above. Nonetheless, transgenic animals were analyzed on DNA, mRNA and sequence level by establishing different assays, including q-RT-PCR assays based on Taqman™ or SYBR® Green. Unfortunately, a quantitative prediction by Taqman™ was not possible as the results were inconsistent, probably resulting from the repetitive pattern that interfered with this assay. Thus, the assay was used to distinguish between the presence or absence of each gRNA in transgenic animals as this does not require the same sensitivity necessary as for quantification. The Taqman™ assay confirmed the presence of all four gRNAs in transgenic animals which was also in line with the results obtained by PCR with a LongAmp® polymerase that covered the 2 kb sequence containing the four expression cassettes (Figure 52). Using a q-RT-PCR assay based on SYBR® Green provided more reliable results and was used for a quantitative estimation of MDV-gRNA expression in transgenic animals. Adapted from Aparicio et al. [233], an assay has been designed (see Figure 24) to detect individual gRNAs. Consistent with LongAmp® and Taqman™, the results confirmed all gRNAs in transgenic animals. However, the expression of gRNAs driven by the human U6 promoter seemed to be rather low and varied strongly between gRNAs and animals (Figure 54). It needs further investigation to understand these differences and more data should be collected as the data shown in Figure 54 represent only one experiment. Although in mammalian systems the human U6 promoter is widely used [290,291], species-specific U6 promoters have been suggested for non-mammalian model organisms such as zebrafish or drosophila [292,293]. Gandhi et al. reported on the use of a chicken U6 promoter in the early chick embryo resulting in a 4-fold increase in transcription compared to the human U6 promoter [294]. The replacement of the human with chicken U6 promoter should therefore be considered which requires, however, the cloning of a new expression construct, followed by the generation of a new transgenic line.

Generation of CRISPR/Cas9-expressing chickens. The CRISPR/Cas9-mediated resistance relies on the cellular availability of both, Cas9 endonuclease and gRNA. By mating ubiquitously Cas9- and MDV-gRNA-expressing chickens, heterozygous Cas9-MDV-gRNA-expressing chickens were obtained. An alternative approach is the generation of a transgenic line by the use of one expression plasmid that contains both CRISPR/Cas9 components which would have been more time-saving, but has several disadvantages. First of all, Cas9-expressing chickens provide a more versatile model without the presence of gRNAs which can cause unwanted off-target effects. Secondly, the breeding strategy provided all control animals (WT, Cas9-only and gRNA-only) needed for an infection challenge with MDV to test this system *in vivo*. This is in contrast to Challagulla et al. who provided only WT and Cas9-only-expressing animals as controls [107].

Because both transgenic lines generated in this work express an antibiotic selectable marker cassette (hygromycin), it was absolutely necessary to monitor double transgenic animals to exclude any negative side effects. In contrast to studies reported from mice, where the inserted selectable marker must be removed to avoid influencing the phenotype [295], our double transgenic chickens are healthy and show no phenotypic abnormalities.

CRISPR/Cas9-expressing chickens are not protected against MDV. To test the hypothesis that the CRISPR/Cas9 system can protect against MDV, an *in vivo* infection challenge with the RB-1B strain was conducted. As the *in vitro* studies suggested that the formation of infectious viral particles was blocked upon the targeting [77], it was also investigated if the CRISPR/Cas9 system in transgenic animals prevents the shedding of the virus to contact birds.

Unlike expected, the experiment showed that heterozygote Cas9-MDV-gRNA-expressing animals were not protected against the virus. They developed MD-induced symptoms (including severe ataxia, paralysis and tumorous lesions) and showed no significant difference in MDV genome copies in blood or feather follicles compared to the control group (Figure 59, Figure 60), indicating that the virus was able to replicate. It was observed that MDV genome copies increased after 4-7 dpi in the blood and 14 dpi in the feather follicles (Figure 60). In the natural pathway of infection, MDV enters the respiratory tract by the inhalation of infectious particles from contaminated dust and replicates within the first 3-5 dpi [58,59]. In the experiment, the virus was directly injected into the animal, therefore viral copies were detectable from the beginning, although at low levels until the virus started to replicate (Figure 60a). The transmission of the virus is highly cell-associated and needs the direct

contact of cells [27]. Infected T-cells transport the virus to the FFE where the second replication phase occurs, typically 12-14 dpi [69] which matches very well to the observation made in this study as viral genome copies increased only after 14 dpi in feathers (Figure 60b). Since Cas9-MDV-gRNA-expressing chickens were not protected, the virus was spread to the contact birds, and the question of shedding could not be addressed. By mistake, one animal was falsely placed into the infected test group. If animals were protected this would have had an impact on the question regarding the viral shedding to the contact group. But since the animals were not protected, this mistake does not affect the outcome of this study. Interestingly, only 2 out of 11 contact animals from test and control groups developed MD (data not shown). The symptoms were less severe and occurred at a later time point compared to the infected group of birds. This is probably due to the fact that the viral spread to those animals could earliest occur at 14 dpi when infectious virions were shed into the environment (Figure 60b) [69]. The outcome of MD is also dependent on the host susceptibility and genotype as e.g. genetic differences in major histocompatibility complex can contribute to a more resistant phenotype [51,52]. Although Valo-SPF chickens are thought to be more susceptible, it needs to be considered that these animals were 14 days older when infected and thus less susceptible due to the developing immune system, providing a certain “age resistance” [53]. In addition, the level of initial exposure to the virus plays an essential role for the onset of the disease [50].

It was observed that some of the infected Cas9-MDV-gRNA-expressing animals developed MD-induced symptoms while others did not show MD at the end of the experiment which led to the assumption that there might be differences between animals. Humoral differences could play a role as chicks used in this experiment originated from mothers that were vaccinated against MDV. The presence of maternal antibodies protects chicks in the first weeks of life [19] which is an important mechanism for the survival of newly born organisms. In retrospect, the use of MDV-maternal-antibody-negative chicks should have been considered to exclude any effects that could result from differences in the antibody composition.

A major concern and reason for the insufficient protection upon infection could be the possibility of low cellular availability of Cas9, MDV-gRNAs or both which are required for the inactivation of the virus. Thus, it was interesting to analyze Cas9 and MDV-gRNA expression in

double transgenic animals to see if there were differences in expressions correlating to the survival or death of these birds. Although there were no differences for the expression of Cas9 within these animals (Figure 61a), it is possible that the overall Cas9 expression *in vivo* is not enough to stop viral replication; but breeding homozygous animals to increase the expression is not an option because homozygosity led to embryonic lethality (see Chapters 3.6 and 4.1). As a proof of concept, a recombinant MDV virus that expresses the Cas9 endonuclease under an inducible early MDV promoter could be introduced. By delivering Cas9 only with the virus, an increased Cas9 expression in infected MDV-gRNA-expressing cells could lead to a higher tolerance and thus to an efficient inactivation of the virus. However, this would only prove the concept and is not practical for the conventional use. It is also possible that the expression of MDV-gRNAs was the limiting factor, leading to insufficient protection in Cas9-MDV-gRNA-expressing chickens. This could be supported by the fact that low expression levels were already observed in MDV-gRNA-expressing animals (Figure 54). The analysis of MDV-gRNAs in birds that survived and birds that died revealed that there was a 10-fold reduction in IT9 and IT7 compared to IT6 and IT12 in birds that died (Figure 61b), although it was not tested if this difference was significant due to insufficient sample sizes. Breeding of heterozygous MDV-gRNA animals to homozygosity was possible (Figure 62) which could increase expression levels *in vivo*. One homozygous MDV-gRNA-expressing animal was generated and its expression should be further analyzed to investigate if levels are indeed increased. Furthermore, it seems that only three of the four MDV-gRNAs were correctly expressed as sequencing of the IT9 cassette revealed the incorrect expression of gRNA against UL49 (Figure 55). Since this was only shown for one MDV-gRNA-expressing animal, it should be tested if this is also true for other animals. Nevertheless, even if the gRNA against UL49 is not correctly expressed, it is unlikely that the loss of one gRNA led to the loss of protection because it was shown that the combination of only two of these gRNAs are necessary to stop virus replication in cell culture [77]. However, these *in vitro* studies were performed in duck cells which can differ from observations made in a chicken *in vivo* system.

5. CONCLUSIONS AND OUTLOOK

In this thesis, a chicken line with ubiquitous Cas9 expression has been generated and was shown to be functional *in vitro* and *in vivo*. This transgenic line will find a broad number of applications in many areas including developmental biology, immunology, biomedicine and agriculture. Already now, these chickens are used to unravel the role of the transcription factor AP-2 delta in the development of the posterior midbrain of chickens. Furthermore, the generated Cas9-expressing chicken line is planned to be used for understanding the role of CD30 in MDV and in human Hodgkin's and non-Hodgkin's lymphoma development. In addition, we received a request from the University of Trento for our Cas9-expressing chickens to help identify the neurobiological bases and molecular pathways of autism spectrum disorders.

The goal of protecting a Cas9-MDV-gRNA-expressing chicken line against MDV was not realized. Despite the elaborate characterization of Cas9 functionality, the *in vivo* functionality of MDV-gRNAs could only be tested in combination with Cas9 through an infection experiment. It is left to be understood if a protection against MDV can be established by higher expression of Cas9, MDV-gRNAs or both. While homozygosity in MDV-gRNA chickens might increase the expression of MDV-gRNAs, the introduction of the Cas9 endonuclease under an inducible early MDV promoter through a recombinant virus could lead to higher expression in only infected cells and thus to more tolerance *in vivo*. Yet, insights from this work will benefit the effort to establish disease resistance against MDV and contribute to CRISPR/Cas9-mediated resistance against other infectious diseases improving the welfare of poultry in the future.

6. ABBREVIATIONS

α	alpha
7AAD	7 Amino actinomycin D
AAV	Adeno-associated virus
ALV	Avian leukosis virus
Amp	Ampicillin
AmpR	Ampicillin resistance
APC	Allophycocyanin
Att	Attenuated
ATP	Adenosine triphosphate
β	beta
B2M	β 2 microglobulin
bp	Base pair
CAG	CMV early enhancer-chicken-β-actin
CAM	Chorioallantoic membrane
Cas9	CRISPR associated protein 9
cDNA	complementary deoxyribonucleic acid
CEF	Chicken embryonic fibroblast
ch	Chicken
CIAP	Calf intestinal alkaline phosphatase
CMV	Cytomegalovirus
Cq	Cycle of quantification
CR	Duck embryo retina cell
CRISPR	Clustered regularly interspaced short palindromic repeats
crRNA	CRISPR-RNA
CXCR4	C-X-C chemokine receptor type 4
δ	delta
ddPCR	Droplet digital PCR
DF-1	Chicken fibroblast cell line Douglas Foster 1
dH_2O	Distilled water

DMEM	Dulbecco's modified eagle medium
DMSO	Dimethyl sulfoxide
DNA	Deoxyribonucleic acid
dpi	Days post infection
ds	Double-stranded
DSB	Double strand break
DsRed	*Discosoma sp.* red fluorescent protein
EBV	Epstein-Barr virus
ECL	Enhanced chemiluminescence
ED	Embryonic day
EDTA	Ethylenediaminetetraacetic acid
EGFP	Enhanced green fluorescent protein
ES	Embryonic stem
E. coli	*Escherichia coli*
EtOH	Ethanol
FACS	Fluorescence-activated cell sorting
FAM	Fluorescein amidite
FBS	Fetal bovine serum
FFE	Feather follicle epithelial
FITC	Fluorescein isothiocyanate
fw	Forward
γ	gamma
g	Gram
GaHV-2	Gallid herpesvirus 2
GAPDH	Glycerinaldehyde-3-phosphate-dehydrogenase
GFP	Green fluorescent protein
gRNA	Guide RNA
h	Hour
HDR	Homology-directed repair
HF	High Fidelity
H&H	Hamburger Hamilton
HHV-6	Human herpes virus 6

HPRS	Houghton Poultry Research Station
HRP	Horse reddish peroxidase
HSV	Herpes simplex virus
hU6	Human U6 promoter
HVT	Herpesvirus of turkey
HygroR	Hygromycin resistance
ICP4	Infected cell protein 4
IDT	Integrated DNA Technologies
IE	Immediate early
IgG	Immunoglobulin G
INDEL	Insertion-deletion
INFAR1	Interferon alpha and beta receptor subunit 1
IOE	World Organization of Animal Health
KCl	Potassium chloride
l	Liter
LB	Lysogeny broth
LSL	Lohmann´s selected Leghorn
MEK/ERK	Ras-Raf-MEK-ERK signaling pathway
MD	Marek´s disease
MDV	Marek´s disease virus
MDV-gRNA	Guide RNA against MDV genes (4x)
MgCl	Magnesium chloride
MHC	Major histocompatibility complex
min	Minute
Mio	Million
ml	Milliliter
mMDV	Mild-MDV
µg	Microgram
µl	Microliter
µM	Micromolar
µU	Microunit
Na+	Sodium

NaCl	Sodium chloride
NCBI	National Center for Biotechnology Information
NHEJ	Non-homologous end joining
NK	Natural killer
NLS	Nuclear location signal
nM	Nanomoles
NTC	No template control
PAM	Protospacer adjacent motif
PBMC	Peripheral blood mononuclear cell
PBS	Phosphate buffered saline
PCR	Polymerase chain reaction
PEG	Polyethylene glycol
Pen/Strep	Penicillin-streptomycin
PFA	Paraformaldehyde
pfu	Plaque-forming unit
PGC	Primordial germ cell
qPCR	Quantitative polymerase chain reaction
RCAS	Replication competent ALV LTR with a splice acceptor
RNA	Ribonucleic acid
RNAi	RNA interference
rpm	Rounds per minute
RPMI	Roswell Park Memorial Institute
RT	Reverse transcriptase
rv	Reverse
SDS	Sodium dodecyl sulfate polyacrylamide
sec	Seconds
sgRNA	Single guide RNA
shRNA	Short harpin RNA
siRNA	Small interfering RNA
SOC	Super optimal broth
SV	Simian-Virus
SpCas9	*Streptococcus pyogenes* Cas9

TAE	TRIS-Acetate-EDTA
TALEN	Transcription activator-like effector nuclease
TBE	TRIS-Borate-EDTA
TCR	T-cell receptor
TEMED	Tetramethylethylendiamin
TG	Thioglycerol
TIDE	Tracing of INDELs by decomposition
TNFR	Tumor necrosis factor receptor
Tm	Melting temperature
TMR	Telomeric repeat
TR/TERC	Telomerase RNA
$TR_{L,S}$	Terminal repeat long, short
tracrRNA	Trans-activating RNA
TUM	Technical University of Munich
UL27	Glycoprotein B
$U_{L,S}$	Unique region long, short
UL30	DNA polymerase
UL49	Tegument protein
UNLB	Unlabeled
UTR	Untranslated region
v	Virulent
VALO-SPF	Vaccine-Lohmann Specific-Pathogen-Free
vv	Very virulent
vv+	Very virulent +
WT	Wild-type
ZFN	Zinc finger nuclease
#	Number

7. LIST OF TABLES

8. LIST OF FIGURES

9. REFERENCES

[1] M.G. Davey, C. Tickle, The chicken as a model for embryonic development, *Cytogenet. Genome Res.* 117 (2007) 231–239. https://doi.org/10.1159/000103184.

[2] D. Parra, F. Takizawa, J.O. Sunyer, Evolution of B cell immunity, *Annu. Rev. Anim. Biosci.* 1 (2013) 65–97. https://doi.org/10.1146/annurev-animal-031412-103651.

[3] S.A. Plotkin, S.L. Plotkin, The development of vaccines: How the past led to the future, *Nat. Rev. Microbiol.* 9 (2011) 889–893. https://doi.org/10.1038/nrmicro2668.

[4] N. Alexandratos, J. Bruinsma, World agriculture towards 2030/2050: The 2012 revision, Rome, 2012.

[5] OECD/FAO, ed., OECD-FAO Agricultural Outlook 2018-2027, OECD Publishing, 2018. https://doi.org/10.1787/agr_outlook-2018-en.

[6] H. Grethe, A. Dembélé, N. Duman, Study: How to feed the World's growing Billions, Berlin, 2011. https://www.boell.de/de/oekologie/publications-study-how-to-feed-the-worlds-growing-billions-fao-12032.html (accessed March 22, 2021).

[7] C. Zhang, R. Wohlhueter, H. Zhang, Genetically modified foods: A critical review of their promise and problems, *Food Sci. Hum. Wellness*. 5 (2016) 116–123. https://doi.org/https://doi.org/10.1016/j.fshw.2016.04.002.

[8] P.W. Aho, The World's Commercial Chicken Meat and Egg Industries, in: W.D.. Bell, D.. Weaver (Eds.), Commer. Chick. Meat Egg Prod., 5th ed., Springer US, 2002: pp. 3–17.

[9] Y.M. Saif, A.M. Fadly, J.R. Glisson, L.R. McDougald, D.E. Swayne, eds., Diseases of Poultry, 12th ed., Blackwell Publishing, 2008.

[10] N. Lawhale, A. Singh, D. Deka, R. Singh, R. Verma, Detection of Marek's disease virus meq gene in feather follicle by loop-mediated isothermal amplification, *IOSR J. Agric. Vet. Sci.* 7 (2014) 19–24. https://doi.org/10.9790/2380-07311924.

[11] I. Othman, E. Aklilu, Marek's disease herpesvirus serotype 1 in broiler breeder and layer chickens in Malaysia, *Vet. World*. 12 (2019) 472–476. https://doi.org/10.14202/vetworld.2019.472-476.

[12] N. Boodhoo, A. Gurung, S. Sharif, S. Behboudi, Marek's disease in chickens: A review with focus on immunology, *Vet. Res.* 47 (2016) 119. https://doi.org/10.1186/s13567-016-0404-3.

[13] Y. Ishino, H. Shinagawa, K. Makino, M. Amemura, A. Nakata, Nucleotide sequence of the iap gene, responsible for alkaline phosphatase isozyme conversion in Escherichia coli, and identification of the gene product, *J. Bacteriol.* 169 (1987) 5429–5433. https://doi.org/10.1128/jb.169.12.5429-5433.1987.

[14] F.J. Mojica, C. Díez-Villaseñor, E. Soria, G. Juez, Biological significance of a family of regularly spaced repeats in the genomes of archaea, bacteria and mitochondria, *Mol. Microbiol.* 36 (2000) 244–246. https://doi.org/10.1046/j.1365-2958.2000.01838.x.

[15] J.A. Doudna, E. Charpentier, Genome editing. The new frontier of genome engineering with CRISPR-Cas9, *Science*. 346 (2014) 1258096. https://doi.org/10.1126/science.1258096.

[16] M. Hryhorowicz, D. Lipiński, J. Zeyland, R. Słomski, CRISPR/Cas9 immune system as a tool for genome engineering, *Arch. Immunol. Ther. Exp. (Warsz).* 65 (2017) 233–240.

https://doi.org/10.1007/s00005-016-0427-5.

[17] T.S. Foley, Animal Cancer Research Act, 96th ed., 1980.

[18] D.W. White, R. Suzanne Beard, E.S. Barton, Immune modulation during latent herpesvirus infection, *Immunol. Rev.* 245 (2012) 189–208. https://doi.org/10.1111/j.1600-065X.2011.01074.x.

[19] F. Davison, V. Nair, Marek's disease: An evolving problem, (2004).

[20] I. Davidson, R. Borenstein, Multiple infection of chickens and turkeys with avian oncogenic viruses: Prevalence and molecular analysis, *Acta Virol.* 43 (1999) 136–142.

[21] S. Kobayashi, K. Kobayashi, T. Mikami, A study of Marek's disease in Japanese quails vaccinated with herpesvirus of turkeys, *Avian Dis.* 30 (1986) 816–819.

[22] P.E. Pellett, B. Roizman, Family Herpesviridae: A Brief Introduction, in: P.M. Howley, D.M. Knipe (Eds.), Fields Virol., 7th ed., Flippincott-Raven, Philadelphia, 2007: pp. 2479–2499. https://books.google.de/books?id=ku4lGwAACAAJ.

[23] A.J. Davison, R. Eberle, B. Ehlers, G.S. Hayward, D.J. McGeoch, A.C. Minson, P.E. Pellett, B. Roizman, M.J. Studdert, E. Thiry, The order herpesvirales, *Arch. Virol.* 154 (2009) 171–177. https://doi.org/10.1007/s00705-008-0278-4.

[24] E.R. Tulman, C.L. Afonso, Z. Lu, L. Zsak, D.L. Rock, G.F. Kutish, The genome of a very virulent Marek's disease virus, *J. Virol.* 74 (2000) 7980–7988. https://doi.org/10.1128/jvi.74.17.7980-7988.2000.

[25] V. V Bulow, P.M. Biggs, Differentiation between strains of Marek's disease virus and turkey herpesvirus by immunofluorescence assays, *Avian Pathol.* 4 (1975) 133–146. https://doi.org/10.1080/03079457509353859.

[26] G.-S. Zhu, T. Ojima, T. Hironaka, T. Ihara, N. Mizukoshi, A. Kato, S. Ueda, K. Hirai, Differentiation of oncogenic and nononcogenic strains of Marek's disease virus type 1 by using polymerase chain reaction DNA amplification, *Avian Dis.* 36 (1992) 637–645. https://doi.org/10.2307/1591759.

[27] L.D. Bertzbach, A.M. Conradie, Y. You, B.B. Kaufer, Latest insights into Marek's disease virus pathogenesis and tumorigenesis, *Cancers (Basel).* 12 (2020) 647-. https://doi.org/10.3390/cancers12030647.

[28] K.A. Schat, B.W. Calnek, Characterization of an apparently nononcogenic Marek's disease Virus23, *JNCI J. Natl. Cancer Inst.* 60 (1978) 1075–1082. https://doi.org/10.1093/jnci/60.5.1075.

[29] D.K. Ajithdoss, S.M. Reddy, P.F. Suchodolski, L.F. Lee, H.-J. Kung, B. Lupiani, In vitro characterization of the Meq proteins of Marek's disease virus vaccine strain CVI988, *Virus Res.* 142 (2009) 57–67. https://doi.org/10.1016/j.virusres.2009.01.008.

[30] N. Osterrieder, N. Wallaschek, B.B. Kaufer, Herpesvirus genome integration into telomeric repeats of host cell chromosomes, *Annu. Rev. Virol.* 1 (2014) 215–235. https://doi.org/10.1146/annurev-virology-031413-085422.

[31] R.F. Silva, L.F. Lee, G.F. Kutish, The genomic structure of Marek's disease virus, *Curr. Top. Microbiol. Immunol.* 255 (2001) 143–158. https://doi.org/10.1007/978-3-642-56863-3_6.

[32] ViralZone, (n.d.). https://viralzone.expasy.org/176?outline=all_by_species.

[33] L.D. Bertzbach, A. Kheimar, F.A.Z. Ali, B.B. Kaufer, Viral factors involved in Marek's disease virus (MDV) pathogenesis, *Curr. Clin. Microbiol. Reports*. 5 (2018) 238–244. https://doi.org/10.1007/s40588-018-0104-z.

[34] G. Morissette, L. Flamand, Herpesviruses and chromosomal integration, *J. Virol.* 84 (2010) 12100–12109. https://doi.org/10.1128/JVI.01169-10.

[35] A. Kheimar, R.L. Previdelli, D.J. Wight, B.B. Kaufer, Telomeres and telomerase: Role in Marek's disease virus pathogenesis, integration and tumorigenesis, *Viruses*. 9 (2017) 173. https://doi.org/10.3390/v9070173.

[36] L. Fragnet, M.A. Blasco, W. Klapper, D. Rasschaert, The RNA subunit of telomerase is encoded by Marek's disease virus, *J. Virol.* 77 (2003) 5985–5996. https://doi.org/10.1128/JVI.77.10.5985-5996.2003.

[37] M. Kishi, G. Bradley, J. Jessip, A. Tanaka, M. Nonoyama, Inverted repeat regions of Marek's disease virus DNA possess a structure similar to that of the a sequence of herpes simplex virus DNA and contain host cell telomere sequences, *J. Virol.* 65 (1991) 2791–2797. http://jvi.asm.org/content/65/6/2791.abstract.

[38] A. Greco, N. Fester, A.T. Engel, B.B. Kaufer, Role of the short telomeric repeat region in Marek's disease virus replication, genomic integration, and lymphomagenesis, *J. Virol.* 88 (2014) 14138–14147. https://doi.org/10.1128/JVI.02437-14.

[39] B.B. Kaufer, K.W. Jarosinski, N. Osterrieder, Herpesvirus telomeric repeats facilitate genomic integration into host telomeres and mobilization of viral DNA during reactivation, *J. Exp. Med.* 208 (2011) 605–615. https://doi.org/10.1084/jem.20101402.

[40] D. Jones, L. Lee, J.L. Liu, H.J. Kung, J.K. Tillotson, Marek disease virus encodes a basic-leucine zipper gene resembling the fos/jun oncogenes that is highly expressed in lymphoblastoid tumors, *Proc. Natl. Acad. Sci. U. S. A.* 89 (1992) 4042–4046. https://doi.org/10.1073/pnas.89.9.4042.

[41] J.L. Liu, H.J. Kung, Marek's disease herpesvirus transforming protein MEQ: A c-Jun analogue with an alternative life style, *Virus Genes*. 21 (2000) 51–64.

[42] A.C. Brown, S.J. Baigent, L.P. Smith, J.P. Chattoo, L.J. Petherbridge, P. Hawes, M.J. Allday, V. Nair, Interaction of MEQ protein and C-terminal-binding protein is critical for induction of lymphomas by Marek's disease virus, *Proc. Natl. Acad. Sci. U. S. A.* 103 (2006) 1687–1692. https://doi.org/10.1073/pnas.0507595103.

[43] S. Haertle, I. Alzuheir, F. Busalt, V. Waters, P. Kaiser, B.B. Kaufer, Identification of the receptor and cellular ortholog of the Marek's disease virus (MDV) CXC chemokine, *Front. Microbiol.* 8 (2017) 2543. https://doi.org/10.3389/fmicb.2017.02543.

[44] A.T. Engel, R.K. Selvaraj, J.P. Kamil, N. Osterrieder, B.B. Kaufer, Marek's disease viral interleukin-8 promotes lymphoma formation through targeted recruitment of B cells and CD4+ CD25+ T cells, *J. Virol.* 86 (2012) 8536–8545. https://doi.org/10.1128/JVI.00556-12.

[45] L.A. Shack, J.J. Buza, S.C. Burgess, The neoplastically transformed (CD30hi) Marek's disease lymphoma cell phenotype most closely resembles T-regulatory cells., *Cancer Immunol. Immunother.* 57 (2008) 1253–1262. https://doi.org/10.1007/s00262-008-0460-2.

[46] S.C. Burgess, J.R. Young, B.J.G. Baaten, L. Hunt, L.N.J. Ross, M.S. Parcells, P.M. Kumar, C.A. Tregaskes, L.F. Lee, T.F. Davison, Marek's disease is a natural model for lymphomas overexpressing Hodgkin's disease antigen (CD30), *Proc. Natl. Acad. Sci. U. S. A.* 101 (2004) 13879–13884. https://doi.org/10.1073/pnas.0305789101.

[47] J.R. Dunn, I.M. Gimeno, Current status of Marek's disease in the United States and worldwide based on a questionnaire survey, *Avian Dis.* 57 (2013) 483–490. https://doi.org/10.1637/10373-091412-ResNote.1.

[48] B.W. Calnek, R.W. Harris, C. Buscaglia, K.A. Schat, B. Lucio, Relationship between the immunosuppressive potential and the pathotype of Marek's disease virus isolates, *Avian Dis.* 42 (1998) 124–132.

[49] J.R. Dunn, K. Auten, M. Heidari, C. Buscaglia, Correlation between Marek's disease virus pathotype and replication, *Avian Dis.* 58 (2014) 287–292. http://www.jstor.org/stable/24595959.

[50] J.R. Dunn, R.L. Witter, R.F. Silva, L.F. Lee, J. Finlay, B.A. Marker, J.B. Kaneene, R.M. Fulton, S.D. Fitzgerald, The effect of the time interval between exposures on the susceptibility of chickens to superinfection with Marek's disease virus, *Avian Dis.* 54 (2010) 1038–1049. https://doi.org/10.1637/9348-033010-Reg.1.

[51] W.E. Briles, H.A. Stone, R.K. Cole, Marek's disease: Effects of B histocompatibility alloalleles in resistant and susceptible chicken lines, *Science*. 195 (1977) 193–195. https://doi.org/10.1126/science.831269.

[52] J. Kaufman, K. Venugopal, The importance of MHC for Rous sarcoma virus and Marek's disease virus—Some Payne-ful considerations, *Avian Pathol.* 27 (1998) S82–S87. https://doi.org/10.1080/03079459808419297.

[53] R.L. Witter, J.M. Sharma, J.J. Solomon, L.R. Champion, An age-related resistance of chickens to Marek's disease: Some preliminary observations, *Avian Pathol.* 2 (1973) 43–54. https://doi.org/10.1080/03079457309353780.

[54] P.M. Biggs, L.N. Payne, Studies on Marek's disease. I. Experimental transmission, *J. Natl. Cancer Inst.* 39 (1967) 267–280.

[55] K. Osterrieder, J.-F. Vautherot, The genome content of Marek's disease-like viruses, *Marek's Dis. An Evol. Probl.* (2004) 17–31. https://doi.org/10.1016/B978-012088379-0/50007-4.

[56] V. Nair, Latency and tumorigenesis in Marek's disease, *Avian Dis.* 57 (2013) 360–365. https://doi.org/10.1637/10470-121712-Reg.1.

[57] A.J. Chaves Hernández, Poultry and avian diseases, in: N. Van Alfen (Ed.), Encycl. Agric. Food Syst., Academic Press, Oxford, 2014: pp. 504–520. https://doi.org/https://doi.org/10.1016/B978-0-444-52512-3.00183-2.

[58] M.F. Abdul-Careem, A. Javaheri-Vayeghan, S. Shanmuganathan, H.R. Haghighi, L.R. Read, K. Haq, D.B. Hunter, K.A. Schat, M. Heidari, S. Sharif, Establishment of an aerosol-based Marek's disease virus infection model, *Avian Dis.* 53 (2009) 387–391. https://doi.org/10.1637/8568-122308-Reg.1.

[59] B.J.G. Baaten, K.A. Staines, L.P. Smith, H. Skinner, T.F. Davison, C. Butter, Early replication in pulmonary B cells after infection with Marek's disease herpesvirus by the respiratory route, *Viral Immunol.* 22 (2009) 431–444. https://doi.org/10.1089/vim.2009.0047.

[60] B. Schusser, E.J. Collarini, H. Yi, S.M. Izquierdo, J. Fesler, D. Pedersen, K.C. Klasing, B. Kaspers, W.D. Harriman, M.-C. van de Lavoir, R.J. Etches, P.A. Leighton, Immunoglobulin knockout chickens via efficient homologous recombination in primordial germ cells, *Proc. Natl. Acad. Sci.* 110 (2013) 20170–20175. https://doi.org/10.1073/pnas.1317106110.

[61] L.D. Bertzbach, M. Laparidou, S. Härtle, R.J. Etches, B. Kaspers, B. Schusser, B.B. Kaufer,

Unraveling the role of B cells in the pathogenesis of an oncogenic avian herpesvirus, *Proc. Natl. Acad. Sci.* 115 (2018) 11603–11607. https://doi.org/10.1073/pnas.1813964115.

[62] J. Schermuly, A. Greco, S. Härtle, N. Osterrieder, B.B. Kaufer, B. Kaspers, In vitro model for lytic replication, latency, and transformation of an oncogenic alphaherpesvirus, *Proc. Natl. Acad. Sci.* 112 (2015) 7279–7284. https://doi.org/10.1073/pnas.1424420112.

[63] L.D. Bertzbach, D.A. van Haarlem, S. Härtle, B.B. Kaufer, C.A. Jansen, Marek's disease virus infection of natural killer cells, *Microorganisms*. 7 (2019). https://doi.org/10.3390/microorganisms7120588.

[64] C. Rozins, T. Day, S. Greenhalgh, Managing Marek's disease in the egg industry, *Epidemics*. 27 (2019) 52–58. https://doi.org/https://doi.org/10.1016/j.epidem.2019.01.004.

[65] I.M. Gimeno, K.A. Schat, Virus-induced immunosuppression in chickens, *Avian Dis.* 62 (2018) 272–285. https://doi.org/10.1637/11841-041318-Review.1.

[66] K.W. Jarosinski, B.K. Tischer, S. Trapp, N. Osterrieder, Marek's disease virus: Lytic replication, oncogenesis and control, *Expert Rev. Vaccines*. 5 (2006) 761–772. https://doi.org/10.1586/14760584.5.6.761.

[67] S.J. Baigent, L.B. Kgosana, A.A. Gamawa, L.P. Smith, A.F. Read, V.K. Nair, Relationship between levels of very virulent MDV in poultry dust and in feather tips from vaccinated chickens, *Avian Dis.* 57 (2013) 440–447. https://doi.org/10.1637/10356-091012-Reg.1.

[68] K.W. Jarosinski, Marek's disease virus late protein expression in feather follicle epithelial cells as early as 8 days postinfection, *Avian Dis.* 56 (2012) 725–731. https://doi.org/10.1637/10252-052212-Reg.1.

[69] K. Nazerian, R.L. Witter, Cell-free transmission and in vivo replication of Marek's disease virus, *J. Virol.* 5 (1970) 388–397. https://doi.org/10.1128/JVI.5.3.388-397.1970.

[70] S.C. Burgess, B.H. Basaran, T.F. Davison, Resistance to Marek's disease herpesvirus-induced lymphoma is multiphasic and dependent on host genotype, *Vet. Pathol.* 38 (2001) 129–142. https://doi.org/10.1354/vp.38-2-129.

[71] V. Nair, Avian immunology, 2nd ed., Academic Press, 2014.

[72] K. Norris, M. Evans, Ecological immunology: Life history trade-offs and immune defense in birds, *Behav. Ecol.* 11 (2000) 19–26.

[73] J. Dunn, Marek Disease in Poultry, (2019). https://www.msdvetmanual.com/poultry/neoplasms/marek-disease-in-poultry (accessed December 15, 2020).

[74] Image Number K9494-1, (n.d.). https://www.ars.usda.gov/oc/images/photos/jul01/k9494-1/ (accessed March 23, 2021).

[75] Marek Disease Market - Global Industry Insights, Trends, Outlook, and Opportunity Analysis, 2018–2026, (n.d.). https://baecold.tumblr.com/post/182446558005/marek-disease-market (accessed March 1, 2021).

[76] L. Wu, A. Cheng, M. Wang, R. Jia, Q. Yang, Y. Wu, D. Zhu, X. Zhao, S. Chen, M. Liu, S. Zhang, X. Ou, S. Mao, Q. Gao, D. Sun, X. Wen, Y. Liu, Y. Yu, L. Zhang, B. Tian, L. Pan, X. Chen, Alphaherpesvirus major tegument protein VP22: Its precise function in the viral life cycle, *Front. Microbiol.* 11 (2020) 1908. https://www.frontiersin.org/article/10.3389/fmicb.2020.01908.

[77] I.T. Hagag, D.J. Wight, D. Bartsch, H. Sid, I. Jordan, L.D. Bertzbach, B. Schusser, B.B. Kaufer, Abrogation of Marek's disease virus replication using CRISPR/Cas9, *Sci. Rep.* 10 (2020) 10919. https://doi.org/10.1038/s41598-020-67951-1.

[78] P.E. Boehmer, A. V Nimonkar, Herpes virus replication, *IUBMB Life*. 55 (2003) 13–22. https://doi.org/10.1080/1521654031000070645.

[79] R.J. Whitley, B. Roizman, Herpes simplex virus infections, *Lancet*. 357 (2001) 1513–1518. https://doi.org/10.1016/S0140-6736(00)04638-9.

[80] M.K. Kukhanova, A.N. Korovina, S.N. Kochetkov, Human herpes simplex virus: Life cycle and development of inhibitors, *Biochemistry. (Mosc).* 79 (2014) 1635–1652. https://doi.org/10.1134/S0006297914130124.

[81] C. Boutell, R.D. Everett, Regulation of alphaherpesvirus infections by the ICP0 family of proteins, *J. Gen. Virol.* 94 (2013) 465–481. https://doi.org/10.1099/vir.0.048900-0.

[82] E. Hildebrandt, J.R. Dunn, M. Niikura, H.H. Cheng, Mutations within ICP4 acquired during in vitro attenuation do not alter virulence of recombinant Marek's disease viruses in vivo, *Virol. Reports*. 5 (2015) 10–18. https://doi.org/https://doi.org/10.1016/j.virep.2014.11.002.

[83] T.C. Mettenleiter, Intriguing interplay between viral proteins during herpesvirus assembly or: The herpesvirus assembly puzzle, *Vet. Microbiol.* 113 (2006) 163–169. https://doi.org/10.1016/j.vetmic.2005.11.040.

[84] T.C. Mettenleiter, Herpesvirus assembly and egress, *J. Virol.* 76 (2002) 1537–1547. https://doi.org/10.1128/jvi.76.4.1537-1547.2002.

[85] K.A. Schat, History of the first-generation Marek's disease vaccines: The science and little-known facts, *Avian Dis.* 60 (2016) 715–724. https://doi.org/10.1637/11429-050216-Hist.

[86] K.A. Schat, V. Nair, Neoplastic diseases, in: Dis. Poult., 2013: pp. 513–673. https://doi.org/https://doi.org/10.1002/9781119421481.ch15.

[87] T.J.D. Knight-Jones, K. Edmond, S. Gubbins, D.J. Paton, Veterinary and human vaccine evaluation methods, *Proceedings. Biol. Sci.* 281 (2014) 20132839. https://doi.org/10.1098/rspb.2013.2839.

[88] A.M. Conradie, L.D. Bertzbach, N. Bhandari, M. Parcells, B.B. Kaufer, A common live-attenuated avian herpesvirus vaccine expresses a very potent oncogene, *MSphere*. 4 (2019) e00658-19. https://doi.org/10.1128/mSphere.00658-19.

[89] A.E. Churchill, L.N. Payne, R.C. Chubb, Immunization against Marek's disease using a live attenuated virus, *Nature*. 221 (1969) 744–747. https://doi.org/10.1038/221744a0.

[90] A.E. Churchill, P. Biggs, Agent of Marek's disease in tissue culture, *Nature*. 215 (1967) 528–530. https://doi.org/10.1038/215528a0.

[91] R.L. Witter, Protection by attenuated and polyvalent vaccines against highly virulent strains of Marek's disease virus, *Avian Pathol.* 11 (1982) 49–62. https://doi.org/10.1080/03079458208436081.

[92] B.H. Rispens, H. van Vloten, N. Mastenbroek, J.L. Maas, K.A. Schat, Control of Marek's disease in the Netherlands. II. Field trials on vaccination with an avirulent strain (CVI 988) of Marek's disease virus, *Avian Dis.* 16 (1972) 126–138.

[93] B.H. Rispens, J. Van Vloten, H.J.L. Maas, Some virological and serological observations on Marek's disease: A preliminary report, *Br. Vet. J.* 125 (1969) 445–453.

https://doi.org/https://doi.org/10.1016/S0007-1935(17)48760-4.

[94] N. Osterrieder, J.P. Kamil, D. Schumacher, B.K. Tischer, S. Trapp, Marek's disease virus: From miasma to model, *Nat. Rev. Microbiol.* 4 (2006) 283–294. https://doi.org/10.1038/nrmicro1382.

[95] F. Davison, V. Nair, Use of Marek's disease vaccines: Could they be driving the virus to increasing virulence?, *Expert Rev. Vaccines*. 4 (2005) 77–88. https://doi.org/10.1586/14760584.4.1.77.

[96] J.R. Dunn, A. Black Pyrkosz, A. Steep, H.H. Cheng, Identification of Marek's disease virus genes associated with virulence of US strains, *J. Gen. Virol.* 100 (2019) 1132–1139. https://doi.org/10.1099/jgv.0.001288.

[97] C.E. Shamblin, N. Greene, V. Arumugaswami, R.L. Dienglewicz, M.S. Parcells, Comparative analysis of Marek's disease virus (MDV) glycoprotein-, lytic antigen pp38- and transformation antigen Meq-encoding genes: Association of meq mutations with MDVs of high virulence, *Vet. Microbiol.* 102 (2004) 147–167. https://doi.org/https://doi.org/10.1016/j.vetmic.2004.06.007.

[98] B.K. Tischer, D. Schumacher, M. Beer, J. Beyer, J.P. Teifke, K. Osterrieder, K. Wink, V. Zelnik, F. Fehler, N. Osterrieder, A DNA vaccine containing an infectious Marek's disease virus genome can confer protection against tumorigenic Marek's disease in chickens, *J. Gen. Virol.* 83 (2002) 2367–2376. https://doi.org/10.1099/0022-1317-83-10-2367.

[99] B.B. Kaufer, S. Arndt, S. Trapp, N. Osterrieder, K.W. Jarosinski, Herpesvirus telomerase RNA (vTR) with a mutated template sequence abrogates herpesvirus-induced lymphomagenesis, *PLoS Pathog.* 7 (2011) e1002333. https://doi.org/10.1371/journal.ppat.1002333.

[100] P. Horvath, R. Barrangou, CRISPR/Cas, the immune system of bacteria and archaea, *Science.* 327 (2010) 167–170. https://doi.org/10.1126/science.1179555.

[101] B. Wiedenheft, S.H. Sternberg, J.A. Doudna, RNA-guided genetic silencing systems in bacteria and archaea, *Nature*. 482 (2012) 331–338. https://doi.org/10.1038/nature10886.

[102] T. Hai, F. Teng, R. Guo, W. Li, Q. Zhou, One-step generation of knockout pigs by zygote injection of CRISPR/Cas system, *Cell Res.* 24 (2014) 372–375. https://doi.org/10.1038/cr.2014.11.

[103] H. Wang, H. Yang, C.S. Shivalila, M.M. Dawlaty, A.W. Cheng, F. Zhang, R. Jaenisch, One-step generation of mice carrying mutations in multiple genes by CRISPR/Cas-mediated genome engineering, *Cell*. 153 (2013) 910–918. https://doi.org/10.1016/j.cell.2013.04.025.

[104] M. Crispo, A. Mulet, L. Tesson, N. Barrera, F. Cuadro, P. Dos Santos Neto, T. Nguyen, A. Crénéguy, L. Brusselle, I. Anegon, A. Menchaca, Efficient generation of myostatin knock-out sheep using CRISPR/Cas9 technology and microinjection into zygotes, *PLoS One*. 10 (2015) e0136690. https://doi.org/10.1371/journal.pone.0136690.

[105] E. Waltz, Gene-edited CRISPR mushroom escapes US regulation, *Nature*. 532 (2016) 293. https://doi.org/10.1038/nature.2016.19754.

[106] K. Selle, R. Barrangou, Harnessing CRISPR-Cas systems for bacterial genome editing, *Trends Microbiol.* 23 (2015) 225–232. https://doi.org/10.1016/j.tim.2015.01.008.

[107] A. Challagulla, K. Jenkins, S. Shi, K. Morris, T. Wise, P. Paradkar, M. Tizard, T. Doran, K. Schat, In vivo inhibition of Marek's disease virus in transgenic chickens expressing Cas9 and gRNA against ICP4, *Microorganisms*. 9 (2021) 164.

https://doi.org/10.3390/microorganisms9010164.

[108] S.G. Tyack, K.A. Jenkins, T.E. O'Neil, T.G. Wise, K.R. Morris, M.P. Bruce, S. McLeod, A.J. Wade, J. McKay, R.J. Moore, K.A. Schat, J.W. Lowenthal, T.J. Doran, A new method for producing transgenic birds via direct in vivo transfection of primordial germ cells, *Transgenic Res.* 22 (2013) 1257–1264. https://doi.org/10.1007/s11248-013-9727-2.

[109] A. Challagulla, K.A. Jenkins, T.E. O'Neil, K.R. Morris, T.G. Wise, M.L. Tizard, A.G.D. Bean, K.A. Schat, T.J. Doran, Germline engineering of the chicken genome using CRISPR/Cas9 by in vivo transfection of PGCs, *Anim. Biotechnol.* (2020) 1–10. https://doi.org/10.1080/10495398.2020.1789869.

[110] J.D. Watson, F.H.C. Crick, Molecular structure of nucleic acids: A structure for deoxyribose nucleic acid, *Nature*. 171 (1953) 737–738. https://doi.org/10.1038/171737a0.

[111] B. Zhu, W. Ge, Genome editing in fishes and their applications, *Gen. Comp. Endocrinol.* 257 (2018) 3–12. https://doi.org/https://doi.org/10.1016/j.ygcen.2017.09.011.

[112] N. Nakashima, K. Miyazaki, Bacterial cellular engineering by genome editing and gene silencing, *Int. J. Mol. Sci.* 15 (2014). https://doi.org/10.3390/ijms15022773.

[113] R.J. Platt, S. Chen, Y. Zhou, M.J. Yim, L. Swiech, H.R. Kempton, J.E. Dahlman, O. Parnas, T.M. Eisenhaure, M. Jovanovic, D.B. Graham, S. Jhunjhunwala, M. Heidenreich, R.J. Xavier, R. Langer, D.G. Anderson, N. Hacohen, A. Regev, G. Feng, P.A. Sharp, F. Zhang, CRISPR-Cas9 knockin mice for genome editing and cancer modeling, *Cell*. 159 (2014) 440–455. https://doi.org/10.1016/j.cell.2014.09.014.

[114] F. Fattah, E.H. Lee, N. Weisensel, Y. Wang, N. Lichter, E.A. Hendrickson, Ku regulates the non-homologous end joining pathway choice of DNA double-strand break repair in human somatic cells, *PLoS Genet.* 6 (2010) e1000855. https://doi.org/10.1371/journal.pgen.1000855.

[115] F.A. Ran, P.D. Hsu, J. Wright, V. Agarwala, D. a Scott, F. Zhang, Genome engineering using the CRISPR-Cas9 system., *Nat Protoc*. 8 (2013) 2281–2308. https://doi.org/10.1038/nprot.2013.143.

[116] L.H. Thompson, D. Schild, Homologous recombinational repair of DNA ensures mammalian chromosome stability, *Mutat. Res. Mol. Mech. Mutagen.* 477 (2001) 131–153. https://doi.org/https://doi.org/10.1016/S0027-5107(01)00115-4.

[117] R. Gerlai, Gene targeting using homologous recombination in embryonic stem cells: The future for behavior genetics?, *Front. Genet.* 7 (2016) 43. https://doi.org/10.3389/fgene.2016.00043.

[118] J.D. Sander, J.K. Joung, CRISPR-Cas systems for editing, regulating and targeting genomes, *Nat. Biotechnol.* 32 (2014) 347–355. https://doi.org/10.1038/nbt.2842.

[119] A.A. Nemudryi, K.R. Valetdinova, S.P. Medvedev, S.M. Zakian, TALEN and CRISPR/Cas genome editing systems: Tools of discovery, *Acta Naturae*. 6 (2014) 19–40. https://pubmed.ncbi.nlm.nih.gov/25349712.

[120] Y.G. Kim, J. Cha, S. Chandrasegaran, Hybrid restriction enzymes: Zinc finger fusions to Fok I cleavage domain, *Proc. Natl. Acad. Sci. U. S. A.* 93 (1996) 1156–1160. https://doi.org/10.1073/pnas.93.3.1156.

[121] J. Bitinaite, D.A. Wah, A.K. Aggarwal, I. Schildkraut, FokI dimerization is required for DNA cleavage, *Proc. Natl. Acad. Sci.* 95 (1998) 10570 LP – 10575. http://www.pnas.org/content/95/18/10570.abstract.

[122] T. Cathomen, J.K. Joung, Zinc-finger nucleases: The next generation emerges, *Mol. Ther.* 16 (2008) 1200–1207. https://doi.org/10.1038/mt.2008.114.

[123] Xenbase, (n.d.). http://www.xenbase.org/other/static-xenbase/CRISPR.jsp (accessed March 1, 2021).

[124] M. Jinek, K. Chylinski, I. Fonfara, M. Hauer, J.A. Doudna, E. Charpentier, A programmable Dual-RNA–guided DNA endonuclease in adaptive bacterial immunity, *Science.* 337 (2012) 816–821. https://doi.org/10.1126/science.1225829.

[125] G.J. Knott, J.A. Doudna, CRISPR-Cas guides the future of genetic engineering, *Science.* 361 (2018) 866–869. https://doi.org/10.1126/science.aat5011.

[126] M. Jinek, F. Jiang, D.W. Taylor, S.H. Sternberg, E. Kaya, E. Ma, C. Anders, M. Hauer, K. Zhou, S. Lin, M. Kaplan, A.T. Iavarone, E. Charpentier, E. Nogales, J.A. Doudna, Structures of Cas9 endonucleases reveal RNA-mediated conformational activation, *Science.* 343 (2014) undefined. https://doi.org/10.1126/science.1247997.

[127] R.M. Gupta, K. Musunuru, Expanding the genetic editing tool kit: ZFNs, TALENs, and CRISPR-Cas9, *J. Clin. Invest.* 124 (2014) 4154–4161. https://doi.org/10.1172/JCI72992.

[128] E. Fernandez, Yes, people can edit the genome in their garage. Can they be regulated?, *Forbes*. (2019). https://www.forbes.com/sites/fernandezelizabeth/2019/09/19/yes-people-can-edit-the-genome-in-their-garage-can-they-be-regulated/.

[129] C. Gustafsson, Nobel Prize Lecture: A tool for genome editing, 2020. www.nobelprize.org/prizes/chemistry/2020/press-release.

[130] Press release: The Nobel Prize in Chemistry 2020, (n.d.). https://www.nobelprize.org/prizes/chemistry/2020/press-release/ (accessed March 23, 2021).

[131] D. Rath, L. Amlinger, A. Rath, M. Lundgren, The CRISPR-Cas immune system: Biology, mechanisms and applications, *Biochimie*. 117 (2015) 119–128. https://doi.org/https://doi.org/10.1016/j.biochi.2015.03.025.

[132] M. Riera Romo, D. Pérez-Martínez, C. Castillo Ferrer, Innate immunity in vertebrates: An overview, *Immunology*. 148 (2016) 125–139. https://doi.org/10.1111/imm.12597.

[133] R. Barrangou, C. Fremaux, H. Deveau, M. Richards, P. Boyaval, S. Moineau, D.A. Romero, P. Horvath, CRISPR provides acquired resistance against viruses in prokaryotes, *Science*. 315 (2007) 1709–1712. https://doi.org/10.1126/science.1138140.

[134] F.J. Mojica, G. Juez, F. Rodríguez-Valera, Transcription at different salinities of Haloferax mediterranei sequences adjacent to partially modified PstI sites, *Mol. Microbiol.* 9 (1993) 613–621. https://doi.org/10.1111/j.1365-2958.1993.tb01721.x.

[135] A. Bolotin, B. Quinquis, A. Sorokin, S.D. Ehrlich, Clustered regularly interspaced short palindrome repeats (CRISPRs) have spacers of extrachromosomal origin, *Microbiology*. 151 (2005) 2551–2561. https://doi.org/10.1099/mic.0.28048-0.

[136] F.J.M. Mojica, C. Díez-Villaseñor, J. García-Martínez, E. Soria, Intervening sequences of regularly spaced prokaryotic repeats derive from foreign genetic elements, *J. Mol. Evol.* 60 (2005) 174–182. https://doi.org/10.1007/s00239-004-0046-3.

[137] C. Pourcel, G. Salvignol, G. Vergnaud, CRISPR elements in Yersinia pestis acquire new repeats by preferential uptake of bacteriophage DNA, and provide additional tools for evolutionary studies, *Microbiology*. 151 (2005) 653–663. https://doi.org/10.1099/mic.0.27437-0.

[138] T.-H. Tang, J.-P. Bachellerie, T. Rozhdestvensky, M.-L. Bortolin, H. Huber, M. Drungowski, T. Elge, J. Brosius, A. Hüttenhofer, Identification of 86 candidates for small non-messenger RNAs from the archaeon Archaeoglobus fulgidus, *Proc. Natl. Acad. Sci. U. S. A.* 99 (2002) 7536–7541. https://doi.org/10.1073/pnas.112047299.

[139] Y. Ishino, M. Krupovic, P. Forterre, History of CRISPR-Cas from encounter with a mysterious repeated sequence to genome editing technology, *J. Bacteriol.* 200 (2018) JB.00580-17. https://doi.org/10.1128/JB.00580-17.

[140] I. Zündorf, T. Dingermann, CRISPR/Cas9 revolutioniert die Gentechnik!, *Trillium Immunol.* (2018). https://www.trillium.de/zeitschriften/trillium-immunologie/archiv/ausgaben-2018/heft-22018/immunologie-leicht-gemacht/crisprcas9-revolutioniert-die-gentechnik.html (accessed March 23, 2021).

[141] J. McGinn, L.A. Marraffini, Molecular mechanisms of CRISPR–Cas spacer acquisition, *Nat. Rev. Microbiol.* 17 (2019) 7–12. https://doi.org/10.1038/s41579-018-0071-7.

[142] R. Jansen, J.D.A. van Embden, W. Gaastra, L.M. Schouls, Identification of genes that are associated with DNA repeats in prokaryotes, *Mol. Microbiol.* 43 (2002) 1565–1575. https://doi.org/10.1046/j.1365-2958.2002.02839.x.

[143] K.S. Makarova, E. V Koonin, Annotation and classification of CRISPR-Cas systems, *Methods Mol. Biol.* 1311 (2015) 47–75. https://doi.org/10.1007/978-1-4939-2687-9_4.

[144] K.S. Makarova, Y.I. Wolf, E. V Koonin, Classification and nomenclature of CRISPR-Cas systems: Where from here?, *Cris. J.* 1 (2018) 325–336. https://doi.org/10.1089/crispr.2018.0033.

[145] Y. Tang, Y. Fu, Class 2 CRISPR/Cas: An expanding biotechnology toolbox for and beyond genome editing, *Cell Biosci.* 8 (2018). https://doi.org/10.1186/s13578-018-0255-x.

[146] F.J.M. Mojica, C. Díez-Villaseñor, J. García-Martínez, C. Almendros, Short motif sequences determine the targets of the prokaryotic CRISPR defence system, *Microbiology*. 155 (2009) 733–740. https://doi.org/10.1099/mic.0.023960-0.

[147] E. Semenova, M.M. Jore, K.A. Datsenko, A. Semenova, E.R. Westra, B. Wanner, J. van der Oost, S.J.J. Brouns, K. Severinov, Interference by clustered regularly interspaced short palindromic repeat (CRISPR) RNA is governed by a seed sequence, *Proc. Natl. Acad. Sci.* 108 (2011) 10098–10103. https://doi.org/10.1073/pnas.1104144108.

[148] R.B. Vercoe, J.T. Chang, R.L. Dy, C. Taylor, T. Gristwood, J.S. Clulow, C. Richter, R. Przybilski, A.R. Pitman, P.C. Fineran, Cytotoxic chromosomal targeting by CRISPR/Cas systems can reshape bacterial genomes and expel or remodel pathogenicity islands, *PLOS Genet.* 9 (2013) e1003454. https://doi.org/10.1371/journal.pgen.1003454.

[149] P. Mandin, F. Repoila, M. Vergassola, T. Geissmann, P. Cossart, Identification of new noncoding RNAs in Listeria monocytogenes and prediction of mRNA targets, *Nucleic Acids Res.* 35 (2007) 962–974. https://doi.org/10.1093/nar/gkl1096.

[150] R. Louwen, D. Horst-Kreft, A.G. de Boer, L. van der Graaf, G. de Knegt, M. Hamersma, A.P. Heikema, A.R. Timms, B.C. Jacobs, J.A. Wagenaar, H.P. Endtz, J. van der Oost, J.M. Wells, E.E.S. Nieuwenhuis, A.H.M. van Vliet, P.T.J. Willemsen, P. van Baarlen, A. van Belkum, A novel link between Campylobacter jejuni bacteriophage defence, virulence and Guillain–Barré syndrome, *Eur. J. Clin. Microbiol. Infect. Dis.* 32 (2013) 207–226. https://doi.org/10.1007/s10096-012-1733-4.

[151] R. Perez-Rodriguez, C. Haitjema, Q. Huang, K.H. Nam, S. Bernardis, A. Ke, M.P. DeLisa, Envelope stress is a trigger of CRISPR RNA-mediated DNA silencing in Escherichia coli, *Mol.*

Microbiol. 79 (2011) 584–599. https://doi.org/https://doi.org/10.1111/j.1365-2958.2010.07482.x.

[152] P.D. Hsu, E.S. Lander, F. Zhang, Development and applications of CRISPR-Cas9 for genome engineering, *Cell*. 157 (2014) 1262–1278. https://doi.org/10.1016/j.cell.2014.05.010.

[153] T. Maruyama, S.K. Dougan, M.C. Truttmann, A.M. Bilate, J.R. Ingram, H.L. Ploegh, Increasing the efficiency of precise genome editing with CRISPR-Cas9 by inhibition of nonhomologous end joining, *Nat. Biotechnol.* 33 (2015) 538–542. https://doi.org/10.1038/nbt.3190.

[154] H. Nishimasu, F.A. Ran, P.D. Hsu, S. Konermann, S.I. Shehata, N. Dohmae, R. Ishitani, F. Zhang, O. Nureki, Crystal structure of Cas9 in complex with guide RNA and target DNA, *Cell*. 156 (2014) 935–949. https://doi.org/https://doi.org/10.1016/j.cell.2014.02.001.

[155] C. Anders, O. Niewoehner, A. Duerst, M. Jinek, Structural basis of PAM-dependent target DNA recognition by the Cas9 endonuclease, *Nature*. 513 (2014) 569–573. https://doi.org/10.1038/nature13579.

[156] R.M. Terns, M.P. Terns, CRISPR-based technologies: Prokaryotic defense weapons repurposed, *Trends Genet.* 30 (2014) 111–118. https://doi.org/https://doi.org/10.1016/j.tig.2014.01.003.

[157] M.R. Bakst, Structure of the avian oviduct with emphasis on sperm storage in poultry, *J. Exp. Zool.* 282 (1998) 618–626.

[158] J. Lee, D.-H. Kim, K. Lee, Current approaches and applications in avian genome editing, *Int. J. Mol. Sci.* 21 (2020) 3937. https://doi.org/10.3390/ijms21113937.

[159] F. Delerue, L.M. Ittner, Generation of genetically modified mice through the microinjection of oocytes, *J. Vis. Exp.* (2017) 55765. https://doi.org/10.3791/55765.

[160] U. Lakshmipathy, B. Pelacho, K. Sudo, J.L. Linehan, E. Coucouvanis, D.S. Kaufman, C.M. Verfaillie, Efficient transfection of embryonic and adult stem cells, *Stem Cells*. 22 (2004) 531–543. https://doi.org/10.1634/stemcells.22-4-531.

[161] F. Robinson, G. Fasenko, R. Renema, Optimizing chick production in broiler breeders, 2003.

[162] S. Kochav, M. Ginsburg, H. Eyal-Giladi, From cleavage to primitive streak formation: A complementary normal table and a new look at the first stages of the development of the chick. II. Microscopic anatomy and cell population dynamics., *Dev. Biol.* 79 (1980) 296–308. https://doi.org/10.1016/0012-1606(80)90117-7.

[163] M.-C. van de Lavoir, J.H. Diamond, P.A. Leighton, C. Mather-Love, B.S. Heyer, R. Bradshaw, A. Kerchner, L.T. Hooi, T.M. Gessaro, S.E. Swanberg, M.E. Delany, R.J. Etches, Germline transmission of genetically modified primordial germ cells, *Nature*. 441 (2006) 766–769. https://doi.org/10.1038/nature04831.

[164] D.W. Salter, E.J. Smith, S.H. Hughes, S.E. Wright, L.B. Crittenden, Transgenic chickens: Insertion of retroviral genes into the chicken germ line, *Virology*. 157 (1987) 236–240. https://doi.org/https://doi.org/10.1016/0042-6822(87)90334-5.

[165] S.H. Hughes, E. Kosik, A.M. Fadly, D.W. Salter, L.B. Crittenden, Design of retroviral vectors for the insertion of foreign deoxyribonucleic acid sequences into the avian germ line, *Poult. Sci.* 65 (1986) 1459–1467. https://doi.org/10.3382/ps.0651459.

[166] A.J. Harvey, G. Speksnijder, L.R. Baugh, J.A. Morris, R. Ivarie, Expression of exogenous protein in the egg white of transgenic chickens, *Nat. Biotechnol.* 20 (2002) 396–399. https://doi.org/10.1038/nbt0402-396.

[167] D.W. Salter, L.B. Crittenden, Artificial insertion of a dominant gene for resistance to avian leukosis virus into the germ line of the chicken, *Theor. Appl. Genet.* 77 (1989) 457–461. https://doi.org/10.1007/BF00274263.

[168] M. Kamihira, K. Ono, K. Esaka, K. Nishijima, R. Kigaku, H. Komatsu, T. Yamashita, K. Kyogoku, S. Iijima, High-level expression of single-chain Fv-Fc fusion protein in serum and egg white of genetically manipulated chickens by using a retroviral vector, *J. Virol.* 79 (2005) 10864–10874. https://doi.org/10.1128/JVI.79.17.10864-10874.2005.

[169] R.A. Bosselman, R.Y. Hsu, T. Boggs, S. Hu, J. Bruszewski, S. Ou, L. Souza, L. Kozar, F. Martin, M. Nicolson, Replication-defective vectors of reticuloendotheliosis virus transduce exogenous genes into somatic stem cells of the unincubated chicken embryo, *J. Virol.* 63 (1989) 2680–2689. https://doi.org/10.1128/JVI.63.6.2680-2689.1989.

[170] M.J. McGrew, A. Sherman, F.M. Ellard, S.G. Lillico, H.J. Gilhooley, A.J. Kingsman, K.A. Mitrophanous, H. Sang, Efficient production of germline transgenic chickens using lentiviral vectors, *EMBO Rep.* 5 (2004) 728–733. https://doi.org/10.1038/sj.embor.7400171.

[171] L. Naldini, U. Blömer, P. Gallay, D. Ory, R. Mulligan, F.H. Gage, I.M. Verma, D. Trono, In vivo gene delivery and stable transduction of nondividing cells by a lentiviral vector, *Science*. 272 (1996) 263–267. https://doi.org/10.1126/science.272.5259.263.

[172] T.J. Doran, C.A. Cooper, K.A. Jenkins, M.L. V Tizard, Advances in genetic engineering of the avian genome: "Realising the promise," *Transgenic Res.* 25 (2016) 307–319. https://doi.org/10.1007/s11248-016-9926-8.

[173] H. Sid, B. Schusser, Applications of gene editing in chickens: A new era is on the horizon, *Front. Genet.* 9 (2018) 456. https://www.frontiersin.org/article/10.3389/fgene.2018.00456.

[174] J. Love, C. Gribbin, C. Mather, H. Sang, Transgenic birds by DNA microinjection, *Bio/Technology*. 12 (1994) 60–63. https://doi.org/10.1038/nbt0194-60.

[175] C. Liu, W. Xie, C. Gui, Y. Du, Pronuclear microinjection and oviduct transfer procedures for transgenic mouse production, *Methods Mol. Biol.* 1027 (2013) 217–232. https://doi.org/10.1007/978-1-60327-369-5_10.

[176] T.S. Park, J.Y. Han, Derivation and characterization of pluripotent embryonic germ cells in chicken, *Mol. Reprod. Dev.* 56 (2000) 475–482. https://doi.org/10.1002/1098-2795(200008)56:4<475::AID-MRD5>3.0.CO;2-M.

[177] J.Y. Han, H.C. Lee, T.S. Park, Germline-competent stem cell in avian species and its application, *Asian J. Androl.* 17 (2015) 421–426. https://doi.org/10.4103/1008-682X.148073.

[178] P.D. Nieuwkoop, L.A. Sutasurya, Primordial germ cells in the chordates: Embryogenesis and phylogenesis, *Q. Rev. Biol.* 55 (1980) 438. https://doi.org/10.1086/412011.

[179] C. Wylie, Germ cells, *Cell*. 96 (1999) 165–174. https://doi.org/10.1016/s0092-8674(00)80557-7.

[180] C.H. Swift, Origin and early history of the primordial germ-cells in the chick, *Am. J. Anat.* 15 (1914) 483–516. https://doi.org/https://doi.org/10.1002/aja.1000150404.

[181] J.N. Kim, T.S. Park, S.H. Park, K.J. Park, T.M. Kim, S.K. Lee, J.M. Lim, J.Y. Han, Migration and proliferation of intact and genetically modified primordial germ cells and the generation of a transgenic chicken, *Biol. Reprod.* 82 (2010) 257–262. https://doi.org/10.1095/biolreprod.109.079723.

[182] T. Fujimoto, T. Ninomiya, A. Ukeshima, Observations of the primordial germ cells in blood

samples from the chick embryo, *Dev. Biol.* 49 (1976) 278–282. https://doi.org/https://doi.org/10.1016/0012-1606(76)90273-6.

[183] C.A. Smith, A.H. Sinclair, Sex determination: Insights from the chicken, *Bioessays*. 26 (2004) 120–132. https://doi.org/10.1002/bies.10400.

[184] M.-C. van de Lavoir, E.J. Collarini, P.A. Leighton, J. Fesler, D.R. Lu, W.D. Harriman, T.S. Thiyagasundaram, R.J. Etches, Interspecific germline transmission of cultured primordial germ cells, *PLoS One*. 7 (2012) e35664. https://doi.org/10.1371/journal.pone.0035664.

[185] B. Burgess-Beusse, C. Farrell, M. Gaszner, M. Litt, V. Mutskov, F. Recillas-Targa, M. Simpson, A. West, G. Felsenfeld, The insulation of genes from external enhancers and silencing chromatin, *Proc. Natl. Acad. Sci.* 99 (2002) 16433–16437. https://doi.org/10.1073/pnas.162342499.

[186] J.W. Choi, S. Kim, T.M. Kim, Y.M. Kim, H.W. Seo, T.S. Park, J.-W. Jeong, G. Song, J.Y. Han, Basic fibroblast growth factor activates MEK/ERK cell signaling pathway and stimulates the proliferation of chicken primordial germ cells, *PLoS One*. 5 (2010) e12968. https://doi.org/10.1371/journal.pone.0012968.

[187] J. Whyte, J.D. Glover, M. Woodcock, J. Brzeszczynska, L. Taylor, A. Sherman, P. Kaiser, M.J. McGrew, FGF, insulin, and SMAD signaling cooperate for avian primordial germ cell self-renewal, *Stem Cell Reports*. 5 (2015) 1171–1182. https://doi.org/10.1016/j.stemcr.2015.10.008.

[188] H. Sang, Transgenesis sunny-side up, *Nat. Biotechnol.* 24 (2006) 955–956. https://doi.org/10.1038/nbt0806-955.

[189] P.A. Leighton, M.-C. van de Lavoir, J.H. Diamond, C. Xia, R.J. Etches, Genetic modification of primordial germ cells by gene trapping, gene targeting, and phiC31 integrase, *Mol. Reprod. Dev.* 75 (2008) 1163–1175. https://doi.org/10.1002/mrd.20859.

[190] P.A. Leighton, D. Pedersen, K. Ching, E.J. Collarini, S. Izquierdo, R. Jacob, M.-C. van de Lavoir, Generation of chickens expressing Cre recombinase, *Transgenic Res.* 25 (2016) 609–616. https://doi.org/10.1007/s11248-016-9952-6.

[191] A. Keravala, M.P. Calos, Site-specific chromosomal integration mediated by phiC31 integrase, *Methods Mol. Biol.* 435 (2008) 165–173. https://doi.org/10.1007/978-1-59745-232-8_12.

[192] P. Leighton, M.-C. Van de Lavoir, J.H. Diamond, C. Xia, R.J. Etches, Genetic modification of primordial germ cells by gene trapping, gene targeting, and ϕC31 integrase, *Mol. Reprod. Dev.* 75 (2008) 1163–1175. https://doi.org/10.1002/mrd.20859.

[193] J.D. Glover, L. Taylor, A. Sherman, C. Zeiger-Poli, H.M. Sang, M.J. McGrew, A novel piggyBac transposon inducible expression system identifies a role for AKT signalling in primordial germ cell migration, *PLoS One*. 8 (2013) e77222. https://doi.org/10.1371/journal.pone.0077222.

[194] T. Park, J.Y. Han, PiggyBac transposition into primordial germ cells is an efficient tool for transgenesis in chickens, *Proc. Natl. Acad. Sci. U. S. A.* 109 (2012) 9337–9341. https://doi.org/10.1073/pnas.1203823109.

[195] M. Muñoz-López, J.L. García-Pérez, DNA transposons: nature and applications in genomics, *Curr. Genomics*. 11 (2010) 115–128. https://doi.org/10.2174/138920210790886871.

[196] S.R. Wessler, Transposable elements and the evolution of eukaryotic genomes, *Proc. Natl. Acad. Sci.* 103 (2006) 17600–17601. https://doi.org/10.1073/pnas.0607612103.

[197] S. Saha, M.H. Wilson, Transposons for Non-Viral Gene Transfer, in: F.M. Molina (Ed.), Gene

Ther. - Tools Potential Appl., 2013: p. 270. https://doi.org/http://dx.doi.org/10.5772/50194.

[198] L.C. Cary, M. Goebel, B.G. Corsaro, H.G. Wang, E. Rosen, M.J. Fraser, Transposon mutagenesis of baculoviruses: Analysis of Trichoplusia ni transposon IFP2i nsertions within the FP-locus of nuclear polyhedrosis viruses, *Virology*. 172 (1989) 156–169. https://doi.org/10.1016/0042-6822(89)90117-7.

[199] K. Kawakami, Tol2: A versatile gene transfer vector in vertebrates, *Genome Biol.* 8 Suppl 1 (2007) S7. https://doi.org/10.1186/gb-2007-8-s1-s7.

[200] J. Macdonald, L. Taylor, A. Sherman, K. Kawakami, Y. Takahashi, H.M. Sang, M.J. McGrew, Efficient genetic modification and germ-line transmission of primordial germ cells using piggyBac and Tol2 transposons, *Proc. Natl. Acad. Sci. U. S. A.* 109 (2012) E1466–E1472. https://doi.org/10.1073/pnas.1118715109.

[201] B. Schusser, E.J. Collarini, D. Pedersen, H. Yi, K. Ching, S. Izquierdo, T. Thoma, S. Lettmann, B. Kaspers, R.J. Etches, M.-C. van de Lavoir, W. Harriman, P.A. Leighton, Expression of heavy chain-only antibodies can support B-cell development in light chain knockout chickens, *Eur. J. Immunol.* 46 (2016) 2137–2148. https://doi.org/https://doi.org/10.1002/eji.201546171.

[202] N. Véron, Z. Qu, P.A.S. Kipen, C.E. Hirst, C. Marcelle, CRISPR mediated somatic cell genome engineering in the chicken, *Dev. Biol.* 407 (2015) 68–74. https://doi.org/10.1016/j.ydbio.2015.08.007.

[203] H.J. Lee, J.W. Yoon, K.M. Jung, Y.M. Kim, J.S. Park, K.Y. Lee, K.J. Park, Y.S. Hwang, Y.H. Park, D. Rengaraj, J.Y. Han, Targeted gene insertion into Z chromosome of chicken primordial germ cells for avian sexing model development., *FASEB J. Off. Publ. Fed. Am. Soc. Exp. Biol.* 33 (2019) 8519–8529. https://doi.org/10.1096/fj.201802671R.

[204] I. Oishi, K. Yoshii, D. Miyahara, H. Kagami, T. Tagami, Targeted mutagenesis in chicken using CRISPR/Cas9 system, *Sci. Rep.* 6 (2016) 23980. https://doi.org/10.1038/srep23980.

[205] J. Lee, J. Ma, K. Lee, Direct delivery of adenoviral CRISPR/Cas9 vector into the blastoderm for generation of targeted gene knockout in quail, *Proc. Natl. Acad. Sci.* 116 (2019) 13288–13292. https://doi.org/10.1073/pnas.1903230116.

[206] Z. Wu, H. Yang, P. Colosi, Effect of genome size on AAV vector packaging, *Mol. Ther.* 18 (2010) 80–86. https://doi.org/10.1038/mt.2009.255.

[207] R. Schirmbeck, J. Reimann, S. Kochanek, F. Kreppel, The immunogenicity of adenovirus vectors limits the multispecificity of CD8 T-cell responses to vector-encoded transgenic antigens, *Mol. Ther.* 16 (2008) 1609–1616. https://doi.org/10.1038/mt.2008.141.

[208] B. Zetsche, S.E. Volz, F. Zhang, A split-Cas9 architecture for inducible genome editing and transcription modulation, *Nat. Biotechnol.* 33 (2015) 139–142. https://doi.org/10.1038/nbt.3149.

[209] Y. Tan, A.H.Y. Chu, S. Bao, D.A. Hoang, F.T. Kebede, W. Xiong, M. Ji, J. Shi, Z. Zheng, Rationally engineered Staphylococcus aureus Cas9 nucleases with high genome-wide specificity, *Proc. Natl. Acad. Sci.* 116 (2019) 20969–20976. https://doi.org/10.1073/pnas.1906843116.

[210] K. Wang, Q. Jin, D. Ruan, Y. Yang, Q. Liu, H. Wu, Z. Zhou, Z. Ouyang, Z. Liu, Y. Zhao, B. Zhao, Q. Zhang, J. Peng, C. Lai, N. Fan, Y. Liang, T. Lan, N. Li, X. Wang, X. Wang, Y. Fan, P.A. Doevendans, J.P.G. Sluijter, P. Liu, X. Li, L. Lai, Cre-dependent Cas9-expressing pigs enable efficient in vivo genome editing, *Genome Res.* 27 (2017) 2061–2071. https://doi.org/10.1101/gr.222521.117.

[211] M. Sadelain, E.P. Papapetrou, F.D. Bushman, Safe harbours for the integration of new DNA in the human genome, *Nat. Rev. Cancer*. 12 (2012) 51–58. https://doi.org/10.1038/nrc3179.

[212] X. Li, Y. Yang, L. Bu, X. Guo, C. Tang, J. Song, N. Fan, B. Zhao, Z. Ouyang, Z. Liu, Y. Zhao, X. Yi, L. Quan, S. Liu, Z. Yang, H. Ouyang, Y.E. Chen, Z. Wang, L. Lai, Rosa26-targeted swine models for stable gene over-expression and Cre-mediated lineage tracing, *Cell Res.* 24 (2014) 501–504. https://doi.org/10.1038/cr.2014.15.

[213] J. Macdonald, J.D. Glover, L. Taylor, H.M. Sang, M.J. McGrew, Characterisation and germline transmission of cultured avian primordial germ cells, *PLoS One*. 5 (2010) e15518. https://doi.org/10.1371/journal.pone.0015518.

[214] M. Laparidou, A. Schlickenrieder, T. Thoma, K. Lengyel, B. Schusser, Blocking of the CXCR4-CXCL12 interaction inhibits the migration of chicken B Cells into the bursa of Fabricius, *Front. Immunol.* 10 (2019) 3057. https://doi.org/10.3389/fimmu.2019.03057.

[215] A.C. Groth, E.C. Olivares, B. Thyagarajan, M.P. Calos, A phage integrase directs efficient site-specific integration in human cells, *Proc. Natl. Acad. Sci. U. S. A.* 97 (2000) 5995–6000. https://doi.org/10.1073/pnas.090527097.

[216] L. Cong, F.A. Ran, D. Cox, S. Lin, R. Barretto, N. Habib, P.D. Hsu, X. Wu, W. Jiang, L.A. Marraffini, F. Zhang, Multiplex genome engineering using CRISPR/Cas systems, *Science*. 339 (2013) 819–823. https://doi.org/10.1126/science.1231143.

[217] D. Maddalo, E. Manchado, C.P. Concepcion, C. Bonetti, J.A. Vidigal, Y.-C. Han, P. Ogrodowski, A. Crippa, N. Rekhtman, E. de Stanchina, S.W. Lowe, A. Ventura, In vivo engineering of oncogenic chromosomal rearrangements with the CRISPR/Cas9 system, *Nature*. 516 (2014) 423–427. https://doi.org/10.1038/nature13902.

[218] S.H. Hughes, J.J. Greenhouse, C.J. Petropoulos, P. Sutrave, Adaptor plasmids simplify the insertion of foreign DNA into helper-independent retroviral vectors, *J. Virol.* 61 (1987) 3004–3012. https://doi.org/10.1128/JVI.61.10.3004-3012.1987.

[219] Zhang lab, (n.d.). http://crispr.mit.edu/index.html (accessed February 27, 2021).

[220] Ensembl, (n.d.). https://www.ensembl.org/index.html (accessed February 27, 2021).

[221] National Library of Medicine, National Center for Biotechnology Information, (1988). https://www.ncbi.nlm.nih.gov/index.html (accessed February 27, 2021).

[222] TIDE: Tracking of Indels by DEcomposition, (n.d.). http://shinyapps.datacurators.nl/tide/ (accessed March 23, 2021).

[223] E.K. Brinkman, T. Chen, M. Amendola, B. van Steensel, Easy quantitative assessment of genome editing by sequence trace decomposition, *Nucleic Acids Res.* 42 (2014) e168. https://doi.org/10.1093/nar/gku936.

[224] L. Chojnacka-Puchta, D. Sawicka, P. Lakota, G. Pluciennicza k, M. Bednarczyk, A. Pluciennicza k, Obtaining chicken primordial germ cells used for gene transfer: In vitro and in vivo results, *J. Appl. Genet.* 56 (2015) 493–504. https://doi.org/10.1007/s13353-015-0276-7.

[225] V. Hamburger, H.L. Hamilton, A series of normal stages in the development of the chick embryo, *Dev. Dyn.* 195 (1992) 231–272. https://doi.org/10.1002/aja.1001950404.

[226] P. Trefil, D. Aumann, A. Koslová, J. Mucksová, B. Benešová, J. Kalina, C. Wurmser, R. Fries, D. Elleder, B. Schusser, J. Hejnar, Male fertility restored by transplanting primordial germ cells into testes: A new way towards efficient transgenesis in chicken, *Sci. Rep.* 7 (2017) 14246. https://doi.org/10.1038/s41598-017-14475-w.

[227] New England Biolabs, Tm calculator, (2020). https://tmcalculator.neb.com/#!/main (accessed February 27, 2021).

[228] R.K. Saiki, D.H. Gelfand, S. Stoffel, S.J. Scharf, R. Higuchi, G.T. Horn, K.B. Mullis, H.A. Erlich, Primer-directed enzymatic amplification of DNA with a thermostable DNA polymerase, *Science*. 239 (1988) 487–491. https://doi.org/10.1126/science.2448875.

[229] P. Keohavong, W.G. Thilly, Fidelity of DNA polymerases in DNA amplification, *Proc. Natl. Acad. Sci. U. S. A.* 86 (1989) 9253–9257. https://doi.org/10.1073/pnas.86.23.9253.

[230] V. Potapov, J.L. Ong, Examining sources of error in PCR by single-molecule sequencing, *PLoS One*. 12 (2017) e0169774. https://doi.org/10.1371/journal.pone.0169774.

[231] Q5® High-Fidelity DNA Polymerase, (n.d.). https://international.neb.com/products/m0491-q5-high-fidelity-dna-polymerase#Product Information (accessed February 27, 2021).

[232] J.L. Hedrick, a J. Smith, Size and charge isomer separation and estimation of molecular weights of proteins by disc gel electrophoresis., *Arch. Biochem. Biophys.* 126 (1968) 155–164. https://doi.org/10.1016/0003-9861(68)90569-9.

[233] E. Aparicio-Prat, C. Arnan, I. Sala, N. Bosch, R. Guigó, R. Johnson, DECKO: Single-oligo, dual-CRISPR deletion of genomic elements including long non-coding RNAs, *BMC Genomics*. 16 (2015) 846. https://doi.org/10.1186/s12864-015-2086-z.

[234] Benchling, (n.d.). https://www.benchling.com/ (accessed February 27, 2021).

[235] Bio-Rad, (n.d.). https://www.bio-rad.com/de-de/product/trans-blot-cell?ID=a9900af6-f596-45c8-859e-9985048a418e (accessed February 27, 2021).

[236] BioRender, (n.d.). https://app.biorender.com (accessed February 27, 2021).

[237] B. Rieblinger, H. Sid, D. Duda, T. Bozoglu, R. Klinger, A. Schlickenrieder, K. Lengyel, K. Flisikowski, T. Flisikowska, N. Simm, A. Grodziecki, C. Perleberg, A. Bähr, L. Carrier, M. Kurome, V. Zakhartchenko, B. Kessler, E. Wolf, L. Kettler, H. Luksch, I.T. Hagag, D. Wise, J. Kaufman, B.B. Kaufer, C. Kupatt, A. Schnieke, B. Schusser, Cas9-expressing chickens and pigs as resources for genome editing in livestock, *Proc. Natl. Acad. Sci.* 118 (2021) e2022562118. https://doi.org/10.1073/pnas.2022562118.

[238] D. Bartsch, H. Sid, B. Rieblinger, R. Hellmich, A. Schlickenrieder, K. Lengyel, K. Flisikowski, T. Flisikowska, N. Simm, A. Grodziecki, C. Perleberg, C. Kupatt, E. Wolf, B. Kessler, L. Kettler, H. Luksch, I.T. Hagag, D. Wise, J. Kaufman, B.B. Kaufer, A. Schnieke, B. Schusser, Resources for genome editing in livestock: Cas9-expressing chickens and pigs, *BioRxiv*. (2020) 2020.04.01.019679. https://doi.org/10.1101/2020.04.01.019679.

[239] J.G. Doench, N. Fusi, M. Sullender, M. Hegde, E.W. Vaimberg, K.F. Donovan, I. Smith, Z. Tothova, C. Wilen, R. Orchard, H.W. Virgin, J. Listgarten, D.E. Root, Optimized sgRNA design to maximize activity and minimize off-target effects of CRISPR-Cas9, *Nat. Biotechnol.* 34 (2016) 184–191. https://doi.org/10.1038/nbt.3437.

[240] P.D. Hsu, D.A. Scott, J.A. Weinstein, F.A. Ran, S. Konermann, V. Agarwala, Y. Li, E.J. Fine, X. Wu, O. Shalem, T.J. Cradick, L.A. Marraffini, G. Bao, F. Zhang, DNA targeting specificity of RNA-guided Cas9 nucleases., *Nat. Biotechnol.* 31 (2013) 827–832. https://doi.org/10.1038/nbt.2647.

[241] N. Itasaki, S. Bel-Vialar, R. Krumlauf, "Shocking" developments in chick embryology: Electroporation and in ovo gene expression., *Nat. Cell Biol.* 1 (1999) E203-7. https://doi.org/10.1038/70231.

[242] H. Nakamura, J. Funahashi, Introduction of DNA into chick embryos by in ovo electroporation, *Methods*. 24 (2001) 43–48. https://doi.org/10.1006/meth.2001.1155.

[243] B. Yang, L.B. Geary, Y.-C. Ma, In ovo electroporation in chick midbrain for studying gene function in dopaminergic neuron development, *J. Vis. Exp.* (2012) e4017. https://doi.org/10.3791/4017.

[244] S. Weigel, T. Flisikowska, A. Schnieke, H. Luksch, Hybrid voltage sensor imaging of eGFP-F expressing neurons in chicken midbrain slices, *J. Neurosci. Methods*. 233 (2014) 28–33. https://doi.org/10.1016/j.jneumeth.2014.05.034.

[245] G. Bourque, K.H. Burns, M. Gehring, V. Gorbunova, A. Seluanov, M. Hammell, M. Imbeault, Z. Izsvák, H.L. Levin, T.S. Macfarlan, D.L. Mager, C. Feschotte, Ten things you should know about transposable elements, *Genome Biol.* 19 (2018) 199. https://doi.org/10.1186/s13059-018-1577-z.

[246] Cre-recombinase-associated toxicity highlights limitations of genome editing, *Dis. Model. Mech.* 6 (2013) 1299–1300. https://www.ncbi.nlm.nih.gov/pmc/articles/PMC3820252/.

[247] A. Fani Maleki, M.H. Sekhavati, Application of phiC31 integrase system in stem cells biology and technology: A review, *Front. Life Sci.* 11 (2018) 1–10. https://doi.org/10.1080/21553769.2018.1447516.

[248] Q. Kong, M. Wu, Y. Huan, L. Zhang, H. Liu, G. Bou, Y. Luo, Y. Mu, Z. Liu, Transgene expression is associated with copy number and cytomegalovirus promoter methylation in transgenic pigs, *PLoS One*. 4 (2009) e6679–e6679. https://doi.org/10.1371/journal.pone.0006679.

[249] B. Thyagarajan, M.P. Calos, Site-specific integration for high-level protein production in mammalian cells, *Methods Mol. Biol.* 308 (2005) 99–106. https://doi.org/10.1385/1-59259-922-2:099.

[250] H. Kim, J.-S. Kim, A guide to genome engineering with programmable nucleases, *Nat. Rev. Genet.* 15 (2014) 321–334. https://doi.org/10.1038/nrg3686.

[251] D. Aumann, Generierung genetisch modifizierter Hühnermodelle für die immunologische Forschung, Ludwig-Maximilians-Universität München, 2017.

[252] L.G. Ahronian, B.C. Lewis, Generation of high-titer RCAS virus from DF1 chicken fibroblasts, *Cold Spring Harb. Protoc.* 2014 (2014) 1161–1166. https://doi.org/10.1101/pdb.prot077974.

[253] B. Schusser, A. Reuter, A. von der Malsburg, N. Penski, S. Weigend, B. Kaspers, P. Staeheli, S. Härtle, Mx is dispensable for interferon-mediated resistance of chicken cells against Influenza A virus, *J. Virol.* 85 (2011) 8307–8315. https://doi.org/10.1128/JVI.00535-11.

[254] A. Reuter, S. Soubies, S. Härtle, B. Schusser, B. Kaspers, P. Staeheli, D. Rubbenstroth, Antiviral activity of lambda interferon in chickens, *J. Virol.* 88 (2014) 2835–43. https://doi.org/10.1128/JVI.02764-13.

[255] C. for C.R. National Cancer Institute, The RCAS System, (n.d.). https://ccr.cancer.gov/hiv-dynamics-and-replication-program/scientific-resources/rcas-system (accessed March 23, 2021).

[256] S.H. Hughes, The RCAS vector system, *Folia Biol. (Praha).* 50 (2004) 107—119. http://europepmc.org/abstract/MED/15373344.

[257] T. Hatziioannou, S.P. Goff, Infection of nondividing cells by Rous sarcoma virus., *J. Virol.* 75 (2001) 9526–9531. https://doi.org/10.1128/JVI.75.19.9526-9531.2001.

[258] R.A. Katz, J.G. Greger, K. Darby, P. Boimel, G.F. Rall, A.M. Skalka, Transduction of interphase cells by avian sarcoma virus., *J. Virol.* 76 (2002) 5422–5434. https://doi.org/10.1128/jvi.76.11.5422-5434.2002.

[259] U.S. National Library of Medicine, blast.ncbi, (n.d.). https://blast.ncbi.nlm.nih.gov/Blast.cgi?PAGE_TYPE=BlastSearch (accessed March 23, 2021).

[260] A. Mukerjee, J. Shankardas, A.P. Ranjan, J.K. Vishwanatha, Efficient nanoparticle mediated sustained RNA interference in human primary endothelial cells, *Nanotechnology*. 22 (2011) 445101. https://doi.org/10.1088/0957-4484/22/44/445101.

[261] N. Le Douarin, A biological cell labeling technique and its use in experimental embryology, *Dev. Biol.* 30 (1973) 217–222. https://doi.org/https://doi.org/10.1016/0012-1606(73)90061-4.

[262] G.F. Couly, P.M. Coltey, N.M. Le Douarin, The developmental fate of the cephalic mesoderm in quail-chick chimeras, *Development*. 114 (1992) 1–15.

[263] N. Sato, K. Matsuda, C. Sakuma, D.N. Foster, R.W. Oppenheim, H. Yaginuma, Regulated Gene Expression in the Chicken Embryo by Using Replication-Competent Retroviral Vectors, *J. Virol.* 76 (2002) 1980 LP – 1985. https://doi.org/10.1128/JVI.76.4.1980-1985.2002.

[264] S. Kothlow, K. Schenk-Weibhauser, M.J.H. Ratcliffe, B. Kaspers, Prolonged effect of BAFF on chicken B cell development revealed by RCAS retroviral gene transfer in vivo, *Mol. Immunol.* 47 (2010) 1619—1628. https://doi.org/10.1016/j.molimm.2010.01.011.

[265] G.L. Andreason, G.A. Evans, Introduction and expression of DNA molecules in eukaryotic cells by electroporation, *Biotechniques*. 6 (1988) 650–660.

[266] M. Takahashi, T. Furukawa, H. Saitoh, A. Aoki, T. Koike, Y. Moriyama, A. Shibata, Gene transfer into human leukemia cell lines by electroporation: Experience with exponentially decaying and square wave pulse, *Leuk. Res.* 15 (1991) 507–513. https://doi.org/https://doi.org/10.1016/0145-2126(91)90062-X.

[267] T. Momose, A. Tonegawa, J. Takeuchi, H. Ogawa, K. Umesono, K. Yasuda, Efficient targeting of gene expression in chick embryos by microelectroporation, *Dev. Growth Differ.* 41 (1999) 335–344. https://doi.org/10.1046/j.1440-169x.1999.413437.x.

[268] T. Muramatsu, Y. Mizutani, Y. Ohmori, J. Okumura, Comparison of three nonviral transfection methods for foreign gene expression in early chicken embryos in ovo, *Biochem. Biophys. Res. Commun.* 230 (1997) 376–380. https://doi.org/10.1006/bbrc.1996.5882.

[269] E.K. Farley, Gene transfer in developing chick embryos: In ovo electroporation, *Methods Mol. Biol.* 1018 (2013) 141–150. https://doi.org/10.1007/978-1-62703-444-9_14.

[270] M.T.P. Gilbert, T. Haselkorn, M. Bunce, J.J. Sanchez, S.B. Lucas, L.D. Jewell, E. Van Marck, M. Worobey, The isolation of nucleic acids from fixed, paraffin-embedded tissues–Which methods are useful when?, *PLoS One*. 2 (2007) e537. https://doi.org/10.1371/journal.pone.0000537.

[271] N. Zhao, J. Qi, Z. Zeng, P. Parekh, C.-C. Chang, C.-H. Tung, Y. Zu, Transfecting the hard-to-transfect lymphoma/leukemia cells using a simple cationic polymer nanocomplex, *J. Control. Release*. 159 (2012) 104–110. https://doi.org/10.1016/j.jconrel.2012.01.007.

[272] A. Hendel, R.O. Bak, J.T. Clark, A.B. Kennedy, D.E. Ryan, S. Roy, I. Steinfeld, B.D. Lunstad, R.J. Kaiser, A.B. Wilkens, R. Bacchetta, A. Tsalenko, D. Dellinger, L. Bruhn, M.H. Porteus, Chemically modified guide RNAs enhance CRISPR-Cas genome editing in human primary cells,

Nat. Biotechnol. 33 (2015) 985–989. https://doi.org/10.1038/nbt.3290.

[273] M. Pallarès Masmitjà, N. Knödlseder, M. Güell, CRISPR-gRNA Design., *Methods Mol. Biol.* 1961 (2019) 3–11. https://doi.org/10.1007/978-1-4939-9170-9_1.

[274] D. Huhle, S. Hirmer, T.W. Göbel, Splenic γδ T cell subsets can be separated by a novel mab specific for two CD45 isoforms, *Dev. Comp. Immunol.* 77 (2017) 229–240. https://doi.org/10.1016/j.dci.2017.08.013.

[275] J.C. Ribot, B. Silva-Santos, Differentiation and activation of γδ T Lymphocytes: Focus on CD27 and CD28 costimulatory receptors, *Adv. Exp. Med. Biol.* 785 (2013) 95–105. https://doi.org/10.1007/978-1-4614-6217-0_11.

[276] R.P. Bucy, C.L. Chen, J. Cihak, U. Lösch, M.D. Cooper, Avian T cells expressing gamma delta receptors localize in the splenic sinusoids and the intestinal epithelium., *J. Immunol.* 141 (1988) 2200–2205.

[277] L.V. Fenzl, Spontane Zytotoxizität von γδ - T - Zellen im Haushuhn, Ludwig-Maximilians-Universität München, 2018.

[278] I.M. Gimeno, Marek's disease vaccines: A solution for today but a worry for tomorrow?, *Vaccine*. 26 (2008) C31–C41. https://doi.org/https://doi.org/10.1016/j.vaccine.2008.04.009.

[279] M. Couteaudier, C. Denesvre, Marek's disease virus and skin interactions, *Vet. Res.* 45 (2014) 36. https://doi.org/10.1186/1297-9716-45-36.

[280] M. Chen, W.S. Payne, J.R. Dunn, S. Chang, H.M. Zhang, H.D. Hunt, J.B. Dodgson, Retroviral delivery of RNA interference against Marek's disease virus in vivo, *Poult. Sci.* 88 (2009) 1373–1380. https://doi.org/https://doi.org/10.3382/ps.2009-00070.

[281] L.S. Lambeth, Y. Zhao, L.P. Smith, L. Kgosana, V. Nair, Targeting Marek's disease virus by RNA interference delivered from a herpesvirus vaccine, *Vaccine*. 27 (2009) 298–306. https://doi.org/https://doi.org/10.1016/j.vaccine.2008.10.023.

[282] M. Chen, W.S. Payne, H. Hunt, H. Zhang, S.L. Holmen, J.B. Dodgson, Inhibition of Marek's disease virus replication by retroviral vector-based RNA interference, *Virology*. 377 (2008) 265–272. https://doi.org/https://doi.org/10.1016/j.virol.2008.03.019.

[283] S. Bivalkar-Mehla, J. Vakharia, R. Mehla, M. Abreha, J.R. Kanwar, A. Tikoo, A. Chauhan, Viral RNA silencing suppressors (RSS): Novel strategy of viruses to ablate the host RNA interference (RNAi) defense system, *Virus Res.* 155 (2011) 1–9. https://doi.org/10.1016/j.virusres.2010.10.003.

[284] L.E. Fry, C.F. Peddle, M. Stevanovic, A.R. Barnard, M.E. McClements, R.E. MacLaren, Promoter orientation within an AAV-CRISPR vector affects Cas9 expression and gene editing efficiency, *Cris. J.* 3 (2020) 276–283. https://doi.org/10.1089/crispr.2020.0021.

[285] C. Ma, M. Liu, Q. Li, J. Si, X. Ren, H. Song, Efficient BoPDS gene editing in cabbage by the CRISPR/Cas9 System, *Hortic. Plant J.* 5 (2019) 164–169. https://doi.org/https://doi.org/10.1016/j.hpj.2019.04.001.

[286] V. Di Donato, F. De Santis, T.O. Auer, N. Testa, H. Sánchez-Iranzo, N. Mercader, J.-P. Concordet, F. Del Bene, 2C-Cas9: A versatile tool for clonal analysis of gene function, *Genome Res.* 26 (2016) 681–692. https://doi.org/10.1101/gr.196170.115.

[287] L. Yin, L.A. Maddison, M. Li, N. Kara, M.C. LaFave, G.K. Varshney, S.M. Burgess, J.G. Patton, W. Chen, Multiplex conditional mutagenesis using transgenic expression of Cas9 and sgRNAs, *Genetics*. 200 (2015) 431–441. https://doi.org/10.1534/genetics.115.176917.

[288] T. Shiraki, K. Kawakami, A tRNA-based multiplex sgRNA expression system in zebrafish and its application to generation of transgenic albino fish, *Sci. Rep.* 8 (2018) 13366. https://doi.org/10.1038/s41598-018-31476-5.

[289] F. Dong, K. Xie, Y. Chen, Y. Yang, Y. Mao, Polycistronic tRNA and CRISPR guide-RNA enables highly efficient multiplexed genome engineering in human cells, *Biochem. Biophys. Res. Commun.* 482 (2017) 889–895. https://doi.org/10.1016/j.bbrc.2016.11.129.

[290] M. Jinek, A. East, A. Cheng, S. Lin, E. Ma, J. Doudna, RNA-programmed genome editing in human cells, *Elife*. 2 (2013) e00471. https://doi.org/10.7554/eLife.00471.

[291] T. Wang, J.J. Wei, D.M. Sabatini, E.S. Lander, Genetic screens in human cells using the CRISPR-Cas9 system, *Science.* 343 (2014) 80–84. https://doi.org/10.1126/science.1246981.

[292] J. Ablain, E.M. Durand, S. Yang, Y. Zhou, L.I. Zon, A CRISPR/Cas9 vector system for tissue-specific gene disruption in zebrafish, *Dev. Cell*. 32 (2015) 756–764. https://doi.org/https://doi.org/10.1016/j.devcel.2015.01.032.

[293] F. Port, H.-M. Chen, T. Lee, S.L. Bullock, Optimized CRISPR/Cas tools for efficient germline and somatic genome engineering in Drosophila, *Proc. Natl. Acad. Sci.* 111 (2014) E2967–E2976. https://doi.org/10.1073/pnas.1405500111.

[294] S. Gandhi, M.L. Piacentino, F.M. Vieceli, M.E. Bronner, Optimization of CRISPR/Cas9 genome editing for loss-of-function in the early chick embryo, *Dev. Biol.* 432 (2017) 86–97. https://doi.org/10.1016/j.ydbio.2017.08.036.

[295] S. Fiering, E. Epner, K. Robinson, Y. Zhuang, A. Telling, M. Hu, D.I. Martin, T. Enver, T.J. Ley, M. Groudine, Targeted deletion of 5'HS2 of the murine beta-globin LCR reveals that it is not essential for proper regulation of the beta-globin locus, *Genes Dev.* 9 (1995) 2203–2213. https://doi.org/10.1101/gad.9.18.2203.

10. ACKNOWLEDGEMENTS

Zuerst möchte ich mich bei meinem Betreuer Herrn Prof. Dr. Benjamin Schusser dafür bedanken, dass er mir die Möglichkeit gegeben hat meine Promotion an diesem Lehrstuhl durchzuführen. Vielen Dank für deine Betreuung und dafür, dass du bei Fragen und Sorgen immer für uns erreichbar bist. Besonders habe ich mich darüber gefreut, dass ich im Jahr 2019 an der „Transgenic animal research conference (TARC)“ Konferenz in den USA teilnehmen durfte, um dort meine Ergebnisse zu präsentieren.

Ein weiterer Dank gilt Prof. Benedikt Kaufer und seinem Team für die angenehme Zusammenarbeit und den Beitrag zu dieser Arbeit. Besonders möchte ich mich an der Stelle bei Andelé Conradie bedanken, die auch noch nach ihrer PhD-Zeit hinaus für mich jederzeit bei Rückfragen zur Verfügung stand.

Auch ein Dankschön an Lutz Kettler, der mit seiner Expertise die *in ovo*-Elektroporationen für uns durchgeführt hat.

Ein riesengroßes Dankeschön gilt meinen Arbeitskollegen - Sabrina Schleibinger, Kamila Lengyel, Hicham Sid, Romina Klinger, Hanna Vikkula und Tom Berghof. Danke, dass ihr immer für mich da wart und mich brav ans Mittagessen erinnert habt. Aber auch möchte ich mich bei den ehemaligen Kollegen bedanken, ohne die meine Promotion auch nur halb so schön gewesen wäre – Theresa Thoma und Antonina Schlickenrieder.

Danke auch an die gesamte AG Schnieke, und besonders den TAs, die mir immer mit Rat und Tat zur Seite gestanden sind.

Zuletzt möchte ich mich von ganzen Herzen bei meiner Familie bedanken. Mama, Papa – vielen Dank, dass ihr immer für mich da seid und mir es ermöglicht habt diesen Weg zu gehen. Danke an meinen Bruder Christopher und seine Frau Jenny, die immer ein offenes Ohr für mich hatten. Am aller meisten möchte ich mich bei meinem Mann Marcel bedanken, der sich abendelang mit Korrekturlesen und Taschentücher bereithalten rumschlagen musste. Vielen Dank, dass du immer für mich da bist!!!